

Cardiorenal Syndrome:
Pathophysiology and Potential Role of Uremic Toxins

Thesis submitted in fulfilment of the requirement for
the degree of Doctor of Philosophy

by

Shan Liu

Centre for Cardiovascular Research and Education in Therapeutics

Department of Epidemiology and Preventive Medicine

School of Public Health and Preventive Medicine

The Alfred Centre, Alfred Hospital

Monash University, 2013

Notice 1

Under the Copyright Act 1968, this thesis must be used only under the normal conditions of scholarly fair dealing. In particular no results or conclusions should be extracted from it, nor should it be copied or closely paraphrased in whole or in part without the written consent of the author. Proper written acknowledgement should be made for any assistance obtained from this thesis.

Summary

Cardiorenal syndrome (CRS) describes both heart and kidney failure initiated by dysfunction in either the heart or kidney. CRS is associated with significant worsened outcomes than disease of either organ alone. The pathophysiology of this condition is still not fully understood. Specifically, there is no preclinical study examining the heart-kidney interactions where chronic heart failure (CHF) is complicated by the addition of chronic kidney disease (CKD). Conversely, the findings remain controversial in a recently described animal model recapitulating features of CKD co-morbid with CHF. Furthermore, one under-explored factor contributory to the development of CRS may be circulating toxins in patients with CKD. Indoxyl sulfate (IS), one such non-dialysable uremic toxin, has direct pro-hypertrophic and pro-fibrotic effects on cardiac myocytes and fibroblasts. Increased cardiac fibrosis in animals with CKD is correlated with IS serum levels. This thesis therefore aimed to further explore the pathophysiology of CRS and the potential role of IS in this condition.

The first part of the thesis evaluated cardiac and renal changes (molecular, structural and functional) and examined potential mechanisms that may underlie the changes observed in a state of chronic abnormalities in cardiac function causing progressive CKD [myocardial infarction (MI) followed by 5/6 nephrectomy (STNx) model in **Chapter 3 and 4**]. This is the first preclinical model (MI+STNx) to demonstrate the left ventricular (LV) dysfunction complicated by the addition of CKD.

This *in vivo* MI+STNx study demonstrated that subsequent STNx accelerated the reduction in left ventricular ejection fraction (LVEF) post-MI. Combined MI and STNx led to increases in heart and lung weights and elevation in myocyte cross-sectional area

and cardiac interstitial fibrosis in the non-infarcted myocardium compared to MI alone. These changes were associated with significant increases in atrial natriuretic peptide (ANP), transforming growth factor β_1 (TGF- β_1) and collagen I gene expression. Co-morbid disease also caused increases in renal tubulointerstitial fibrosis compared to STNx alone, with no further deterioration in renal function.

The second part of this thesis assessed pathophysiological changes and potential mechanisms in a condition of CKD contributing to decreased cardiac function and cardiac hypertrophy [STNx followed by MI (STNx+MI) model in **Chapter 5 and 6**]. This *in vivo* study demonstrated that STNx+MI caused a non-significant decrease in changes of LVEF over time compared to MI alone. Compared to STNx alone, combined STNx and MI increased renal tubulointerstitial fibrosis and kidney injury molecule-1 (KIM-1) tissue levels in the kidney, and elevated myocyte cross-sectional area and cardiac interstitial fibrosis in the non-infarcted myocardium. These changes were associated with increases in collagen I gene expression, and activation of p38 mitogen-activated protein kinase (MAPK) and p44/42 MAPK protein in the non-infarcted myocardium.

The third part of the thesis focused on potential approaches to block IS-induced cardiac remodelling (**Chapter 7**). Organic anion transporters 1 and 3 (OAT1/3) have been found to be involved in the trans-cellular transport of IS in renal cells. Furthermore, apoptosis signal-regulating kinase-1 (ASK1) is a potential therapeutic target for cardiac disease. The activation of ASK1 associated signalling pathways, namely p38, p44/42 MAPK and nuclear factor-kappa B (NF κ B), has been demonstrated to be involved in IS-induced cardiac remodelling. Hence, we investigated the role of OAT1/3 and/or

ASK1 in cardiac remodelling *in vitro* via the approaches to block pro-hypertrophic and pro-fibrotic actions of IS in cardiac myocytes and fibroblasts. Inhibition of OAT1/3 and ASK1 suppressed IS-activated cardiac myocyte hypertrophy and fibroblast collagen synthesis, in a dose-dependent manner. OAT1/3 and ASK1 antagonists appear to attenuate these effects by blocking the uptake of IS into cardiac cells and downstream actions post-uptake, respectively.

Together, this thesis has demonstrated that accelerated cardiac remodelling and increased renal tubulointerstitial fibrosis appear to be the common pathophysiological changes in the setting of MI+STNx and STNx+MI. MI+STNx animals had decreased LVEF compared to the STNx+MI animals, suggesting animals with pre-morbid CHF had worsening cardiac outcomes. A non-significant reduction in glomerular filtration rate (GFR) was observed in STNx+MI vs MI+STNx animals, indicating that animals with pre-morbid CKD were likely to develop more severe renal outcomes. Thus, the severity of heart and kidney damage appears to be best related to the primary failing organ.

OAT1/3 and ASK1 appear to play a role in IS-induced pathological cardiac remodelling, which are suppressed by their antagonists, in a dose-dependent manner. They may represent potential novel therapeutic approaches to ameliorate uremic toxin-stimulated cardiac effects in the setting of co-morbid CHF and CKD.

Table of Contents

Summary	i
General Declaration	xii
Acknowledgements	xiv
Publications, Awards and Conference Communications	xvi
Abbreviations List	xix
Chapter 1 Literature Review	2
1.1 Introduction	3
1.2 Definition	3
1.2.1 Acute cardio-renal syndrome (Type 1)	4
1.2.2 Chronic cardio-renal syndrome (Type 2)	5
1.2.3 Acute reno-cardiac syndrome (Type 3)	5
1.2.4 Chronic reno-cardiac syndrome (Type 4)	5
1.2.5 Secondary cardio-renal syndromes (Type 5)	6
1.3 Epidemiology	6
1.3.1 The heart as primary failing organ	6
1.3.2 The kidney as primary failing organ	10
1.3.3 Systemic conditions causing cardiac and renal dysfunction	13
1.4 Pathophysiology of CRS	13
1.4.1 Pathophysiological contributors to CRS	14
1.4.1.1 Hemodynamic derangements	14
1.4.1.2 Neurohormonal activation	15
1.4.1.3 Oxidative stress	17
1.4.1.4 Inflammation	19

1.4.1.5 Hypertension	20
1.4.1.6 Anemia	21
1.4.1.7 Calcium and phosphate abnormalities	21
1.4.1.8 Uremic toxins	22
1.4.2 Consequences when heart/kidney is the primary insult	25
1.4.2.1 Cardiac changes	25
1.4.2.2 Renal changes	27
1.5 Diagnosis of CRS	28
1.5.1 Imaging	28
1.5.2 Biomarkers	29
1.5.2.1 Natriuretic peptides	30
1.5.2.2 Cardiotrophin-1	30
1.5.2.3 Suppression of tumorigenicity 2	31
1.5.2.4 Galectin-3	31
1.5.2.5 Creatinine and cystatin C	32
1.5.2.6 Neutrophil gelatinase-associated lipocalin	32
1.5.2.7 Kidney injury molecule-1	33
1.5.2.8 Interleukin-18	33
1.5.2.9 <i>N</i> -acetyl- β -(D)-glucosaminidase	33
1.6 Preclinical models	34
1.6.1 MI model	34
1.6.1.1 Cardiac effects	34
1.6.1.2 Renal effects	35
1.6.2 STNx model	35
1.6.2.1 Cardiac effects	35

1.6.2.2 Renal effects.....	36
1.6.3 Combination of MI and STNx models.....	37
1.7 Management of CRS.....	39
1.7.1 Diuretics and ultrafiltration.....	42
1.7.2 Angiotensin converting enzyme inhibitors	44
1.7.3 Angiotensin II receptor blockers.....	45
1.7.4 β -adrenergic receptor blockers.....	45
1.7.5 Mineralocorticoid receptor antagonists.....	46
1.7.6 Treatments for uremic toxins	46
1.8 Conclusion	48
1.9 Hypotheses and Aims.....	49
1.9.1 CRS when cardiac dysfunction is the primary insult.....	49
1.9.2 CRS when renal dysfunction is the primary insult	49
1.9.3 Potential novel treatments for CRS.....	50
Chapter 2 Materials and Methods	51
2.1 <i>In vivo</i> studies.....	52
2.1.1 Animals and ethics approval	52
2.1.2 Myocardial infarction.....	52
2.1.3 Subtotal nephrectomy	53
2.1.4 Blood pressure.....	53
2.1.5 Echocardiography	53
2.1.6 Cardiac catheterization.....	54
2.1.7 Glomerular filtration rate	55
2.1.8 Metabolic caging.....	55
2.1.9 IS measurements	56

2.1.10 Tissue collection	56
2.1.11 Histopathology	57
2.1.12 Infarct size.....	57
2.1.13 Interstitial fibrosis	58
2.1.14 Haematoxylin and eosin staining	58
2.1.15 Immunohistochemistry.....	59
2.1.15.1 Collagen type I and III	60
2.1.15.2 Kidney injury molecule-1	60
2.1.15.3 Macrophage infiltration.....	61
2.1.16 Quantitative mRNA expression	61
2.1.17 Protein extraction	64
2.1.18 Bradford assay.....	64
2.1.19 Western blot analysis	64
2.1.19.1 Reagents and solutions.....	64
2.2.19.2 Preparation	66
2.1.19.3 SDS-PAGE.....	68
2.1.19.4 Transfer	68
2.1.19.5 Immunoblotting.....	68
2.1.20 Statistical analysis	70
2.2 <i>In vitro</i> studies.....	70
2.2.1 Animal and ethics approval.....	70
2.2.2 Materials.....	70
2.2.3 Reagents and solutions.....	71
2.2.4 NCMs and NCFs isolation	73
2.2.5 Measurement of NCM hypertrophy	74

2.2.6 Measurement of NCF collagen synthesis.....	75
2.2.7 Measurement of cell viability in NCFs	76
2.2.8 Statistical analysis	76
Chapter 3 Functional and Structural Changes in the MI+STNx Model	77
3.1 Introduction.....	78
3.2 Aims	79
3.3 Materials and Methods.....	79
3.4 Results.....	80
3.4.1 Survival rate and infarct size.....	80
3.4.2 Blood pressure.....	81
3.4.3 Tissue weights.....	82
3.4.4 Echocardiography	83
3.4.5 Hemodynamic parameters.....	86
3.4.6 Cardiac interstitial fibrosis	87
3.4.7 Cardiac myocyte cross-sectional area	89
3.4.8 Renal function and indoxyl sulfate plasma levels.....	91
3.4.9 Renal tubulointerstitial fibrosis.....	92
3.5 Discussion	94
Chapter 4 Pathological and Mechanistic Investigations in the MI+STNx Model	98
4.1 Introduction.....	99
4.2 Aims	99
4.3 Materials and Methods.....	99
4.4 Results.....	100
4.4.1 Cardiac collagen I and III.....	100
4.4.2 Cardiac mRNA expression.....	103

4.4.3 Cardiac signalling pathway activation	105
4.4.4 Renal injury biomarker	106
4.4.5 Renal macrophage infiltration.....	108
4.4.6 Renal mRNA expression.....	109
4.4.7 Renal signalling pathway activation	110
4.5 Discussion	113
Chapter 5 Functional and Structural Changes in the STNx+MI Model	116
5.1 Introduction.....	117
5.2 Aims	118
5.3 Materials and Methods.....	118
5.4 Results.....	119
5.4.1 Survival rate and infarct size.....	119
5.4.2 Blood pressure.....	121
5.4.3 Tissue weights.....	121
5.4.4 Echocardiography	122
5.4.5 Hemodynamic parameters.....	125
5.4.6 Cardiac interstitial fibrosis	126
5.4.7 Cardiac myocyte cross-sectional area	128
5.4.8 Renal function and indoxyl sulfate plasma levels.....	129
5.4.9 Renal tubulointerstitial fibrosis.....	130
5.5 Discussion	133
Chapter 6 Pathological and Mechanistic Investigations in the STNx+MI Model	136
6.1 Introduction.....	137
6.2 Aims	137
6.3 Materials and Methods.....	138

6.4 Results	138
6.4.1 Cardiac collagen I and III	138
6.4.2 Cardiac mRNA expression	141
6.4.3 Cardiac signalling pathway activation	144
6.4.4 Renal injury biomarker	146
6.4.5 Renal macrophage infiltration	147
6.4.6 Renal mRNA expression	149
6.4.7 Renal signalling pathway activation	150
6.5 Discussion	153
Chapter 7 Treatments for Indoxyl Sulfate-induced Cardiac Effects	155
7.1 Introduction	156
7.2 Aims	158
7.3 Materials and Methods	159
7.4 Results	159
7.4.1 OAT1/3 inhibition in cardiac myocytes	159
7.4.2 OAT1/3 inhibition in cardiac fibroblasts	161
7.4.3 ASK1 inhibition in cardiac myocytes	163
7.4.4 ASK1 inhibition in cardiac fibroblasts	165
7.4.5 Effect of OAT1/3 and ASK1 inhibitors on cardiac cell viability	166
7.5 Discussion	167
Chapter 8 Thesis Summary, Conclusions and Future Directions	169
8.1 <i>In vivo</i> MI+STNx and STNx+MI studies	170
8.2 Study limitations	173
8.3 <i>In vitro</i> IS study	174
8.4 Future directions	174

References	177
------------------	-----

Appendices

Appendix 1: Cardiorenal syndrome: Pathophysiology, preclinical models, management and potential role of uraemic toxins

Appendix 2: Antagonists of organic anion transporters 1 and 3 ameliorate adverse cardiac remodelling induced by uremic toxin indoxyl sulfate

Appendix 3: Subtotal nephrectomy accelerates pathological cardiac remodeling post-myocardial infarction: Implications for cardiorenal syndrome

General Declaration

Monash University

Monash Research Graduate School

Declaration for thesis based or partially based on conjointly published or unpublished work

In accordance with Monash University Doctorate Regulation 17/ Doctor of Philosophy and Master of Philosophy (MPhil) regulations the following declarations are made:

I hereby declare that this thesis contains no material which has been accepted for the award of any other degree or diploma at any university or equivalent institution and that, to the best of my knowledge and belief, this thesis contains no material previously published or written by another person, except where due reference is made in the text of the thesis. Efforts have been made to obtain permissions for using data/figures for the literature where possible, otherwise proper reference details have been provided.

This thesis includes three original papers published in peer-reviewed journals and one unpublished paper. The core theme of the thesis is ‘Pathophysiology of Cardiorenal Syndrome and Potential Role of Uremic Toxins’. The ideas, development and writing up of all the papers in the thesis were the principal responsibility of myself, the candidate, working within the Department of Epidemiology and Preventive Medicine

under the supervision of A/Prof Bing H. Wang, Dr Andrew R. Kompa, and Professor Henry Krum.

The inclusion of co-authors reflects the fact that the work came from active collaboration between researchers and acknowledges input into team-based research.

Signed:

Date:

Acknowledgements

There are many people who have made it possible for the completion of this thesis. Firstly I would like to thank my supervisors A/Prof Bing H. Wang, Dr Andrew R. Kompa and Prof Henry Krum. They have been very supportive all the time. Thank you for your guidance and knowledgeable assistance throughout the PhD. To A/Prof Bing H. Wang, I will be always grateful for your mentoring and facilitating, especially in the field of cell culture work and tissue analyses. To Dr Andrew R. Kompa, thank you for your insight, useful opinions, great patience, and everything you have taught me over the past few years. To Prof Henry Krum, you have been always supportive and available with a quick response. Thank you for never letting me lose sight of the big picture in my whole PhD years.

I am grateful to all the staff and students at Department of Epidemiology and Preventive Medicine, Monash University, particularly those in Centre of Cardiovascular Research and Education in Therapeutics (CCRET). Special thanks goes to Lavinia, Patty, Suree, Ingrid, Hendrik, Grace, Masataka, Thomas, Sirinart, Qiang, Longxing for their encouragement and friendship.

To the delicate bunch of staff from Department of Medicine, University of Melbourne, thanks for your continuous support and contribution towards the work presented in this thesis. Special thank you goes to Dr Yuan Zhang for assistance with immunohistochemistry. I'd like to thank Ms Mariana Pacheco, Ms Jemma Court and Ms Alysha Holland for their technical assistance with the animal work, Mrs Sylwia Glowacka for assistance with Cobas assays. To my PhD colleagues, Christina, Min, Mark, thank you for the chats, laughs and sharing the journey with me.

Special thanks goes to Dr Fuyuhiko Nishijima from Pharmaceutical Department, Kureha Corporation, Tokyo, Japan. I am grateful for the collaboration and assistance with chromatographic analysis.

I also would like to acknowledge Australian government and Monash University for postgraduate scholarships supporting my PhD study. Special acknowledgements also go to my mother county for her award and great care when I am in overseas.

Last but most importantly, Mum, Dad and Junfei deserve my heartfelt thanks for having been a source of endless love, encouragement and support.

Publications, Awards and Conference Communications

Publications

Liu S, Lekawanvijit S, Kompa AR, Wang BH, Kelly DJ, Krum H. Cardiorenal syndrome: Pathophysiology, preclinical models, management and potential role of uraemic toxins. (2012) *Clinical and Experimental Pharmacology and Physiology* 39: 692–700

Liu S, Wang BH, Kompa AR, Lekawanvijit S, Krum H. Antagonists of organic anion transporters 1 and 3 ameliorate adverse cardiac remodelling induced by uremic toxin indoxyl sulfate. (2012) *International Journal of Cardiology* 158(3):457-458

Liu S, Kompa AR, Kumfu S, Nishijima F, Kelly DJ, Krum H, Wang BH. Subtotal nephrectomy accelerates pathological cardiac remodeling post-myocardial infarction: Implications for cardiorenal syndrome. (2013) *International Journal of Cardiology* DOI: 10.1016/j.ijcard.2012.12.065

Awards

Mini Oral Prize in 61st Annual Scientific Meeting of the Cardiac Society of Australia and New Zealand, Gold Coast, Australia, 2013

Chinese Government Award for Outstanding Self-financed Students Abroad, 2012

Baker IDI Heart and Diabetes Institute Prize for Cardiovascular Research at Alfred Week, Melbourne, Australia, 2012

Monash Postgraduate Travel Grant Award to attend American Heart Association Scientific Sessions, Orlando, USA, 2011

Presentation Award of 3rd Australia-China Biomedical Research Conference, Melbourne, Australia, 2011

Conference communications

Liu S, Kompa AR, Kelly DJ, Krum H and Wang BH. Myocardial infarction accelerates pathological cardiac remodeling and renal impairment post subtotal nephrectomy. European Society of Cardiology Congress, Amsterdam, Netherlands (2013) *European Heart Journal* 34:S928

Liu S, Kompa AR, Kelly DJ, Krum H and Wang BH. Myocardial infarction after subtotal nephrectomy accelerates pathological cardiac remodeling and renal impairment. 61st Annual Scientific Meeting of the Cardiac Society of Australia and New Zealand, Gold Coast, Australia (2013) *Heart, Lung and Circulation* 22:S83

Liu S, Kompa AR, Kelly DJ, Krum H and Wang BH. Myocardial infarction accelerates renal and cardiac impairment post subtotal nephrectomy: Implications for cardiorenal syndrome. American Society of Nephrology: KidneyWeek, San Diego, USA (2012) *Journal of the American Society of Nephrology* 23:514A

Liu S, Kompa AR, Kelly DJ, Krum H and Wang BH. Subtotal nephrectomy accelerates pathological cardiac remodeling post myocardial infarction: Implications for the cardiorenal syndrome. European Society of Cardiology Congress, Munich, Germany (2012) *European Heart Journal* 33:S1052

Liu S, Kompa AR, Krum H, Kelly DJ and Wang BH. Subtotal nephrectomy accelerates pathological cardiac remodeling post myocardial infarction: Implications for the cardiorenal syndrome. 60th Annual Scientific Meeting of the Cardiac Society of

Australia and New Zealand, Brisbane, Australia (2012) *Heart, Lung and Circulation* 21:S93-94

Liu S, Kompa AR, Krum H, Kelly DJ and Wang BH. Myocardial infarction accelerates pathological cardiac remodeling and renal fibrosis post subtotal nephrectomy: Implications for the cardiorenal syndrome. 60th Annual Scientific Meeting of the Cardiac Society of Australia and New Zealand, Brisbane, Australia (2012) *Heart, Lung and Circulation* 21:S86-87

Liu S, Kompa AR, Kelly DJ, Krum H and Wang BH. Subtotal nephrectomy accelerates pathological cardiac remodelling post myocardial infarction: Recapitulating the phenotype of cardiorenal syndrome? American Heart Association Scientific Sessions, Orlando, USA (2011) *Circulation* 124:A11507

Liu S, Kompa AR, Kelly DJ, Krum H and Wang BH. Combined subtotal nephrectomy and myocardial infarction accelerates heart and kidney disease: A new model of the cardiorenal syndrome. 59th Annual Scientific Meeting of the Cardiac Society of Australia and New Zealand, Perth, Australia (2011) *Heart, Lung and Circulation* 20:S61

Liu S, Lekawanvijit S, Xu G, Kompa AR, Krum H and Wang BH. Organic ion transporters ameliorate the adverse cardiac effects of the non-dialysable uremic toxin indoxyl sulfate in cardiac cell culture: Implications for the treatment of the cardiorenal syndrome. 58th Annual Scientific Meeting of the Cardiac Society of Australia and New Zealand, Adelaide, Australia (2010) *Heart, Lung and Circulation* 19:S77

Abbreviations List

ACE	Angiotensin converting enzyme
ACEi	Angiotensin converting enzyme inhibitors
ADHF	Acute decompensated heart failure
AKI	Acute kidney injury
Ang II	Angiotensin II
ANP	Atrial natriuretic peptide
APS	Ammonium persulfate
ARB	Angiotensin II receptor blockers
ASK1	Apoptosis signal-regulating kinase-1
BNP	B-type natriuretic peptide
BP	Blood pressure
BrDu	5-bromo-deoxyuridine
BSA	Bovine serum albumin
BW	Body weight
cDNA	Complimentary deoxyribonucleic acid
CHF	Chronic heart failure
Cil	Cilastatin
CKD	Chronic kidney disease
CRS	Cardiorenal syndrome
CTGF	Connective tissue growth factor
CVD	Cardiovascular disease
DAB	Diaminobenzidine
dH ₂ O	Distilled water

DMEM	Dulbecco's modified eagle medium
DMSO	Dimethyl sulfoxide
DT	Deceleration time
DTT	Dithiothreitol
Echo	Echocardiography
EDPVR	End diastolic pressure-volume relationship
eGFR	Estimated glomerular filtration rate
EPO	Erythropoietin
ESPVR	End systolic pressure-volume relationship
ESRD	End-stage renal disease
FBS	Fetal bovine serum
FS	Fractional shortening
GAPDH	Glyceraldehydes 3-phosphate dehydrogenase
GFR	Glomerular filtration rate
G226	GSK2261818A
G235	GSK2358939
HBSS	Hank's buffered salt solution
HCl	Hydrogen chloride
HF	Heart failure
HPLC	High performance liquid chromatography
HRP	Horseradish peroxidase
ICU	Intensive care unit
i.p.	Intraperitoneal
i.v.	Intravenous
IgG	Immunoglobulin G

IL-1	Interleukin-1
IL-1 β	Interleukin-1 β
IL-1	Interleukin-1
IL-6	Interleukin-6
IS	Indoxyl sulfate
IVRT	Isovolumic relaxation time
JNK	c-Jun NH ₂ -terminal kinases
KIM-1	Kidney injury molecule-1
LAD	Left anterior descending
LV	Left ventricle/ventricular
LVEDP	Left ventricular end diastolic pressure
LVEF	Left ventricular ejection fraction
LVH	left ventricular hypertrophy
LVIDd	Left ventricular internal diameter at end-diastole
LVIDs	Left ventricular internal diameter at end-systole
LVPWd	Left ventricular posterior wall thickness in diastole
MAP	Mitogen-activated protein
MAPK	Mitogen-activated protein kinase
MEM	Minimum essential media
MI	Myocardial infarction
MRI	Magnetic resonance imaging
mRNA	Messenger ribonucleic acid
MRS	Magnetic resonance spectroscopy
MTT	3-(4,5-dimethylthiazol-2-yl)-2,5-diphenyltetrazolium bromide
NaOH	Sodium hydroxide

NBCS	New born calf serum
NBF	Neutral-buffered formalin
NCF	Neonatal rat cardiac fibroblast
NCM	Neonatal rat cardiac myocyte
NFκB	Nuclear factor-kappa B
NGAL	Neutrophil gelatinase-associated lipocalin
NO	Nitric oxide
NT-proBNP	N-terminal pro-B-type natriuretic peptide
OAT1/3	Organic anion transporters 1 and 3
PBS	Phosphate buffered saline
PCR	Polymerase chain reaction
PET	Positron emission tomography
Pro	Probenecid
PRSW	Preload recruitable stroke work
RAAS	Renin-angiotensin-aldosterone system
RAS	Renin-angiotensin system
RNA	Ribonucleic acid
ROS	Reactive oxygen species
RPM	Revolutions per minute
RT-PCR	Real-time polymerase chain reaction
RVU	Relative Volume Units
RWT	Relative wall thickness
s.c.	Subcutaneous
SD	Sprague Dawley
SDS	Sodium dodecyl sulfate

SDS-PAGE	Sodium dodecyl sulfate polyacrylamide gel electrophoresis
SEM	Standard error of the mean
SNS	Sympathetic nervous system
SPARC	Secreted protein acidic and rich in cysteine
SPECT	Single-photon emission computed tomography
ST2	Suppression of tumorigenicity 2
STNx	Subtotal nephrectomy
TBS	Tris-buffered saline
TBST	Tris-buffered saline - Tween 20
TCA	Trichloroacetic acid
⁹⁹ Tc-DTPA	⁹⁹ Technetium-diethylene triamine pentaacetic acid
TEMED	Tetramethylethylenediamine
TGF- β	Transforming growth factor- β
TNF- α	Tumor necrosis factor- α
UNX	Unilateral nephrectomy
v/v	Volume by volume
w/v	Weight by volume
β -blockers	β -adrenergic receptor blockers
β -MHC	β -myosin heavy chain

Chapter 1 Literature Review

1.1 Introduction

Cardiorenal syndrome (CRS) is a condition in which a complex inter-relationship between cardiac dysfunction and renal impairment co-exists. A diseased heart has numerous negative effects on kidney function, whilst renal insufficiency can significantly impair cardiac function leading to the progression of failure of both organs.^{1,2} CRS has been generally classified into 5 subtypes to recognize the potential pathophysiological disorder of both the heart and kidney, whereby acute or chronic dysfunction of one organ may induce acute or chronic dysfunction of the other.³ The primary failing organ can be either heart or kidney. Systemic conditions leading to simultaneous injury and/or dysfunction of the heart and kidney are also proposed to be one of the subtypes of CRS.³ Our understanding of the complex hemodynamic, neurohormonal, immunological and biochemical derangements that encompass CRS is deficient, and may not be able to provide the rationale for specific management. Thus, further investigation in its pathophysiology and underlying mechanisms is needed to explore the complex nature of CRS.

1.2 Definition

According to Ronco et al,³ The CRS has been classified into 5 subtypes to highlight the time course of heart-kidney interaction and the primacy of the diseased organ leading to the syndrome (Table 1.1).

Table 1.1 Subtypes of the cardiorenal syndrome.

	Acute cardio-renal syndrome (type 1)	Chronic cardio-renal syndrome (type 2)	Acute reno-cardiac syndrome (type 3)	Chronic reno-cardiac syndrome (type 4)	Secondary cardiorenal syndromes (type 5)
Primary events	Acute heart failure, acute coronary syndrome, cardiogenic shock	Chronic heart disease	Acute kidney injury	Chronic kidney disease	Systemic disease (sepsis, amyloidosis, etc.)
Secondary events	Acute kidney injury	Chronic kidney disease	Acute heart failure, acute coronary syndrome, arrhythmias, shock	Chronic heart disease, acute heart failure, acute coronary syndrome	Acute heart failure, acute coronary syndrome, chronic heart disease, acute kidney injury, chronic kidney disease

Used with permissions from Ronco C, *et al.*⁴

1.2.1 Acute cardio-renal syndrome (Type 1)

The term of acute kidney injury (AKI) has been used to describe the conditions that cover the spectrum from mild prerenal azotemia with no renal pathologic changes and no functional failure to severe oliguric renal dysfunction associated with tubular necrosis with failure of function.⁵ Type 1 acute cardio-renal syndrome is defined as acute worsening of heart function leading to AKI.³ This is a syndrome of the initial acute heart failure and/or acute coronary syndrome complicated by kidney injury and/or dysfunction.⁴ Approximately 27-40% of patients administrated for acute decompensated heart failure (ADHF) develop AKI and fall into this clinical entity.⁴

1.2.2 Chronic cardio-renal syndrome (Type 2)

Type 2 chronic cardio-renal syndrome is defined as chronic abnormalities in heart function leading to kidney injury or dysfunction.³ This subtype refers to chronic heart disease (CHF) complicated by chronic state of kidney disease.⁴ This syndrome is common and appears to happen in 63% of patients hospitalized with congestive heart failure.^{4, 6}

Due to the co-existence of heart and kidney dysfunction, there is yet a clear separation in time to distinguish the occurrence of kidney disease from heart disease.⁷ Therefore, a clear discrimination between type 2 and type 4 CRS (see below) is not available in current literature.⁷

1.2.3 Acute reno-cardiac syndrome (Type 3)

Type 3 acute reno-cardiac syndrome is defined as acute worsening kidney function leading to heart injury and/or dysfunction.³ This subtype refers to cardiac dysfunction secondary to AKI.³ AKI is a growing disorder in hospital and intensive care unit (ICU) patients, and has been identified in approximately 9% of hospital patients and more than 35% of ICU patients.^{8, 9} AKI can affect the heart through several pathways and the recent definition and classification of AKI may help to investigate this syndrome further.¹⁰⁻¹²

1.2.4 Chronic reno-cardiac syndrome (Type 4)

Type 4 chronic reno-cardiac syndrome is defined as a condition of primary chronic kidney disease (CKD) contributing to decreased cardiac function, ventricular hypertrophy and/or increased risk of cardiovascular disease (CVD).³ This subtype

refers to disease or dysfunction of the heart occurring secondary to CKD. It is widely prevalent since it involves the progression of CKD, often due to diabetes mellitus and hypertension, with accelerated calcific atherosclerosis, progressive left ventricular hypertrophy (LVH), and the development of left ventricular (LV) dysfunction.¹³

1.2.5 Secondary cardio-renal syndromes (Type 5)

Type 5 secondary cardio-renal syndromes are defined as systemic conditions leading to simultaneous injury and/or dysfunction of heart and kidney.³ Although this subtype does not have primary and/or secondary organ dysfunction, it refers to situations where both organs are simultaneously affected by systemic illnesses, either acute or chronic.⁴ Severe sepsis represents the most commonly acute condition, which can affect both heart and kidney, while diabetes represents the most commonly chronic cause of combined cardiac and renal dysfunction.¹⁴ Other examples include systemic lupus erythematosus, amyloidosis, or other chronic inflammatory conditions that can lead to these syndromes.⁴

1.3 Epidemiology

1.3.1 The heart as primary failing organ

Heart failure (HF) is a complex clinical condition that can result from any cardiac disorder of the pericardium, myocardium, endocardium and large blood vessels. The impairment of the ability of the ventricle to eject blood during systole is recognized as LV systolic dysfunction.¹⁵ A left ventricular ejection fraction (LVEF) of 40% or less usually indicates impaired LV systolic function. HF can also occur in patients with normal LVEF in whom higher filling pressures are needed to obtain a normal end-diastolic volume of the ventricle. This is so called HF with preserved LVEF or diastolic

HF.^{16, 17} Approximately half of the patients diagnosed with symptomatic HF have systolic dysfunction while the other half have diastolic dysfunction.¹⁵ HF is generally in a chronic state in which worsening symptoms and signs may occur.¹⁶ Alternatively, HF may develop within 24-hour, presenting in forms of acute pulmonary oedema, cardiogenic shock or ADHF.¹⁶ HF affects 1-2% of the population in developed countries and appears to be increasing, and health cost of CHF accounts for 1-2% of the total health care budget.^{15, 18, 19}

HF, being a common disease in the elderly,¹⁵ does not present as sole disease in clinic. Anemia, cachexia, diabetes mellitus, obstructive sleep apnoea, chronic pulmonary disease and renal impairment are conditions frequently observed in HF patients often with a poor prognosis.¹⁶ Specifically, renal function significantly deteriorates in patients with CVD.²⁰ Approximately 27% of acute heart failure are complicated by AKI as defined by an increase in serum creatinine of 26.5 $\mu\text{mol/L}$ or greater, resulting in increased complications, prolonged hospitalisations and increased risk of death.²¹ The incidence estimates for worsening renal function associated with ADHF and acute coronary syndrome are 24-45% and 9-19%, respectively.⁷

In the setting of CHF, the prevalence of renal dysfunction is close to 25%,²²⁻²⁴ and the development of renal dysfunction is associated with poor clinical outcomes.^{25, 26} For example, a recent study recruits patients with CVD with a mean baseline serum creatinine of 79.6 $\mu\text{mol/L}$ and estimated glomerular filtration rate (eGFR) of 86.2 ml/min/1.73 m^2 .²⁷ After a follow-up of 9.3 years, 7.2% of CVD patients have increases in creatinine of 35.4 $\mu\text{mol/L}$ or greater and 34% of patients have reductions in eGFR of

15 ml/min/1.73 m² or more. During the observational period, 2.3% and 5.6% of patients develop kidney disease, respectively.²⁷

Renal impairment leads to a poor prognosis and confers further mortality among HF patients. The degree of renal dysfunction is a powerful independent risk factor for all-cause mortality in HF patients. The prevalence and mortality of renal dysfunction in CHF patients has been summarized in Table 1.2, indicating that even slightly worsening renal function is associated with increased mortality and prolonged hospital stay for CHF patients.^{22, 24, 28-34} For every increase in creatinine by 44.25 µmol/L, the 1-year death risk increases by approximately 10-15%.³⁵ These findings clearly highlight the common co-existence of heart and kidney dysfunction and associated poor prognosis. However, the clinical circumstances often present a challenge to determine which disease process is the primary cause.⁷

Table 1.2 Summary of studies on the prevalence and mortality of renal dysfunction with an eGFR less than 60 ml/min/1.73 m² in major heart failure clinical trials.

Study	Population	% eGFR <60	% LVEF	Outcomes (%)
Hillege ²² (PRIME-II)	1906	50	<35	Matched HR: (CKD versus non-CKD) all-cause death 2.1
Hillege ²⁴ (CHARM)	2680	36	All*	All-cause death (HR): eGFR ≥90, 1.0; eGFR 75–89, 1.13; eGFR 60–74, 1.14; eGFR 45–59, 1.50; eGFR <45, 1.91
Al-Ahmad ³⁰ (SOLVD)	6630	32	≤35	Matched HR: (CKD versus non-CKD) all-cause death 1.064
Ahmed ³² (DIG trial)	7788	45	All*	Matched HR: (CKD versus non-CKD) all-cause death, 1.71
Campbell ³³ (DIG trial)	7788	45	All*	Matched HR: (CKD versus non-CKD) all-cause hospitalisation, 1.18

* Symptomatic CHF patients (New York Heart Association class II–IV) with reduced and preserved LVEF. PRIME-II, Second Prospective Randomized Study of Ibopamine on Mortality and Efficacy; CHARM, Candesartan in Heart Failure: Assessment of Reduction in Mortality and Morbidity; SOLVD, Studies of Left Ventricular Dysfunction; DIG trial, Digitalis Investigation Group trial. eGFR, estimated glomerular filtration rate; LVEF, left ventricular ejection fraction; HR, hazard ratio; CKD, chronic kidney disease.

1.3.2 The kidney as primary failing organ

Renal diseases are worldwide public health problems with a rising incidence and prevalence of kidney failure, and high healthcare cost. According to the US Renal Data System (<http://www.usrds.org>), the prevalence of CKD increased from 12.3 to 14.0% between 1988-1994 and 2005-2010, with 594,374 patients receiving treatment for end-stage renal disease (ESRD) at the end of 2010.³⁶

The national kidney foundation's Kidney Disease Outcomes Quality Initiative (KDOQI) classification divides CKD into 5 stages based on severity of kidney damage and glomerular filtration rate (GFR) (Table 1.3). A graded and independent association exists between the severity of CKD and adverse cardiac outcomes.⁴ There is higher prevalence of CVD in dialysis patients than in the general population (Table 1.4).³⁷

Table 1.3 Classification of the stages of renal disease. Used with permissions from Levey A, *et al.*³⁸

Stage	GFR (ml/min/1.73m ²)	Description
1	≥90	Kidney damage with normal or increased GFR
2	60-89	Kidney damage with mild reduction of GFR
3A 3B*	30-59	Moderate reduction of GFR
4	15-29	Severe reduction of GFR
5 5D 5T [#]	<15	Kidney failure

People with urine albumin-to-creatinine ratio ≥ 30 mg/g (the threshold commonly accepted for ‘microalbuminuria’) or eGFR < 60 ml/min/1.73m² are defined as having CKD, and staged according to the level of GFR. *Because of greater CVD risk and risk of disease progression at lower GFRs, CKD Stage 3 is subdivided into Stages 3A (45-59 ml/min/1.73m²) and 3B (30-44 ml/min/1.73m²). #CKD Stage 5 includes patients that may require or are undergoing kidney replacement therapy. Designations 5D and 5T indicate ESRD patients who undergo chronic dialysis (5D) treatment or have undergone kidney transplantation (5T).

Table 1.4 Prevalence of CVD in the general population and CKD patients.

	Ischemic Heart Disease	Left Ventricular Hypertrophy	Heart Failure
General population	8–13	20	3-6
CKD stages 3–4 (diabetic and non-diabetic kidney disease)	NA	25–50*	NA
CKD stages 1–4 (kidney transplant recipients)	15	50-70	NA
CKD stage 5 (hemodialysis/peritoneal dialysis)	40	75	40

Values are expressed in percentages. * Prevalence varies with levels of kidney function.

Used with permissions from Sarnak MJ, *et al.*³⁹

Patients with renal diseases are at extremely high cardiovascular risk (Figure 1.1).^{39, 40}

Acceleration of arterial vascular disease and cardiomyopathy are major cardiac

problems observed in patients with renal failure and may be contributory to HF that is frequently an accompaniment in patients with impaired renal function.^{1,41} Patients with CKD have 10 to 30 times greater risk of cardiac death compared with general population.⁴² In a prospective study where 433 ESRD patients with dialysis therapy are followed, 15% had systolic dysfunction, 44% had concentric LVH, and 32% had LV dilatation.⁴³

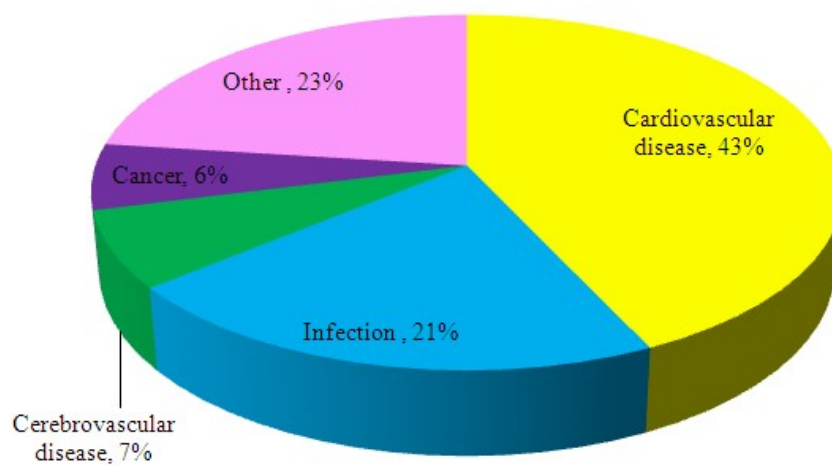


Figure 1.1 Causes of death in dialysis patients. Approximately 43% of deaths are due to cardiovascular events. Adopted from Ritz E, *et al.*⁴⁴

Patients on dialysis who have acute cardiac injury have poor long-term survival.⁴⁵ The 2-year mortality rate after myocardial infarction (MI) in patients with ESRD is approximately 50%.⁴⁶ In comparison, the 10-year mortality rate post-infarct for the general population is estimated to be 25%.³ Individuals with CKD are more likely to die of CVD than to develop kidney failure.⁴⁰ Mortality rate for ESRD patients is above 20% annually, with more than half of the deaths related to cardiovascular events.⁴⁷

1.3.3 Systemic conditions causing cardiac and renal dysfunction

There is limited data on the epidemiology of type 5 CRS. Sepsis occurs at a rate of 3 cases per 1000 population and is increasing by an estimated 8.7% per year.⁷ Approximately 11-64% of the septic patients develop AKI, with 46-58% having sepsis as a major contributing factor to the development of AKI.⁷ Patients with concomitant sepsis and AKI have higher mortality compared to those with either sepsis or AKI alone.⁷ Similarly, abnormalities in cardiac function commonly exist in sepsis patients. Approximately 30-80% of sepsis patients have troponin elevation that often correlates with reduced cardiac function.⁷

1.4 Pathophysiology of CRS

The pathophysiological mechanisms of heart-kidney interactions have not been fully investigated. The proposed CRS subtypes (1 to 5) are likely to share some similarities in pathophysiology. The primary failing organ causes activation of a series of response mechanisms. Although in some cases these mechanisms are initially compensatory, many contribute to further functional worsening and even initiate the disorders of the secondary organ (Figure 1.2).

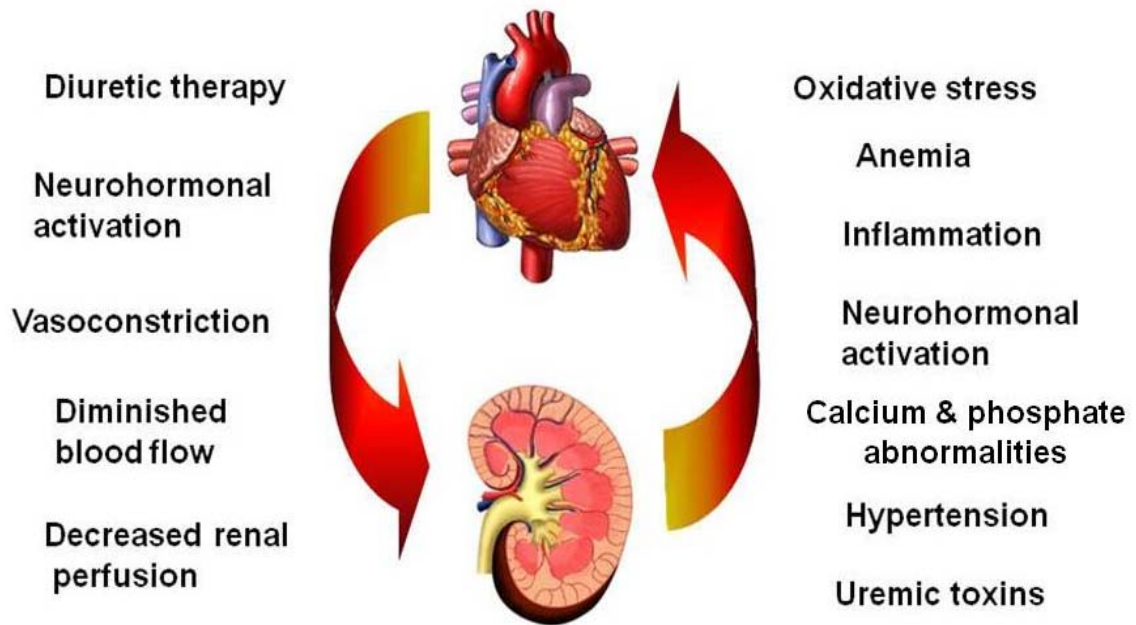


Figure 1.2 Major pathophysiological interactions between heart and kidney in cardiorenal syndrome.

1.4.1 Pathophysiological contributors to CRS

1.4.1.1 Hemodynamic derangements

Volume overload appears to be a common problem in CRS irrespective of the organ of origin or the time frame defined.¹⁴ LV systolic dysfunction associated with CHF leads to diminished cardiac output and decreased renal perfusion, which causes neurohormonal activation and volume overload. On the other hand, volume overload is the result of failure in maintenance of fluid homeostasis in the setting of CKD, and intractable volume overload commonly develops congestive HF that carries a poor prognosis. In addition, diuretic resistance, a condition in which diuretics fail to effectively control sodium and water retention despite the use of appropriate doses of diuretics, occurs frequently in patients with congestive HF.

1.4.1.2 Neurohormonal activation

As previously mentioned, renal hypo-perfusion leads to activation of neurohormonal systems, including renin-angiotensin-aldosterone system (RAAS), sympathetic nervous system (SNS), arginine vasopressin system, endothelin system and natriuretic peptide system. These occur mainly *via* sodium and water reabsorption, baroreceptor-mediated renal vasoconstriction, and release of catecholaminergic hormones.² The excess of the RAAS further activates the SNS, and causes dysregulation of endothelial function, progression of atherosclerosis, and inhibition of the fibrinolytic system.⁴⁸ The activation of the SNS contributes to peripheral and renal vasoconstriction, and to sodium retention.²

Increased hemodynamic stress in the kidney is mediated by neurohormonal factors, such as angiotensin II (Ang II). Ang II constricts blood vessels, **promotes renal tubule sodium reabsorption, and** stimulates the secretion of aldosterone **from the adrenal gland**.⁴⁹ Aldosterone further increases reabsorption of sodium in the collecting duct.⁴⁹ The increase in blood pressure and volume, resulting from the effects of Ang II and aldosterone contributes to the pathophysiology of diseases such as hypertension, and cardiac and renal injury.^{50, 51} Apart from the hypertensive effects, neurohormonal activation also has direct deleterious effects on the myocytes and interstitium, altering the performance and phenotype of these cells.⁵² Thus the hemodynamic consequences of systemic hypertension as well as the direct pro-fibrotic and pro-inflammatory actions of Ang II and aldosterone adversely affect (alone or in concert) the structure and function of the heart and kidney and promote end organ injury.⁵³

Elevated central sympathetic tone caused by activation of renal somatic afferent nerve is closely associated with hypertension and systolic HF; and the consequences of excessive efferent sympathetic signals adversely affect the kidney (Figure 1.3).⁵⁴ Various stimuli such as renal ischemia, hypoxia, oxidative stress and intrinsic renal diseases are likely to activate renal sensory afferent signalling.⁵⁵ Activation of these signalling pathways affects the hypothalamus, which provides the basis for targeting the renal somatic afferent nerves as modulators of central integration in the brain stem.^{54, 55} This integration subsequently causes increased sympathetic efferent signalling to kidney, and directly influences the entire sympathetic system.^{54, 56}

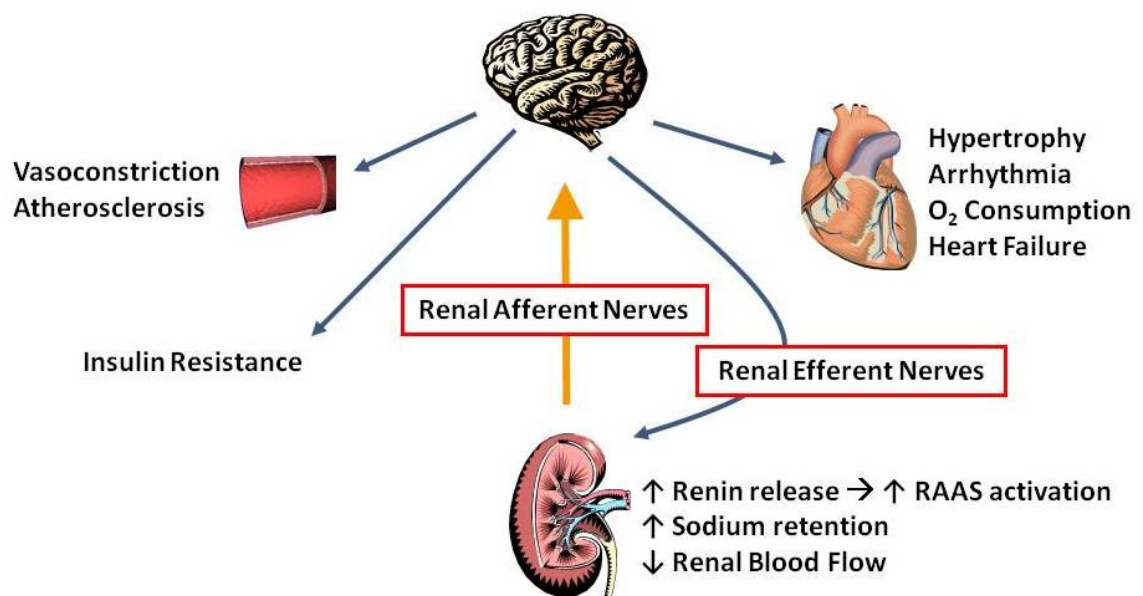


Figure 1.3 Contribution of the kidney's afferent and efferent (pre- and post-glomerular) nerves to a variety of chronic conditions, linked through chronic elevated central sympathetic signalling. Adopted from Sobotka PA, *et al.*⁵⁴

1.4.1.3 Oxidative stress

Activation of the RAAS and the SNS and inflammation may increase oxidative stress,^{57, 58} defined as an imbalance between anti-oxidants (e.g. nitric oxide, NO) and reactive oxygen species (ROS) (Figure 1.4). NO enhances vasodilation, inhibits platelet aggregation, and prevents neutrophil adhesion, thereby controlling vascular tone and preventing atherogenesis.⁵⁹ Increased oxidative stress in the vascular wall is associated with CKD, occurring through reduced bioavailability of NO.⁶⁰ Increased oxidative stress may cause myocyte apoptosis and necrosis, and it is associated with arrhythmias and endothelial dysfunction.^{3, 61}



Figure 1.4 An imbalance between decreased nitric oxide (NO) and increased reactive oxygen species (ROS).

Experimental evidence demonstrates Ang II activates ROS in cardiomyocytes, and pre-treatment with anti-oxidants suppresses Ang II-induced cardiac hypertrophy.⁶² These findings suggest a critical role for ROS-dependent signal transduction in cardiac hypertrophy. Exposure to ROS also impairs myocardial contractility, alters the electrophysiological properties of cardiac cells through modification of ion channels, and stimulates inflammatory cytokines (e.g. tumour necrosis factor- α (TNF- α), interleukin (IL)-1 β and IL-6).⁶³⁻⁶⁶

Increased oxidative stress plays an important role in multiple biochemical pathway activation. Apoptosis signal-regulating kinase-1 (ASK1) is a ROS-sensitive, mitogen-activated protein kinase kinase kinase (MAPKKK).⁶⁷ ASK1 is identified to activate two different subgroups of MAP kinase kinases (MAPKK), MKK3/6 and MKK4/7, these in turn activate p38 MAPK and c-Jun N-terminal kinase (JNK) subgroups (Figure 1.5).⁶⁸

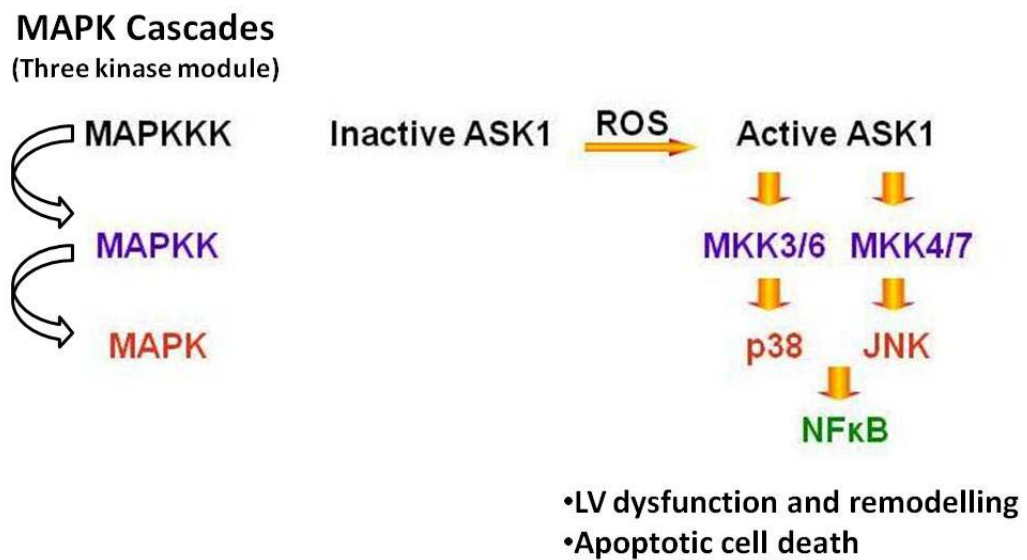


Figure 1.5 Schematic representation of the MAPK signalling constituents constructed as a hierarchy beginning at the MAPKKK (ASK1), to the MAPKKs (MKK3/6 and MKK4/7), down through the MAPKs (p38 and JNK). Used with permissions from Baines CP, *et al.*⁶⁹

ASK1 has been demonstrated to be involved in the pathogenesis of HF progression.⁷⁰ The ROS/ASK1 pathway is associated with stress- and cytokine- induced apoptosis and non-apoptotic cardiomyocyte death.^{68, 71, 72} ASK1 and the downstream kinases of JNK and p38 MAPK are critical signalling pathways in Ang II-induced LV hypertrophy and

remodelling.⁷³⁻⁷⁶ ASK1 also plays a role in G-protein-coupled receptor agonist-induced transcription factor NFκB (nuclear factor-kappa B) activation and results in cardiomyocyte hypertrophy.⁷⁷ Thus, ASK1 is proposed to be a potential therapeutic target for cardiac disease.

1.4.1.4 Inflammation

Systemic inflammatory activation and enhanced cytokine expression are associated with the progression of CRS. C-reactive protein, the prototype marker of inflammation, has an inverse relationship with renal function; it is also strongly associated with CVD.^{78, 79} Increases in C-reactive protein predict cardiovascular events in both general population and CKD patients.⁸⁰⁻⁸²

Cardiac injury results in the migration of macrophages, monocytes and neutrophils into the myocardium. This initiates neurohormonal activation and intracellular signalling, which localizes the inflammatory response.⁸³ Inflammatory mediators IL-1β, IL-6 and TNF-α are increased early post-infarct to acutely regulate myocyte survival or apoptosis and trigger additional cellular inflammatory response.⁸⁴⁻⁸⁶ Such pro-inflammatory cytokines have been demonstrated to mediate the activation of p38 and p44/42 MAPKs and NFκB pathways in subsequent cardiac remodelling and progressive LV dysfunction.⁸⁷⁻⁸⁹

Inflammation is also a common feature in ESRD patients,⁵⁸ and it is even observed among patients with moderate renal impairment.⁹⁰ Levels of the inflammatory markers IL-6 and fibrinogen are significantly higher in patients with renal insufficiency.⁹¹ These inflammatory products may be important mediators leading to the increased

cardiovascular risk in CKD patients.⁹¹ Furthermore, levels of immunoreactive TNF- α and interleukin-1 (IL-1) are increased in the heart after experimental renal ischemia,⁹² and this is associated with cardiac dysfunction, myocyte apoptosis, and leukocyte infiltration of the heart.^{93, 94}

1.4.1.5 Hypertension

Hypertension is an independent predictor of worsening renal function, and commonly develops in patients with underlying renal disease.^{14, 95} Co-existence of hypertension with renal disease greatly accelerates the progression of renal failure.⁹⁵

Hypertension is also the most common risk factor for HF, accounting for more than 40% of the cases (Figure 1.6).⁹⁶ Hypertension results in pressure overload, and it is the major precursor for the development of concentric LVH, and the alterations in the extracellular matrix with increases in fibrosis.^{37, 97, 98} This remodelling inevitably causes diastolic dysfunction. Hypertension also increases the risk of MI *via* acceleration of atherosclerosis, leading to systolic dysfunction.^{99, 100}

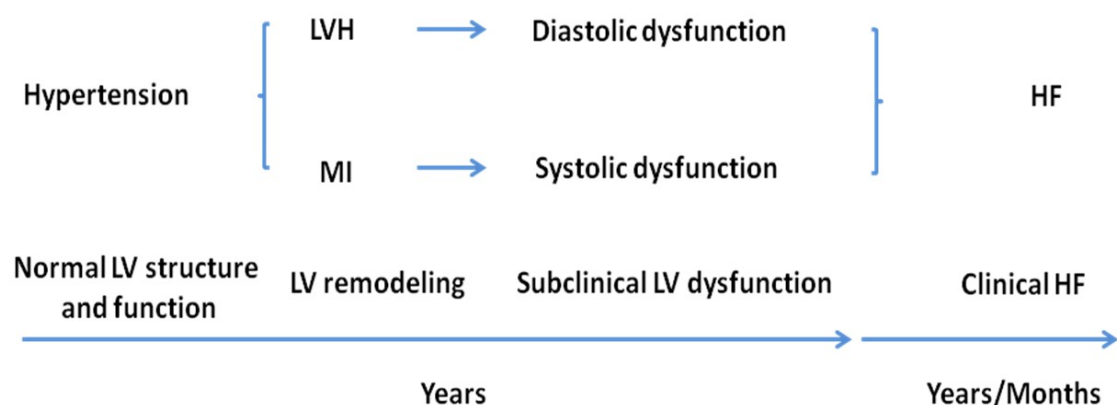


Figure 1.6 Progression from hypertension to heart failure (HF). Used with permissions from Klapholz M.¹⁰¹

1.4.1.6 Anemia

Anemia, as a result of erythropoietin (EPO) insufficiency, is frequently associated with CHF and CKD.¹⁰²⁻¹⁰⁵ Anemia, CHF and CKD interact in a vicious circle to cause or worsen each other.^{104, 106} The prolonged renal hypoxia caused by both anemia and CHF can lead to chronic renal ischemia, and eventual nephron loss and renal fibrosis.¹⁰⁷ Anemia, as a contributory factor to volume overload, also leads to LV dilatation with LVH in patients with renal insufficiency.^{39, 108}

Erythrocytes contains many anti-oxidants, thus anemia may cause increases in oxidative stress.^{106, 109} The lack of oxygen supply to the heart associated with anemia, is compensated for by increasing heart rate and stroke volume, and this may activate the SNS and RAAS, causing renal vasoconstriction and fluid retention.^{106, 110}

Exogenous EPO treatment elevates haemoglobin and has anti-apoptotic, anti-oxidative and anti-inflammatory effects with improved cardiac and renal function in patients with CHF, CKD and anemia.^{14, 111} However, higher haemoglobin concentrations when treating CKD-induced anemia patients may be associated with increased risk of stroke, hypertension, vascular thrombosis, cardiovascular events, progression to ESRD and death.¹¹²

1.4.1.7 Calcium and phosphate abnormalities

The kidney, bone, and parathyroid gland act in concert in regulation of calcium and phosphorus homeostasis; however progression of CKD appears to be a far more common cause of abnormal calcium-phosphate metabolism.¹¹³ Elevated serum

phosphorus is a predictable accompaniment seen in ESRD patients. The consequence of hyperphosphatemia leads to the development of secondary hyperparathyroidism and a predisposition to metastatic calcification when the product of serum calcium and phosphorus ($\text{Ca} \times \text{PO}_4$) is elevated.¹¹⁴ Both of these conditions may contribute to the substantial morbidity and mortality seen in patients with ESRD.¹¹⁴

High phosphate levels are also linked to coronary calcification in hemodialysis patients.¹¹⁵ The presence of coronary calcification is strongly predictive of ischemic heart disease despite absence of significant luminal obstruction.^{116, 117} The progressive loss of renal function leads to several changes that occur in bone and mineral metabolism, resulting in increased parathyroid hormone.¹¹⁸ Parathyroid hormone seems to damage cardiac myocytes and promote cardiac fibrosis.^{119, 120} High levels of calcium, phosphorus and parathyroid hormone have been suggested to be associated with overall mortality attributed to CVD in hemodialysis patients.^{114, 121, 122}

1.4.1.8 Uremic toxins

In the setting of CKD, there is systemic accumulation of uremic toxins, many of which can be eliminated by conventional dialysis treatment.¹²³ However, removal of some toxins, including indoxyl sulfate (IS), *m/p*-cresol, *m/p*-cresylsulfate and phenyl acetic acid, is limited due to their high protein-binding capacity.^{124, 125} Amongst these non-dialysable uremic toxins, IS has strong dose-dependent pro-fibrotic and pro-hypertrophic effects in cultured neonatal rat cardiac fibroblasts and myocytes, whereas other protein-bound uremic toxins have little or no effect (Table 1.5).^{124, 126} These findings suggest a new potential link between the kidney and the heart, that being non-dialysable uremic toxins contributing to LV remodelling.¹²⁶

Table 1.5 Direct cardiac effects of non-dialysable uremic toxins.

Non-dialysable uremic toxins	Cardiac effects
Indoxyl sulfate	Increase cardiac fibroblast collagen synthesis and cardiac myocyte hypertrophy <i>in vitro</i> ¹²⁶ Correlate with cardiac fibrosis <i>in vivo</i> ¹²⁷ Increase cardiac oxidative stress <i>in vivo</i> ¹²⁸
p-cresyl sulfate	Increase cardiac fibroblast collagen synthesis and cardiac myocyte hypertrophy <i>in vitro</i> ¹²⁶
p-cresol *	Induce disassembly of gap junctions of cardiomyocytes <i>in vitro</i> ¹²⁹ Increase cardiac myocyte hypertrophy <i>in vitro</i> ¹²⁴
Phenylacetic acid	Increase cardiac myocyte hypertrophy <i>in vitro</i> ¹²⁶
Phenol	Suppress contractility of cardiac muscle <i>in vitro</i> ¹³⁰

* Mainly present as p-cresyl sulfate. Used with permissions from Lekawanvijit S, *et al.*¹²⁴

IS is synthesized in the liver from dietary tryptophan, and is excreted into urine through renal tubules (Figure 1.7).¹³¹ Serum IS transports across the basolateral membrane of renal proximal and distal tubular cells *via* organic anion transporters 1 and 3 (OAT1/3).¹³² Administration of IS to uremic rats results in IS being detected in the proximal and distal tubules where OAT1/3 have been localized.¹³³

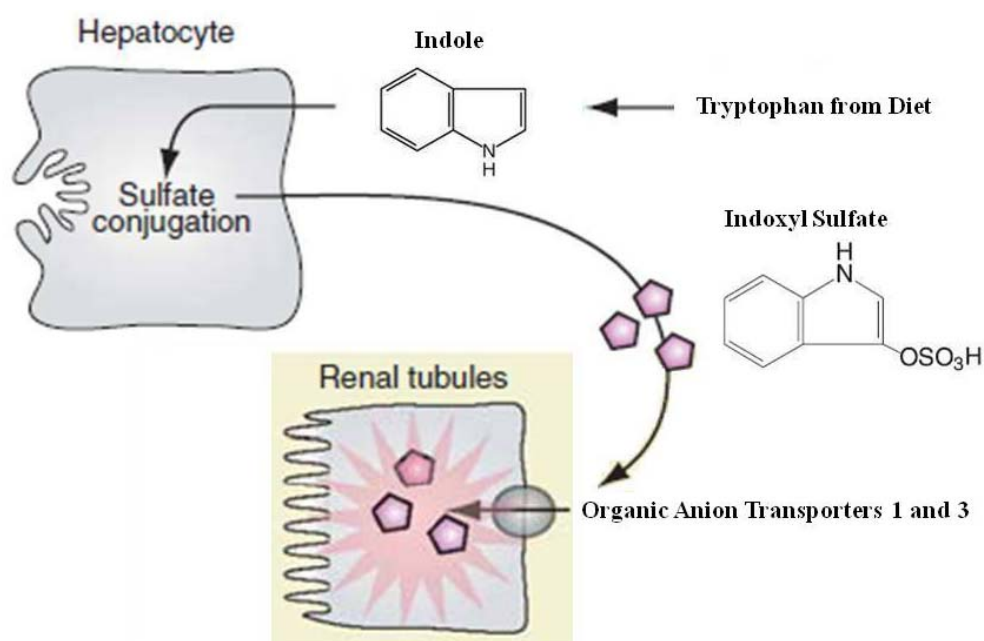


Figure 1.7 Nephrotoxicity induced by indoxyl sulfate is mediated by organic anion transporters 1 and 3. Tryptophan from diet is converted into indole by tryptophanase from the gut micro flora, and the indole is absorbed across the gastrointestinal tract before being metabolized to indoxyl sulfate by hepatic sulfation.¹²⁴ Adopted from Enomoto A, *et al.*¹³¹

Accumulation of IS in serum is due to the reduced renal clearance.¹³² In the progression of CKD, a loss of functioning intact nephrons results in an increase in serum IS levels and an overload of IS in the remnant nephrons, especially in tubular epithelial cells.^{131, 134-136} The total IS concentration is as high as 500 μM in CKD patients compared to less than 2.4 μM in healthy cohorts.^{134, 137-139} The free IS is estimated to be 10% of the total IS in CKD patients; however, it is not detectable in normal population.¹⁴⁰

Accumulated IS in the renal tubular cells induces nephrotoxicity and accelerates progressive CKD mainly due to its pro-fibrotic and oxidative effects. Oral administration of IS in rats with CKD induces further renal tubular injury, renal

interstitial fibrosis, glomerular sclerosis, and impaired renal superoxide scavenging activity, leading to enhanced renal dysfunction.^{134, 141-143} These adverse effects are partially mediated *via* activation of NFκB (p53) pathway through ROS.¹³²

IS exerts its direct cardiac effects *via* p38, p44/42 MAPK and NFκB pathways,¹²⁶ yet there is a lack of mechanistic studies that have examined the activation of other signalling cascades that are involved in IS-induced cardiac effects. Furthermore, it is unknown whether the OAT1/3 contribute to the uptake of IS in the cardiac cells.

In animals with CKD, IS serum level is associated of and positively correlates with cardiac fibrosis,¹²⁷ suggesting IS is at least partly responsible for the development of cardiac fibrosis in the CKD setting.¹²⁴

IS also demonstrates pro-inflammatory effects as determined by significant increases in IL-1β, IL-6, and TNF-α mRNA in cultured human leukaemia monocytic cells (THP-1).¹²⁶

1.4.2 Consequences when heart/kidney is the primary insult

1.4.2.1 Cardiac changes

Individuals with prevalent CVD but without overt symptomatic HF include those whose hearts are undergoing progressive maladaptive LV remodelling, which ultimately leads to HF.¹⁴⁴ LV remodelling refers to changes in the geometry and structure of the LV in response to the injury to the myocardium.¹⁴⁵ Although such changes in chamber size and structure offset increased load, attenuate progressive dilation and stabilize the contractile function, remodelling leads to a worse prognostic

outcome *via* either sudden death or progressive cardiac dysfunction over the long term.¹⁴⁶

Adverse changes in cellular pathophysiology occur early post-infarction. Infarct expansion occurs within hours of myocyte injury, and results in myocyte hypertrophy, wall thinning and ventricular dilatation, accompanied by accelerated apoptosis or necrosis.^{83, 145, 147} Myocyte hypertrophy leads to LVH, which is an adaptive response during LV remodelling.⁸³ Cardiac fibroblasts undergo phenotypic transformation to myofibroblasts, which have increased capacity for collagen synthesis.^{148, 149} Collagen deposition in the heart increases both at the site of infarct to prevent further ventricular deformation, and in remote regions including the peri-infarct region and the inter-ventricular septum.^{150, 151} Fibroblast activation and collagen synthesis are regulated by signals of local and systemic origin, including Ang II, endothelin-1 and transforming growth factor- β_1 (TGF- β_1).¹⁵² Increased cardiac fibrosis results in exaggerated mechanical stiffness and contributes to diastolic dysfunction.¹⁴⁵ Progressive increases in fibrosis may also cause systolic dysfunction and LVH as well as electrical instability leading to fatal arrhythmias.^{119, 145, 153, 154}

Cardiac abnormalities in dialysis patients are mainly due to ischemic heart disease and/or uremic cardiomyopathy.¹⁵⁵ Ischemia causes myocyte death, leading to LV remodelling and the loss of contractility.¹⁵⁵ Cardiomyopathy results from pressure and volume overload, and causes eccentric hypertrophy and LV dilatation.¹⁵⁶ These events are well-established antecedents of clinical HF.¹⁴⁴ Furthermore, uremic cardiomyopathy can exacerbate the perfusion abnormalities. Cardiomyopathy almost invariably involves not only myocyte hypertrophy, cardiac fibrosis but also a decrease

in myocardial capillary density,^{37, 119, 157} such microvascular changes increase the risk of ischemic heart disease.

1.4.2.2 Renal changes

In the cases of HF, the excessive Ang II has hemodynamic/cellular effects that influence renal handling of sodium and water.¹⁵⁸ These include systemic vasoconstriction with efferent arteriolar vasoconstriction and mesangial cell contraction, contributory to a gradual loss of nephron function.⁴⁹ Compensatory response to the loss of sufficient nephrons leads to glomerular injury and secondary glomerulosclerosis.¹⁵⁹

Renal injury or stimuli also leads to an increase in Ang II, and subsequently causes an elevation in TGF- β_1 gene expression in tubular cells.¹⁶⁰ TGF- β plays a key role in the pathogenesis of fibrosis, not only by stimulating cells already committed to the task of matrix production but also by activating epithelial and endothelial cells to behave similarly. Thus over-expression of TGF- β_1 eventually leads to the progression of renal failure associated with connective tissue formation.¹⁶¹⁻¹⁶⁴

During the development of CKD, accumulated type IV collagen in the tubulointerstitium is cross-linked and resistant to degradation, which invariably results in fibrogenesis and loss of function when normal tissues are replaced with scar tissue.^{165, 166} Interestingly, despite the glomerulus as often being the primary site of injury in renal disease, it is the extent of tubulointerstitial rather than glomerular injury which correlates most closely with, and predicts the ultimate loss of renal function in patients with primary glomerular disease.¹⁶⁷

1.5 Diagnosis of CRS

Imaging of the heart and the kidney can provide valuable information in the diagnosis of CRS. Detection of laboratory biomarkers has an additional role as it may enhance and extend our ability to quantify the damage and function of both organs. Early diagnosis and a clear definition of the progression of organ damage using well-established imaging techniques and/or novel biomarkers may be critical for timely therapeutic intervention.

1.5.1 Imaging

Echocardiography (Echo) is the main clinical tool used to non-invasively assess cardiac function of patients. The Echo-Doppler imaging as well as the performance of all the standard measurements (e.g. chamber volumes, LV mass) obtained with the various ultrasound modalities [M-mode, two-dimensional (2D), and Doppler] are of considerable diagnostic value in patients suspicious of having cardiac dysfunction.^{168, 169} LV diameters (at end-diastole and end-systole) and wall thickness (at end-diastole) can be obtained from correctly aligned M-mode or direct 2D echo.^{170, 171} The calculation of LV volumes is used for the determination of LV chamber size.¹⁶⁹ Echocardiograms are also valuable in assessing regional wall motion abnormalities (tissue Doppler), condition and function of heart valves (Doppler), and hemodynamics.¹⁶⁸ The presence of coronary artery disease can be excluded by stress echocardiogram or stress myocardial perfusion [single-photon emission computed tomography (SPECT)/ positron emission tomography (PET)] in types 3, 4, and 5 CRS and in types 1 and 2 CRS when the primary cardiac disease is valvular, congenital, or myopathic.⁴ Protocols have been developed using magnetic resonance imaging (MRI)

to assess ischemia and myocardial viability, and to diagnose infiltrative disorders.¹⁷² However, MRI is not widely available.

Renal ultrasonography is used in the workup of kidney disease, and in differentiating between AKI and CKD and ruling out obstruction as a cause of worsening renal function.¹⁶⁸ Such data can be correlated with renal biomarkers and complemented with techniques designed to quantify and control renal blood flow, ultimately preserving kidney function.⁴ This is because increased central venous pressure seems to be associated with impaired renal function and all-cause mortality in a broad spectrum of CVD patients.¹⁷³

Future studies will be able to utilize molecular imaging techniques [MRI, magnetic resonance spectroscopy (MRS), PET, etc.] for *in vivo* specific markers for diagnosis and severity evaluation of the different types of CRS.⁴

1.5.2 Biomarkers

Although biomarkers are usually considered individually, combination of multiple biomarkers may improve prediction of death from cardiovascular causes.¹⁷⁴ In type 1 and 3 CRS, the early diagnosis of AKI remains a challenge.^{3,5} In both cases, creatinine increases when AKI has already been established and very little can be done to prevent it or to protect the kidney.³ On this background, a recent evolution is the discovery of AKI biomarkers. With the quantification of gene expression and proteomics as screening techniques, ventricular and renal injury can be discovered within the first few hours.^{61, 175, 176} Several biomarkers have been recently highlighted as potential diagnostic tools in patients affected by suspected CRS.

1.5.2.1 Natriuretic peptides

Natriuretic peptides, particularly B-type natriuretic peptide (BNP) and its amino-terminal co-metabolite, N-terminal pro-BNP (NT-proBNP), are diagnostic tools in ADHF and represent independent predictors of cardiovascular events.^{4, 177} Patients with a BNP level less than 130 pg/ml had a 1% risk of sudden cardiac death versus 19% risk at higher BNP concentration.¹⁷⁸ BNP secreted from the ventricles, causes natriuresis and vasodilation after cardiac injury. A cutoff level of 100 pg/ml yields 90% sensitivity and 76% specificity for separating cardiac from non-cardiac aetiologies of dyspnea.¹⁷⁸ Natriuretic peptides have also shown prognostic utility in patients with various stages of renal insufficiency.⁴ Patients with CKD have higher levels of BNP and NT-proBNP, even in the absence of clinical CHF.⁴ However, the BNP and NT-proBNP levels vary substantially over the day and are not related to the progression of underlying disease.¹⁷⁹

1.5.2.2 Cardiotrophin-1

Cardiotrophin-1 is a member of the IL-6 family of cytokines, and it activates various signalling pathways leading to cardiomyocyte hypertrophy and myocardial fibrosis.^{180, 181} Addition to its potential mechanistic contribution to the development of hypertensive heart disease, its plasma level is elevated in relation to the severity of LVH and LV systolic dysfunction in patients with hypertrophic cardiomyopathy.^{180, 182-184} Cardiotrophin-1 can be considered as a potential therapeutic target to prevent and treat hypertensive heart disease beyond blood pressure control.¹⁸¹ Furthermore, combined use of cardiotrophin-1 and BNP may be more accurate at predicting mortality in patients with CHF than either alone.¹⁸⁵

1.5.2.3 Suppression of tumorigenicity 2

Serum suppression of tumorigenicity 2 (ST2), an IL-1 receptor family member, increases early in patients with acute MI and reaches maximum at 12-hour.^{186, 187} This finding suggests that ST2 participates in the cardiovascular response to injury, and thus serum ST2 may be a useful cardiac biomarker.¹⁸⁷ In addition, an increase in ST2 in patients with HF is strong predictive of a poor prognosis.¹⁸⁸ ST2 levels at 12-hour post-infarct are independently associated with death at 30-day.¹⁸⁶

No study has published on the potential role of ST2 in guiding therapy or as a direct target for therapy so far.¹⁸⁸

1.5.2.4 Galectin-3

Galectin-3, a member of the galectin family, is a useful marker to evaluate patients with suspected or proven CHF and acute HF.^{189, 190} Galectin-3 plays an important role in the ventricular remodelling process.¹⁷⁹ It has stimulatory effects on macrophage migration, fibroblast proliferation and fibrosis synthesis.¹⁷⁹ Galectin-3 expression reaches maximum at peak fibrosis and is absent after recovery, thus it can be considered as a novel biomarker to predict the development and progression of HF.¹⁷⁹ The use of galectin-3 complementary to NT-proBNP has been suggested to the best predictor for prognosis in patients with acute HF.¹⁹¹⁻¹⁹³

Serum galectin-3 level is also associated with renal dysfunction and is an independent predictor of poor outcome in patients with ESRD.¹⁹⁴

1.5.2.5 Creatinine and cystatin C

Traditionally, GFR has been estimated by measurement of serum creatinine and 24-hour urine collection for creatinine clearance. In clinical practice, it generally relies on serum creatinine alone due to the difficulty in urine collection.¹⁹⁵ Some factors limit the accuracy of serum creatinine including influence of muscle mass, dietary intake and age.¹⁹⁶ Despite limitations, serum creatinine remains the most commonly used standard for assessment of renal function.¹⁹⁷⁻¹⁹⁹

Recently serum cystatin C, an endogenous biochemical marker of glomerular filtration,²⁰⁰ has been suggested as a better predictor of glomerular function than serum creatinine because it is not affected by age, gender, race, or muscle mass.¹⁹⁶ Moreover, urinary cystatin C predicts the requirement for renal replacement therapy earlier than serum creatinine in the case of AKI.⁴

1.5.2.6 Neutrophil gelatinase-associated lipocalin

Neutrophil gelatinase-associated lipocalin (NGAL) in plasma and urine appears to be early biomarker detected in patients with AKI.^{201, 202} Urinary NGAL is able to distinguish those with AKI from normal function, prerenal azotemia and CKD, with 90% sensitivity and 99% specificity.²⁰³ The increase in serum NGAL occurs 24-48 hours earlier than the rise of serum creatinine.²⁰⁴ Acute HF leading to worsening renal function has been classified as type 1 CRS. NGAL could be used as an earlier marker of impending renal dysfunction during the acute episode of HF.²⁰⁴ Thus the early identification of patients with type 1 CRS may represent an opportunity to preserve kidney function.²⁰⁴

1.5.2.7 Kidney injury molecule-1

Kidney injury molecule-1 (KIM-1) is a novel urinary biomarker, and it is initially identified and evaluated in patients with AKI. It is detectable in the urine after ischemic or nephrotoxic insults to proximal tubular cells, and is earlier and more sensitive indicator of AKI than serum creatinine.²⁰⁵⁻²⁰⁸ Both clinical and laboratory evidences show the elevation of KIM-1 and NGAL in urinary concentrations and tissue levels in the setting of CHF.^{209, 210} These findings suggest an important role for tubular injury and tubular biomarkers in cardiorenal interaction in the setting of CHF.²⁰⁷

1.5.2.8 Interleukin-18

Interleukin-18 (IL-18) is a pro-inflammatory cytokine that is detected in the urine after acute ischemic proximal tubular damage.^{4, 211} It increases 48-hour prior to the increase in serum creatinine for ischemic AKI.⁴ Such biomarker is useful to describe kidney injury before increases in serum creatinine become manifest in patients who subsequently develop AKI. However in a prospective observational cohort study, the findings show negative in identification of AKI using early measurement of urinary IL-18 following cardiac surgery.²¹²

1.5.2.9 *N*-acetyl- β -(D)-glucosaminidase

N-acetyl- β -(D)-glucosaminidase is a lysosomal brush border enzyme of proximal tubular cells, and it acts as a kidney injury biomarker, reflecting particularly the degree of tubular damage.^{4, 213} The urinary *N*-acetyl- β -(D)-glucosaminidase increases not only in acute renal failure,²¹⁴ but also in patients with HF.²¹⁵

1.6 Preclinical models

A variety of experimental models with cardiac and/or renal impairment has been developed, with rat models predominating.²¹⁶ MI, a severe manifestation of coronary artery disease, is the most potent risk factor for HF.²¹⁷ Left anterior descending coronary artery ligation is commonly used to induce myocardial injury.²¹⁶ To induce renal injury, 5/6 subtotal nephrectomy (STNx) alters intraglomerular hemodynamics and ultimately causes progressive renal failure.^{167, 218}

These well-established models may not necessarily mirror the clinical settings. However, they recapitulate features of the phenotype of cardiac and/or renal impairment which occur clinically. Several examples have illustrated that these models are critical to the development of new therapies in the management of heart failure and renal failure.

1.6.1 MI model

1.6.1.1 Cardiac effects

In animals with infarction, maximum cardiac output and pressure generating capacity are impaired in proportion to infarct size.²¹⁹ Post-infarction, animals develop cardiac dysfunction indicated by reduced LVEF.²¹⁰ Animals also have increased LV and lung weights, myocardial hypertrophy and infarcted wall thinning with interstitial tissue scarring.²²⁰⁻²²² Immunohistochemical analysis demonstrates increased immunostaining for collagen I and III, TGF- β , phospho-Smad2, α -smooth muscle actin and macrophages in the LV region remote to the infarct, known as the non-infarct zone.²²⁰ Tissue expression of angiotensin converting enzyme (ACE) co-localizes with that of ACE2 in the heart of MI animals.²²³ The ACE2 has been suggested to play a

cardioprotective role.²²⁴ Increased ACE2 mRNA expression is observed in the injured myocardial tissue (infarct and border zone) early after MI, with further increases occurring in the viable myocardium by 28 days.²²³

This MI model has been used to assess whether the adverse process following HF could be altered favourably by administration of the potential pharmacological therapies. For example, ACE inhibitors (ACEi) and/or Ang II receptor blockers (ARB) have been proved to reduce LV chamber dilation, improve LV function and structure, and increase survival in animals with moderate or large MI.²²⁵⁻²²⁷ These findings lead to clinical trials to explore their utility in post-MI patients with reduced LV function.²²⁸⁻²³⁰

1.6.1.2 Renal effects

Renal changes have been recently investigated in the MI model.²¹⁰ GFR reduces in MI animals at 1 and 4 weeks post-MI, and returns back to sham levels at 8 and 12 weeks, before returning to borderline reduction at 16 weeks.²¹⁰ These changes are accompanied by progressive increases in renal cortical interstitial fibrosis and immunoreactive KIM-1 expression.²¹⁰

1.6.2 STNx model

1.6.2.1 Cardiac effects

STNx animals develop LV diastolic dysfunction indicated by increases in peak velocity of atrial filling (A and A' waves) and decreases in E/A and E'/A' ratios obtained by echocardiography early after injury.¹²⁷ Diastolic dysfunction is also shown by significant increase in the time constant for isovolumic relaxation (tau logistic).^{127, 231}

STNx causes significant increases in heart weight, myocyte cross-sectional area and LV interstitial fibrosis.^{127, 232} STNx animals also have increased gene expression of pro-fibrotic [TGF- β and connective tissue growth factor (CTGF)] and hypertrophic [atrial natriuretic peptide (ANP), β -myosin heavy chain (β -MHC) and α -skeletal muscle actin] markers, and elevated protein levels of TGF- β and phosphorylated NF κ B.¹²⁷

Increased cardiac ACE2 activity and its mRNA expression have been observed in STNx animals, and the ACE2 activity is normalized by ACEi.²³³ This cardioprotective effect of ACE2 may be mediated by promoting the production of the anti-remodelling peptide Ang-(1-7) from Ang II.^{234, 235}

1.6.2.2 Renal effects

STNx leads to a compensatory hyperfiltration of the remaining nephrons initially to maintain overall GFR,²³⁶ however, STNx animals invariably develop hypertension, proteinuria, reduced creatinine clearance and a loss of GFR over time.^{127, 237-239} Following STNx, animals have increased water intake and urine excretion.²³¹

Kidney injury also leads to activation of Smad2 pathway and increased TGF- β protein levels in addition to deposition of excessive quantities of extracellular matrix in both the glomerulus and tubulointerstitium.^{237, 238, 240} These pathological changes, recognised as glomerulosclerosis and tubulointerstitial fibrosis, encroach on surrounding structures ultimately causing capillary rarefaction with consequent hypoxia, tubular atrophy and inflammatory cell infiltration.²⁴¹ Consistent with increased TGF- β protein levels, TGF- β_1 gene expression increases throughout the sclerotic glomeruli and areas of tubulointerstitial injury.²⁴²

The amelioration of glomerular and tubulointerstitial injury with treatment by ACEi and ARB supports the notion of a pathogenetic link between the renin-angiotensin system (RAS) and progressive renal injury.²⁴² In the form of primary glomerular injury, there is also activation of RAS within the tubular epithelium.¹⁶⁷ This finding reveals that local and intrarenal RAS system is activated within renal tubules in the setting of STNx and suggests that this tubular RAS may be involved in the progression of tubulointerstitial injury that accompanies the glomerular injury.¹⁶⁷

Secreted protein acidic and rich in cysteine (SPARC) is an extracellular matrix that modulates cell adhesion, proliferation, matrix deposition, and tissue remodelling.^{243,}²⁴⁴ After STNx, SPARC protein levels are increased along with concordant changes in SPARC mRNA expression in glomerular and interstitial cells, and *de novo* expression by tubular epithelial cells at sites of renal injury.²⁴⁵ The SPARC over-expression is suppressed by ACEi and/or ARB.²⁴⁵

The above studies clearly indicate that impairment of one organ has detrimental effects on the other, with changes at functional, structural and molecular levels. To accelerate the progression of dysfunction in both organs, several attempts have been made at combining the two models as described below.

1.6.3 Combination of MI and STNx models

There is a lack of investigation on the pathophysiological mechanisms for concomitant cardiac failure and renal failure. So far no study has specifically examined the heart-kidney interactions where MI-induced CHF is complicated by the addition of CKD. A

new animal model recapitulating the features of this condition will be established and investigated in Chapter 3 and 4 of this thesis.

Animal model of mild CKD [induced by unilateral nephrectomy (UNX)] followed by MI does not induce further cardiac dysfunction compared with the model of MI alone.²⁴⁶ The UNX co-morbid with MI induces progressive renal injury in comparison with UNX alone.^{246, 247} The deterioration is independent of blood pressure and probably through the activation of renal angiotensin type 1 receptor.²⁴⁶ However, this model does not fully recapitulate the phenomenon of primary renal failure as renal function is preserved in animals receiving UNX.²⁴⁶⁻²⁴⁹ It suggests that it takes longer for renal impairment to evolve post-UNX.

In a recently described model of combined STNx and MI (STNx+MI), animals with STNx+MI develop more severe cardiac dilatation compared with animals with MI alone.²⁵⁰ Animals with STNx+MI also demonstrate reduced LVEF, increased LV end diastolic pressure and prolonged tau logistic compared with animals with STNx or MI alone.²⁵⁰ However, there is no difference in cardiac fibrosis comparing animals with MI only and STNx+MI to sham-operated animals. In fact there is also a decrease in cardiac fibrosis in animals receiving STNx only compared to sham-operated animals. These findings are not consistent with previous studies examining cardiac fibrosis in MI or STNx only models.^{127, 251, 252}

The subsequent MI does not cause further reduction in GFR in STNx animals.^{250, 253} There are differences in results examining the further structural damage in STNx animals.^{250, 253} A study demonstrates more severe focal glomerulosclerosis in

STNx+MI compared to STNx only.²⁵⁰ In contrast, another study indicates no significant changes in glomerulosclerosis between the two groups.²⁵³ Moreover, the underlying mechanisms including activation and signalling of the potential pathways have not been understood.

Despite the above investigation in the model of STNx+MI, many aspects in this field remain controversial. Further exploration on the pathophysiological processes may lead to discovery of potential therapies in attenuating both cardiac and renal injury in CRS. More detailed pathophysiological mechanisms will be examined in Chapter 5 and 6 of this thesis.

1.7 Management of CRS

Although there are clinical guidelines for managing HF and renal failure, there are no agreed guidelines for managing patients with CRS (Table 1.6).⁴ In the management of CRS, it is important to control volume status and blood pressure, restrict sodium intake (and water if patient is hyponatremic), check for intrinsic renal pathology and avoid nephrotoxic agents.

In the setting of HF, successful therapies have focused on diuretics and key neurohormonal systems activated as part of the pathophysiology of this disease process.²⁵⁴ However, many of the interventions used to control HF can worsen renal function, and *vice versa*. For example, ACEi and ARB may cause increases in serum creatinine when treatment is initiated. Most patients with HF can tolerate mild to moderate degrees of renal insufficiency.⁵² In these patients, changes in serum urea and serum creatinine can usually be managed without the withdrawal of drugs for the

management of HF.⁵² However, if the serum creatinine increases up to 265 $\mu\text{mol/L}$, the presence of renal impairment can severely limit the efficacy and enhance the toxicity of established treatments.^{52, 255-257} If the serum creatinine increases up to 442.5 $\mu\text{mol/L}$, hemofiltration or dialysis are recommended to relieve symptoms of renal failure and allow the patient to respond to and tolerate the drugs routinely used to treat HF.^{52, 258, 259} In patients unable to tolerate these agents, combination of hydralazine and nitrates may be an option.²⁶⁰

Table 1.6 Management strategies for each subtype of cardiorenal syndrome.

Acute cardio-renal syndrome (type 1)	<p>Specific - depends on precipitating factors.</p> <p>General supportive - oxygenate, relieve pain & pulmonary congestion, treat arrhythmias appropriately, differentiate left from right heart failure, treat low cardiac output or congestion according to ESC guidelines.</p> <p>Avoid nephrotoxins, closely monitor kidney function.</p>
Chronic cardio-renal syndrome (type 2)	<p>Treat CHF according to ESC guidelines, excluding precipitating pre-renal AKI factors (hypovolaemia and/or hypotension).</p> <p>Avoid nephrotoxins, while monitoring renal function and electrolytes.</p> <p>Extracorporeal ultrafiltration</p>
Acute reno-cardiac syndrome (type 3)	<p>Follow ESC guidelines depending on underlying aetiology, may need to exclude renovascular disease and consider early renal support, if diuretic resistant.</p>
Chronic reno-cardiac syndrome (type 4)	<p>Follow KDOQI guidelines for CKD management, excluding precipitating causes (cardiac tamponade).</p> <p>Treat HF according to ESC guidelines, consider early renal replacement support.</p>
Secondary cardiorenal syndromes (type 5)	<p>Specific - according to etiology.</p> <p>General - as advised by ESC guidelines.</p>

ESC guidelines, European Society of Cardiology guidelines 2008;²⁶⁰ KDOQI, Kidney Disease Outcomes Quality Initiative. Used with permissions from Ronco C, *et al.*⁴

1.7.1 Diuretics and ultrafiltration

Diuretics remove fluid in volume-overloaded patients and maintain normal body fluid volume afterwards.²⁶¹ Thus diuretic therapy provides symptom relief, and has been a mainstay of ADHF management. Diuretics are always combined with an ACEi to maintain euvolaemia in patients with systolic LV dysfunction.¹⁷² However, diuretics improve symptoms in CHF but have no effect on mortality.¹⁷² Furthermore diuretic therapy in CHF may cause electrolyte abnormalities and develop pre-renal azotemia and worsening renal function.

Thiazide diuretics inhibit sodium reabsorption in the distal tubules and cause increased sodium excretion. These tend to be less effective in patients with advanced renal failure. Thus loop diuretics are preferred over thiazide diuretics in patients with creatinine clearance less than 30 ml/min/1.73m² (Figure 1.8).^{262, 263} However, loop diuretics predispose to electrolyte imbalances and hypovolaemia leading to neurohormonal activation, reduction of renal glomerular flow, and further rises in serum urea and creatinine. Thus an optimal dose is needed to be titrated for the highest efficacy with the least neurohormonal activation.²⁶⁴⁻²⁶⁶

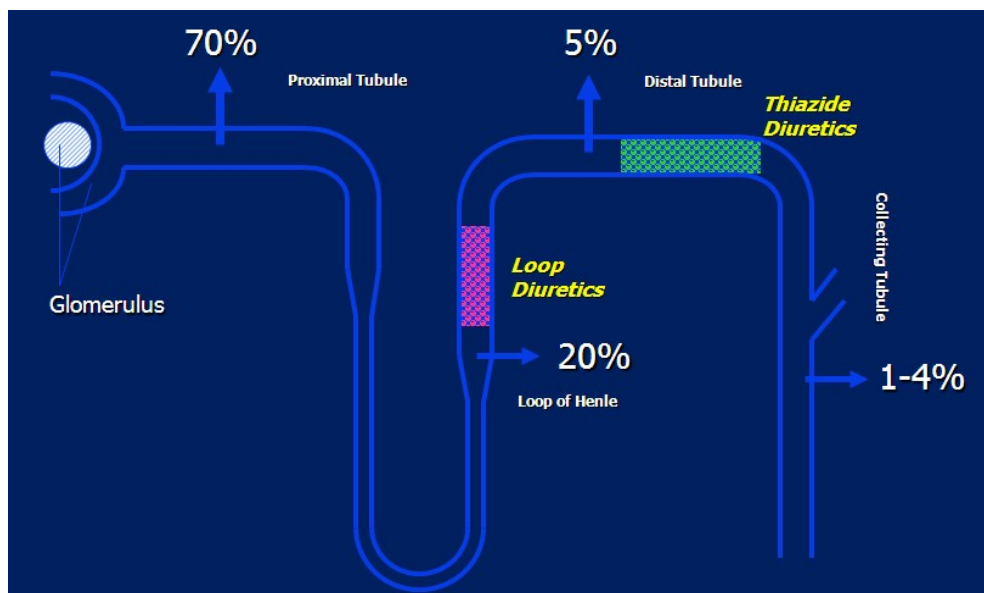


Figure 1.8 Thiazide and loop diuretics acting at distal tubule and loop of Henle respectively. The loop diuretics excrete 20% of the filtered load of sodium, thus enhancing water clearance. In contrast, the thiazide diuretics excrete only 4% of the filtered load, and tend to lose their effectiveness in patients with impaired renal function. Used with permissions from Krum H.²⁶⁷

Many patients with CRS become resistant to conventional diuretic treatment, indicated by persistent pulmonary congestion and the need for higher doses. In this ‘diuretic resistant’ setting, higher doses of diuretics are needed to achieve effective concentration in renal tubules.²⁶⁸ However renal blood flow may be more potently reduced than congestive HF symptoms improved. A recent clinical study reports that there is no difference in 60-day clinical outcomes when diuretic therapy has been administered among patients with ADHF at a high dose as compared with a low dose.²⁶⁹ Higher loop diuretic dosages for patients with advanced HF have been suggested to be associated with high risk of mortality.²⁷⁰

Extracorporeal ultrafiltration can be used in ADHF patients if diuretic resistance does develop.²⁶⁶ Early ultrafiltration safely results in greater weight and fluid loss than loop diuretics in ADHF patients, and it significantly reduces the re-hospitalisations for HF.²⁷¹ Furthermore the large molecules retained in uremia may be further cleared by adding ultrafiltration to dialysis process.¹²³ However, ultrafiltration is suggested to be inferior to a strategy of stepped pharmacologic therapy for the preservation of renal function at 96 hours, with a similar amount of weight loss with the two approaches in patients with HF and worsening renal function.²⁷² Ultrafiltration is associated with a higher rate of adverse events compared with pharmacologic therapy.²⁷²

1.7.2 Angiotensin converting enzyme inhibitors

ACEi are first-line treatment for patients with LV dysfunction, and those without known ventricular dysfunction.^{228, 273} ACEi reduce blood pressure and cardiac afterload, and exert direct beneficial effects on cardiovascular function and homeostasis.²⁷⁴ ACEi may be used in combination with ARB.

ACEi also prevent progressive renal dysfunction in diabetic nephropathy and other forms of CKD.²⁷⁵ Unfortunately, in the presence of underlying renal disease, use of ACEi may be associated with elevation in serum creatinine, thereby creating a therapeutic dilemma.²⁷⁵ Patients with renal artery stenosis and CKD are at a high risk of developing renal dysfunction in response to introducing ACEi therapies. Treatments with ACEi also cause potassium retention; thus CKD patients are advised to restrict dietary sodium and potassium.²⁷⁶

1.7.3 Angiotensin II receptor blockers

ARB are considered as an alternative for patients who are not tolerant to ACEi due to kinin-mediated adverse effects, such as a cough and angioedema,^{277, 278} and they are also recommended for systolic CHF patients who remain symptomatic despite receiving ACEi.²⁷⁹ ARB act differently to ACEi, and their effects include inhibiting the Ang II induced vasoconstriction, sodium reabsorption, activation of SNS and stimulation of cardiac fibrosis.²⁸⁰ These inhibitory effects are mediated by preventing Ang II from binding to its type 1 receptor.²⁸¹ Candesartan, an Ang II type 1 receptor antagonist, improves outcomes in patients with preserved LVEF who are intolerant of ACEi in CHARM Preserved trial.²⁸² However, ARB are likely to cause hypotension, worsening renal function, and hyperkalemia as ACEi.⁵²

1.7.4 β -adrenergic receptor blockers

β -adrenergic receptor blockers (β -blockers) are commonly prescribed to patients with HF and low LVEF.⁵² β -blockers appear to be effective in reducing the risk of death or hospitalisation in CHF patients,²⁸³ and they are used for the treatment of patients who remain mildly to moderately symptomatic despite appropriate doses of an ACEi.²⁷⁹

In addition to the blockade of RAAS,⁵⁰ β -blockers principally inhibit the adverse effects of activation of the SNS.²⁸⁴ The adverse effects of sympathetic activation on the myocardium are mediated *via* β -adrenergic receptors and/or α_1 -adrenergic receptors.^{172, 285} β -blockers act by suppressing the action of endogenous catecholamines, released from nerve ending of the SNS, on β -adrenergic receptors.^{286, 287} The magnitude of the prognostic benefits conferred by β -blockers is similar to or even exceeds that of ACEi in patients with systolic CHF.²⁸⁸ In the Cardiac Insufficiency Bisoprolol Study II, a

highly selective β_1 adrenergic receptor antagonist bisoprolol, is found to be effective in patients with HF and concomitant renal dysfunction.^{283, 289}

1.7.5 Mineralocorticoid receptor antagonists

Mineralocorticoid receptor (also known as the aldosterone receptor) antagonists play an important role in the management of CHF.²⁹⁰ Aldosterone receptor blockade with spironolactone, in addition to receiving standard therapies (e.g. ACEi), substantially reduces the risk of morbidity and mortality among patients with severe HF.²⁹⁰ Aldosterone blockade with eplerenone improves mortality in patients with mild LV systolic dysfunction and post-acute MI HF.^{291, 292} These benefits appear to be additive to those of ACEi and β -blockers. However, hyperkalaemia is a major concern in patients with a reduced eGFR receiving mineralocorticoid antagonists for HF.²⁶⁵ Dietary restriction may be required in these patients.⁴

1.7.6 Treatments for uremic toxins

Cardiovascular mortality is significantly higher in dialysis patients compared to age-matched patients receiving kidney transplantation, suggesting a possible role for non-dialysable uremic toxins in the pathogenesis and progression of CVD.¹²⁴ Thus reduction of non-dialysable uremic toxins appears to be a further potentially beneficial therapeutic strategy. Prolonged dialysis time, increasing the treatment frequency and/or using higher permeability membranes may reduce the concentrations of protein-bound uremic toxins.²⁹³⁻²⁹⁶

In addition to enhancing uremic toxin removal, another option is to alleviate the accumulation of uremic toxins using non-pharmacological strategies. AST-120

(Kremezin), an oral charcoal adsorbant, shows a strong adsorptive ability for uremic toxins.²⁹⁷ In uremic patients, AST-120 delays dialysis initiation and the progression to ESRD.^{135, 298}

Concentration of serum IS and intensity of IS staining in the proximal tubules are reduced after the administration of the AST-120 in preclinical CKD models; this is accompanied with amelioration in renal dysfunction and structural damage.^{124, 127, 131, 299} Furthermore, AST-120 reduces LV fibrosis (68%) and decreases protein levels of TGF- β and activation of NF κ B pathway in the heart of CKD animals.¹²⁷

In addition, many uremic toxins that are OAT substrates interact with other substrates such as drugs due to the competition for OAT transport, thus increasing the half-life and extra-renal toxicity of the drugs. Therefore, the effective elimination of circulating uremic toxins *via* AST-120 may decrease the competition for OAT transport, and this may potentially contribute to the attenuation of the progression of renal failure.¹³¹

Apart from the management addressed above, there have been several novel therapeutic strategies that target CRS, such as selective adenosine A₁ receptor blockers, natriuretic peptides, vasopressin antagonists, soluble guanylate cyclase activators, and many others.²⁶⁵ Ongoing clinical trials of these potential pharmacologic agents will examine their safety and efficacy in the prevention and management of the CRS.

1.8 Conclusion

The combined impairment in both heart and the kidney with primary dysfunction in either heart or kidney is increasingly encountered in a large proportion of patients admitted to hospital. To assist further understanding the interrelationship of these disorders and the bidirectional nature of heart-kidney interactions, the CRS has been generally classified into 5 subtypes that reflect the pathophysiology, the time-frame, and the cardiac and renal co-dysfunction.

Despite the growing recognition of the definition, epidemiology and management for each subtype of CRS, it is still associated with high mortality. Lack of significant progress in the prevention and management of CRS may be attributed, in part, to failure to clearly identify the pathophysiology in this condition. Therefore, further understanding of the pathophysiological mechanisms during co-dysfunction of heart and kidney has important clinical implications. Mechanism-targeted therapies may provide benefits in attenuating both cardiac and renal injury in well-defined patient populations. However, there is no preclinical study examining the heart-kidney interactions where CHF is complicated by the addition of CKD. Conversely, there are conflicting results in a recently described animal model recapitulating features of CKD co-morbid with CHF. There are significant knowledge gaps in the literature in need for further investigation, and this provides direction for future basic research.

Furthermore, circulating uremic toxins in patients with CKD may have detrimental effects on cardiac function. Thus, reducing uremic toxin levels and/or amelioration of

adverse cardiac effects induced by uremic toxins may provide therapeutic benefits for patients with CRS.

1.9 Hypotheses and Aims

1.9.1 CRS when cardiac dysfunction is the primary insult

Hypothesis: CHF followed by CKD may cause more severe functional, structural and molecular impairment compared with CHF or CKD only.

The aim of this *in vivo* study was to test the hypothesis using a rat model of MI followed by a kidney injury (induced by STNx), recapitulating CHF with co-morbid CKD. Functional, histological/immunohistological, biochemical and molecular assays will be conducted to assess the pathophysiological changes and potential mechanisms that may underlie the changes.

1.9.2 CRS when renal dysfunction is the primary insult

Hypothesis: CKD followed by CHF may cause further pathophysiological changes compared with CKD or CHF only.

The aim of this *in vivo* study was to test the hypothesis using a rat model of STNx followed by MI, implicating CKD co-morbid with CHF. Similarly to the above *in vivo* study, pathophysiological changes and underlying mechanisms will be investigated to understand the effects of the subsequent MI on the initial renal injury on heart and kidney.

1.9.3 Potential novel treatments for CRS

Hypothesis: Antagonists of uremic toxin uptake *via* OAT1/3 or inhibition of downstream signalling pathway *via* ASK1 may ameliorate adverse cardiac remodelling induced by uremic toxin IS.

The objective of this *in vitro* study was to determine potential approaches to block IS-induced cardiac myocyte hypertrophy and cardiac fibroblast collagen synthesis, which contribute to pathological cardiac remodelling. This study will specifically investigate the potential therapeutic effects of OAT1/3 antagonists and ASK1 inhibitors on the suppression of the pro-hypertrophic and pro-fibrotic actions of IS.

Chapter 2 Materials and Methods

2.1 *In vivo* studies

2.1.1 Animals and ethics approval

Outbred male Sprague Dawley (SD) rats weighing 200-250g were obtained from the Animal Resource Centre (Murdoch, WA, Australia). They were given free access to commercial standard rat chow (Norco Co-Operative Ltd., NSW, Australia) and tap water and housed in stable conditions at 22°C with a 12 h light/dark cycle during the entire study unless mentioned somewhere else.

All experiments adhered to the guidelines of the Animal Welfare and Ethics Committee of the St. Vincent's Hospital and the National Health and Medical Research Council (NHMRC) of Australia. The animal Ethics Committee Approval Number was 027/10.

2.1.2 Myocardial infarction

MI was induced in SD rats by ligation of left anterior descending (LAD) coronary artery.³⁰⁰ Animals were anaesthetized with Alfaxan *via* tail vein injection (1.5 ml/kg, i.v.), intubated and placed on a respirator and maintained anesthetized with isoflurane (2%).³⁰¹ A left thoractomy was performed; the LAD coronary artery was identified and permanently ligated 3 mm below its origin with a 6-0 prolene suture. The chest was then closed, and the muscle and skin were closed in layers. Immediately post-surgery, animals were administrated buprenorphine (0.03 mg/kg, s.c.) for post-operative pain. Sham animals were treated identically except that the prolene suture was not tied.

2.1.3 Subtotal nephrectomy

Animals were anesthetized with isoflurane (3%) in a perspex chamber, and maintained of 2% isoflurane administrated *via* a nose cone.²³⁹ Under aseptic conditions, rats underwent STNx performed by right subcapsular nephrectomy and infarction of approximately 2/3 of the left kidney by selectively ligating two of 3-4 extra-renal branches of the left renal artery.^{238, 242, 245} Immediately post-surgery, animals were administrated buprenorphine (0.03 mg/kg, s.c.) for post-operative pain. Sham animals were treated with laparotomy and manipulation of both kidneys before wound closure.

2.1.4 Blood pressure

Systolic blood pressure (BP) was measured in conscious rats using an occlusive tail-cuff plethysmography attached to a pneumatic pulse transducer (PowerLab, ADInstruments, Australia).^{302, 303} The reading was recorded using the software Chart 5 (PowerLab, ADInstruments, Australia). For each animal blood pressure was taken until 5 readings were obtained within a range of 5 mmHg and averaged.

2.1.5 Echocardiography

Echocardiography was performed in lightly anaesthetized animals (ketamine 3.75 mg/100g and xylazine 0.5 mg/100g, i.p.) using a Vivid 7 (GE Vingmed, Horten, Norway) echocardiography machine with a 10 MHz phased array probe.³⁰⁴ Parasternal short-axis views of the heart at the mid-papillary level were used to obtain measures of LV anterior wall thickness in diastole, LV posterior wall thickness in diastole (LVPWd), and left ventricular internal dimension in diastole (LVIDd) and systole (LVIDs). Fractional shortening (FS) and relative wall thickness (RWT) were calculated according to standard formula:

$$FS(\%)=[(LVIDd-LVIDs)/LVIDd]\times 100; RWT=(2\times LVPWd)/LVIDd.$$

Doppler images were obtained from the apical 4-chamber views of the heart. Early and late transmitral peak diastolic flow velocity (E and A waves) and mitral valve inflow E wave deceleration time (DT), isovolumic relaxation time (IVRT) were measured. Diastolic filling was evaluated by determining the E/A ratio from the peak velocity of E and A mitral flow and DT. Tissue Doppler imaging was also performed to assess peak early and late (E' and A') diastolic tissue velocity at the septal side of the mitral annulus. All parameters were assessed using an average of three consecutive cardiac cycles and calculations were made in accordance with the American Society of Echocardiography guidelines.³⁰⁵ All data were acquired and analysed by a single blinded observer with Echo PAC (GE Vingmed, Horten, Norway) using offline processing.

2.1.6 Cardiac catheterization

Cardiac catheterization was performed at the end of the study as previously published.³⁰⁶ Briefly, animals under anaesthesia with pentobarbitone (Nembutal) (6 mg/100g, i.p.) were placed on a warming pad (37 °C) and ventilated. A 2-F_r miniaturized combined catheter-micromanometer (Model SPR-838 Millar instruments, TX, USA) was inserted into the right common carotid artery to obtain aortic blood pressure and then advanced into the LV to obtain LV pressure-volume loops when stable.³⁰⁷ The loops were recorded at steady state and during transient preload reduction, achieved by occlusion of the inferior vena cava and portal vein with the ventilator turned off and the animal apnoeic. Parallel conductance values of the heart muscle were obtained by the injection of approximately 100 µL of 10% NaCl into the right atrium.^{308, 309} Calibration from Relative Volume Units (RVU) conductance signal to

absolute volumes (in μL) was undertaken using a previously validated method of comparison to known volumes in Perspex wells.^{306, 310} The following validated parameters were assessed using Millar conductance data acquisition and analysis software PVAN 3.2: LV end diastolic pressure (LVEDP), the slope of the end systolic pressure-volume relationship (ESPVR), the slope of the end diastolic pressure-volume relationship (EDPVR), the maximal rate of pressure rise (dP/dt_{max}) and fall (dP/dt_{min}), tau logistic, and the slope of the preload recruitable stroke work (PRSW) relationship.

2.1.7 Glomerular filtration rate

GFR was measured by the clearance of a single shot ^{99}Tc -diethylene triamine penta-acetic acid (^{99}Tc -DTPA) (i.v.).^{210, 311} Blood (1 ml) was drawn 43 min after injection,²⁴² and was centrifuged in lithium heparin tubes at 3000 revolutions per minute (rpm) for 15 min to obtain plasma. The supernatant was then collected for GFR and plasma creatinine measures, and 200 μL was aliquot for each analysis.

Plasma radioactivity was measured and compared with a reference prepared at time of injection.³¹² GFR was calculated using the following formula: Clearance (ml/min) = $V \times \ln(P_0/P_t)/t$, where V is the estimated volume of distribution, P_0 is the theoretical plasma space concentration at injection, and P_t is the observed plasma concentration at t minutes after injection.³¹² The GFR was corrected for body weight (BW) recorded before the procedure and reported as GFR/kg.

2.1.8 Metabolic caging

Rats were individually housed in metabolic cages for 24 hr, where they were given free access to tap water and standard laboratory chow.³¹³ Food and water intake, and urine

volume was recorded. An aliquot of urine (1 ml) was collected from the 24-hour urine sample and stored at -20°C for subsequent analysis of urine creatinine and urinary protein.²³⁷ Urine creatinine, plasma creatinine and urinary protein were measured by autoanalyzer (Roche Instruments Inc., CA, USA). Creatinine clearance and 24h proteinuria were calculated using the following formula.¹²⁷

24h Proteinuria (mg/day) = Urinary protein (g/L) x 24h urine volume (ml)

Creatinine clearance (ml/min) = $\frac{\text{Urine creatinine } (\mu\text{mol/day})}{\text{Plasma creatinine } (\mu\text{mol/L})} \times 1000 \times \frac{1}{24 \times 60}$

2.1.9 IS measurements

IS levels were measured by a high performance liquid chromatography (HPLC) method (Shimadzu, Kyoto, Japan).¹⁴² Samples (10 µl) were analysed in the mobile phase, 5% tetrahydrofuran/0.1 M KH₂PO₄ (pH 6.5) at a flow rate of 1 ml/min with fluorescence detection (excitation 295 nm and emission 390 nm).¹⁴²

2.1.10 Tissue collection

At the completion of obtaining pressure-volume loops, blood was withdrawn from the abdominal aorta for determination of conductance measures and analysis of IS. The hearts and lungs were then removed and weighed. The LV was dissected from the atria and right ventricle and weighed. The LV was cross sectioned into 3 portions. The base of the LV was embedded in Tissue-Tek® O.C.T compound. The middle portion was fixed in 10% neutral-buffered formalin (NBF). The apex was separated into infarcted and non-infarcted tissue in MI-induced animals and cut into smaller pieces before being snap-frozen in liquid nitrogen for gene and protein analyses.

The remnant kidney was excised, decapsulated, weighed, and then sliced sagittally with one-half immersion fixed in 10% NBF, and the other half was dissected into smaller pieces of tissue before being snap-frozen in liquid nitrogen for gene and protein analyses.^{239, 314}

2.1.11 Histopathology

Formalin-fixed heart and kidney tissues were placed in histo-cassettes and processed overnight (Department of Pathology, St. Vincent's Hospital, Melbourne, Australia). Tissues were then embedded in paraffin moulds and 4 µm sections were cut using a rotary microtome (Leica Biosystems). Tissue sections were floated in a 42°C water bath and collected on silanated glass microscope slides. Prior to staining, sections were dewaxed in 2 changes (2x) of histolene for 5 min each time and hydrated through graded ethanols: 100% ethanol 2x 3 min, 70% ethanol 1x 3 min.³¹⁴ Sections were then rehydrated in distilled water (dH₂O) for 3x 5 min washes.

2.1.12 Infarct size

LV tissue sections were incubated in picrosirius red (Merck, VIC, Australia) reagent for 1 hr. Slides were then washed briefly in 2 changes of acidified water (1% acetic acid). Sections were dehydrated through graded ethanol (2 x70%, 2x 100%) for 3 min each and histolene (2x 5 min) before being mounted with DPX (BDH laboratory supplies, Poole, UK).³¹⁴

Infarct size was assessed morphologically and slides were digitally scanned using Aperio ScanScope Console v.8.0.0.1058 (Aperio Technologies, Inc) for infarct size analysis. Infarct size was expressed as an averaged percentage of the endocardial and

epicardial scarred circumferences of the LV, ventricular septum was not included.³⁰¹
Animals with small infarcts (<20%) were omitted from the analysis.

2.1.13 Interstitial fibrosis

LV and kidney tissue sections stained with picrosirius red,^{314, 315} were analysed for interstitial fibrosis using Aperio ScanScope Console v.8.0.0.1058 (Aperio Technologies, Inc) at X200 magnification. Interstitial fibrosis in the non-infarcted zone of the LV and kidney, excluding perivascular fibrosis, was selected for its intensity of red staining, and the percentage area was calculated using a pre-set algorithm. The intensity and algorithm was maintained constant for the analysis of all sections.

2.1.14 Haematoxylin and eosin staining

LV tissue sections were stained with haematoxylin and eosin to assess the morphology of cardiomyocytes.⁷⁴ After dewaxing and rehydration, sections were incubated in Mayer's haematoxylin (Amber Scientific, WA, Australia) for 15 min and washed under running tap water for 5 min. Sections were dipped into Scott's tap water and washed under running tap water for 3 min. Slides were then incubated in eosin (BASF Australia Ltd., Auckland, New Zealand) for 10 min to give the cytoplasm shades of pink colour. Sections were dehydrated in 3x100% ethanol briefly to minimize the loss of stain and cleared in histolene (2x 5 min) and coverslipped using DPX.

Sections were scanned and analysed for each animal using Aperio ScanScope Console v.8.0.0.1058 (Aperio Technologies, Inc). Myocytes in the same plane, as assessed by selecting cells with similar sized nuclei and intact cellular membranes in the non-

infarcted zone of the myocardium, were outlined and the average myocyte cross-sectional area calculated from 50 myocytes per LV.

2.1.15 Immunohistochemistry

Sections were placed into histolene to remove the paraffin wax, hydrated in graded ethanol, and immersed in dH₂O as described in 2.1.11. Antigen retrieval was performed to unmask cross linked antigens. Sections were placed in pre-heated 0.01 M citrate buffer, pH 6.0, and boiled in a microwave oven at medium power for 10 min before being washed with 0.1 M phosphate buffered saline (PBS) (3x 5 min). Sections were then incubated with 3% H₂O₂ (Sigma Aldrich, USA) for 15 min to quench endogenous peroxidase activity. Slides were washed with PBS before incubation with diluted normal goat serum or normal swine serum (1:5) for 30 min at room temperature.³¹⁴ Sections were then incubated with primary antibody (Table 2.1) overnight at 4°C. On the following day, slides were washed with PBS (3x 5 min) and incubated with secondary antibody for 30 min or 1 hr, followed by PBS wash. Localisation of the peroxidase conjugates was achieved using 3,3'-diaminobenzidine tetrahydrochloride (DAB; Dako, CA, USA) as a chromagen.³¹³ DAB was applied to all sections until the target stained brown under microscope according to manufacturer's instruction (10-15 sec). Slides were washed thoroughly with running tap water for 10 min. Sections were then counter-stained with haematoxylin by submerging slides in Harris' modified haematoxylin for 10 sec and washed in running tap water until water clear. After that, slides were differentiated in Scott's tap water for 15 sec and rinsed in tap water. Sections were then dehydrated, cleared and mounted as described in 2.1.12.

Table 2.1 Antibodies for immunohistochemistry.

Serum	Primary antibody	Type	Dilution	Secondary antibody	Dilution	Duration
Swine	Collagen I (Southern Biotech)	Goat IgG	1:200	Rabbit-anti-goat IgG * (DAKO)	1:200	1 h
Goat	Collagen III (Biogenex)	Mouse monoclonal IgG	1:2	Anti-mouse IgG # (DAKO)	Nil	30 min
Swine	KIM-1 (R&D systems)	Goat IgG	1:200	Rabbit-anti-goat IgG * (DAKO)	1:200	30 min
Goat	Macrophage infiltration (Serotec)	Mouse monoclonal IgG	1:300	Anti-mouse IgG # (DAKO)	Nil	1 h

KIM-1, kidney injury molecule-1; IgG, Immunoglobulin G.

* Immunoglobulins conjugated to a horseradish peroxidase (HRP)

Dakocytomation Envision, HRP linked

2.1.15.1 Collagen type I and III

LV tissue sections were stained with antibodies specific for collagen I and III.³¹⁵ Images were captured using AxioVision software (Carl Zeiss Inc.) connected to Axio Imager A1 light microscope (Carl Zeiss Inc.) at X200 magnification. The levels of DAB staining were quantified by a single blinded researcher using the Analytic Imaging Station software (AIS, Version 6, Imaging research Inc., ON, Canada). Results were expressed as average percentage area of 10 random fields for each section obtained in the sub-endocardial region of the LV non-infarcted zone.

2.1.15.2 Kidney injury molecule-1

Tissue expression of KIM-1 in the non-infarcted zone of the kidney cortex was assessed using goat anti-KIM-1 antibodies. Sections were scanned and images were

analysed using Aperio ScanScope Console v.8.0.0.1058 (Aperio Technologies, Inc). The positive brown staining in the non-infarcted zone of the kidney cortex was selected for its intensity, and results were expressed as percentage area calculated using a pre-set algorithm. The intensity and the algorithm was maintained constant for the analysis of all sections.

2.1.15.3 Macrophage infiltration

Tissue expression of macrophage infiltration in the non-infarcted zone of the kidney cortex was assessed using mouse anti-CD 68 antibodies. Sections were scanned using Aperio ScanScope Console v.8.0.0.1058 (Aperio Technologies, Inc). The total number of macrophages (CD 68 immunoreactive cells) in the non-infarcted zone of the kidney cortex was individually counted for each animal.

2.1.16 Quantitative mRNA expression

Total RNA was extracted from frozen tissues using Ambion RNAqueous® kit (Ambion, TX, USA) according to manufacturer's instruction. RNA (20 ng/μl for genes of interest and 2 ng/μl for the housekeeping gene) was reversed transcribed to complimentary deoxyribonucleic acid (cDNA) with MultiScribe (Table 2.2).³¹⁵ Reverse transcription was performed in a thermocycler. Reaction mixture was heated to 25°C for 10 min, 42°C for 12 min, 95°C for 5 min, and cooled to 4°C. The cDNA was stored at -20°C.

Table 2.2 Composition of reverse transcription reaction mixture.

Reagent	volume (µl)/reaction
PCR Buffer II (10X)	4
MgCl ₂	8
dNTPs	16
Random Hexamers	2
Nuclease free water	2
RNAse inhibitor	2
MultiScribe	2
RNA	4
Total	40

Triplicate cDNA aliquots were amplified using sequence-specific primers (Geneworks, SA, Australia) (Table 2.3) with SYBR Green detection (Applied Biosystems, NY, USA). Composition of the Real-Time Polymerase Chain Reaction (RT-PCR) reaction mixture is shown in Table 2.4. Following the addition of the reaction mixture into PCR plates, the plates were covered with optical adhesive film (Applied Biosystems, CA, USA) and spun in a centrifuge at 3,000 rpm for 10 min at 4°C to remove air bubbles. RT-PCR was performed with ABI prism 7900HT sequence Detection System (Applied Biosystems, CA, USA) to quantify mRNA expression of TGFβ₁, CTGF, collagen I, collagen IV, ANP, β-MHC and IL-6. Quantitation was standardized to the housekeeping genes glyceraldehydes 3-phosphate dehydrogenase (GAPDH; cardiac tissues) and 18S (renal tissues).³¹⁵

Table 2.3 Primer sequences for RT-PCR.

Gene	Primer sequence
TGF β_1	Forward: 5' CCA GCC GCG GGA CTC T 3'
	Reverse: 5' TTC CGT TTC ACC AGC TCC AT 3'
CTGF	Forward: 5' GCG GCG AGT CCT TCC AA 3'
	Reverse: 5' CCA CGG CCC CAT CCA 3'
Collagen I	Forward: 5' TGC CGA TGT CGC TAT CCA 3'
	Reverse: 5' TCT TGC AGT GAT AGG TGA TGT TCTG 3'
Collagen IV	Forward: 5'-ATCCGGCCCTTCATTAGCA-3'
	Reverse: 5'- GACTGTGCACCGCCATCA-3'
ANP	Forward: 5'- ATCTGATGGATTTC AAGAACC-3'
	Reverse: 5'-CTCTGAGACGGGTTGACTTC-3'
β -MHC	Forward: 5'-TTGGCACGGACTGCGTCATC-3'
	Reverse: 5'- GAGCCTCCAGAGTTTGCTGAAGGA -3'
IL-6	Forward: 5' GCT ATG AAG TTT CTC TCC GCA AGA 3'
	Reverse: 5' GGC AGT GGC TGT CAA CAA CAT 3'
GAPDH	Forward:5'-GACATGCCGCCTGGAGAAAC-3'
	Reverse: 5'-AGCCCAGGATGCCCTTTAGT-3'
18S	Forward: 5' TCG AGG CCC TGT AAT TGG AA 3'
	Reverse: 5' CCC TCC AAT GGA TCC TCG TT 3'

Table 2.4 Composition of RT-PCR mixture.

Reagent	Volume (μ l)
SYBR Green master mix	5
Forward Primer	0.5
Reverse Primer	0.5
Nuclease free water	3
cDNA	1
Total	10

2.1.17 Protein extraction

Frozen tissue was homogenized with 1 ml of tissue lysis buffer (see Section 2.1.19.1) using a polytron homogenizer. After centrifugation for 15 min at 4°C, the supernatant was collected for subsequent Bradford assay and western blot analysis.

2.1.18 Bradford assay

Protein concentrations were measured by Bradford assay. Protein samples were diluted 1:5 with dH₂O. A bovine serum albumin (BSA) standard curve with a concentration range from 0.025 to 1.6 µg/ml was generated from serial 1:2 dilutions in dH₂O using a 4 µg/ml BSA stock solution. Protein samples and BSA standards (5 µl each) were added in triplicate to 96-well plates. 200 µl of diluted (1:5) Bradford reagent (Bio-Rad, CA, USA) was added to each well. Plates were mixed for 10 min using a microplate mixer. Absorbance was measured using a microplate reader (Bio-rad, CA, USA) at a wavelength of 595 nm. Protein concentrations of the samples were calculated from the standard curve.

2.1.19 Western blot analysis

Western blot analysis was performed as previously described.^{126, 127, 210} Protein was separated using sodium dodecyl sulfate polyacrylamide gel electrophoresis (SDS-PAGE) on the basis of molecular weight. After that, western blot analysis was used to determine the activation of signal transduction pathways in cardiac and renal tissues..³¹⁶

2.1.19.1 Reagents and solutions

All chemical products were purchased from Sigma Aldrich (St. Louis, MO, USA).

Tissue lysis buffer

Composition: Tris-HCl 20 mM, NaCl 250 mM, EDTA 2 mM, EGTA 2 mM, Glycerol 10%, β -glycerophosphate 40 mM, 0.5% Triton X-100, Leupeptin 10 $\mu\text{g}/\mu\text{l}$, Aprotinin 10 $\mu\text{g}/\mu\text{l}$, Pepstatin 1 μM , Phenylmethylsulfonylfluoride 1 mM, Dithiothreitol (DTT) 1 mM, Phosphatase inhibitor cocktail-1 1 $\mu\text{l}/\text{ml}$, Phosphatase inhibitor cocktail-2 1 $\mu\text{l}/\text{ml}$, NaF 0.5 mM, Sodium Pyrophosphate 2.5 mM.

The lysis buffer was made fresh with dH₂O water.

2xSample buffer

Composition: Tris-HCl (pH 6.8) 125 mM, Sodium dodecyl sulfate (SDS) 4% w/v, Glycerol 20% v/v, β -mercaptoethanol 10% v/v, Bromophenol blue 0.02 mg/ml.

The sample buffer was stored at -20°C.

5xRunning buffer

Composition: Tris base 0.124 M, Glycine 0.96 M, SDS 0.5% w/v.

The concentrated running buffer was made with dH₂O, stored at 4°C and diluted 1:5 with dH₂O water when required.

Transfer buffer

Composition: Tris base 0.025 M, Glycine 0.192 M, CH₃OH 20% v/v.

The transfer buffer was made fresh with dH₂O water.

10xTris buffered saline (TBS)

Composition: Tris base 0.2 M, NaCl 1.37 M.

The concentrated TBS was adjusted to pH 7.6 with concentrated HCl and stored at 4°C.

Tris buffered saline - Tween 20 (TBST)

Composition: 10xTBS 100 ml, dH₂O 900 ml, Tween 20 1 ml.

The TBST was made fresh when required.

5% blotto in TBST

Composition: Skim milk powder 5 g, TBST 100 ml.

The 5% blotto was made fresh when required.

5% BSA in TBST

Composition: BSA powder 5 g, TBST 100 ml.

The 5% BSA was made fresh when required.

2.2.19.2 Preparation

Sample buffer was added to equal amounts of protein (30 or 60 µg) at 1:1 (v/v) ratio.

Mixtures were boiled at 98°C for 10 min before centrifuging at maximum speed for 5 min.

The gel apparatus was assembled using a glass plate sandwich in a gel casting stand. A 10% separating gel (Table 2.5) was prepared and the gel mix was cast between the glasses using a pipette followed by an overlay of 1 ml of water saturated n-butanol to create a level. The gel was allowed to set (~ 45 min) prior to removing the water saturated n-butanol. A 4% stacking gel (Table 2.6) was prepared and poured on top of the set separating gel until the gel reached the top of the glass plate. A comb was

inserted to create wells and the gel was allowed to set (~30 min). After gel set, the comb was removed from the stacking gel.

Table 2.5 Separating gel recipe (1.5 mm gel). SDS, sodium dodecyl sulfate; APS, ammonium persulfate; TEMED, tetramethylethylenediamine.

Reagent	10%
dH ₂ O	4.05 ml
1.5M Tris-HCl pH 8.8	2.50 ml
30% Acrylamide/bis	3.30 ml
10% SDS	100 µl
10% APS	50 µl
TEMED	5 µl
Total	10 ml

Table 2.6 Stacking gel recipe (1.5 mm gel).

Reagent	4%
dH ₂ O	6.40 ml
0.5M Tris-HCl pH 6.8	2.50 ml
30% Acrylamide/bis	1.00 ml
10% SDS	100 µl
10% APS	200 µl
TEMED	20 µl
Total	~10 ml

2.1.19.3 SDS-PAGE

The gel was placed into clamping frame and electrode assembly. The inner chamber was placed into a mini tank, and running buffer was then added into the inner chamber (between gels) up to the top of the glass plate and outer chamber ~ 4 cm high. After loading prepared protein samples and molecular weight marker (BenchMark™ Pre-Stained Protein Ladder, 10 µl, Invitrogen) into wells of gels, the gels were run at voltage of 120V until dye front reached the bottom of the gel (~ 2 hr).

2.1.19.4 Transfer

Nitrocellulose membrane (Amersham Hybond ECL, GE Healthcare, Freiburg, Germany), filter paper and fiber pad were soaked in transfer buffer for 30 min. Transfer sandwich was set up as laying a fiber pad, 3x filter paper, 1x nitrocellulose membrane, 1x gel, 3x filter paper and a fiber pad in order. The transfer sandwich was clamped in a cassette and placed into an electrode module (the black side of the cassette facing the black side of the electrode module). The module was then placed into a tank containing transfer buffer. The separated protein samples were electrophoretically transferred to the membrane under a voltage of 100V for ~ 2 hr at 4°C. After transferring, the membrane was taken out, stained with Ponceau solution for 2-3 min to locate the protein bands, and washed with dH₂O.

2.1.19.5 Immunoblotting

The membrane was incubated with 5% BSA/blotto in TBST for 1 hr at room temperature. Diluted primary antibody (10 ml) was added onto the membrane and incubated overnight at 4°C (Table 2.7). The membrane was washed with TBST for 3x 5

min before adding secondary antibody diluted in 5% blotto in TBST (10 ml). The membrane was then incubated for 1 hr at room temperature following washing with TBST for 5x 5 min. Specific bands were visualized by enhanced chemiluminescent HRP substrate (Thermo Scientific, Rockford, IL, USA),³¹⁷ and then the intensity was analysed using ImageJ software (National Center for Biotechnology Information).

Table 2.7 Antibodies for western blot analysis

Primary antibody	Isotype	Dilution	Secondary antibody	Dilution
Phospho-p38 MAPK #9215 (Cell Signaling Technology)	Rabbit monoclonal IgG	1:1000 in 5% BSA	Anti-rabbit IgG, HRP-linked #7074 (Cell Signaling Technology)	1:2000
Phospho-p44/42 MAPK #9101 (Cell Signaling Technology)	Rabbit polyclonal	1:1000 in 5% BSA	Anti-rabbit IgG, HRP-linked #7074 (Cell Signaling Technology)	1:2000
Phospho-NFκB #3033 (Cell Signaling Technology) *	Rabbit monoclonal IgG	1:1000 in 5% BSA	Anti-rabbit IgG, HRP-linked #7074 (Cell Signaling Technology)	1:2000
TGF-β #3709 (Cell Signaling Technology)	Rabbit monoclonal Ab	1:1000 in 5% blotto	Anti-rabbit IgG, HRP-linked #7074 (Cell Signaling Technology)	1:2000
Pan-actin #ACTN 05 (Neomarkers)	Mouse monoclonal IgG	1:2000 in 5% blotto	Anti-mouse IgG, HRP-linked #7076 (Cell Signaling Technology)	1:4000

* Nuclear proteins, including activated transcription factor subunits of NFκB complex, such as p65, were extracted with high detergent (0.5% Triton X-100) lysis buffer to obtain total cell lysis and detected with Western blot analysis. Phospho-NFκB Rabbit mAb detected NFκB subunit p65.

2.1.20 Statistical analysis

Data are expressed as mean \pm SEM. Significance was determined by a one-way ANOVA followed by Bonferroni post hoc test. For comparisons between 2 groups, unpaired Student t-test was used. All statistical analyses were performed using GraphPad Prism 5. A two-sided P-value of less than 0.05 was considered statistically significant.

2.2 *In vitro* studies

Cultured neonatal rat cardiac myocytes (NCMs) and fibroblasts (NCFs) were used to determine pro-hypertrophic and pro-fibrotic effects of indoxyl sulfate (IS).

2.2.1 Animal and ethics approval

NCMs and NCFs were isolated from 1-2 day old SD pups. Animal experiments were conducted in accordance with Alfred Medical Research and Education Precinct (AMREP) Animal Ethics Committee approved protocols and conformed to the requirements of the National Health and Medical Research Council of Australia (NHMRC) *Code of Practice for the Care and Use of Animals for Scientific Purposes*. The ethics approval number was E/0980/2010/M.

2.2.2 Materials

IS was purchased from Sigma Aldrich (St. Louis, MO, USA). IS stock solution was prepared with endotoxin-free sterilized PBS and kept at -20°C.

OAT antagonists, Probenecid (Pro) and Cilastatin (Cil), were purchased from Sigma Aldrich (St. Louis, MO, USA). ASK1 inhibitors, GSK2261818A (G226) and GSK2358939 (G235), were a kind gift from GlaxoSmithKline (Heart Failure Discovery Performance Unit, King of Prussia, PA, USA). Stock solutions of Pro, Cil, G226 and G235 at concentrations of 1000 folds of final treatment concentrations were prepared in dimethyl sulfoxide (DMSO) and kept at -20°C.

All cell culture media were purchased from Gibco life technologies, Invitrogen, NY, USA. ³H-leucine and ³H-proline was purchased from PerkinElmer, Boston, MA, USA. All chemical products were purchased from Sigma Aldrich (St. Louis, MO, USA).

2.2.3 Reagents and solutions

Hanks buffered salt solution (HBSS)

Composition: NaCl 135.0 mM; KCl 5.4 mM; MgSO₄ 0.8 mM; Glucose 5.6 mM; KH₂PO₄ 4.4 mM; Na₂HPO₄ 3.5 mM; HEPES 20 mM.

The HBSS was adjusted to pH 7.2, sterilized using Steritop filters (Millipore, MA, USA) and stored at 4°C.

Enzyme digestion solution

HBSS containing 0.8 mg/ml pancreatin and 125 U/ml collagenase.

Minimum essential media (MEM) with 10% new born calf serum (NBCS)

Composition: Powdered MEM dissolved in MilliQ-water; NaHCO₃ 26 mM; 1xessential amino acids; non-essential amino acids 100 µM; L-glutamine 2 mM; 1xMEM vitamins; 10% v/v NBCS; 1xantibiotics and antimycotics.

It was adjusted to pH 7.2, sterilized using Steritop filters and stored at 4°C.

10x Ads buffer

Composition: NaCl 116 mM; KCl 50 mM; MgSO₄ 8 mM; Glucose 60 mM; Na₂HP0₄ 0.008 mM.

The concentrated Ads buffer was adjusted to pH 7.35, stored at 4°C, and diluted to 1x Ads with sterilized Milli-Q water (Millipore) when required.

Percoll stock

9 parts Percoll: 1 part 10xAds.

Percoll stock was stored at 4°C.

Top Percoll layer

9 parts Percoll stock: 11 parts 1xAds.

Top Percoll layer was made fresh when required.

Bottom Percoll layer

13 parts Percoll stock: 7 parts 1xAds.

Bottom Percoll layer was made fresh when required.

NCM media for culture/treatment

Composition: Dulbecco's modified eagle medium (DMEM; Invitrogen, Mount Waverly, VIC, Australia); NaHCO₃ 26 mM; 1xessential amino acids; non-essential amino acids 100 µM; sodium pyruvate 1 mM; 1xMEM vitamins.

Media was adjusted to pH 7.2, sterilized using Steritop filters, stored at 4°C and supplemented with insulin 2 mg/L, apo-transferrin 10 mg/L, and 5-bromo-deoxyuridine (BrDu) 0.1 mM before use.

NB: BrDu was only used in the first three days to inhibit proliferation of fibroblasts.

2.2.4 NCMs and NCFs isolation

NCMs and NCFs were isolated from 1-2 day old SD pups with enzymatic digestion as described in detail previously.^{318, 319} Hearts were harvested under aseptic conditions and placed into cold HBSS solution. After removing the main blood vessels and atria, the remaining ventricular tissues were washed and gently cut into 6-8 pieces (1-2 mm²). The chopped tissues were digested by 10x 10 min sequential stirring in a Celstir apparatus containing enzyme digestion solution (0.3 ml per heart). The Celstir system was placed on a magnetic stirrer using the lowest speed and maintained at 37°C. For each cycle, undigested tissue was allowed to settle; and following each digestion period, the supernatants containing dissociated NCMs and NCFs were transferred into 50 ml sterile tubes (on ice) in the presence of 10% NBCS to inhibit enzyme activity. The first supernatant was discarded because it contained red blood cells and cell debris. The remaining supernatant was centrifuged at 1,200 rpm (300xg) for 10 min and the cell pellets were collected, resuspended in MEM with 10% NBCS and combined. Cells were centrifuged for 10 min and the pellets collected. Cell pellets were resuspended in 1x Ads buffer.

The resuspended cells were loaded above the top layer of a Percoll gradient, consisting of the top and bottom Percoll layers, and centrifuged at 3,000 rpm for 30 min at 4°C without using the brake. Upon completion of centrifugation, the NCFs were collected

in the upper gradient band and the NCMs were collected in the lower band. After transferring each band into separated tubes, cells were washed with 1x Ads by centrifuging at 1,200 rpm for 6 min, and resuspended in MEM with 10% NBCS.

2.2.5 Measurement of NCM hypertrophy

NCM hypertrophy was determined by ^3H -leucine incorporation.³¹⁹⁻³²¹ After isolation, the number of NCMs was counted using an Bright-LineTM Hemacytometer (Hausser Scientific, Horsham, PA, USA). Purified NCMs were seeded at 10,000 cells/cm² in 12-well plates (BD Falcon, NJ, USA) coated with 0.1% gelatin and maintained in serum-free DMEM in the presence of 1% antibiotic/antimycotic (100x; Gibco life technologies, Invitrogen, NY, USA) supplemented with insulin and apo-transferrin.³¹⁵ NCMs were incubated overnight at 37°C with 5% CO₂. Media was then changed and NCMs were incubated for another 48 hr before treatment. KCl (50 mM) was added to the media to prevent contact-induced spontaneous contraction of the plated NCMs.³²²

On treatment day, media was changed. NCMs were then pre-treated with or without of OAT antagonists (0.1 to 100 μM) or ASK1 inhibitors (0.03 to 1.0 μM). After 2 hr of pre-treatment, IS at a concentration of 10 μM was added to cells. ^3H -leucine (1 μCi) was added to each well. Cells were incubated at 37°C with 5% CO₂ for a further 48 hr. After 3 washes with cold 1x PBS, cells were harvested by precipitation with 10% trichloroacetic acid (TCA) on ice for 30 min before solubilisation with 1M NaOH overnight at 4°C. The samples were then neutralized with 1M HCl, and ^3H levels were counted in scintillation fluid on a beta counter to determine the levels of ^3H -leucine incorporation.

2.2.6 Measurement of NCF collagen synthesis

NCF collagen synthesis was determined at passage 2 NCFs by ^3H -proline incorporation.^{320, 323} After isolation, NCFs (passage 0) were seeded into T75 cell culture flasks (BD Falcon, NJ, USA) and maintained in high-glucose (25 mM) DMEM (Invitrogen, VIC, Australia) in the presence of 1% antibiotic/antimycotic (100x; Gibco life technologies, Invitrogen, NY, USA) and 10% fetal bovine serum (FBS; JRH Biosciences, Lenexa, KA, USA). Cells were incubated at 37°C with 5% CO₂ for 48 hr.

At 80% of confluence, the NCFs were sub-cultured. After removing media, NCFs were washed 2 times with warm 1x PBS, 2 ml of warm 0.05% trypsin-EDTA was added to each flask. Flasks were placed back into a 37°C incubator for 1-2 min to allow cells to lift off the surface of the flasks. Trypsin was inactivated by adding 8 ml of DMEM containing 10% FBS. NCF (passage 1) were centrifuged at 1,300 rpm for 6 min at room temperature. Cell pellets were washed 3 times and resuspended with DMEM containing 10% FBS. Cells were then split into new flasks (1:3) and incubated at 37°C with 5% CO₂ for 48 hr.

To seed NCFs, steps from trypsinization to resuspension described above were repeated. NCFs (passage 2) were counted and seeded at a density of 50,000 cells/well in 12 well plates in DMEM containing 10% FBS. Plated NCFs were incubated at 37°C with 5% CO₂ overnight before serum starving with media containing 1% vitamin C and 0.5% BSA for 48 hr.

After changing media, cells were pre-treated with or without OAT antagonists (0.1 to 100 μM) or ASK1 inhibitors (0.03 to 1.0 μM) for 2 hr before stimulation with IS at a

concentration of 10 μ M. ^3H -proline (1 μCi) was added to each well. After a 48 hr of further incubation, cells were harvested by TCA precipitation and ^3H -proline incorporation was determined similar to NCM hypertrophy assessment described above.

2.2.7 Measurement of cell viability in NCFs

MTT [3-(4,5-dimethylthiazol-2-yl)-2,5-diphenyltetrazolium bromide] assay was used to determine cell viability of NCFs as previously described.^{126, 315} NCFs were prepared as described in 2.2.6 and seeded in 96 well plates at a density of 10,000 cells/well. After serum starving for 48 hr, NCFs were treated with OAT antagonists and ASK1 inhibitors. MTT (Sigma Aldrich, St Louis, MO, USA) (5.0 mg/ml) was added to each well (10 μl per 100 μl medium) and the cells were incubated at 37°C with 5% CO_2 for 4 hr.³²⁴ The media was removed and isopropanol (100 μl) was added, the plates were placed back into the incubator for 30 min. Absorbance was measured on a microplate reader (Bio-rad, CA, USA) at a wavelength of 570 nm with background subtraction at 690 nm.

2.2.8 Statistical analysis

Absolute values from each triplicate experiment for each condition were recorded. Percentages were calculated by taking the mean of triplicate absolute values and comparing as a per cent change to the mean of triplicates of absolute mean values of control within each individual experiment. Data are presented as means \pm SEM. Experiments were performed at least three times in triplicate. One-way ANOVA followed by Neuman-Keul post hoc test was used for data analysis with GraphPad Prism 5. A two-tailed P-value of less than 0.05 was considered statistically significant.

Chapter 3 Functional and Structural Changes in the MI+STNx Model

3.1 Introduction

Renal dysfunction frequently coexists in situations of cardiac dysfunction such as MI and HF, manifesting in the so-called CRS.³ The prevalence of renal disease in patients with CHF is approximately 25%.²²⁻²⁴ The degree of renal dysfunction is a powerful independent risk factor for all-cause mortality in HF patients.^{22, 24, 28-31} Studies have indicated that even a slight worsening of renal function is associated with increased mortality and prolonged hospitalisation.³⁴

The pathophysiology underlying CRS is poorly understood. The heart and the kidney exert reciprocal control in maintaining constant blood volume and organ perfusion under continuously changing conditions. A complex combination of hemodynamic, neurohormonal, immunological, biochemical feedback pathways and other unknown factors such as uremic toxins contribute to CRS.³²⁵ IS, a non-dialysable uremic toxin, has been demonstrated as a contributory factor in cardiac hypertrophy and fibrosis.^{126, 326} Cardiac fibrosis correlates closely with IS serum levels in a rat model of CKD.¹²⁷

A number of experimental rat models with cardiac or renal impairment have been developed.³²⁵ However, very few have attempted to combine elements of cardiac and renal dysfunction as a potential model of CRS.^{246, 248-250, 253} Specifically, no study has been performed where MI-induced LV systolic dysfunction is complicated by the addition of CKD. Given the multiplicity of heart-kidney interactions and lack of systematic investigation of CRS, the purpose of this study was to establish a new model of MI (induced by left anterior descending coronary ligation) followed by a kidney insult (induced by 5/6 nephrectomy - STNx) in rats. We sought to identify subsequent

functional and structural changes in heart and kidney in this setting. The pathology and potential mechanisms that may underlie the changes will be described in Chapter 4.

3.2 Aims

To evaluate functional and structural changes in heart and kidney in the setting of MI followed by STNx in rats.

3.3 Materials and Methods

Male Sprague Dawley rats (n=43) weighing 200-250 g were randomized into four groups: Sham-operated MI+Sham-operated STNx (Sham+Sham), MI+Sham-operated STNx (MI+Sham), Sham-operated MI+STNx (Sham+STNx) and MI+STNx. MI/Sham was induced initially and STNx/Sham performed 4 weeks later; the animals were then followed for a further 10 weeks (Figure 3.1).

Tail-cuff blood pressure (BP) and cardiac and renal function was assessed prior to STNx/Sham and at study's end. Hemodynamic parameters were measured prior to sacrifice. Surgical procedure and functional measurements were performed using protocols as per Chapter 2.1.2-2.1.9. Paraffin-embedded sections were stained with picrosirius red for fibrosis analysis and hematoxylin and eosin for cardiac myocyte cross-sectional area as per Chapter 2.1.10-2.1.14.

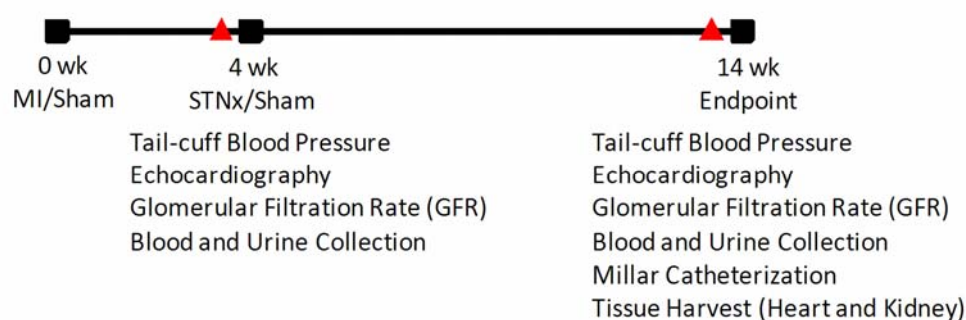


Figure 3.1 Experimental design of MI+STNx model. MI/Sham was induced initially and STNx/Sham performed 4 weeks later; the animals were then followed for a further 10 weeks. Blood pressure, echocardiography and GFR was assessed, and blood and urine was collected prior to STNx/Sham and at endpoint. Millar catheterization was performed prior to sacrifice. Tissues were weighed and collected for pathological and molecular changes. MI, myocardial infarction; STNx, 5/6 subtotal nephrectomy.

3.4 Results

3.4.1 Survival rate and infarct size

Totally 80 animals were randomized into each group initially and 43 animals were survived at the end of the study. Survival rates were 100%, 59.7%, 91.7% and 44.1% for Sham+Sham, MI+Sham, Sham+STNx and MI+STNx animals respectively (Figure 3.2). The number of animals in each group at the end of the study is shown in Table 3.1. There was no difference in infarct size between both MI groups (Sham-operated STNx and STNx) (Table 3.1).

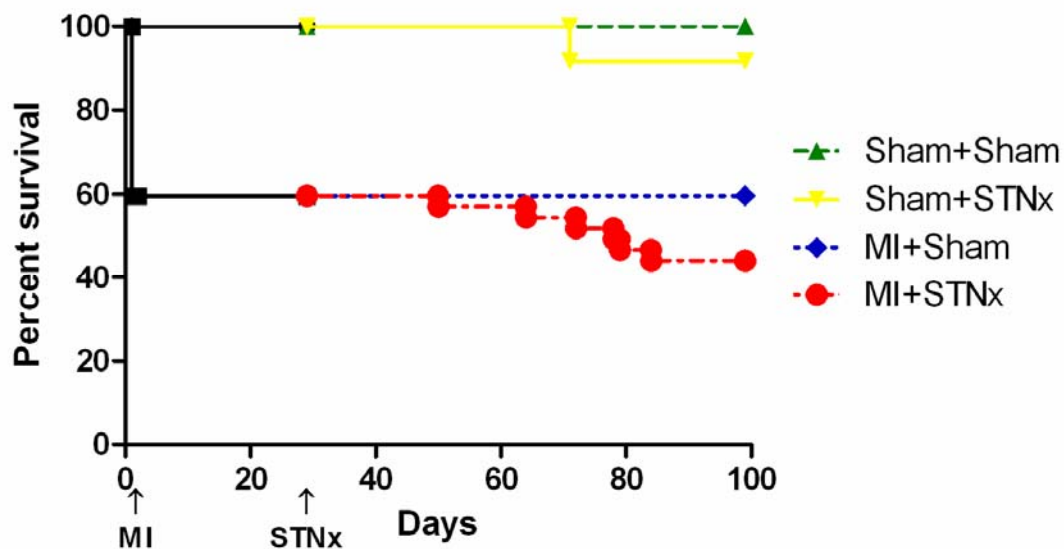


Figure 3.2 Kaplan-Meier curves for groups of Sham+Sham, MI+Sham, Sham+STNx and MI+STNx respectively.

Table 3.1 Animal number and infarct size. There was no difference in infarct size between MI+Sham and MI+STNx groups. Values are expressed as mean \pm SEM.

	Sham+Sham	MI+Sham	Sham+STNx	MI+STNx
Animal Number	10	11	11	11
Infarct size (%)	-	34.6 \pm 2.2	-	33.7 \pm 1.5

3.4.2 Blood pressure

There was no difference in BP between all groups before STNx/Sham surgery at week 4 (Table 3.2). As a consequence of the kidney insult, both STNx groups (Sham-operated MI and MI) developed substantial and persistent hypertension. MI+STNx animals had reduced systolic BP compared to the Sham+STNx group ($p < 0.01$).

Table 3.2 Blood pressure (BP) assessed at week 4 and 14. Sham+STNx and MI+STNx animals were hypertensive at 14 weeks. Values are expressed as mean \pm SEM.

***p<0.001 vs Sham+Sham; §§§p<0.001 vs MI+Sham; ##p<0.01 vs Sham+STNx.

	Week 4				Week 14			
	Sham+Sham	MI+Sham	Sham+STNx	MI+STNx	Sham+Sham	MI+Sham	Sham+STNx	MI+STNx
BP (mmHg)	128.2 \pm 6.8	115.5 \pm 6.3	122.3 \pm 3.5	111.4 \pm 4.2	125.8 \pm 6.0	118.8 \pm 4.7	221.8 \pm 10.9 ***, §§§	176.6 \pm 9.3 ***, §§§, ##

3.4.3 Tissue weights

Heart, LV, atria, lung and left kidney weights as a ratio of body weight (BW) were significantly greater in MI+STNx animals compared to the MI+Sham group (Table 3.3). Heart and LV weights as a ratio of BW were higher in Sham+STNx animals compared with MI+Sham animals (p<0.001), this was also evident in the echocardiography measure of anterior (p<0.001) and posterior wall thickness (p<0.05) (Table 3.4), suggesting that more muscle mass in the STNx group. A major driver of this was the increase in BP that was observed in the Sham+STNx group compared to the MI+Sham group (Table 3.2). Heart, LV, right ventricular and atria weights as a ratio of BW were identical in both STNx groups, independent of MI.

Table 3.3 Animal tissue weights that are corrected for body weight. Heart, LV, atria, lung and left kidney weights were significantly greater in MI+STNx animals compared to the MI+Sham group. Values are expressed as mean \pm SEM. BW, body weight.

p<0.01, *p<0.001 vs Sham+Sham; §p<0.05, §§p<0.01, §§§p<0.001 vs MI+Sham.

	Sham+Sham	MI+Sham	Sham+STNx	MI+STNx
Heart weight/BW ratio (mg/g)	2.4 \pm 0.1	2.8 \pm 0.1 ***	3.9 \pm 0.2 ***, §§§	3.9 \pm 0.2 ***, §§§
Lung weight/BW ratio (mg/g)	3.0 \pm 0.1	3.1 \pm 0.1	3.6 \pm 0.1 **, §§	3.6 \pm 0.2 **, §§
LV weight/BW ratio (mg/g)	1.73 \pm 0.07	1.94 \pm 0.03 **	2.93 \pm 0.14 ***, §§§	2.88 \pm 0.10 ***, §§§
Right ventricular weight/BW ratio (mg/g)	0.45 \pm 0.02	0.57 \pm 0.02 ***	0.60 \pm 0.02 ***	0.64 \pm 0.04 ***
Atria weight/BW ratio (mg/g)	0.24 \pm 0.01	0.32 \pm 0.02 **	0.35 \pm 0.03 **	0.42 \pm 0.04 ***, §
Left kidney weight/BW ratio (mg/g)	3.1 \pm 0.1	3.1 \pm 0.1	4.6 \pm 0.1 ***, §§§	5.0 \pm 0.2 ***, §§§
BW (g)	576.6 \pm 34.5	551.1 \pm 16.6	488.2 \pm 19.4 *, §	516.0 \pm 16.7

3.4.4 Echocardiography

Significant reductions in LVEF and FS were observed in both MI groups compared to sham-operated animals at 4 weeks post-infarction (Table 3.4). Anterior wall thickness was significantly reduced in both MI groups due to scar tissue replacement post-MI (p<0.001).

Animals that underwent MI+STNx had further reductions in LVEF (20.8%) and FS (20.9%) compared to the MI+Sham group at 10 weeks post-STNx (p<0.01). Although

no difference in A wave velocity, a measure of late transmitral peak diastolic flow velocity, was observed between all groups at 4 weeks post-MI; a significant increase was seen in MI+STNx animals compared to the MI+Sham group at 10 weeks post-STNx ($p<0.05$), indicating an increase in diastolic dysfunction. Sham+STNx animals had increased LV mass ($p<0.01$), anterior wall thickness ($p<0.001$), posterior wall thickness ($p<0.001$) and developed diastolic dysfunction indicated by reduced E'/A' ratio ($p<0.05$) and increased A' wave velocity ($p<0.01$) compared to the Sham+Sham group at week 14. LVEDV, LVESV and IVRT were significantly increased in both MI groups compared to sham-operated animals. There was no difference in DT, transmitral early peak velocity (E), septal mitral annulus velocity (E'), E/E' ratio and E/A ratio between the groups post-STNx.

Table 3.4 Echocardiography assessed at week 4 and 14. Left ventricular ejection fraction was significantly decreased in MI+STNx animals compared to the MI+Sham group at week 14. Values are expressed as mean \pm SEM. FS, fractional shortening; LVEF, left ventricular ejection fraction; LVEDV and LVESV, left ventricular end diastolic and end systolic volume; DT, deceleration time; IVRT, isovolumetric relaxation time. * $p<0.05$, ** $p<0.01$, *** $p<0.001$ vs Sham+Sham; § $p<0.05$, §§ $p<0.01$, §§§ $p<0.001$ vs MI+Sham; # $p<0.05$, ## $p<0.01$, ### $p<0.001$ vs Sham+STNx.

	Week 4				Week 14			
	Sham+Sham	MI+Sham	Sham+STNx	MI+STNx	Sham+Sham	MI+Sham	Sham+STNx	MI+STNx
FS (%)	40.5±1.5	21.4±1.5 ***	45.3±1.5 §§§	18.1±0.5 ***, ###	40.4±2.9	19.1±0.9 ***	47.6±3.3 §§§	15.1±0.9 ***, §§, ###
Anterior wall thickness (mm)	1.45±0.03	0.91±0.04 ***	1.49±0.05 §§§	0.83±0.03 ***, ###	1.64±0.04	0.78±0.02 ***	2.04±0.06 ***, §§§	0.73±0.03 ***, ###
Posterior wall thickness (mm)	1.57±0.05	1.81±0.06 *	1.67±0.06	1.65±0.04	1.69±0.06	1.93±0.05 **	2.24±0.08 ***, §	1.69±0.08 §, ###
LVEF (%)	67.1±2.2	42.7±2.3 ***	72.2±2.0 §§§	37.7±1.4 ***, ###	67.8±2.9	39.4±1.8 ***	71.8±3.1 §§§	31.2±1.3 ***, §§, ###
LVEDV (mL)	0.66±0.02	0.83±0.05 **	0.60±0.04 §§	0.90±0.05 ***, ###	0.76±0.04	1.11±0.05 ***	0.81±0.04 §§	1.23±0.07 ***, ###
LVESV (mL)	0.22±0.05	0.48±0.04 ***	0.17±0.02 §§§	0.56±0.04 ***, ###	0.25±0.03	0.68±0.04 ***	0.22±0.03 §§§	0.85±0.06 ***, §, ###
LV mass (gram/m²)	1.41±0.04	1.47±0.05	1.40±0.04	1.51±0.03	1.70±0.04	1.80±0.11	2.13±0.07 **, §	1.78±0.08 #
DT (msec)	31.3±1.5	36.0±1.8	38.3±1.1 *	39.0±1.5 **	32.1±1.8	37.2±1.8	31.8±2.1	36.7±2.3
IVRT (msec)	23.0±1.4	31.3±1.2 ***	21.9±1.3 §§§	30.3±1.6 **, ###	24.2±1.6	34.7±1.7 **	26.2±1.6 §	35.4±2.5 **, ##
E wave velocity (m/sec)	1.04±0.04	1.07±0.04	1.06±0.03	1.05±0.04	0.99±0.04	0.97±0.04	1.10±0.04	1.03±0.05
A wave velocity (m/sec)	0.64±0.06	0.49±0.03	0.53±0.04	0.48±0.03	0.45±0.05	0.37±0.04	0.66±0.05 *, §§	0.53±0.06 §
E' wave velocity (cm/sec)	4.8±0.3	4.0±0.3	4.4±0.2	3.7±0.2 *	4.0±0.2	3.6±0.3	4.4±0.4	4.1±0.3
A' wave velocity (cm/sec)	3.3±0.3	2.7±0.3	3.5±0.4	2.5±0.1	2.7±0.4	2.5±0.3	4.4±0.3 **, §§	3.1±0.3 #
E/E' ratio	22.4±1.1	26.7±1.1	25.1±1.5	28.3±1.7 *	25.0±1.4	28.2±2.2	26.2±2.3	26.0±1.8
E/A ratio	1.8±0.1	2.3±0.2	2.1±0.2	2.3±0.2	2.6±0.5	3.0±0.4	1.7±0.1	2.2±0.4
E'/A' ratio	1.5±0.1	1.6±0.3	1.4±0.1	1.5±0.1	1.7±0.2	1.6±0.3	1.1±0.1 *	1.5±0.2

3.4.5 Hemodynamic parameters

Significant increases in systolic and diastolic BP were observed in MI+STNx animals compared to the MI+Sham group ($p<0.01$) (Table 3.5). It should be noted here, the systolic/diastolic BP was measured when animals were under anaesthesia; therefore the values were different from the BP recording presented in Table 3.2.

LV end diastolic pressure (LVEDP) in MI+STNx animals compared to the MI+Sham group did not reach significance ($p=0.08$). MI+STNx animals had a 31% reduction in cardiac output compared to the MI+Sham group ($p=0.06$). There was no difference in heart rate between the groups.

The rate of rise and fall of pressure in the LV, dp/dt_{max} and dp/dt_{min} , was significantly reduced in both MI groups compared to the sham-operated animals; however, no difference was observed comparing MI+STNx animals with the MI+Sham group. Parameters of systolic function including the slope of preload recruitable stroke work relationship (PRSW) and the gradient of end systolic pressure-volume relationship (ESPVR) were significantly reduced in MI groups compared to Sham+Sham control animals; while the diastolic measures pertaining to the time constant of active relaxation, tau logistic, was significantly prolonged by 38% in MI+STNx animals compared to the MI+Sham group ($p<0.01$), indicating an impairment of ventricular relaxation and diastolic function.

Table 3.5 Hemodynamic parameters assessed at week 14. Tau logistic was significantly increased in MI+STNx animals compared to the MI+Sham group. Values are expressed as mean \pm SEM. dP/dt_{max} and dP/dt_{min} , the maximal rate of pressure rise and fall; LVEDP, left ventricular end diastolic pressure; ESPVR and EDPVR, slope of end systolic and end diastolic pressure-volume relationship; PRSW, slope of preload recruitable stroke work relationship. * $p<0.05$, ** $p<0.01$, *** $p<0.001$ vs Sham+Sham; § $p<0.05$, §§ $p<0.01$, §§§ $p<0.001$ vs MI+Sham; # $p<0.05$, ### $p<0.001$ vs Sham+STNx.

	Sham+Sham	MI+Sham	Sham+STNx	MI+STNx
Systolic blood pressure (mmHg)	104.4 \pm 6.3	91.8 \pm 2.0	116.7 \pm 6.4 §§	111.8 \pm 6.0 §§
Diastolic blood pressure (mmHg)	77.3 \pm 5.7	66.3 \pm 2.4	87.6 \pm 5.4 §§	88.6 \pm 5.7 §§
Heart rate (beats/min)	306 \pm 19	302 \pm 23	309 \pm 17	314 \pm 17
dP/dt_{max} (mmHg/sec)	6123 \pm 215	4763 \pm 163 ***	6193 \pm 301 §§§	4633 \pm 253 ***, ###
$-dP/dt_{min}$ (mmHg/sec)	5229 \pm 295	3212 \pm 180 ***	4124 \pm 356 *, §	3065 \pm 207 ***, #
LVEDP (mmHg)	3.9 \pm 0.6	7.3 \pm 0.9 *	10.1 \pm 1.4 **	10.7 \pm 1.5 **
ESPVR (mmHg/μl)	0.58 \pm 0.07	0.29 \pm 0.04 **	0.47 \pm 0.07 §	0.32 \pm 0.04 **
EDPVR (mmHg/μl)	0.03 \pm 0.01	0.03 \pm 0.01	0.05 \pm 0.01	0.04 \pm 0.01
PRSW (mmHg)	78.9 \pm 5.5	58.2 \pm 6.1 *	62.7 \pm 8.9	49.2 \pm 4.5 ***
Cardiac output (mmHg)	45070 \pm 3670	44678 \pm 4975	53724 \pm 8169	30761 \pm 4775 *, #
Tau logistic (msec)	10.0 \pm 0.5	12.3 \pm 0.7 *	16.5 \pm 1.6 ***, §	17.0 \pm 1.4 ***, §§

3.4.6 Cardiac interstitial fibrosis

Cardiac interstitial fibrosis in the LV non-infarcted myocardium, determined from picrosirius red staining, was significantly increased in MI+STNx animals compared to

the MI+Sham group ($p<0.01$) (Figure 3.3). LV fibrosis was also greater in MI+Sham and Sham+STNx animals compared to Sham+Sham control animals ($p<0.05$ and $p<0.001$ respectively).

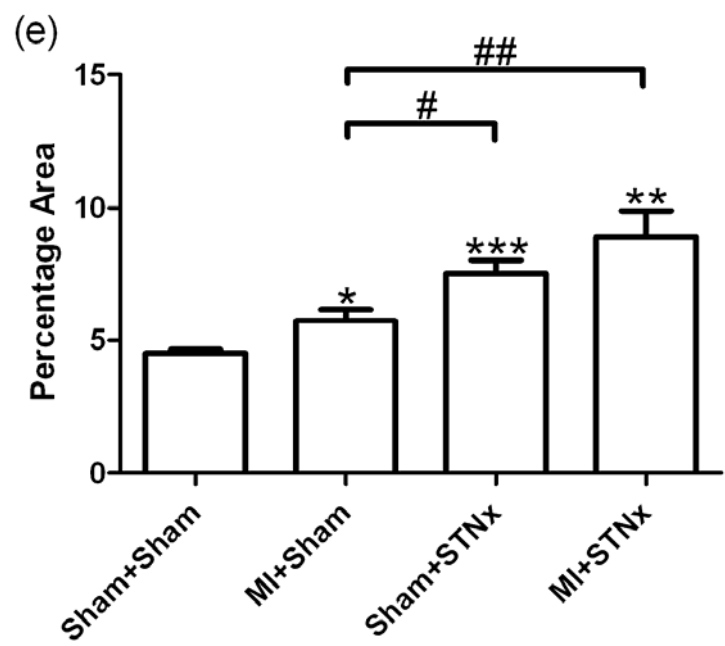
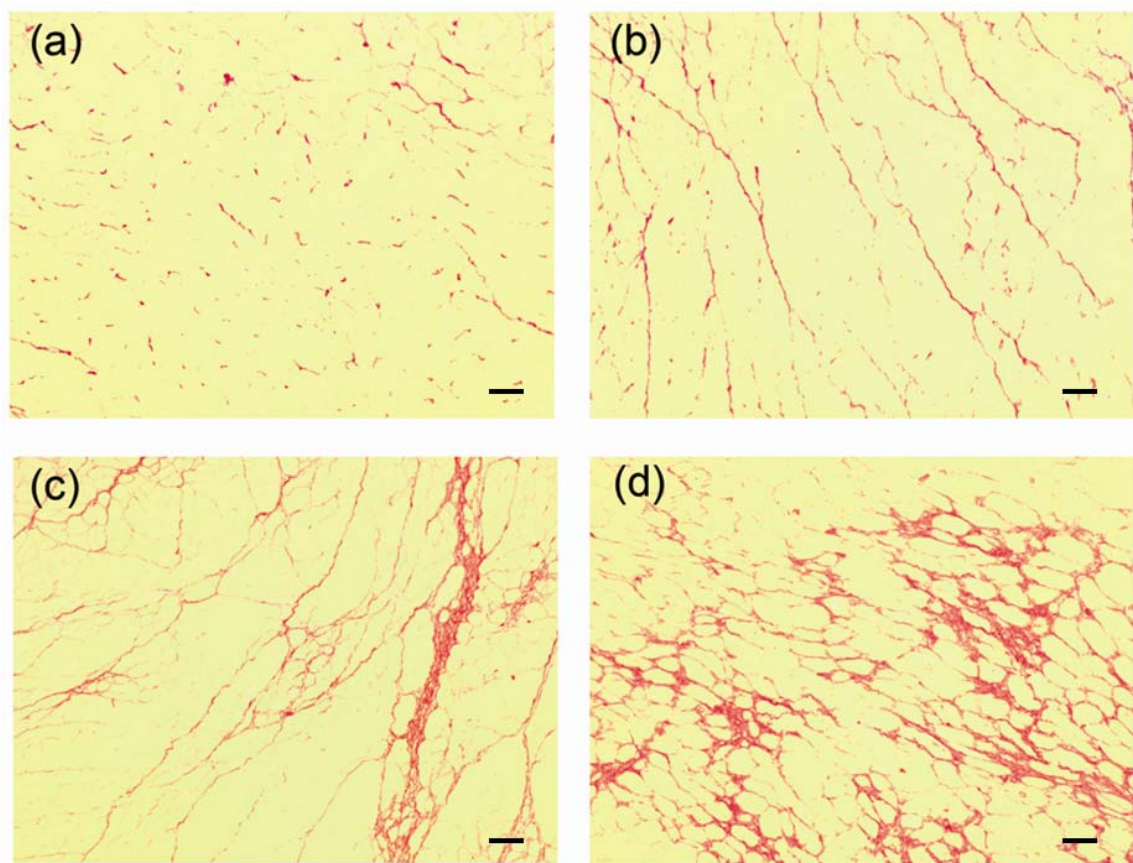


Figure 3.3 Representative images of the LV non-infarcted zone showing picrosirius red staining from the following groups (a) Sham+Sham, (b) MI+Sham, (c) Sham+STNx and (d) MI+STNx. Scale bar, 100 μ m. Quantitation of picrosirius red staining (e) showing MI+STNx animals had significantly greater cardiac interstitial fibrosis compared to the MI+Sham group. Data are expressed as mean \pm SEM. * p <0.05, ** p <0.01, *** p <0.001 vs Sham+Sham; # p <0.05, ## p <0.01 for between group comparisons.

3.4.7 Cardiac myocyte cross-sectional area

Cardiac myocyte cross-sectional area in the LV non-infarcted zone, determined from hematoxylin and eosin stained sections, was elevated by 44% in MI+STNx animals compared to the MI+Sham group (p <0.001) (Figure 3.4). The myocyte cross-sectional area was also greater in MI+Sham and Sham+STNx animals compared to Sham+Sham control animals (p <0.01 and p <0.001 respectively).

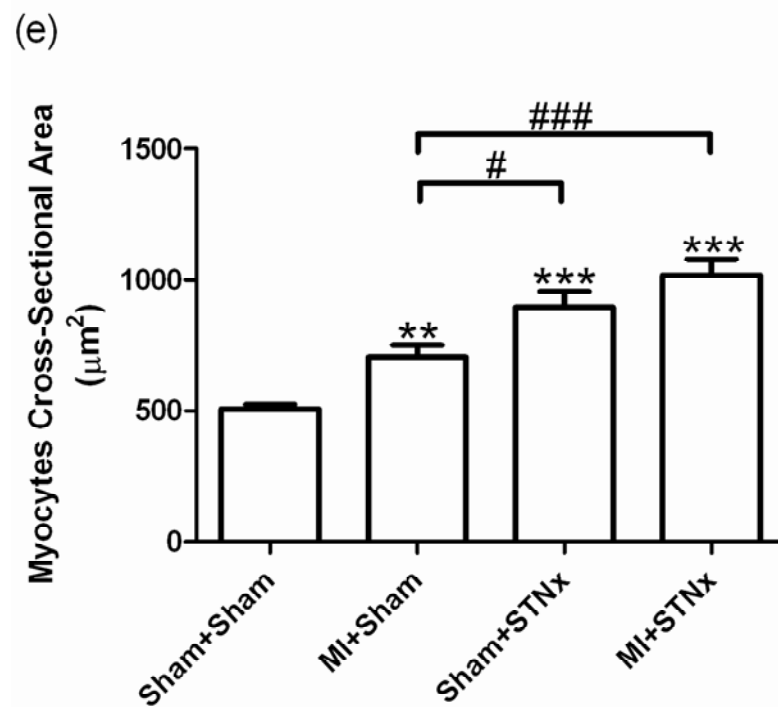
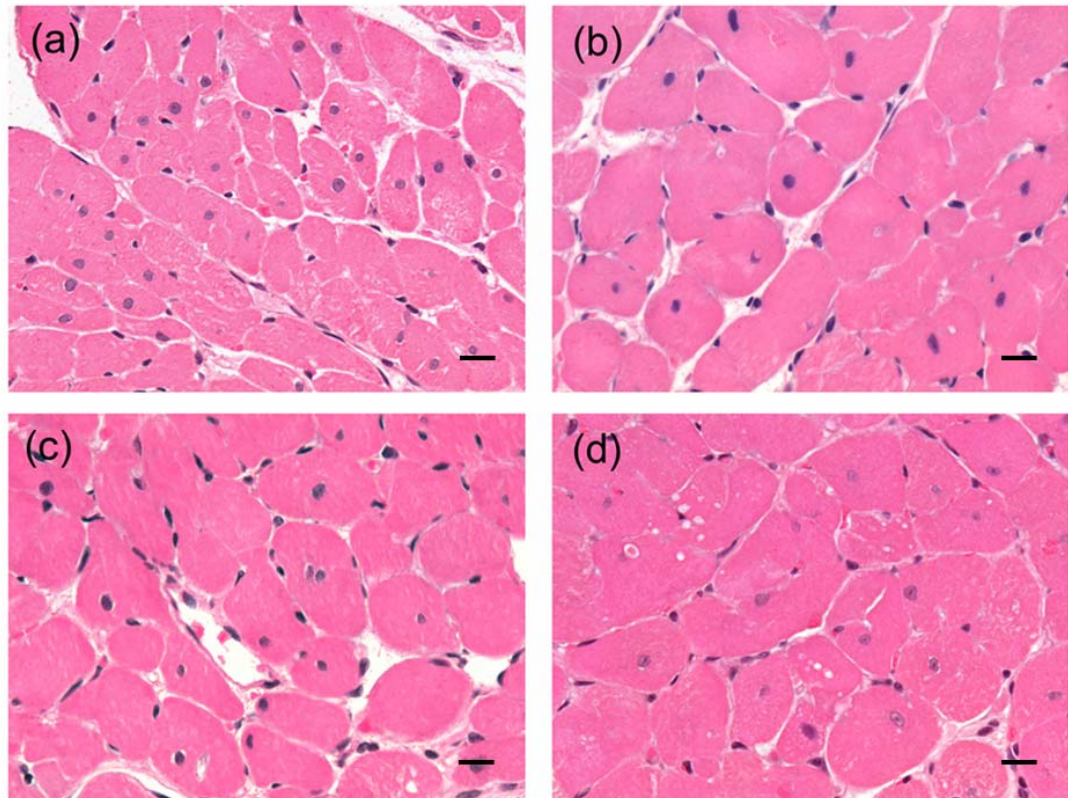


Figure 3.4 Representative images of the LV non-infarcted zone showing hematoxylin and eosin staining in myocytes from the following groups (a) Sham+Sham, (b) MI+Sham, (c) Sham+STNx and (d) MI+STNx. Scale bar, 30 μm. Quantitation of the

data (e) showing that MI+STNx animals had significantly larger cardiomyocytes compared to the MI+Sham group. Data are expressed as mean \pm SEM. ** $p < 0.01$, *** $p < 0.001$ vs Sham+Sham; # $p < 0.05$, ### $p < 0.001$ for between group comparisons.

3.4.8 Renal function and indoxyl sulfate plasma levels

There was no difference in renal function among the groups at week 4 (Table 3.6). At week 14, both STNx groups developed severe renal dysfunction as indicated by reduced GFR, reduced creatinine clearance and increased proteinuria compared to the sham-operated animals. However, no further deterioration was observed between MI+STNx and Sham+STNx groups.

There was no difference in IS plasma levels among the groups at week 4 (Table 3.6). Both STNx groups had significantly higher IS plasma levels at week 14, and there was no significant difference between the STNx groups.

Table 3.6 Renal function and indoxyl sulfate plasma levels at week 4 and 14. Both STNx groups developed severe renal dysfunction and had increased indoxyl sulfate levels compared to the sham-operated animals at week 14. Values are expressed as mean \pm SEM. GFR, glomerular filtration rate; CrCl, creatinine clearance; IS, indoxyl sulfate. * $p<0.05$, ** $p<0.01$, *** $p<0.001$ vs Sham+Sham; § $p<0.05$, §§ $p<0.01$, §§§ $p<0.001$ vs MI+Sham.

	Week 4				Week 14			
	Sham+Sham	MI+Sham	Sham+STNx	MI+STNx	Sham+Sham	MI+Sham	Sham+STNx	MI+STNx
GFR (ml/min/kg)	10.0 \pm 1.1	11.2 \pm 0.9	12.1 \pm 0.4	11.3 \pm 0.9	8.4 \pm 0.3	6.9 \pm 0.8	1.1 \pm 0.5 ***, §§§	1.5 \pm 0.4 ***, §§§
CrCl (ml/min)	206.4 \pm 14.5	162.3 \pm 22.4	202.1 \pm 24.1	185.1 \pm 13.1	222.8 \pm 27.5	192.6 \pm 36.9	33.7 \pm 12.4 ***, §§	33.8 \pm 7.9 ***, §§§
Serum creatinine (μmol/L)	28.2 \pm 1.0	29.3 \pm 1.1	30.6 \pm 0.7	29.4 \pm 0.5	37.9 \pm 4.7	45.3 \pm 6.7	101.8 \pm 12.3 ***, §§	110.4 \pm 25.3 *
Proteinuria (mg/24 hr)	20.1 \pm 1.5	16.9 \pm 1.1	19.6 \pm 1.4	14.8 \pm 1.9	24.8 \pm 2.2	20.4 \pm 1.7	391.4 \pm 60.1 ***, §§§	433.7 \pm 87.1 ***, §§§
IS (μmol/L)	13.08 \pm 0.81	14.43 \pm 4.16	16.79 \pm 2.32	19.58 \pm 2.54	11.93 \pm 2.87	13.77 \pm 1.66	67.28 \pm 17.20 **, §	64.05 \pm 13.85 *, §

3.4.9 Renal tubulointerstitial fibrosis

MI+Sham ($p<0.05$), Sham+STNx ($p<0.001$) and MI+STNx ($p<0.001$) animals demonstrated significantly greater tubulointerstitial fibrosis in the non-infarcted zone of the kidney compared to Sham+Sham control group (Figure 3.5). Sham+STNx and MI+STNx groups had greater renal tubulointerstitial fibrosis compared to the MI+Sham group ($p<0.001$). MI+STNx animals had incrementally greater fibrosis compared to the Sham+STNx group ($p<0.001$).

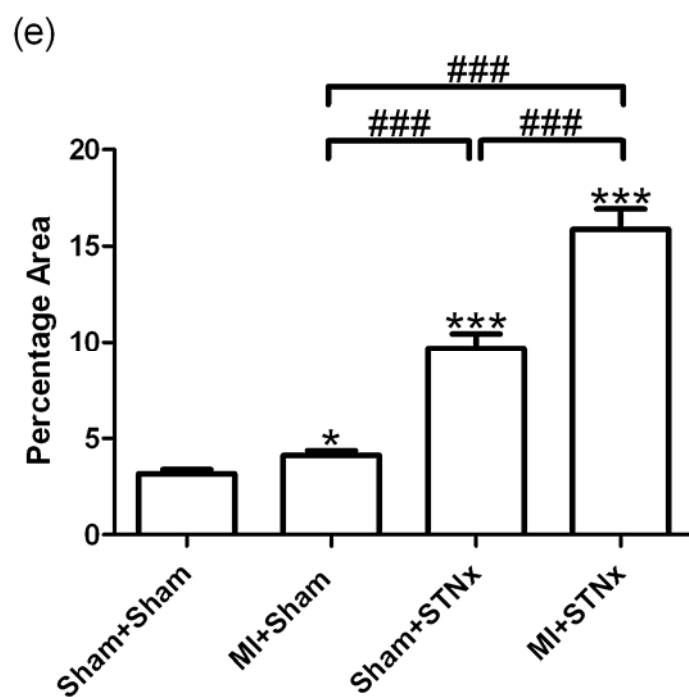
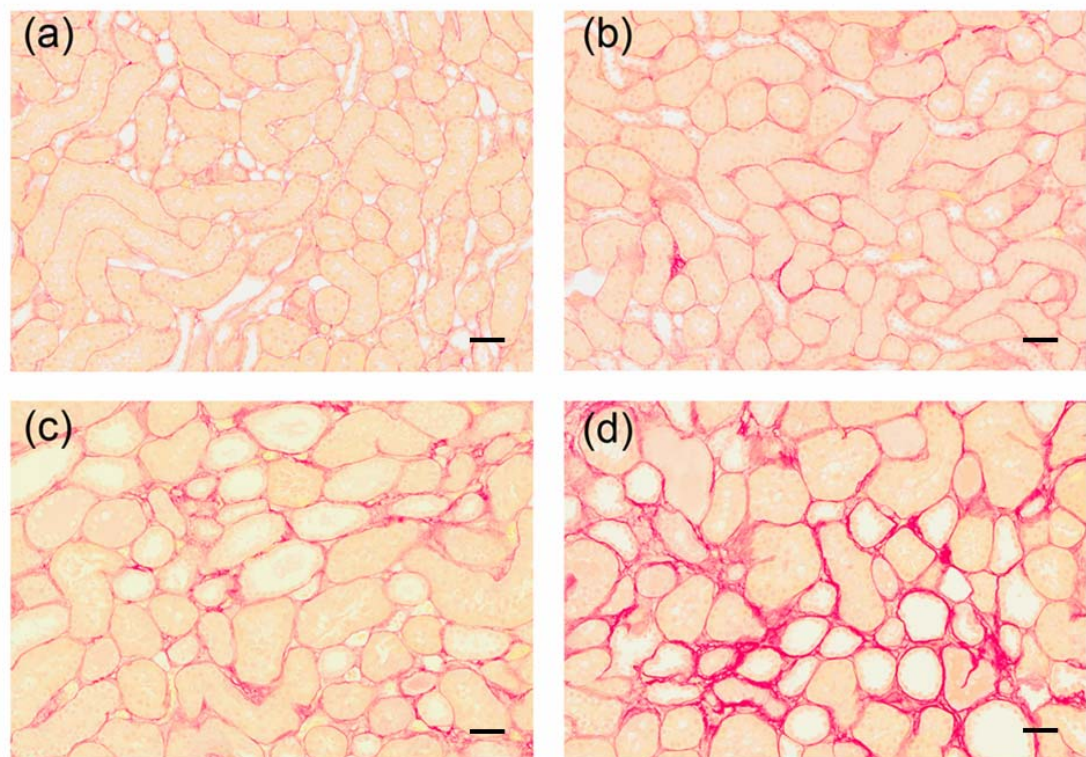


Figure 3.5 Representative images of the non-infarcted zone of the kidney showing picosirius red staining from the following groups (a) Sham+Sham, (b) MI+Sham, (c) Sham+STNx and (d) MI+STNx. Scale bar, 50 μ m. Quantitation of renal fibrosis (e)

showing MI+STNx animals had significantly greater tubulointerstitial fibrosis compared to all other groups. Data are expressed as mean \pm SEM. * $p < 0.05$, *** $p < 0.001$ vs Sham+Sham; ### $p < 0.001$ for between group comparisons.

3.5 Discussion

This chapter demonstrates that MI followed by STNx may be a potentially useful model to assess the functional and structural changes underlying CRS in this setting. Impairment of cardiac function and accelerated cardiac remodelling as well as increased renal tubulointerstitial fibrosis was observed in animals that underwent MI followed by STNx. These findings are of considerable interest as this model appears to successfully recapitulate features of the phenotype of both ventricular remodelling and kidney impairment which occurs clinically.

Few studies have investigated the effects of MI on animals with primary CKD, however no report has described the effects of kidney injury on animals with a primary cardiac disease.³²⁷ A previous study examining a model of UNX followed by MI did not reproduce the condition of primary CKD contributing to decreased cardiac function as renal function was preserved in those animals,^{246, 248} suggesting UNX takes longer for renal impairment to evolve. In this study, we allowed 4 weeks post-MI for animals to develop cardiac dysfunction before inducing STNx, a further 10-week allows for the development of CKD whilst at the same time preserving survival as much as possible to permit adequate tissue analysis. To our knowledge, this study is the first description of progressive functional and structural changes on heart and kidney in a preclinical model of MI followed by STNx that implicates features of the phenotype of CRS.³

Worsening renal function in the context of HF is associated with adverse outcomes.⁴ Reflecting this, mortality was increased by 26% in MI+STNx animals compared to the MI+Sham group, despite no difference in infarct size. Survival rate was reduced by 51.9% compared to Sham+STNx animals with an attenuation rather than an increase in BP in MI+STNx animals.

Both MI groups developed systolic dysfunction, as indicated by significant decreases in LVEF and FS at 4 weeks post-MI. The subsequent STNx accelerated the progression of cardiac remodelling leading to a further reduction in LVEF and FS in MI+STNx animals compared to the MI+Sham group.

A prominent cardiac remodelling event associated with functional alterations is myocardial fibrosis. STNx increased cardiac interstitial fibrosis in the non-infarcted myocardium. This increased fibrosis in the LV impeded cardiac relaxation and led to a deterioration in diastolic function as observed by significant increases in A wave velocity and tau logistic in MI+STNx animals compared to the MI+Sham group.

Compensatory eccentric hypertrophy of the viable myocardium also contributes to ventricular dysfunction.³²⁸ Enlargements in cardiac myocyte cross-sectional area and increases in heart weight were observed in MI+STNx animals compared to the MI+Sham group, which may be contributory to and reflective of the detrimental effects of pathological cardiac remodelling.^{83, 329}

Cardiac remodelling was also accompanied by pulmonary congestion as lung weight was significantly increased in MI+STNx animals compared to the MI+Sham group. It is therefore likely that MI+STNx animals had some degree of decompensated HF.

Renal tubulointerstitial fibrosis, another pathological process occurring post-MI was accelerated by STNx. Renal tubulointerstitial fibrosis in the non-infarcted region of the kidney was increased in MI+STNx animals despite a significantly lower BP compared to the Sham+STNx group, indicating that this detrimental effect had a BP-independent component.

Myocardial fibrosis was more pronounced post-STNx with no difference between Sham+STNx and MI+STNx groups, irrespective of the presence of a MI. However, post-MI renal tubulointerstitial fibrosis was accelerated by STNx. These suggest that the pre-existing CHF may exacerbate CKD more than the development of CKD could accelerate myocardial fibrosis. Myocardial dysfunction may impact more on kidney pathology than CKD on cardiac dysfunction.

Two insults within a 4-week period may not ideally replicate the clinical scenario of heart failure followed by renal insufficiency and is a limitation of the current study. However, the features of accelerated organ worsening have clinical implications. Functional changes in the kidney between MI+STNx and Sham+STNx animals were not observed, at least at the 14-week time-point. We did, however, observe structural changes in the kidney which were greater in MI+STNx compared to Sham+STNx animals. This may translate to functional changes over a time period beyond our study duration (10 weeks post STNx). Alternatively, the insult induced by STNx may be so

aggressive that a further reduction in renal function following MI was difficult to observe.

In conclusion, this chapter has systematically examined the functional and structural changes in the heart and kidney in the setting of MI followed by STNx. STNx accelerates cardiac hypertrophy, fibrosis and cardiac dysfunction post-MI, whilst MI accelerates STNx-induced renal fibrosis. These findings have clinical implications with regard to the pathophysiology of the so-called CRS in man specifically renal impairment post MI, and it may represent a useful preclinical model that recapitulates some of the clinical features of this condition. We have thus established a new proof-of-concept CRS model to improve our understanding of organ crosstalk and assess the efficacy of potential therapies in attenuating both cardiac and renal injury in the CRS setting.

Chapter 4 Pathological and Mechanistic Investigations in the MI+STNx Model

4.1 Introduction

In Chapter 3, a new model of MI followed by STNx was established and the functional and structural changes in heart and kidney were investigated in this setting. The findings showed that STNx further accelerated cardiac dysfunction compared to the MI alone group. Cardiac interstitial fibrosis and cardiac myocyte cross-sectional area was increased in MI+STNx vs MI+Sham animals. In comparison with the Sham+STNx group, renal tubulointerstitial fibrosis was increased in MI+STNx animals, with no further deterioration in renal function. The pathology and mechanisms by which the onset of CHF leads to CKD are multiple and complex.^{3, 330} In this chapter we sought to systematically examine the pathological and mechanistic alterations linked with the observed cardiac and renal changes in above setting.

4.2 Aims

To investigate the pathological and mechanistic alterations contributory to the functional and structural changes in the setting of MI followed by STNx.

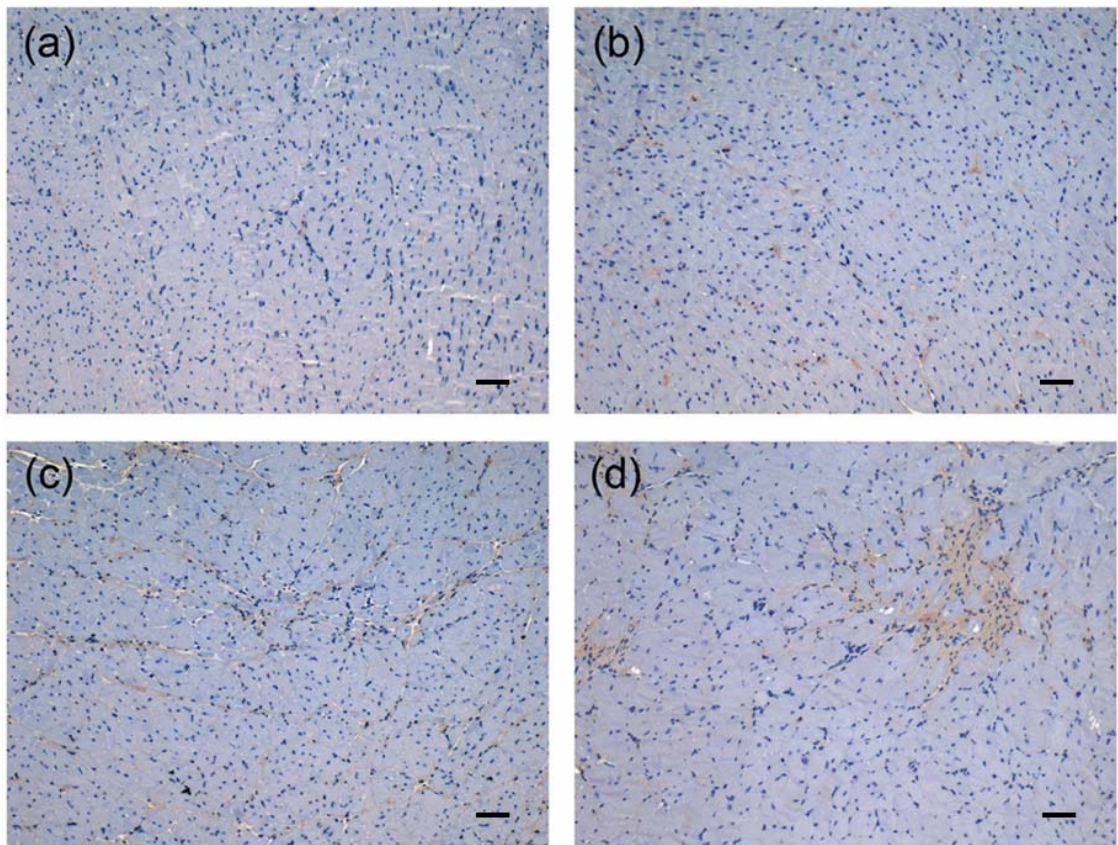
4.3 Materials and Methods

Molecular changes in heart and kidney were determined by tissue assessments using immunohistochemistry, real-time PCR and western blot analyses as per Chapter 2.1.15-2.1.19.

4.4 Results

4.4.1 Cardiac collagen I and III

Antibody staining for collagen I in the non-infarcted myocardium was significantly increased in MI+STNx animals compared to the MI+Sham group ($p<0.01$) (Figure 4.1). MI+Sham, Sham+STNx and MI+STNx animals had significantly increased levels of collagen I compared to the Sham+Sham control group.



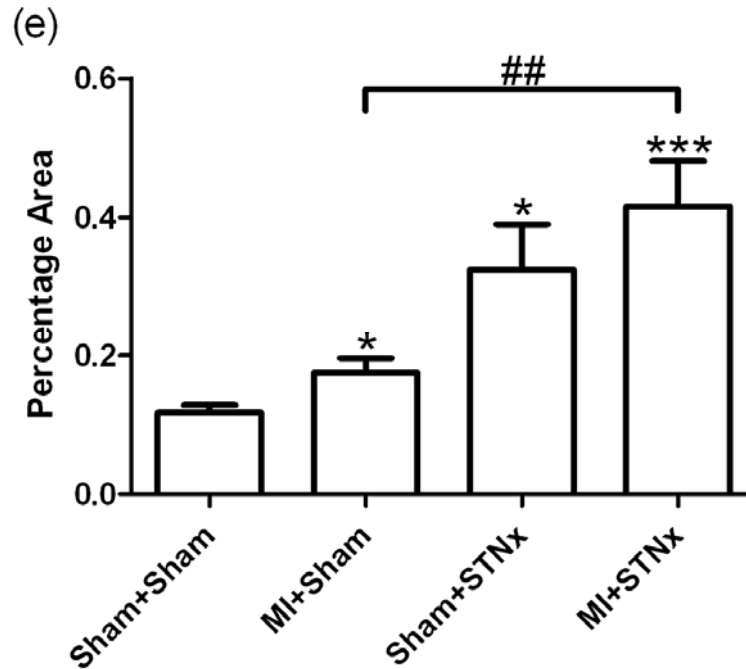


Figure 4.1 Representative images of the LV non-infarcted zone showing collagen I immunostaining from the following groups (a) Sham+Sham, (b) MI+Sham, (c) Sham+STNx and (d) MI+STNx. Scale bar, 30 μ m. Quantitation of collagen I (e) showing MI+STNx animals had significantly greater immunostaining compared to the MI+Sham group. Data are expressed as mean \pm SEM. * p <0.05, *** p <0.001 vs Sham+Sham; ## p <0.01 for between group comparisons.

Antibody staining for collagen III in the LV non-infarcted zone was non-significantly elevated between MI+STNx and MI+Sham groups (p =0.08) (Figure 4.2). Sham+STNx and MI+STNx animals had greater collagen III immunostaining compared to the Sham+Sham control group (p <0.05).

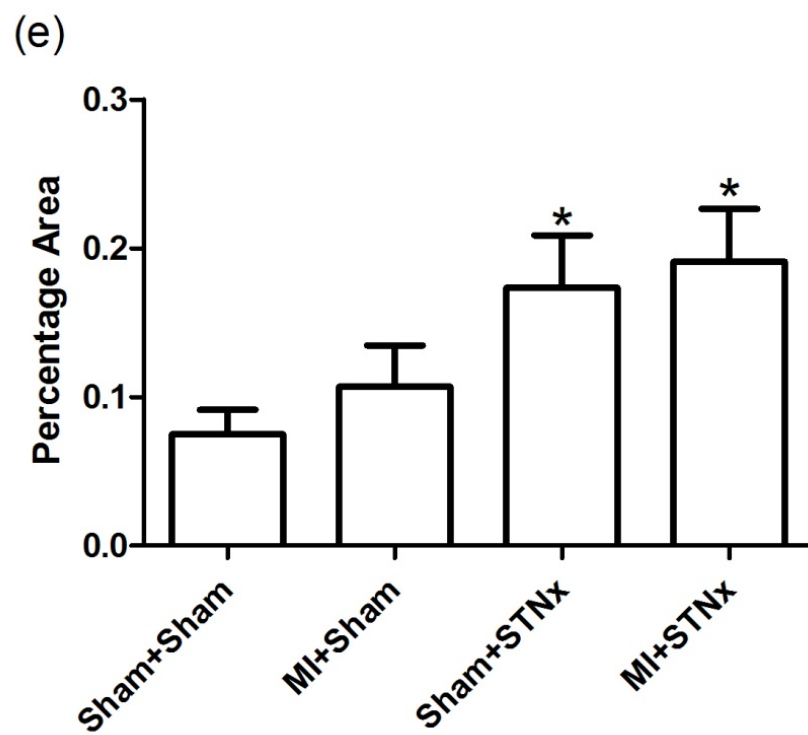
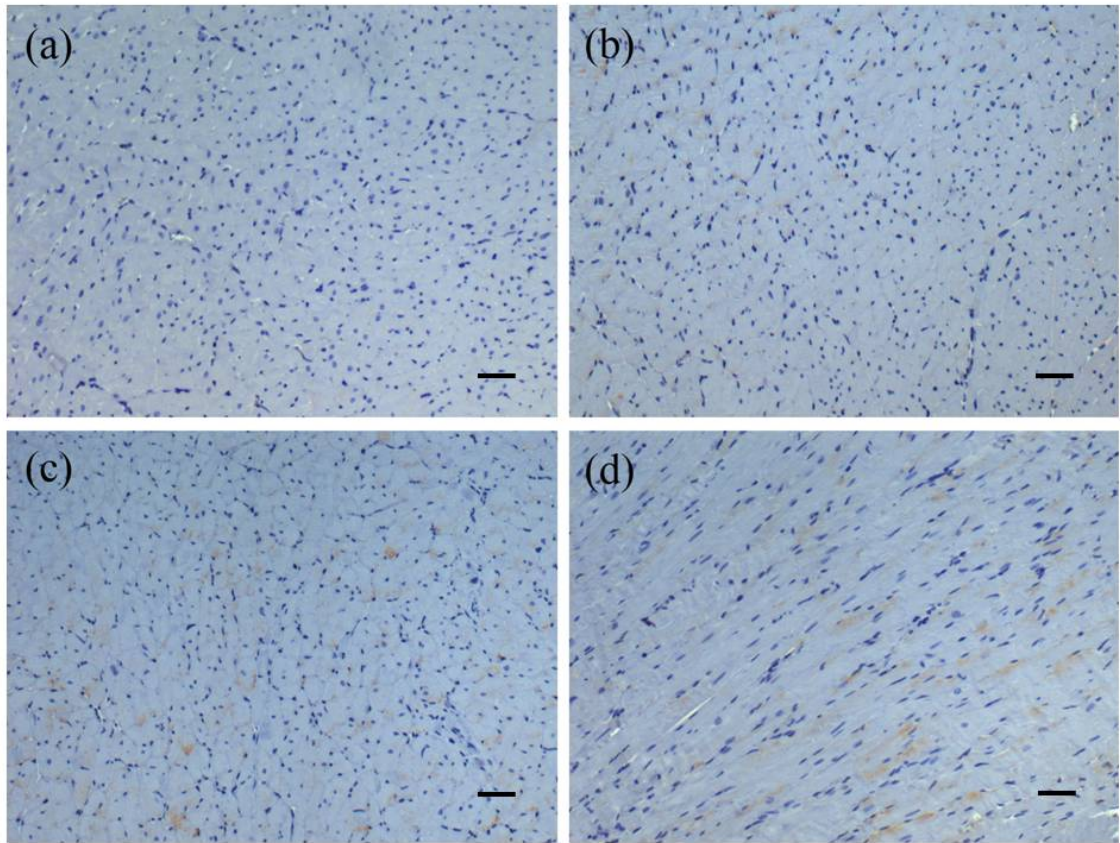


Figure 4.2 Representative images of the LV non-infarcted zone showing collagen III immunostaining from the following groups (a) Sham+Sham, (b) MI+Sham, (c) Sham+STNx and (d) MI+STNx. Scale bar, 30 μ m. Quantitation of collagen III (e) showing Sham+STNx and MI+STNx animals had significantly greater immunostaining compared to the Sham+Sham group. Data are expressed as mean \pm SEM. * $p < 0.05$ vs Sham+Sham.

4.4.2 Cardiac mRNA expression

Real time PCR was used to determine gene expression of the pro-fibrotic markers TGF β_1 , CTGF and collagen I in the LV non-infarcted zone (Figure 4.3 a-c). Compared to the Sham+Sham control animals, TGF β_1 and collagen I were significantly increased in the Sham+STNx and MI+STNx groups ($p < 0.05$), whereas CTGF expression was significantly elevated in the MI+Sham and MI+STNx groups ($p < 0.05$). TGF β_1 and collagen I, but not CTGF showed significant increases in MI+STNx animals compared to the MI+Sham group ($p < 0.05$).

The hypertrophic marker ANP was increased in Sham+STNx and MI+STNx animals compared to the Sham+Sham control group ($p < 0.05$ and $p < 0.001$ respectively) (Figure 4.3 d). In MI+STNx animals ANP was significantly elevated compared to either MI+Sham or Sham+STNx group ($p < 0.001$ and $p < 0.01$ respectively). The hypertrophic marker β -MHC was significantly increased in MI+Sham and MI+STNx animals compared to the Sham+Sham control group ($p < 0.05$), but there was no significant difference between MI+STNx and MI+Sham groups (Figure 4.3 e).

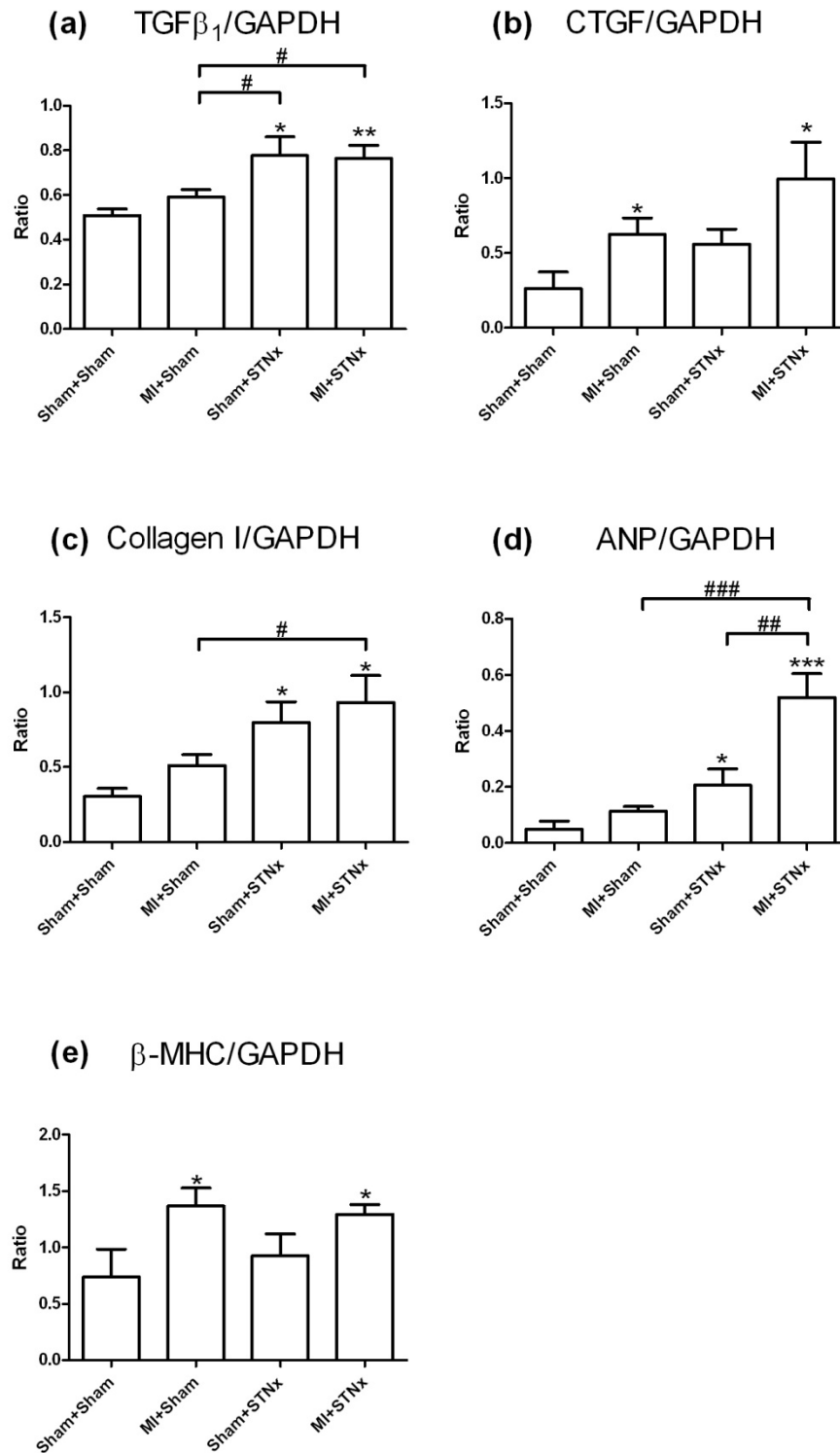
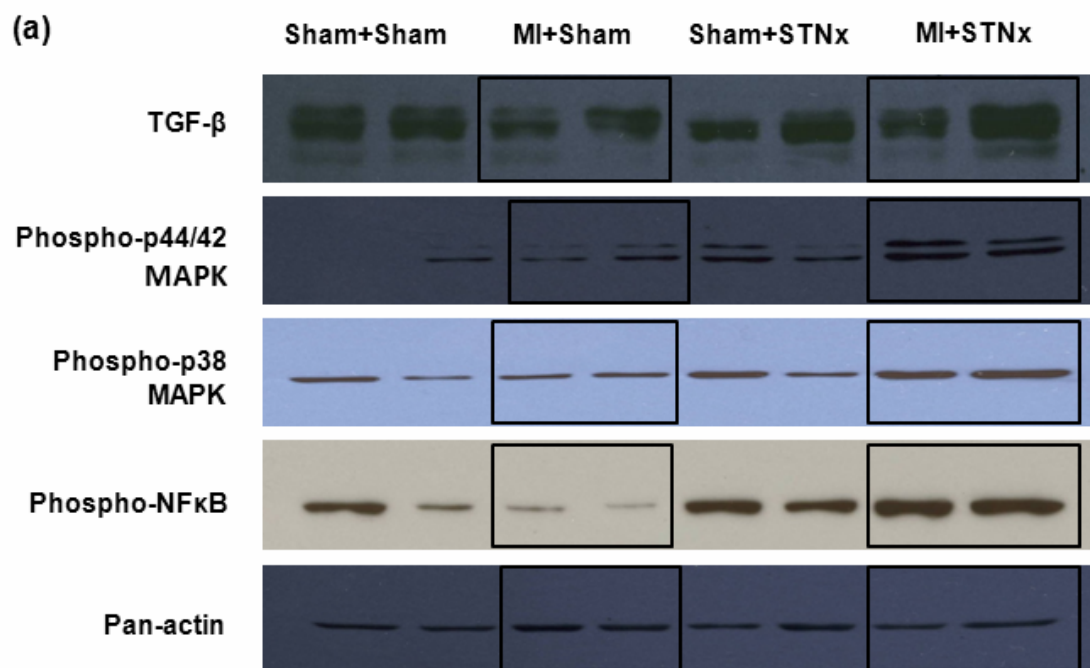


Figure 4.3 Cardiac mRNA expression of pro-fibrotic markers TGF β_1 (a), CTGF (b) and collagen I (c), and hypertrophic markers ANP (d) and β -MHC (e), expressed as a ratio of GAPDH in the LV non-infarcted zone. Data are expressed as mean \pm SEM.

* $p < 0.05$, ** $p < 0.01$, *** $p < 0.001$ vs Sham+Sham; # $p < 0.05$, ## $p < 0.01$, ### $p < 0.001$ for between group comparisons.

4.4.3 Cardiac signalling pathway activation

Activation of phospho-smad2 was not detectable in the LV non-infarcted zone using western blot analysis. Although no significant differences in the levels of TGF- β , phospho-p44/42 MAPK, phospho-p38 MAPK and phospho-NF κ B were found among the groups, there was an indicating trend towards an increase in TGF- β between Sham+Sham and MI+STNx groups (Figure 4.4).



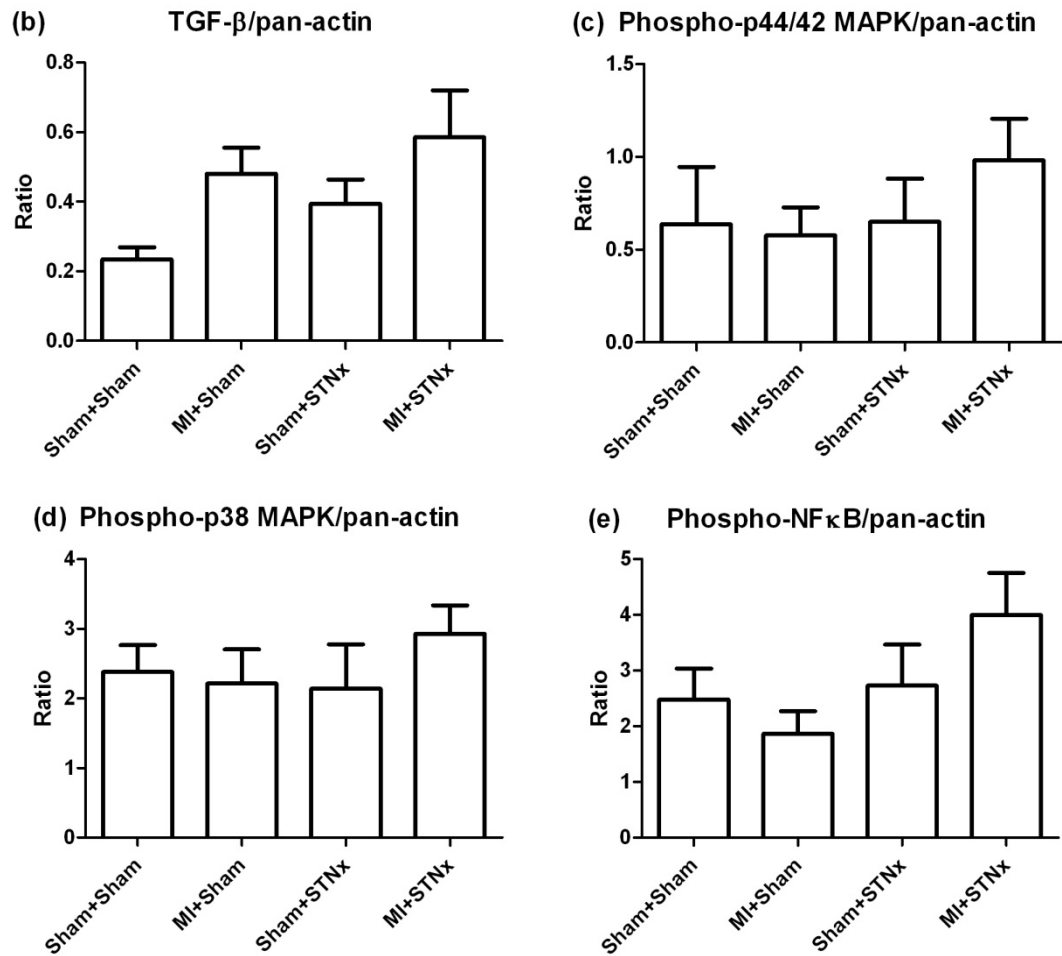


Figure 4.4 Representative images of the western blot analysis results showing cardiac protein levels in the LV non-infarcted zone from Sham+Sham, MI+Sham, Sham+STNx and MI+STNx groups (a). Quantitation of the protein levels of TGF-β (b), phospho-p44/42 MAPK (c), phospho-p38 MAPK (d), and phospho-NFκB (e) in the non-infarcted myocardium after normalization with pan-actin. Data are expressed as mean ± SEM.

4.4.4 Renal injury biomarker

Both STNx groups (Sham-operated MI and MI) demonstrated significantly greater tissue levels of kidney injury molecule-1 (KIM-1) in the non-infarcted cortex region of

the kidney compared to the sham-operated animals (Figure 4.5). No significant difference was observed between the STNx groups.

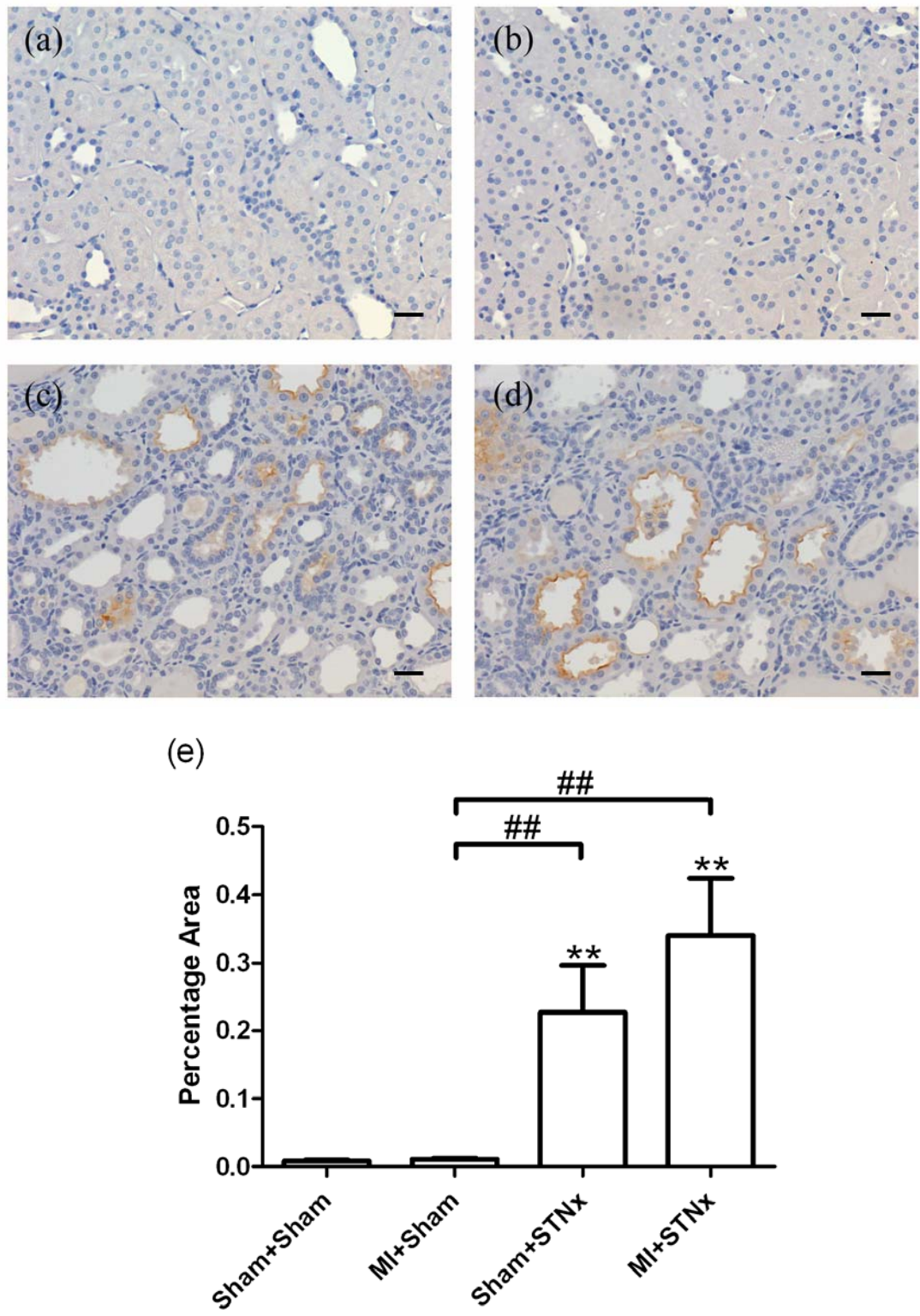
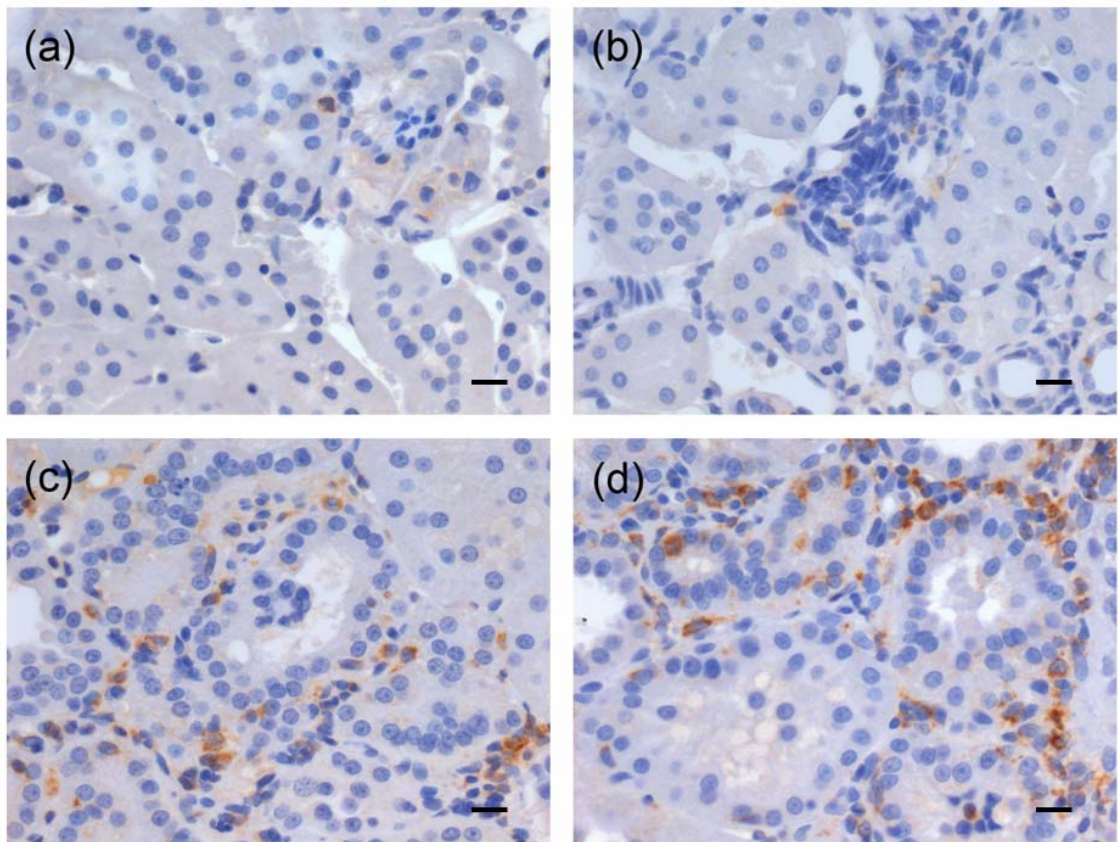


Figure 4.5 Representative images of the non-infarcted cortex region of the kidney showing immunostaining of the kidney injury molecule-1 (KIM-1) from the following groups (a) Sham+Sham, (b) MI+Sham, (c) Sham+STNx and (d) MI+STNx. Scale bar, 30 μ m. Quantitation of KIM-1 (e) showing STNx groups had significantly greater immunostaining compared to the sham-operated animals. Data are expressed as mean \pm SEM. ** $p < 0.01$ vs Sham+Sham; $^{##}p < 0.01$ for between group comparisons.

4.4.5 Renal macrophage infiltration

Both STNx groups had increased renal macrophage infiltration in the non-infarcted cortex region of the kidney compared to the sham-operated animals (Figure 4.6). No significant difference was observed between the STNx groups.



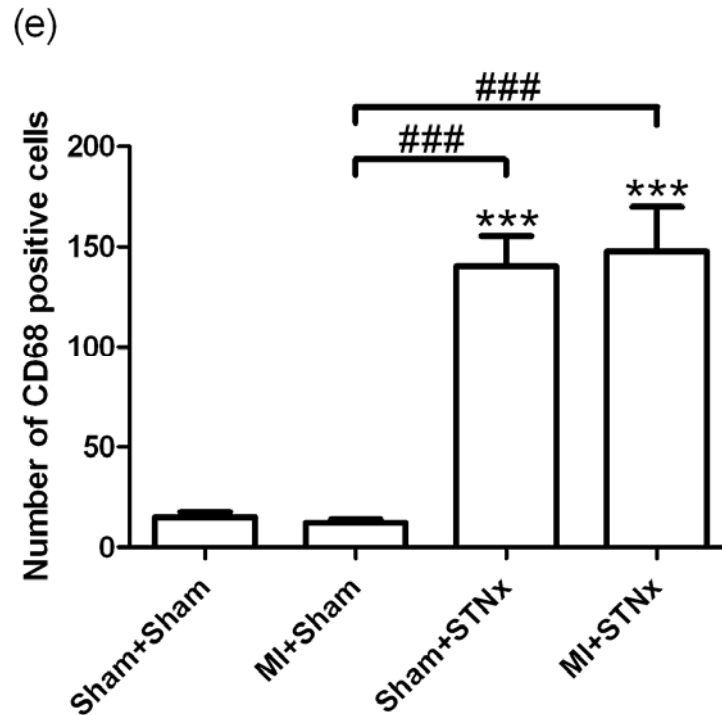


Figure 4.6 Representative images of the non-infarcted cortex region of the kidney showing immunostaining of macrophage infiltration from the following groups (a) Sham+Sham, (b) MI+Sham, (c) Sham+STNx and (d) MI+STNx. Scale bar, 30 μ m. Quantitation of number of CD68 positive cells (e) showing STNx groups had significantly increased macrophage infiltration compared to the sham-operated animals. Data are expressed as mean \pm SEM. ***p<0.001 vs Sham+Sham; ###p<0.001 for between group comparisons.

4.4.6 Renal mRNA expression

Renal pro-fibrotic markers TGF β ₁ and collagen IV as well as pro-inflammatory cytokine IL-6 were significantly increased in STNx groups compared to the sham-operated animals (Figure 4.7); and no further increase was observed between the STNx groups.

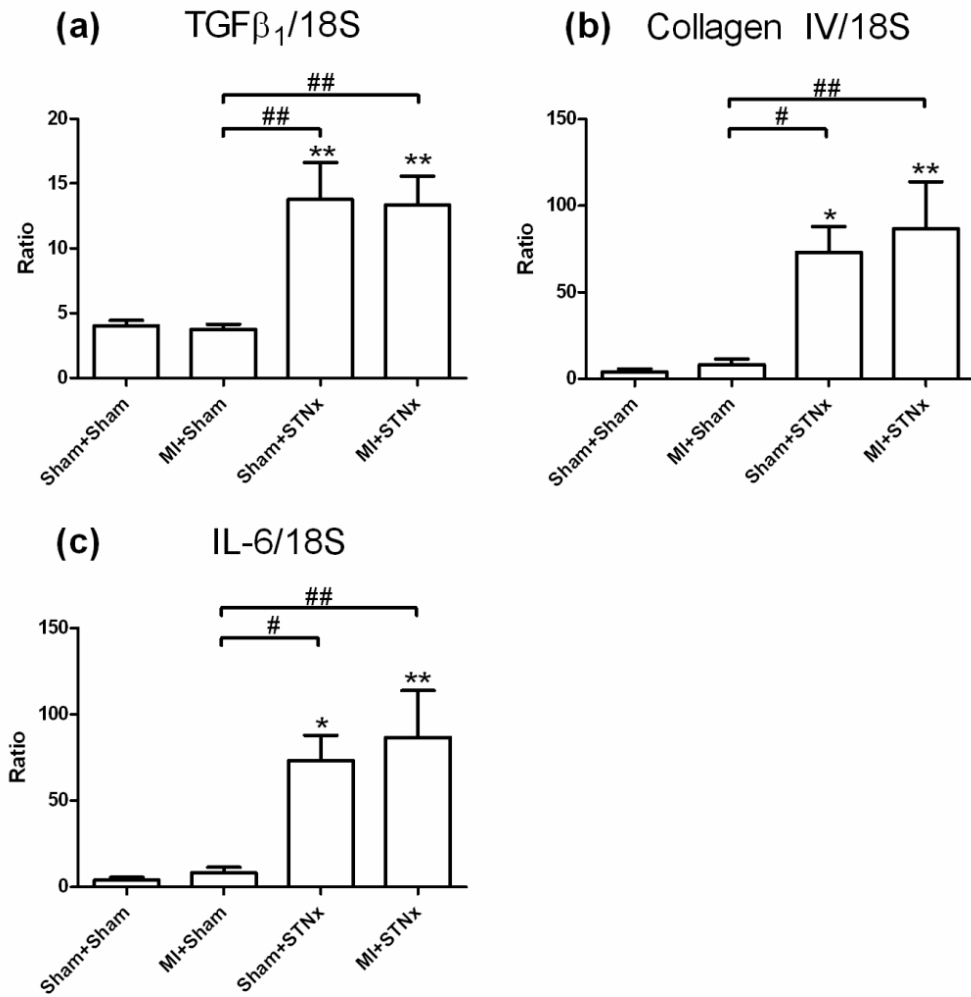
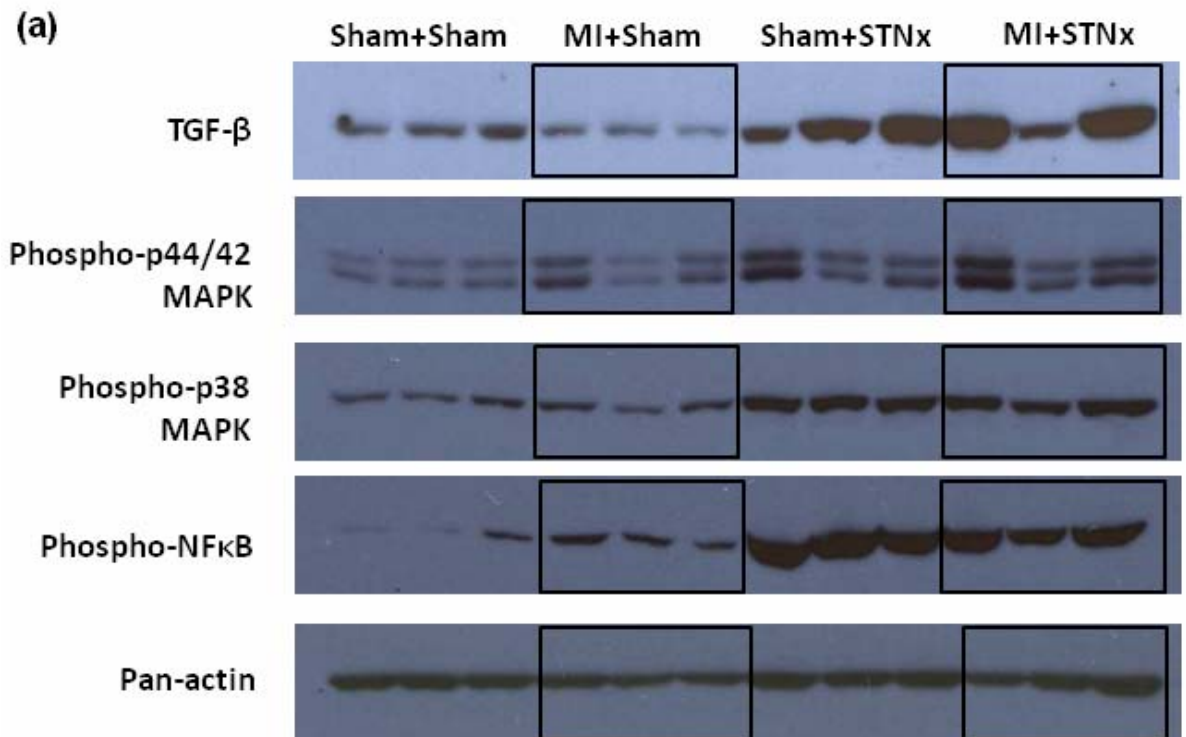


Figure 4.7 Renal mRNA expression of pro-fibrotic markers TGFβ₁ (a) and collagen IV (b); and the pro-inflammatory cytokine IL-6 (c) in the kidney, expressed as a ratio of 18S. STNx groups had greater TGFβ₁, collagen IV and IL-6 gene expression compared to the sham-operated animals. Data are expressed as mean ± SEM. *p<0.05, **p<0.01 vs Sham+Sham; #p<0.05, ##p<0.01 for between group comparisons.

4.4.7 Renal signalling pathway activation

Activation of phospho-smad2 was not detectable in the kidney on western blot. There were significant increases in the levels of TGF-β, phospho-NFκB and phospho-p38 MAPK but not phospho-p44/42 MAPK when normalized with pan-actin comparing

Sham+STNx and MI+STNx groups to the Sham+Sham control animals (Figure 4.8). The levels of TGF- β , phospho-NF κ B and phospho-p38 MAPK normalized with pan-actin were significantly up-regulated in MI+STNx animals compared to the MI+Sham group.



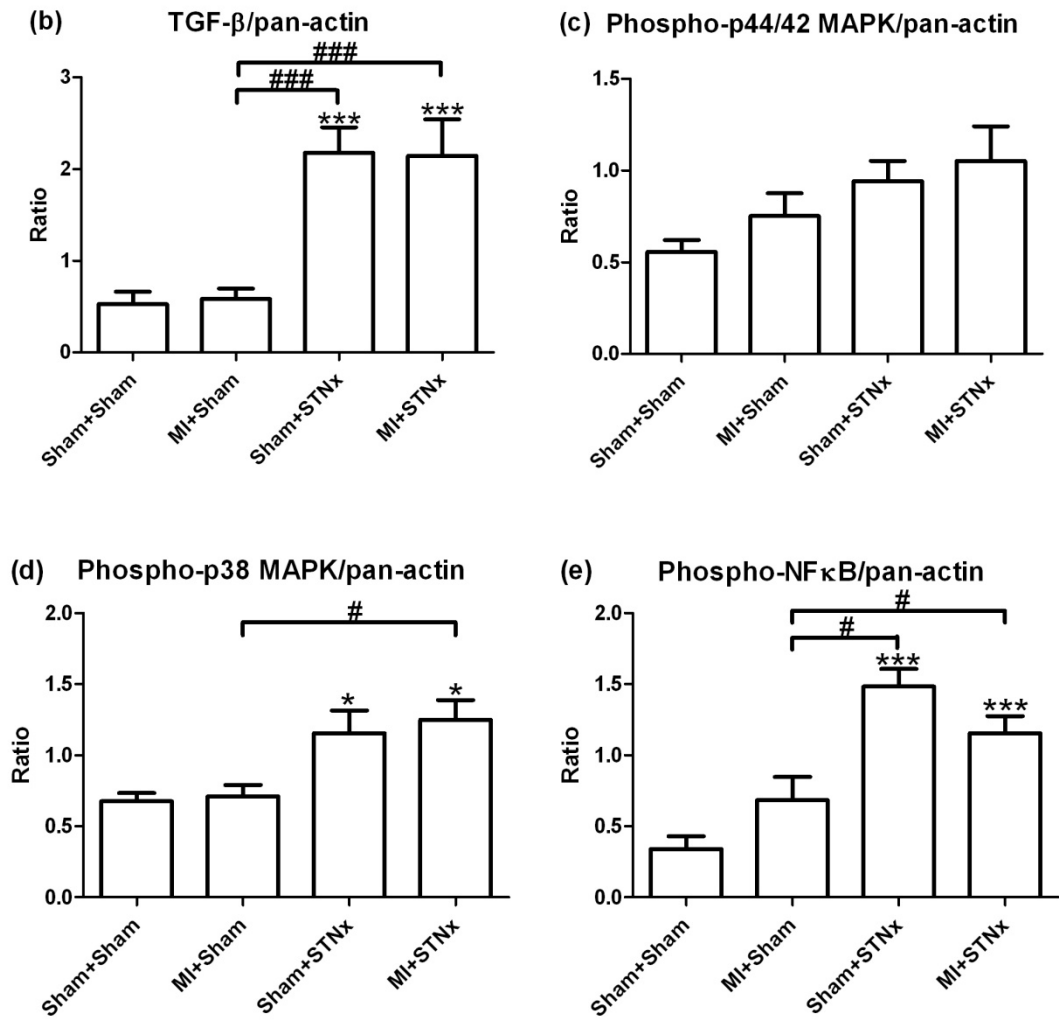


Figure 4.8 Representative images of the western blot analysis results showing renal protein levels from Sham+Sham, MI+Sham, Sham+STNx and MI+STNx groups (a). Quantitation of the protein levels of TGF-β (b), phospho-p44/42 MAPK (c), phospho-p38 MAPK (d), and phospho-NFκB (e) were normalized with pan-actin. Data are expressed as mean ± SEM. * $p < 0.05$, *** $p < 0.001$ vs Sham+Sham; # $p < 0.05$, ### $p < 0.001$ for between group comparisons.

4.5 Discussion

This chapter demonstrates the pathological and mechanistic changes contributory to LV and renal dysfunction in the setting of MI followed by STNx. The findings revealed that the hypertrophy of the viable myocardium was accompanied with significant increases in LV gene expression of the hypertrophic marker ANP in MI+STNx animals compared to the MI+Sham group.

MI+STNx animals had significantly greater protein levels of collagen I in the non-infarcted myocardium compared to the MI+Sham group, consistent with a significant elevation in cardiac interstitial fibrosis as described in Chapter 3.4.6. These changes were associated with significant increases in LV gene expression of fibrotic markers TGF β ₁ and collagen I in MI+STNx animals compared to the MI+Sham group.

A non-significant trend toward an increase in the protein levels of TGF- β between MI+STNx and Sham+Sham animals was observed in the non-infarcted LV tissues, indicating this pathway may be operating in the setting of MI+STNx. A lack of significant differences among the groups may be related to the time point of the analysis. Cardiac signalling pathway activation occurs immediately or very early in the cardiac remodelling in response to the injury.³³¹ TGF- β levels increase within the first day post-MI.³³² After inflammation has subsided, peak levels of differently activated signalling pathways are likely to decrease. Therefore, the alterations were difficult to observe at the 14 weeks time-point at which tissues were harvested.

The reduction in renal function was accompanied by significant increases in tubular injury biomarker KIM-1 and renal macrophage infiltration in STNx groups, all of

which may be contributory to the subsequent renal fibrosis as described in Chapter 3.4.9.^{333, 334}

Up-regulated gene expression of the fibrotic markers TGF β ₁ and collagen IV as well as pro-inflammatory cytokine IL-6 were observed in the kidney in STNx groups. Although differences in gene expression changes between MI+STNx and Sham+STNx animals were not observed, these are likely to have occurred considerably earlier than the 14 weeks time-point. Activation of gene expression is a dynamic process,³³⁵ hence the increases in transcription in MI+STNx animals at 14 weeks post-MI may have returned back to the levels in the Sham+STNx group.

Intensive investigation into the pathogenesis of both experimental and human renal disease has consistently implicated the role of the locally active growth factor, TGF- β in tissue fibrosis.³³⁶ Activation of TGF- β signalling subsequently enables MAPK and NF κ B activation.³³⁷ Cooperation between TGF- β induced Smad signalling and the TGF- β dependent and independent MAPK signalling contributes to the final cellular response to the renal injury.³³⁷ Increases in TGF- β , phospho-p38 MAPK and phospho-NF κ B protein levels in association with renal dysfunction and renal tubulointerstitial fibrosis were found in STNx groups compared to the Sham+Sham control group. Thus activation of fibrotic related pathways, namely TGF- β , MAPK and NF κ B, may at least in part contribute to the functional worsening and structural damage observed in STNx groups.

In conclusion, the chapter has examined pathological and mechanistic alterations underlying cardiac and renal functional changes in the setting of MI followed by STNx.

STNx accelerates cardiac protein levels of collagen I and cardiac mRNA expression of fibrotic markers $\text{TGF}\beta_1$ and collagen I post-MI. STNx also triggers increases in cardiac mRNA expression of hypertrophic marker ANP post-MI. Increases in extent of tubular injury biomarker and macrophage infiltration have been found in the kidney post-STNx. Up-regulated mRNA expression of $\text{TGF}\beta_1$, collagen IV and IL-6 and activation of fibrotic related pathways, namely $\text{TGF-}\beta$, p38 MAPK and $\text{NF}\kappa\text{B}$ have also been observed in the kidney in STNx groups. All these may at least in part contribute to the subsequent renal dysfunction.

The present animal model with functional cardiac and renal manifestations offers a proof-of-principle approach to explore the pathophysiology and mechanisms underlying CRS and its progression; and assess the efficacy of specific therapies. Given that the clinical relevance of such rodent model has to be validated based on the predictive power for both negative and positive clinical trials; further investigation needs to be directed toward determining interventional efficiency consistency with findings in human clinical studies, thus validating the relevance of this model.

Chapter 5 Functional and Structural Changes in the STN_x+MI Model

5.1 Introduction

Cardiovascular diseases and ventricular dysfunction are highly prevalent among patients with renal insufficiency. Cardiac-specific mortality rates are 10- to 20-fold higher compared with non-CKD populations.^{45, 46, 338-340} There is a graded and independent association between the severity of CKD and adverse cardiac outcomes.^{4, 47, 208, 341}

Despite several epidemiological descriptions of the kidney-heart interaction, there is some confusion regarding the pathology and mechanisms in the preclinical model of combined STNx and MI. Previous study examining the model of MI occurring secondary to STNx has been reported to cause more severe cardiac dilatation compared to MI alone.²⁵⁰ Furthermore in the combined STNx and MI animals, reduced LVEF, increased LV end diastolic pressure and prolonged time constant for isovolumic relaxation (tau logistic), but no further changes in cardiomyocyte hypertrophy were demonstrated in comparison with animals with STNx or MI alone.²⁵⁰ Surprisingly however, there was no difference in cardiac fibrosis between MI alone and the STNx followed by MI compared to sham-operated animals. In fact there was also a decrease in cardiac fibrosis in animals receiving STNx only compared to sham-operated animals. These findings are not consistent with previous studies examining cardiac fibrosis in MI or STNx only models.^{127, 251, 252}

The STNx co-morbid with MI has not caused further renal functional impairment indicated by similar levels of kidney function in STNx animals.^{250, 253} There are however differences in results examining the further structural damage in STNx

animals.^{250, 253} A previous study demonstrated more severe focal glomerulosclerosis in the combined STNx and MI compared to STNx alone.²⁵⁰ In contrast, another study indicated that an MI does not significantly induce more glomerulosclerosis between the two groups.²⁵³ Furthermore, the underlying mechanisms including activation and signalling of the potential pathways have not been investigated.

Therefore, the functional and structural changes in the model of STNx followed by MI will be investigated in this chapter. The mechanistic insights into the pathological changes will be described in Chapter 6.

5.2 Aims

To evaluate functional and structural changes in heart and kidney in a preclinical model of STNx followed by MI.

5.3 Materials and Methods

Male Sprague Dawley (SD) rats (n=36) weighing 200-250 g were randomized into four groups: Sham-operated STNx + Sham-operated MI (Sham+Sham), Sham-operated STNx + MI (Sham+MI), STNx+Sham-operated MI (STNx+Sham) and STNx+MI.

STNx or Sham surgery was induced initially and animals underwent MI or Sham surgery 4 weeks later (Figure 5.1). Systolic blood pressure (BP) was measured, and cardiac and renal function was assessed as per Chapter 2.1.4-2.1.9 prior to the MI or Sham surgery and again 8 weeks later. Hemodynamic parameters were measured prior to sacrifice, and tissues then collected for further analysis.

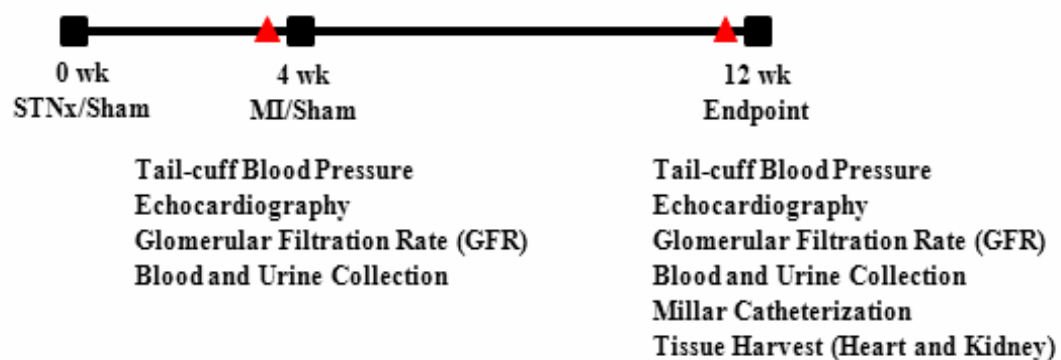


Figure 5.1 Experimental design of the STNx+MI model. STNx or Sham surgery was performed initially with each group randomised to receive MI or Sham surgery 4 weeks later. Animals were then followed for a further 8 weeks. Echocardiography, glomerular filtration rate (GFR) and blood pressure was assessed prior to the second surgery and at the end of the study. Thereafter, hemodynamic parameters were measured and tissues collected for analysis. STNx, 5/6 nephrectomy; MI, myocardial infarction.

5.4 Results

5.4.1 Survival rate and infarct size

Totally 84 animals were randomized into each group initially and 36 animals were survived at the end of the study. Survival rate was 100%, 77.8%, 60.9% and 39.8% in Sham+Sham, Sham+MI, STNx+Sham and STNx+MI animals respectively (Figure 5.2). The number of animals in each group at the endpoint is shown in Table 5.1. Animals with MI included in this study had a minimum infarct size of 20% as determined by the averaged percentage of the endocardial and epicardial scarred circumferences of the LV. No difference in infarct size was observed in both MI groups (Sham-operated STNx and STNx) (Table 5.1).

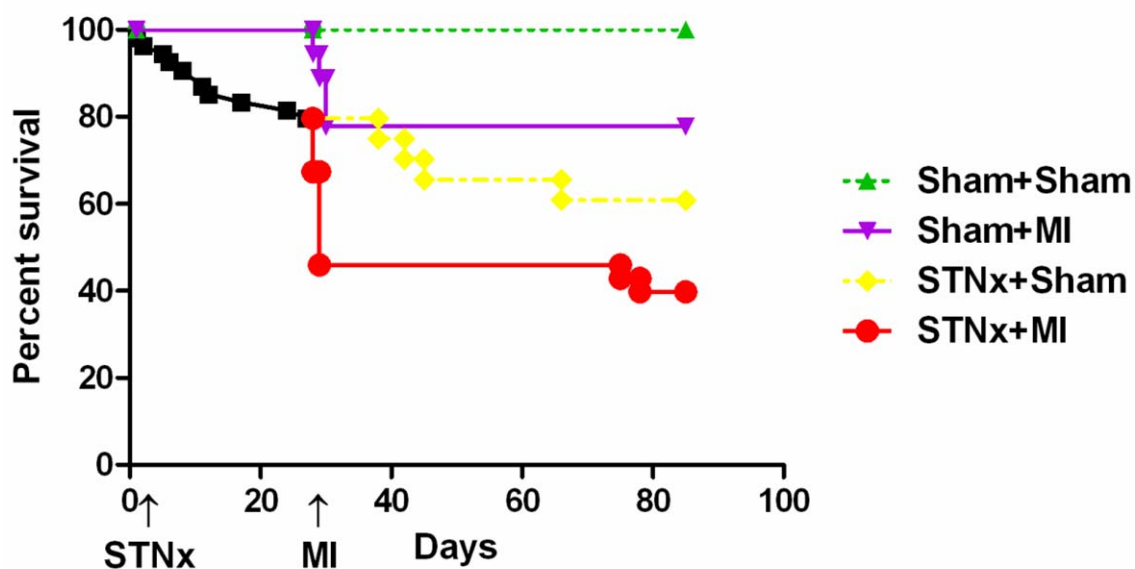


Figure 5.2 Kaplan-Meier curves for groups of Sham+Sham, Sham+MI, STNx+Sham and STNx+MI animals respectively.

Table 5.1 Animal number and infarct size. There was no difference in infarct size between Sham+MI and STNx+MI animals. Values are mean \pm SEM.

	Sham+Sham	Sham+MI	STNx+Sham	STNx+MI
Animal Number	10	7	12	7
Infarct size (%)	-	36.3 \pm 3.6	-	34.4 \pm 2.4

5.4.2 Blood pressure

As a consequence of kidney injury, both STNx groups (Sham-operated MI and MI) had significantly increased BP compared to sham-operated animals as measured at week 4 and 12 respectively (Table 5.2). No difference in BP was observed between the STNx groups.

Table 5.2 Blood pressure (BP) assessed at week 4 and 12. Values are mean \pm SEM.

***p<0.001 vs Sham+Sham; \$\$\$p<0.001 vs Sham+MI.

	Week 4				Week 12			
	Sham+Sham	Sham+MI	STNx+Sham	STNx+MI	Sham+Sham	Sham+MI	STNx+Sham	STNx+MI
BP (mmHg)	120.3 \pm 5.7	117.9 \pm 3.0	193.3 \pm 6.2 ***, \$\$\$	178.3 \pm 6.7 ***, \$\$\$	138.3 \pm 4.4	130.1 \pm 8.8	221.8 \pm 9.1 ***, \$\$\$	204.9 \pm 11.6 ***, \$\$\$

5.4.3 Tissue weights

STNx+MI animals had significantly increased heart, LV, right ventricular, atria and left kidney weights compared to the Sham+MI group (Table 5.3). Heart and right ventricular weights were significantly higher in STNx+MI compared to STNx+Sham animals. A non-significant increase in left kidney weight was observed in STNx+MI compared to STNx+Sham animals (p=0.06).

Table 5.3 Animal tissue weights that are corrected for body weight (BW). Values are mean \pm SEM. *p<0.05, **p<0.01, ***p<0.001 vs Sham+Sham; §p<0.05, §§p<0.01, §§§p<0.001 vs Sham+MI; #p<0.05, ###p<0.001 vs STNx+Sham.

	Sham+Sham	Sham+MI	STNx+Sham	STNx+MI
Heart weight/BW ratio (mg/g)	2.43 \pm 0.03	2.90 \pm 0.11 ***	3.74 \pm 0.12 ***, §	4.57 \pm 0.44 ***, §§§, #
Lung weight/BW ratio (mg/g)	2.87 \pm 0.17	3.73 \pm 0.54	3.74 \pm 0.07	4.10 \pm 0.41 *
Left ventricular weight/BW ratio (mg/g)	1.69 \pm 0.02	1.98 \pm 0.10	2.85 \pm 0.11 **, §§§	3.41 \pm 0.40 ***, §§§
Right ventricular weight/BW ratio (mg/g)	0.49 \pm 0.01	0.60 \pm 0.04 *	0.54 \pm 0.02 *	0.72 \pm 0.04 ***, §, ###
Atria weight/BW ratio (mg/g)	0.23 \pm 0.01	0.33 \pm 0.04 *	0.35 \pm 0.01 ***	0.44 \pm 0.07 ***, §§
Left kidney weight/BW ratio (mg/g)	3.09 \pm 0.08	3.22 \pm 0.07	4.32 \pm 0.11 ***, §§§	4.77 \pm 0.22 ***, §§§
BW (g)	547.8 \pm 10.9	537.7 \pm 14.1	459.7 \pm 7.8 ***, §§§	440.4 \pm 26.3 ***, §§§

5.4.4 Echocardiography

STNx-induced kidney impairment resulted in significant hypertension-induced cardiac hypertrophy as indicated by increased anterior wall thickness, posterior wall thickness and relative wall thickness in STNx+Sham animals compared to Sham+Sham and Sham+MI animals at week 4 and 12 (Table 5.4). Both STNx groups had increased LV mass compared to Sham+Sham animals at week 4 and 12.

At week 12, subsequent MI caused significant decreases in anterior wall thickness in both MI groups, with no effects on posterior wall thickness (Table 5.4). Sham+MI animals had increased LVEDV and LVESV compared to Sham+Sham and

STNx+Sham animals. Increases in LVIDd and LVIDs and reductions in LVEF and FS were observed in the MI groups compared to sham-operated animals. STNx+MI animals had further non-significant reduction in changes of LVEF and FS (delta LVEF and delta FS) over time compared to the Sham+MI group ($p=0.085$ and $p=0.074$ respectively).

The addition of STNx resulted in reduced E'/A' ratio and increased A' wave in animals receiving MI, however no difference in E/E' ratio between the groups was observed at week 12 (Table 5.4). STNx+Sham animals had elevated A wave and A' wave and decreased E/A ratio and E' wave, but no change in E wave compared to Sham+Sham and Sham+MI animals. DT and IVRT were significantly increased in Sham+MI, STNx+Sham and STNx+MI animals compared to the Sham+Sham group.

Table 5.4 Echocardiographic parameters at week 4 (prior to MI or Sham surgery) and week 12. Values are mean \pm SEM. FS, fractional shortening; LVIDd and LVIDs, left ventricular internal diameter in diastole and systole; LVEF, left ventricular ejection fraction; LVEDV and LVESV, LV end diastolic and end systolic volume; DT, deceleration time; IVRT, isovolumetric relaxation time. * $p<0.05$, ** $p<0.01$, *** $p<0.001$ vs Sham+Sham; § $p<0.05$, §§ $p<0.01$, §§§ $p<0.001$ vs Sham+MI; # $p<0.05$, ## $p<0.01$, ### $p<0.001$ vs STNx+Sham.

	Week 4				Week 12			
	Sham+Sham	Sham+MI	STNx+Sham	STNx+MI	Sham+Sham	Sham+MI	STNx+Sham	STNx+MI
FS (%)	41.4±0.7	39.1±1.5	45.8±1.3 *, §§	47.1±2.0 *, §§	40.0±1.2	16.5±0.9 ***	43.8±2.6 §§	18.1±1.2 ***, ##
Anterior wall thickness (mm)	1.37±0.01	1.32±0.02	1.84±0.06 ***, §§§	1.83±0.05 ***, §§§	1.56±0.03	0.78±0.02 ***	2.14±0.07 ***, §§§	0.82±0.01 ***, ###
Posterior wall thickness (mm)	1.70±0.05	1.60±0.04	1.97±0.07 *, §§	2.12±0.12 **, §§§	1.72±0.04	1.85±0.06	2.26±0.09 ***, §§	2.38±0.12 ***, §§
LVIDd	8.81±0.14	8.98±0.09	8.41±0.21	8.73±0.26	9.36±0.13	11.69±0.23 ***	8.78±0.26 §§§	11.45±0.69 **, ###
LVIDs	5.16±0.13	5.47±0.18	4.57±0.19 *, §§	4.63±0.27 §	5.61±0.16	9.77±0.29 ***	4.98±0.33 §§§	9.39±0.61 ***, ###
Relative wall thickness	0.39±0.01	0.36±0.01	0.47±0.03 *, §§	0.49±0.03 *, §§	0.37±0.01	0.32±0.01 **	0.52±0.03 ***, §§§	0.43±0.03 §, #
LVEF (%)	68.8±2.1	66.3±3.1	74.3±2.0	79.2±3.0 §	66.9±1.9	42.0±2.4 ***	74.3±2.7 §§§	42.7±3.5 ***, ###
LVEDV (mL)	0.54±0.04	0.56±0.03	0.50±0.03	0.54±0.05	0.81±0.06	1.14±0.04 **	0.65±0.04 *, §§§	0.97±0.10 ##
LVESV (mL)	0.17±0.02	0.19±0.02	0.13±0.01	0.11±0.02 §	0.25±0.02	0.66±0.04 ***	0.18±0.03 §§§	0.55±0.07 ***, ###
LV mass (gram/m²)	1.42±0.02	1.40±0.01	1.62±0.04 ***, §§	1.77±0.08 ***, §§§	1.6±0.02	1.72±0.07	1.95±0.08 ***	2.0±0.16 **
DT (msec)	29.7±1.0	30.3±0.9	33.2±0.6 **, §	33.4±1.2 *	28.8±0.7	34.7±1.0 **	39.0±1.0 ***, §	37.6±1.9 ***
IVRT (msec)	21.1±0.9	20.2±1.2	24.0±1.2	24.2±0.9 *, §	23.0±1.2	29.2±1.6 **	28.4±1.6 *	29.7±2.1 *
E wave velocity (m/sec)	1.14±0.03	1.08±0.06	1.05±0.03	1.14±0.06	1.08±0.02	1.12±0.08	1.0±0.04	1.04±0.11
A wave velocity (m/sec)	0.53±0.03	0.54±0.05	0.75±0.05 **, §	0.83±0.05 ***, §§§	0.45±0.03	0.31±0.04 **	0.81±0.05 ***, §§§	0.51±0.06 §, ###
E' wave velocity (cm/sec)	5.2±0.3	4.8±0.3	4.1±0.2 *	4.5±0.3	4.8±0.2	4.5±0.3	3.5±0.3 **, §	3.9±0.5
A' wave velocity (cm/sec)	2.9±0.2	2.7±0.2	3.8±0.2 *, §§	4.7±0.3 ***, §§§	2.4±0.2	1.9±0.2 *	4.2±0.3 ***, §§§	3.3±0.2 **, §§§, #
E/E' ratio	22.6±1.2	23.1±1.8	25.8±1.1	25.8±1.8	23.3±1.4	25.9±2.7	30.0±2.1	28.9±5.3
E/A ratio	2.2±0.1	2.1±0.1	1.5±0.1 ***, §§	1.4±0.1 ***, §	2.5±0.2	4.1±0.7 *	1.3±0.1 ***, §§§	2.5±0.7 #
E'/A' ratio	1.8±0.1	1.9±0.2	1.1±0.1 **, §§	1.0±0.1 **, §	2.1±0.2	2.4±0.2	0.9±0.1 ***, §§§	1.2±0.2 ***, §§§

5.4.5 Hemodynamic parameters

On completion of the study, hemodynamic measurements were obtained for all animals (Table 5.5). There was no difference in heart rate between the groups. The rate of rise and fall of pressure in the LV, dp/dt_{max} and dp/dt_{min} were significantly reduced in both MI groups compared to the Sham+Sham group. LVEDP and EDPVR were significantly increased in Sham+MI, STNx+Sham and STNx+MI animals compared to the Sham+Sham group. There was an indicating trend towards an increase in LVEDP between STNx+MI and STNx+Sham animals. Measurements of systolic function including PRSW and ESPVR were significantly reduced in Sham+MI compared to Sham+Sham animals. A measurement of diastolic function, tau logistic, was significantly prolonged in both STNx groups compared to sham-operated animals at week 12.

Table 5.5 Hemodynamic parameters assessed at week 12. Values are mean \pm SEM. dP/dt_{max} , dP/dt_{min} , the maximal rate of pressure rise and fall; LVEDP, left ventricular end diastolic pressure; ESPVR and EDPVR, slope of end systolic and end diastolic pressure-volume relationship; PRSW, slope of preload recruitable stroke work relationship. * $p<0.05$, ** $p<0.01$, *** $p<0.001$ vs Sham+Sham; § $p<0.05$, §§ $p<0.01$, §§§ $p<0.001$ vs Sham+MI; # $p<0.05$ vs STNx+Sham.

	Sham+Sham	Sham+MI	STNx+Sham	STNx+MI
Heart Rate (beats/min)	297 \pm 21	316 \pm 10	312 \pm 19	320 \pm 27
dP/dt_{max} (mmHg/sec)	6306 \pm 138	4478 \pm 182 ***	6589 \pm 295 §§§	5667 \pm 255 *, §§
$-dP/dt_{min}$ (mmHg/sec)	5479 \pm 314	3192 \pm 161 ***	4315 \pm 396 *, §	3605 \pm 348 **
LVEDP (mmHg)	2.6 \pm 0.6	8.8 \pm 1.4 ***	5.7 \pm 1.1 *	8.8 \pm 1.8 **
ESPVR (mmHg/μl)	0.47 \pm 0.07	0.25 \pm 0.03 *	0.89 \pm 0.12 *, §§§	0.38 \pm 0.03 §, #
EDPVR (mmHg/μl)	0.013 \pm 0.002	0.055 \pm 0.011 ***	0.037 \pm 0.006 *	0.045 \pm 0.007 *
PRSW (mmHg)	84.2 \pm 6.3	42.9 \pm 6.7 **	80.4 \pm 8.0 §	62.0 \pm 11.4
Tau logistic (msec)	11.4 \pm 0.6	13.0 \pm 0.8	17.6 \pm 1.2 ***, §	17.0 \pm 1.6 **, §

5.4.6 Cardiac interstitial fibrosis

Cardiac interstitial fibrosis in the non-infarcted myocardium with picrosirius red staining was significantly increased in STNx+MI animals compared to Sham+Sham and Sham+MI animals (Figure 5.3). The addition of MI to STNx increased the extent of interstitial fibrosis in STNx+MI compared to STNx+Sham animals ($p<0.05$).

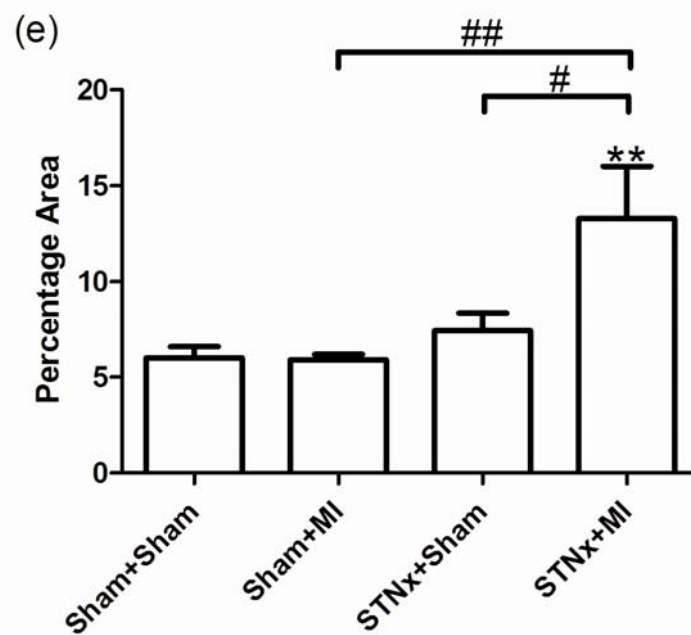
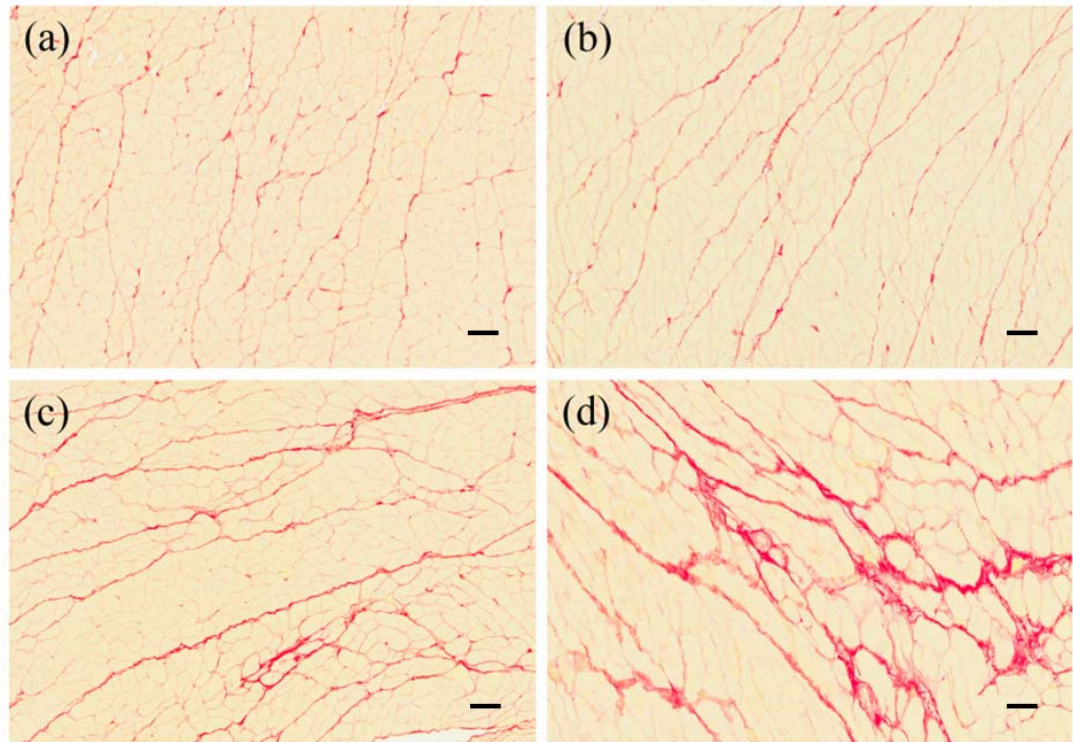
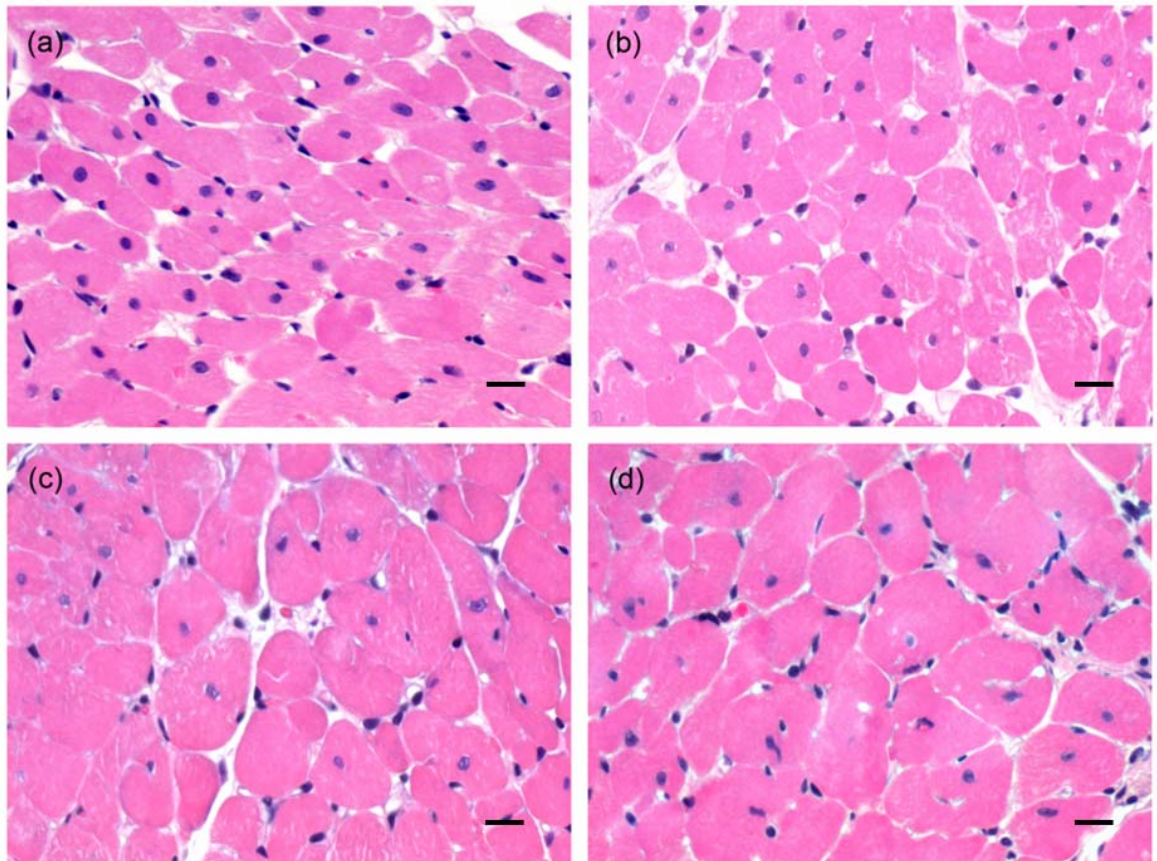


Figure 5.3 Representative images of the LV non-infarcted zone with picrosirius red staining for the following groups (a) Sham+Sham, (b) Sham+MI, (c) STNx+Sham and (d) STNx+MI. Scale bar, 100 μ m. Quantitation of picrosirius red staining (e) showing STNx+MI animals had significantly greater cardiac interstitial fibrosis compared to all

other groups. Data are expressed as mean \pm SEM. ** $p < 0.01$ vs Sham+Sham; # $p < 0.05$, ### $p < 0.01$ for between group comparisons.

5.4.7 Cardiac myocyte cross-sectional area

Myocyte cross-sectional area in the non-infarcted myocardial was elevated in Sham+MI ($p < 0.05$), STNx+Sham ($p < 0.001$) and STNx+MI ($p < 0.001$) animals compared to the Sham+Sham group (Figure 5.4). STNx+Sham ($p < 0.01$) and STNx+MI ($p < 0.001$) animals had greater myocyte cross-sectional area compared to the Sham+MI group. STNx+MI animals also had greater cardiomyocyte size compared to the STNx+Sham group ($p < 0.01$).



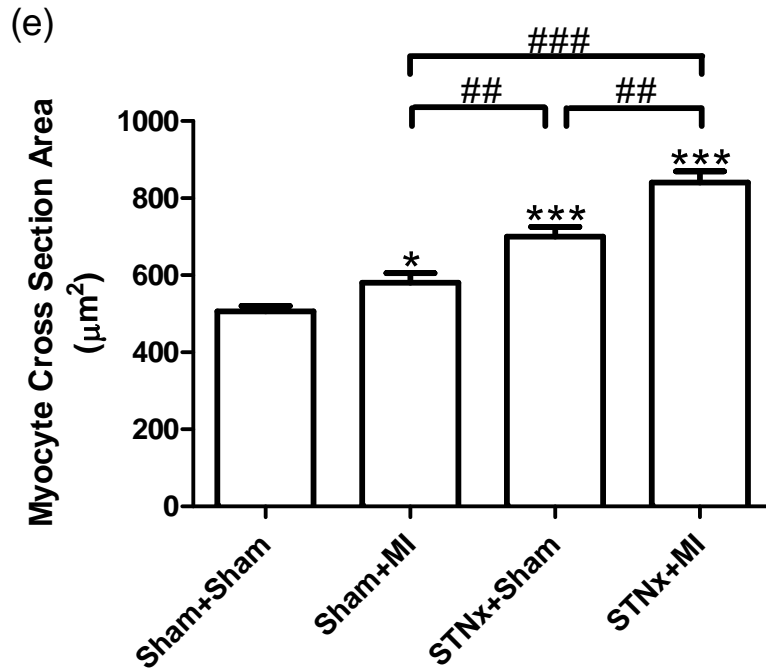


Figure 5.4 Representative images of the LV non-infarcted zone with hematoxylin and eosin staining of myocytes for the following groups (a) Sham+Sham, (b) Sham+MI, (c) STNx+Sham and (d) STNx+MI. Scale bar, 30 μm . Quantitation of the data (e) showing that STNx+MI animals had significantly larger cardiomyocytes compared to all other groups. Data are expressed as mean \pm SEM. * $p < 0.05$, *** $p < 0.001$ vs Sham+Sham; ## $p < 0.01$, ### $p < 0.001$ for between group comparisons.

5.4.8 Renal function and indoxyl sulfate plasma levels

Both STNx groups developed severe renal dysfunction as indicated by reduced GFR and creatinine clearance and increased proteinuria, and those animals also had significantly higher IS plasma levels compared to sham-operated animals at week 4 and 12 (Table 5.6). However, no further deterioration in renal function nor difference in IS plasma levels were observed between STNx+MI and STNx+Sham animals.

Table 5.6 Renal function and indoxyl sulfate plasma levels at week 4 (prior to MI or Sham surgery) and week 12. STNx+Sham and STNx+MI animals developed severe renal dysfunction compared to Sham+Sham and Sham+MI groups. Values are mean \pm SEM. GFR, glomerular filtration rate; CrCl, creatinine clearance; IS, indoxyl sulfate. * p <0.05, ** p <0.01, *** p <0.001 vs Sham+Sham; § p <0.05, §§ p <0.01, §§§ p <0.001 vs Sham+MI.

	Week 4				Week 12			
	Sham+Sham	Sham+MI	STNx+Sham	STNx+MI	Sham+Sham	Sham+MI	STNx+Sham	STNx+MI
GFR (ml/min/kg)	9.9 \pm 0.6	9.4 \pm 0.7	2.5 \pm 0.2 ***, §§§	3.3 \pm 0.4 ***, §§§	8.6 \pm 0.5	8.1 \pm 0.5	0.9 \pm 0.4 ***, §§§	0.4 \pm 0.3 ***, §§§
CrCl (ml/min)	232.9 \pm 10.4	246.5 \pm 17.0	36.9 \pm 4.5 ***, §§§	45.1 \pm 4.7 ***, §§§	242.6 \pm 26.6	255.5 \pm 39.7	32.2 \pm 8.7 ***, §§§	33.9 \pm 12.4 ***, §§§
Serum creatinine (μmol/L)	23.2 \pm 0.9	22.8 \pm 0.7	63.7 \pm 3.2 ***, §§§	58.5 \pm 1.9 ***, §§§	36.1 \pm 5.2	29.0 \pm 0.7	111.8 \pm 15.6 **, §§	145.0 \pm 27.8 ***, §§§
Proteinuria (mg/24 hr)	20.3 \pm 2.0	16.2 \pm 3.3	76.7 \pm 16.0 *, §	75.9 \pm 20.2 *, §	23.1 \pm 2.0	16.2 \pm 1.6	344.4 \pm 48.9 ***, §§§	380.0 \pm 89.1 ***, §§§
IS (μmol/L)	18.79 \pm 2.39	16.69 \pm 1.17	94.05 \pm 11.65 ***, §§§	66.16 \pm 6.97 **, §§	13.03 \pm 1.14	10.21 \pm 1.02	58.03 \pm 11.86 **, §§	66.19 \pm 13.17 ***, §§

5.4.9 Renal tubulointerstitial fibrosis

STNx groups demonstrated significantly greater tubulointerstitial fibrosis in the non-infarcted zone of the kidney compared to sham-operated animals (p <0.001) (Figure 5.5). STNx+MI animals had greater tubulointerstitial fibrosis compared to the STNx+Sham group (p <0.05).

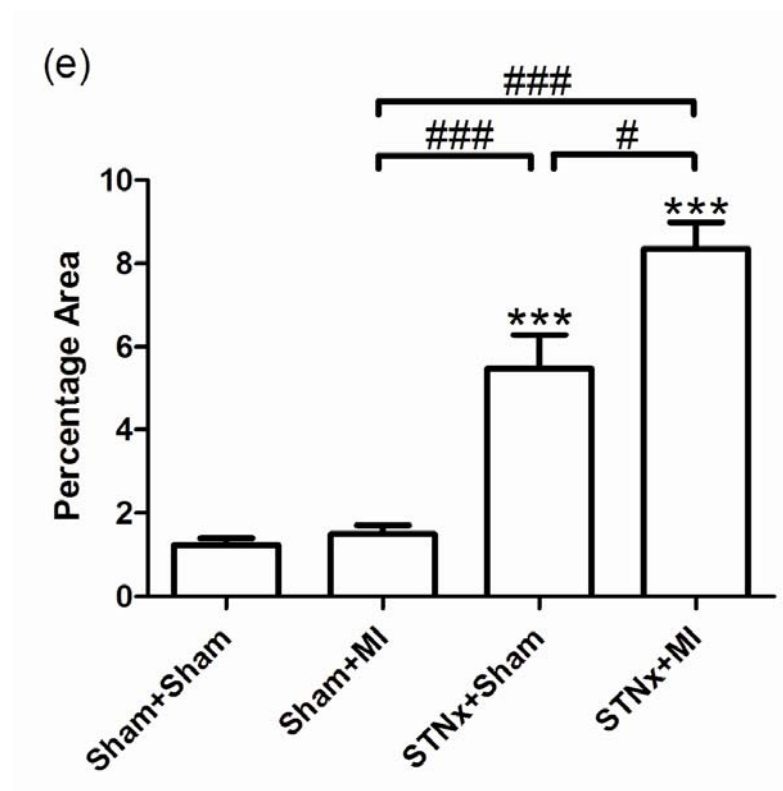
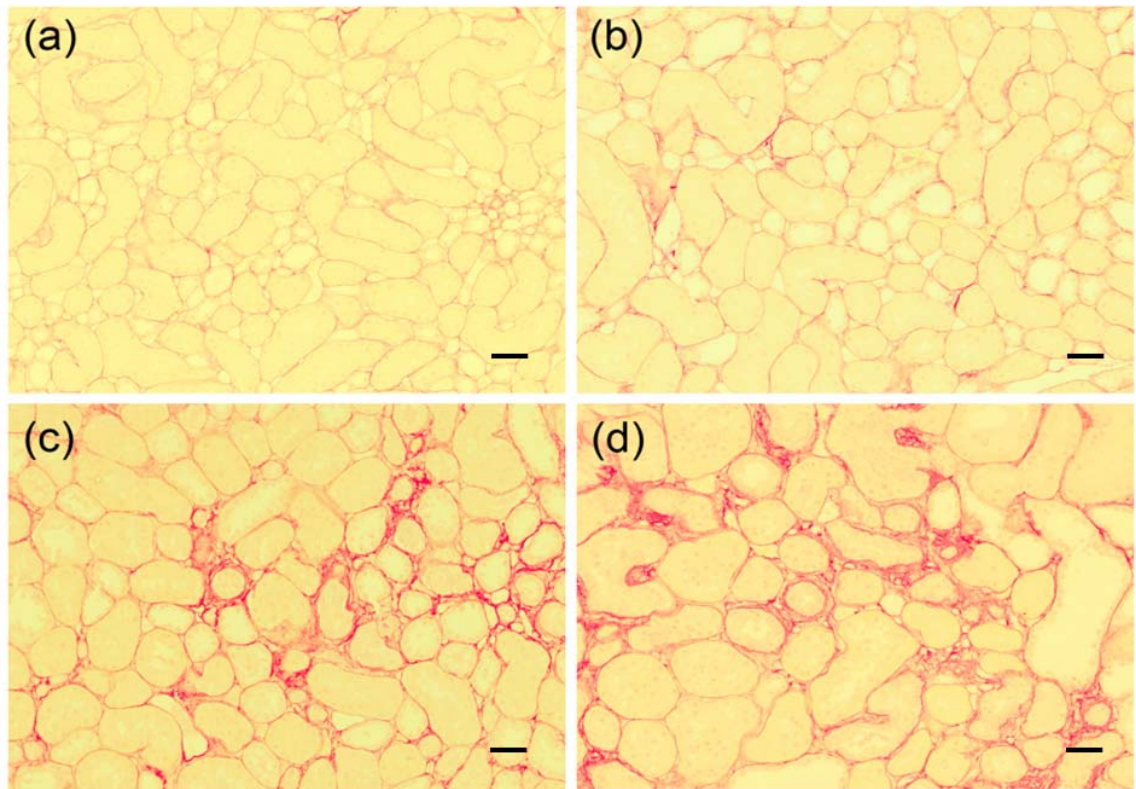


Figure 5.5 Representative images of the non-infarcted zone of the kidney with picosirius red staining for the following groups (a) Sham+Sham, (b) Sham+MI, (c) STNx+Sham and (d) STNx+MI. Scale bar, 50 μm . Quantitation of renal tubulointerstitial fibrosis (e) showing STNx+MI animals had significantly greater tubulointerstitial fibrosis than all other groups. Data are expressed as mean \pm SEM. *** $p < 0.001$ vs Sham+Sham; # $p < 0.05$, ### $p < 0.001$ for between group comparisons.

5.5 Discussion

In the setting of CKD, cardiovascular disease is the most common cause of death, responsible for 40-50% of all deaths. The present chapter investigates pathophysiological changes in the preclinical model of progressive kidney disease followed by cardiac injury. Not only increases in heart weight, cardiomyocyte size and cardiac interstitial fibrosis have been found between STNx+MI and Sham+MI animals, elevations have been demonstrated between STNx+MI and STNx+Sham animals. Non-significant decreases in delta LVEF and delta FS were observed between STNx+MI and Sham+MI animals. STNx+MI animals also had increased renal tubulointerstitial fibrosis compared to the STNx+Sham animals, although MI did not further impair renal function between the two groups.

The mortality in STNx+MI animals was increased by 49% compared to the Sham+MI group without any difference in infarct size, and it was elevated by 35% compared to the BP-matched STNx+Sham group. These findings are of considerable clinical significance given the large burden of cardiovascular morbidity and mortality in patients with CKD.

STNx-induced CKD is a major contributor to cardiovascular disease and may accelerate cardiac dysfunction post-infarction. Non-significant decreases in delta LVEF and delta FS were observed between STNx+MI and Sham+MI animals at week 12. A deterioration in cardiac diastolic function was observed between the two groups, as indicated by decreased E'/A' ratio, increased A' wave and prolonged tau logistic. However, no difference was observed in tau logistic between STNx+MI and

STNx+Sham animals. This is in contrast to a previous study that has showed an increase in tau logistic in a similar model but at a more distant time point of 17 weeks.²⁵⁰ Difference in results between the previous study and this study may be explained by a further 6-week time delay between the initial STNx and subsequent MI.

In the setting of CKD followed by CHF, heart and right ventricular weights were significantly increased in STNx+MI vs STNx+Sham animals, indicating heart and right ventricular hypertrophy representative of cardiac failure. Increases in cardiomyocyte cross-sectional area and cardiac interstitial fibrosis were observed in STNx+MI animals compared to the Sham+MI group and BP-matched STNx+Sham group. These changes may be contributory to and reflective of the detrimental effects of pathological cardiac remodelling induced by the model.^{83, 329, 342} It also suggests that the subsequent MI increased cardiomyocyte size and myocardial interstitial fibrosis in CKD rats by mechanisms independent of hypertension.³⁴³

Progression of renal dysfunction and accumulation of circulating IS were observed in CKD animals at week 4 and 12, as indicated by reduced GFR and creatinine clearance, and increased proteinuria and plasma IS levels. However, subsequent MI post-CKD did not cause further renal dysfunction in STNx+MI compared to STNx+Sham animals at least by 12 weeks, as similarly observed from an early study.²⁵⁰ The differences may become evident with a longer follow-up period.

The central pathological feature of kidney disease that leads to kidney failure in human is the accumulation of extracellular matrix.²⁴⁰ Despite not being able to cause further functional derangements, STNx+MI animals had significantly greater renal

tubulointerstitial fibrosis compared to BP-matched STNx+Sham animals, indicating that this detrimental effect may not be mediated by systemic hemodynamic factors.

In this chapter, the functional and structural changes on heart and kidney have been systematically examined in the setting of STNx followed by MI. In Chapter 3.4.6, STNx causes more abnormality in myocardial fibrosis and cardiac hypertrophy than that of MI; in this STNx+MI model, the STNx followed by MI accelerates cardiac fibrosis and hypertrophy compared to STNx only. Furthermore subsequent MI exacerbates the renal tubulointerstitial fibrosis post-STNx. All of these effects are BP-independent. These findings continue to refine our understanding to the pathophysiology of CRS. Further pathological and mechanistic investigations may help to further explore the pathophysiology of cardiac and renal changes observed in the present study.

Chapter 6 Pathological and Mechanistic Investigations in the STN_x+MI Model

6.1 Introduction

In Chapter 5, the direct adverse effects were investigated in the setting of myocardial injury occurring secondary to CKD. The addition of MI following STNx results in disturbances in cardiac structure, including myocyte hypertrophy and extracellular matrix deposition that may contribute to the progression of disease. These observations, together with elevated tubulointerstitial fibrosis in the kidney, are traits reported in the field of pathophysiological changes typical for the CRS. However, the pathology and mechanisms by which subsequent MI leads to accelerated cardiac remodelling and renal impairment are not well understood.

The findings of similar GFRs in the animals with combined CKD and CHF compared with animals with CKD only lead to the question whether individuals with CKD plus CHF develop worsening renal impairment that goes undetected using standard renal functional measurements.²⁵⁰ Effective clinical tools are needed for the early detection of subtle and progressive renal impairment.³ Given the above considerations, in the present study we sought to identify the role of tubular injury biomarker KIM-1 for the early detection, prevention and management of CKD co-morbid with CHF.

6.2 Aims

To determine the pathology and mechanisms in a rodent model of STNx+MI in which cardiac remodelling and tubulointerstitial injury are well established features.

6.3 Materials and Methods

STNx or Sham surgery was induced initially and animals underwent MI or Sham surgery 4 weeks later and maintained for 8 weeks before sacrifice as per Chapter 5.3. Totally 36 animals were randomized into four groups: Sham+Sham, Sham+MI, STNx+Sham and STNx+MI. After sacrifice, the heart and kidney were collected for immunohistochemical, gene expression and protein level analyses as per Chapter 2.1.15-2.1.19.

6.4 Results

6.4.1 Cardiac collagen I and III

Analysis of immunoreactivity data for extracellular matrix proteins showed a significant increase in cardiac collagen I in the non-infarcted myocardium in STNx+MI animals compared to Sham+Sham and Sham+MI animals (Figure 6.1).

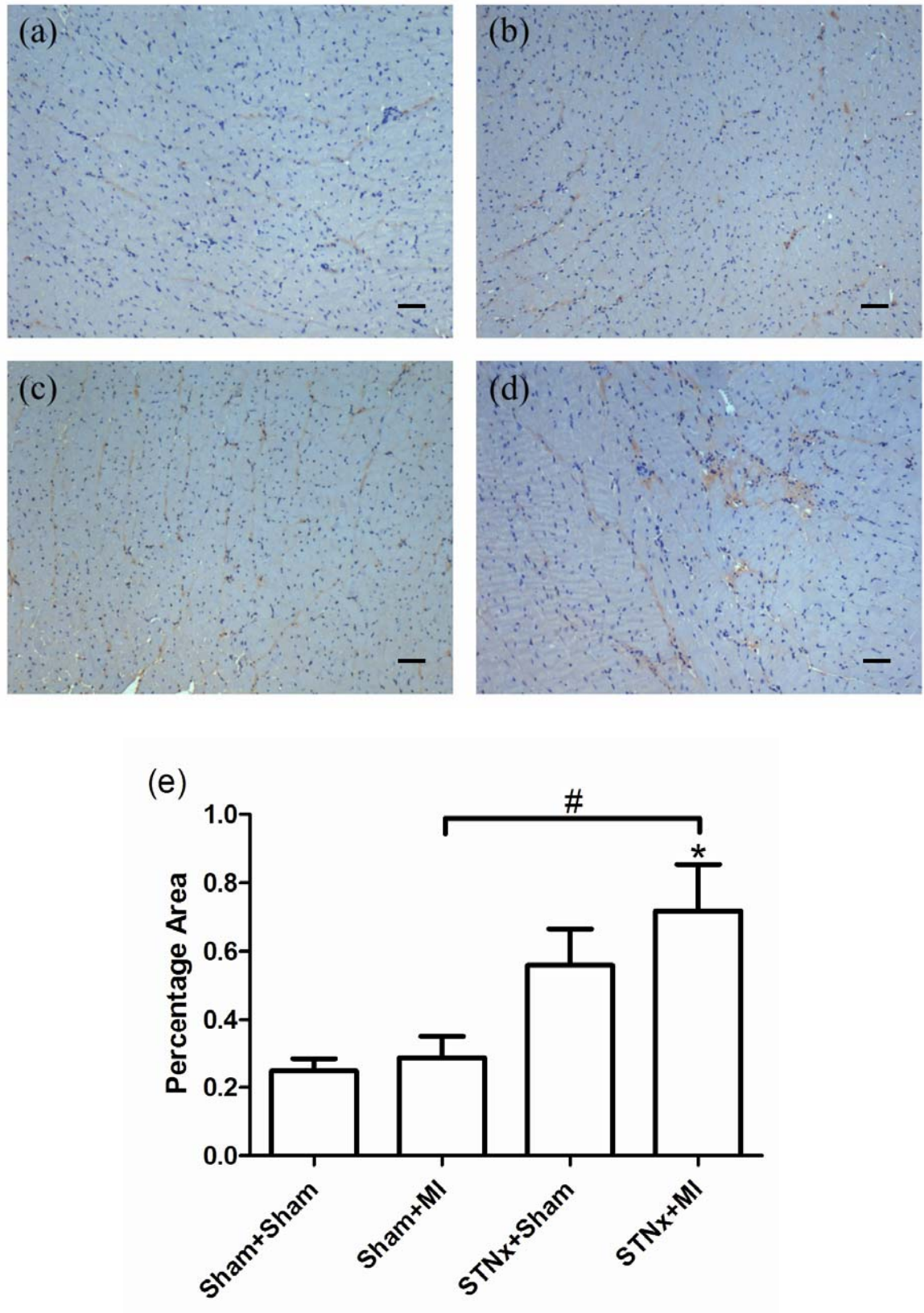
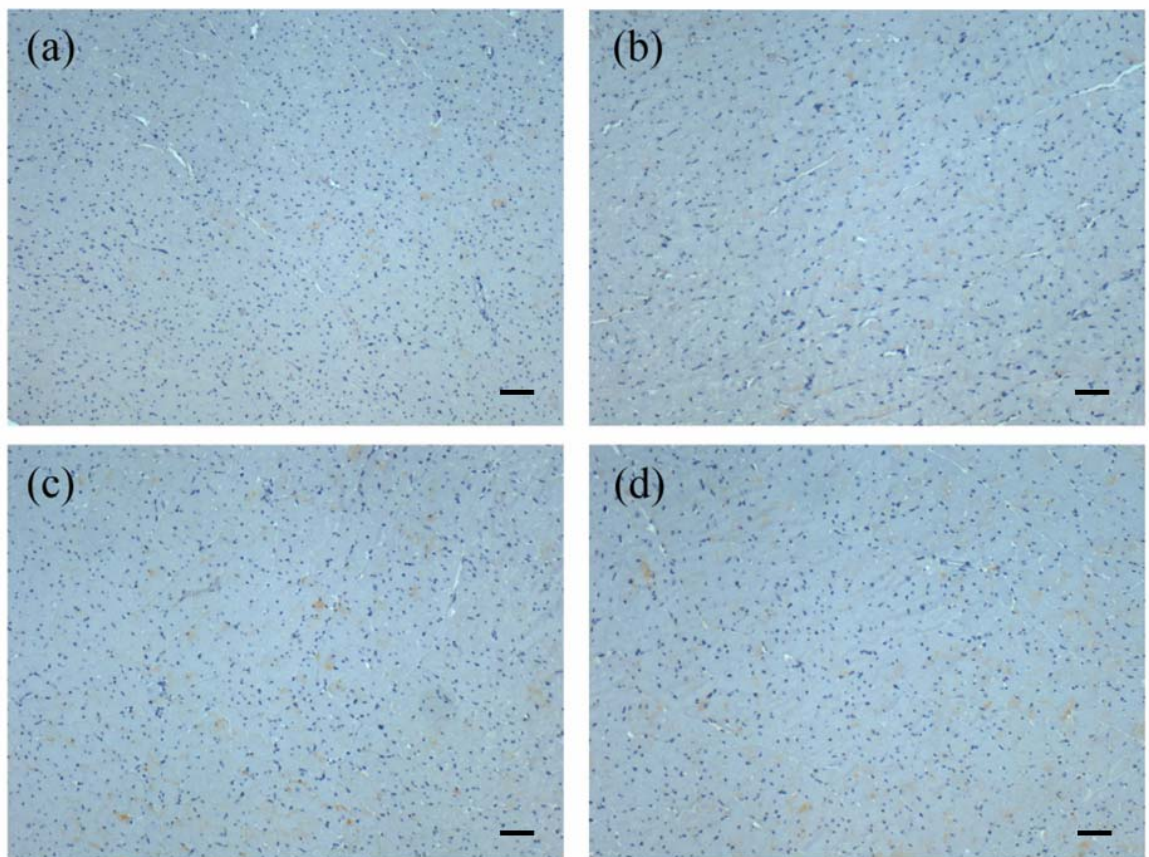


Figure 6.1 Representative images of the LV non-infarcted zone with collagen I immunostaining for the following groups (a) Sham+Sham, (b) Sham+MI, (c)

STNx+Sham and (d) STNx+MI. Scale bar, 30 μ m. Quantitation of collagen I (e) showing STNx+MI animals had significantly greater immunostaining than Sham+Sham and Sham+MI groups. Data are expressed as mean \pm SEM. * p <0.05 vs Sham+Sham; # p <0.05 for between group comparisons.

Cardiac collagen III in the non-infarcted myocardium was significantly increased in STNx groups compared to sham-operated animals (Figure 6.2). There was an indicating trend towards an increase in cardiac collagen III in STNx+MI animals compared to the STNx+Sham group (p =0.070).



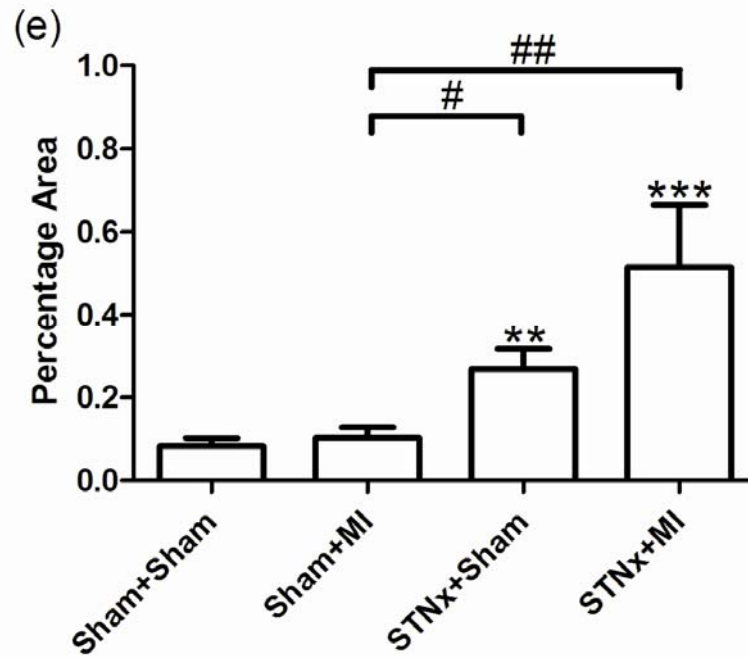


Figure 6.2 Representative images of the LV non-infarcted zone with collagen III immunostaining for the following groups (a) Sham+Sham, (b) Sham+MI, (c) STNx+Sham and (d) STNx+MI. Scale bar, 30 μ m. Quantitation of collagen III (e) showing STNx+Sham and STNx+MI animals had significantly greater immunostaining compared to the Sham+Sham and Sham+MI groups. Data are expressed as mean \pm SEM. ** $p<0.01$, *** $p<0.001$ vs Sham+Sham; # $p<0.05$, ## $p<0.01$ for between group comparisons.

6.4.2 Cardiac mRNA expression

Gene expression of the pro-fibrotic markers CTGF and collagen I, but not TGF β_1 showed significant increases in STNx groups compared to the Sham+Sham group (Figure 6.3 a-c). Significant increases in collagen I mRNA expression were observed in STNx+MI animals compared to Sham+MI and STNx+Sham groups ($p<0.05$).

The hypertrophic marker ANP gene expression was increased in STNx groups compared to sham-operated animals (Figure 6.3 d). ANP gene expression was non-significantly increased in STNx+MI compared to STNx+Sham animals ($p=0.089$). Compared to the Sham+Sham group, the hypertrophic marker β -MHC gene expression was significantly increased in all other groups (Figure 6.3 e).

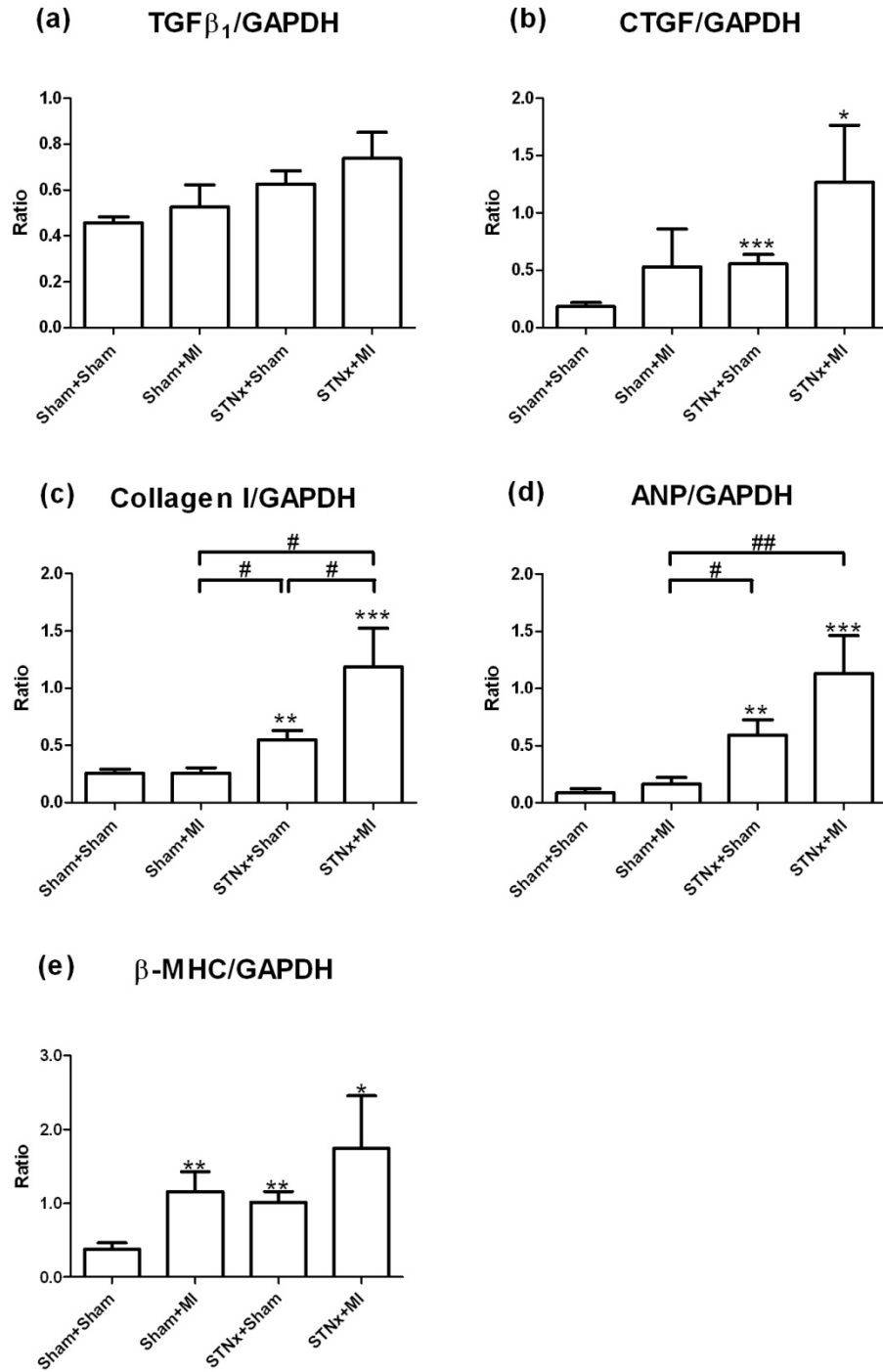
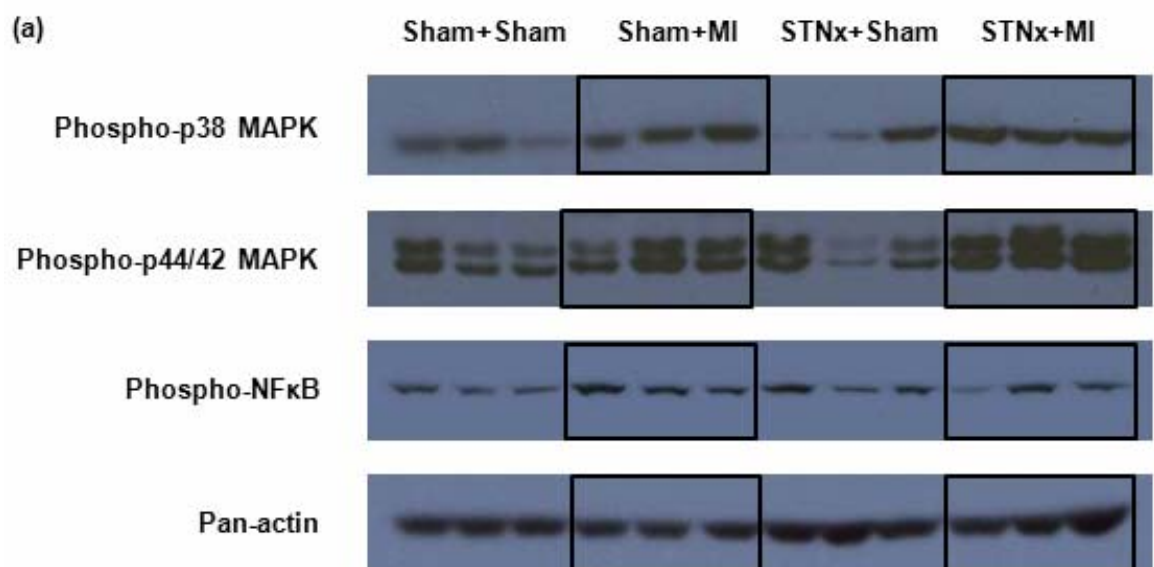


Figure 6.3 Gene expression of pro-fibrotic markers TGF β_1 (a), CTGF (b) and collagen I (c) and hypertrophic markers ANP (d) and β -MHC (e) in the LV non-infarcted zone. Results are expressed as a ratio of GAPDH. Data are expressed as mean \pm SEM. * $p < 0.05$, ** $p < 0.01$, *** $p < 0.001$ vs Sham+Sham; # $p < 0.05$, ## $p < 0.01$ for between group comparisons.

6.4.3 Cardiac signalling pathway activation

Significant increases in the protein levels of phospho-p38 MAPK were observed in MI groups compared to sham-operated animals (Figure 6.4). STNx+MI animals had significantly greater levels of phospho-p44/42 MAPK compared to Sham+Sham ($p<0.05$) and STNx+Sham ($p<0.01$) groups. TGF- β was undetectable in the non-infarcted myocardium with western blot analysis using 60 μ g per sample. No significant difference was observed in phospho-NF κ B levels between the groups.



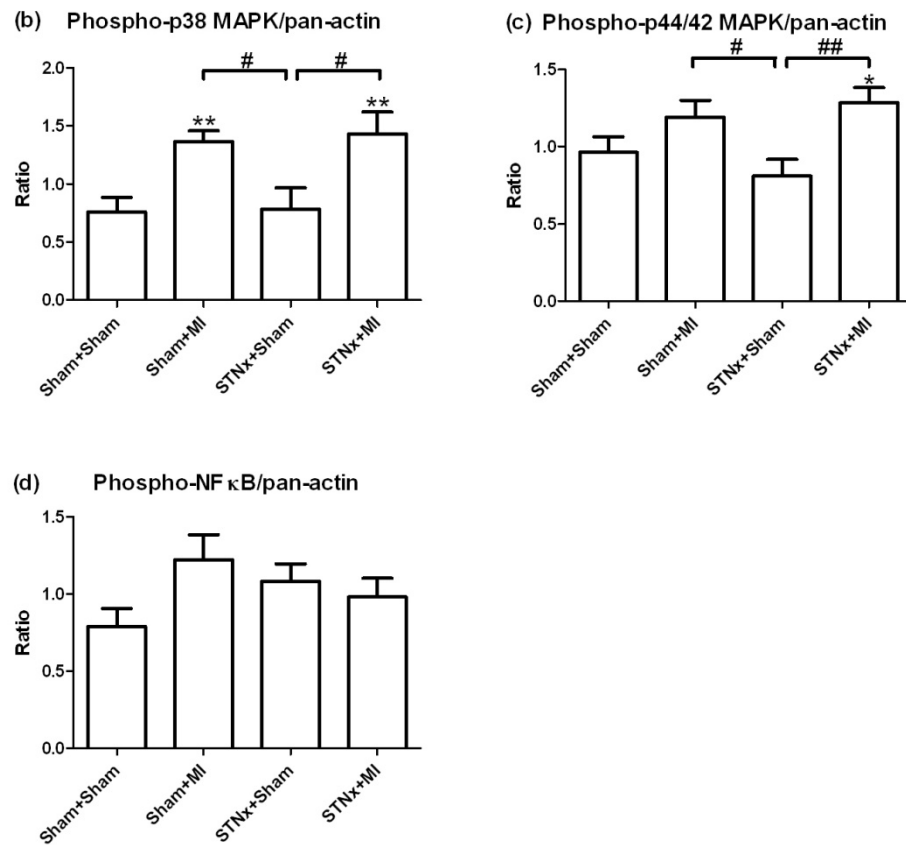
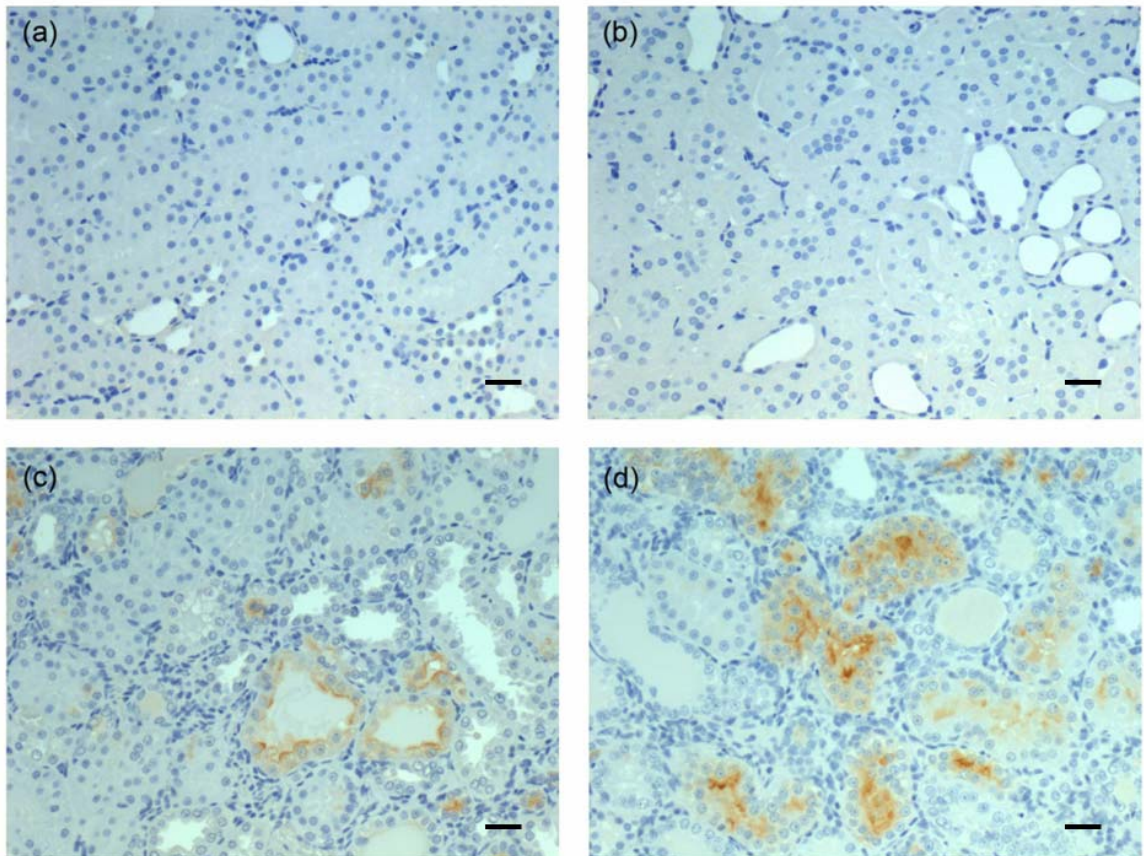


Figure 6.4 Representative images of the western blot analysis results for cardiac protein levels in the LV non-infarcted zone for the Sham+Sham, Sham+MI, STNx+Sham and STNx+MI groups (a). Quantitation of the protein levels of phospho-p38 MAPK (b), phospho-p44/42 MAPK (c), and phospho-NFκB (d) are normalized with pan-actin. STNx+MI animals had greater protein levels of phospho-p38 MAPK and phospho-p44/42 MAPK, but not phospho-NFκB compared to Sham+Sham and STNx+Sham groups. Data are expressed as mean \pm SEM. * $p < 0.05$, ** $p < 0.01$ vs Sham+Sham; # $p < 0.05$, ## $p < 0.01$ for between group comparisons.

6.4.4 Renal injury biomarker

STNx groups demonstrated significantly elevated tissue levels of KIM-1 in the kidney compared to sham-operated animals (Figure 6.5). STNx+MI animals had increased tissue levels of KIM-1 compared to the STNx+Sham group ($p<0.001$).



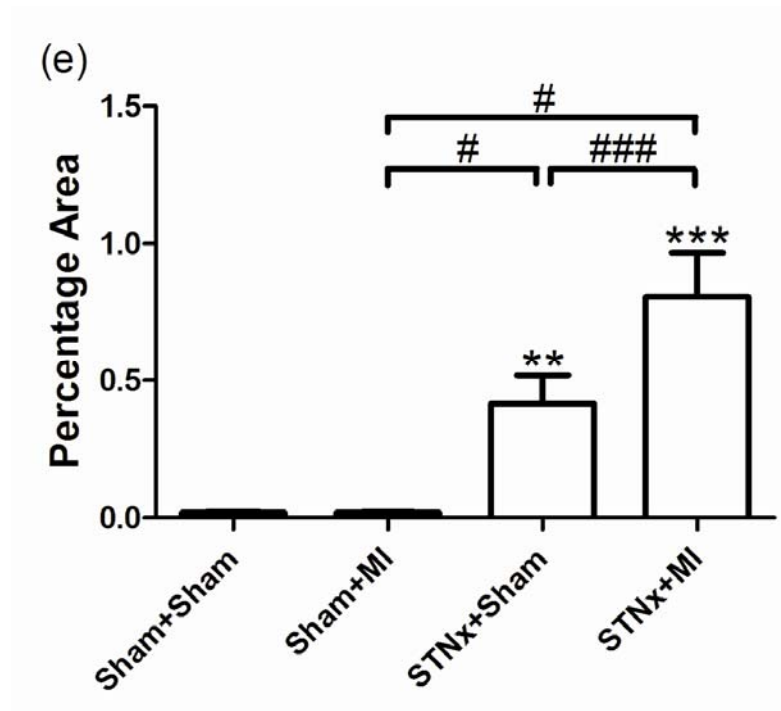


Figure 6.5 Representative images of the non-infarcted cortex region of the kidney with immunostaining of kidney injury molecule-1 (KIM-1) for the following groups (a) Sham+Sham, (b) Sham+MI, (c) STNx+Sham and (d) STNx+MI. Scale bar, 30 μ m. Quantitation of KIM-1 (e) showing STNx+MI animals had significantly greater tissue levels of KIM-1 compared to all other groups. Data are expressed as mean \pm SEM. ** $p < 0.01$, *** $p < 0.001$ vs Sham+Sham; # $p < 0.05$, ### $p < 0.001$ for between group comparisons.

6.4.5 Renal macrophage infiltration

STNx groups demonstrated significantly increased tubulointerstitial macrophage accumulation (CD68 cells) in the kidney compared to sham-operated animals (Figure 6.6), hence increasing the overall inflammatory contribution to progressive kidney disease.

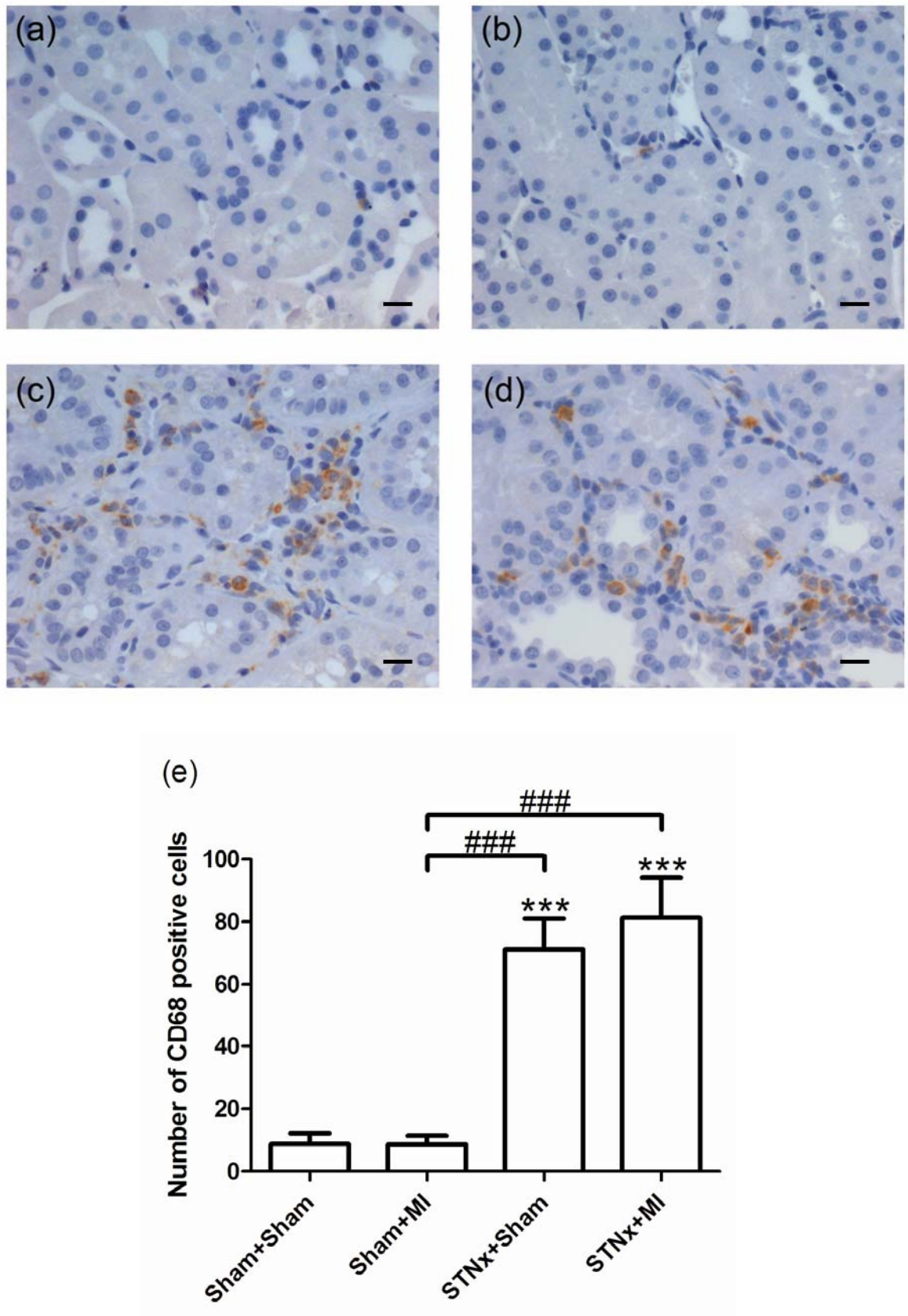


Figure 6.6 Representative images of the non-infarcted cortex region of the kidney with immunostaining of macrophage infiltration for the following groups (a) Sham+Sham,

(b) Sham+MI, (c) STNx+Sham and (d) STNx+MI. Scale bar, 30 μ m. Quantitation of number of CD68 positive cells (e) showing STNx+Sham and STNx+MI animals had significantly greater macrophages infiltration compared to Sham+Sham and Sham+MI groups. Data are expressed as mean \pm SEM. ***p<0.001 vs Sham+Sham; ###p<0.001 for between group comparisons.

6.4.6 Renal mRNA expression

Renal pro-fibrotic markers TGF β ₁ and collagen IV, along with pro-inflammatory cytokine IL-6 gene expression were significantly increased in STNx groups compared to sham-operated animals (Figure 6.7); and no further increase was observed in STNx+MI vs STNx+Sham animals.

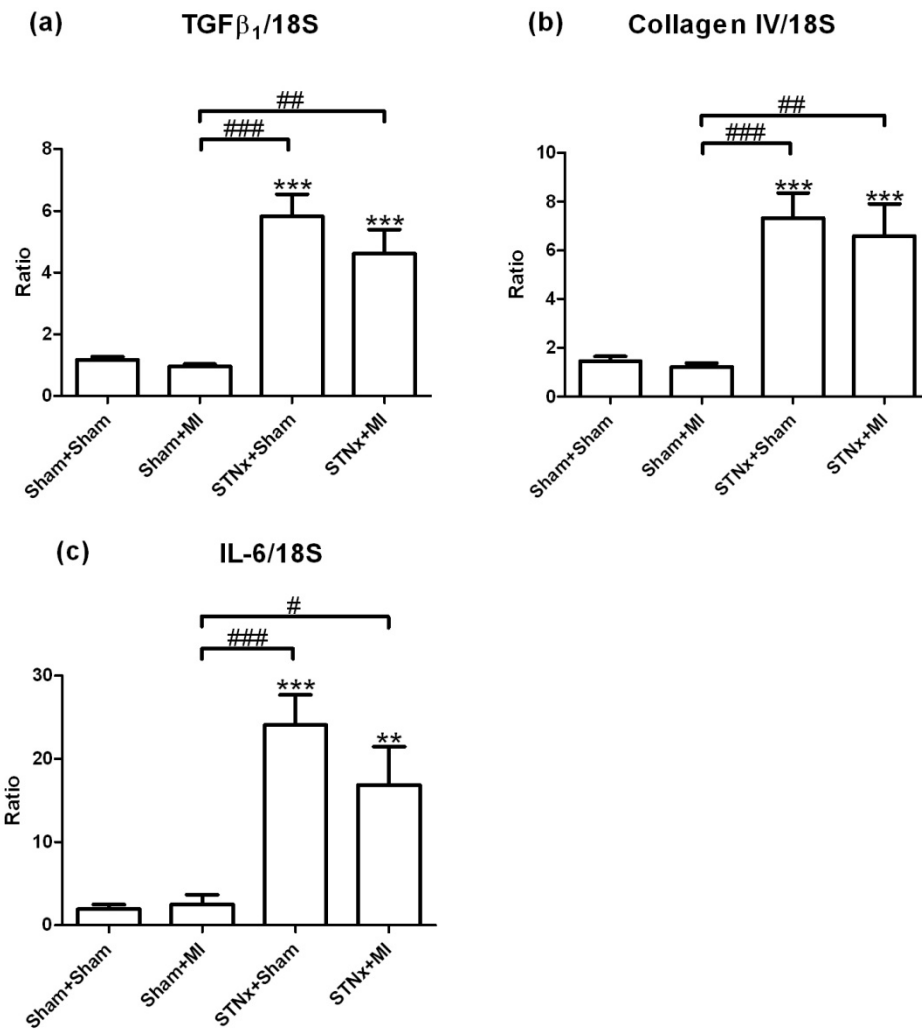
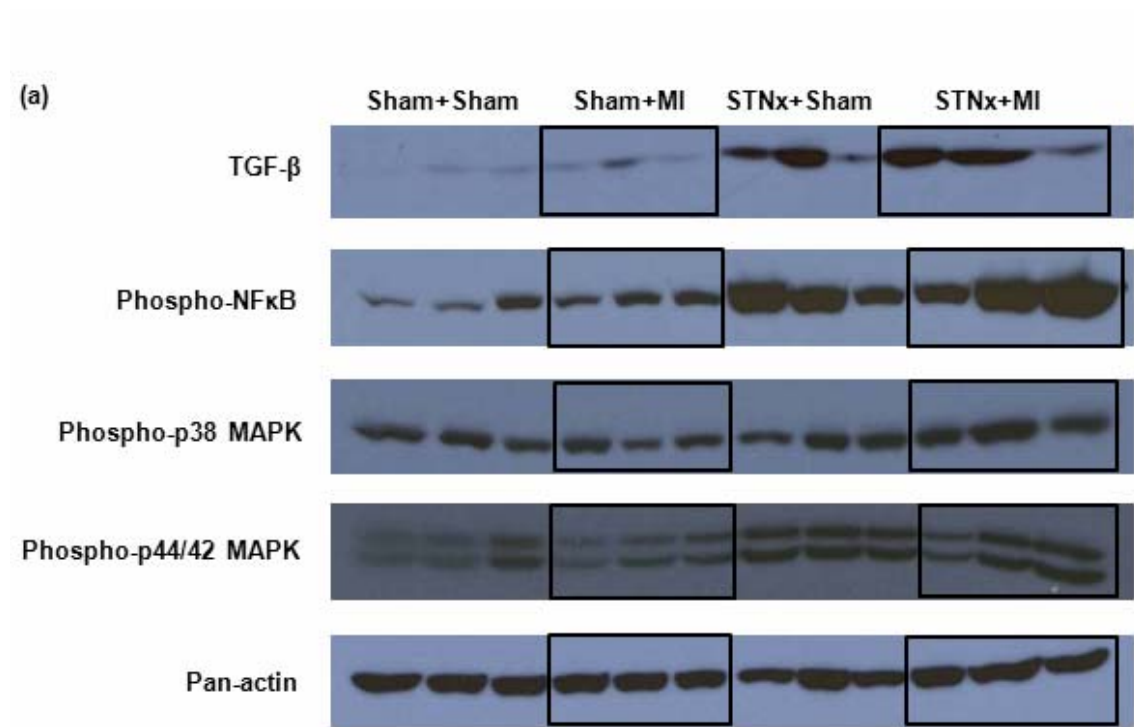


Figure 6.7 Pro-fibrotic markers TGFβ₁ (a) and collagen IV (b); and the pro-inflammatory cytokine IL-6 (c) gene expression in the kidney. Results are expressed as a ratio of 18S. Data are expressed as mean ± SEM. **p<0.01, ***p<0.001 vs Sham+Sham; #p<0.05, ##p<0.01, ###p<0.001 for between group comparisons.

6.4.7 Renal signalling pathway activation

Protein levels of TGF-β were significantly increased in Sham+MI compared to Sham+Sham animals (p<0.01) (Figure 6.8). These were also significantly increased in STNx groups compared to sham-operated animals (p<0.001). Protein levels of phospho-NFκB in STNx+Sham (p<0.05) and STNx+MI (p<0.01) animals were greater

compared to the Sham+Sham group. There was an increasing trend in phospho-NFκB protein levels between STNx+MI and Sham+MI animals ($p=0.052$). No significant difference was observed in phospho-p38 MAPK and phospho-p44/42 MAPK protein levels between the groups.



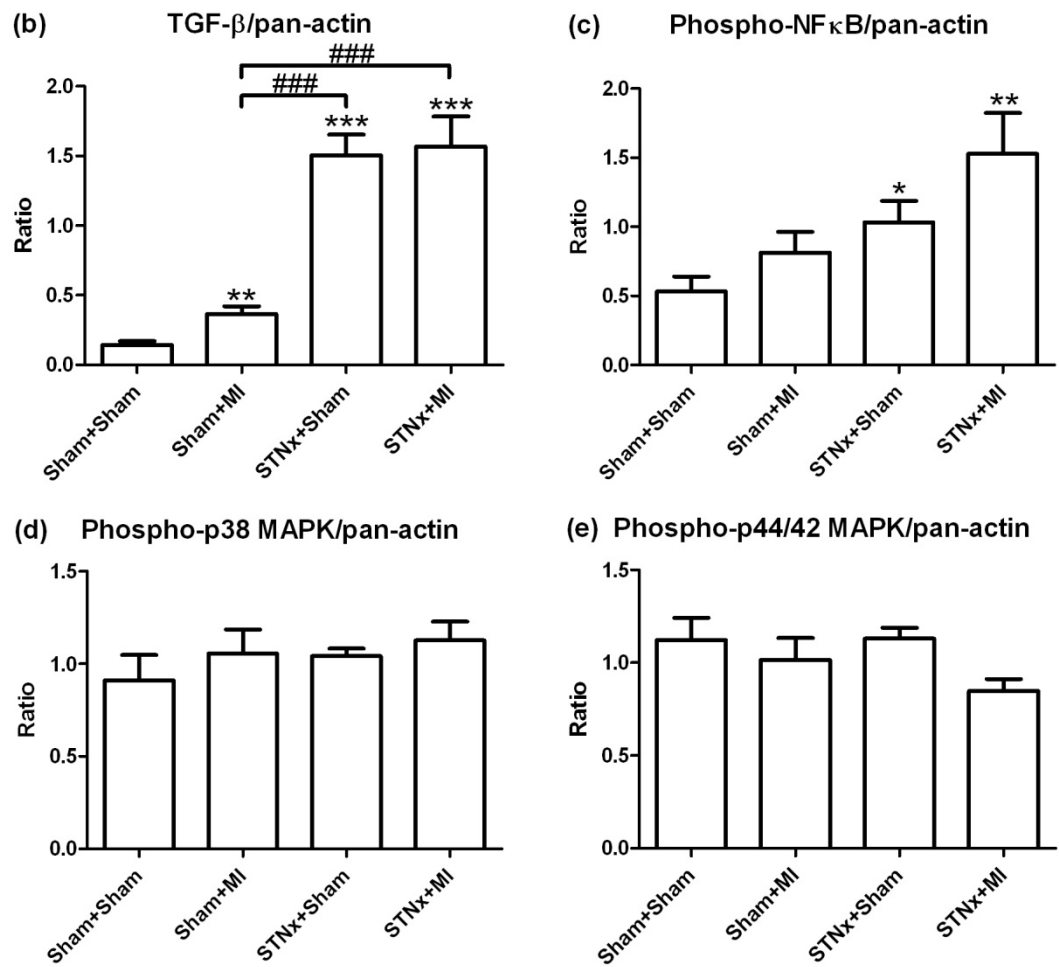


Figure 6.8 Representative images of the western blot analysis results of renal protein levels for Sham+Sham, Sham+MI, STNx+Sham and STNx+MI groups (a). Quantitation of the protein levels of TGF-β (b), phospho-NFκB (c), phospho-p38 MAPK (d) and phospho-p44/42 MAPK (e) after normalization with pan-actin. The results showed TGF-β protein levels significantly increased in the kidney of STNx+Sham and STNx+MI animals compared to Sham+Sham and Sham+MI animals. Data are expressed as mean ± SEM. **p<0.01, ***p<0.001 vs Sham+Sham; ##p<0.01, ###p<0.001 for between group comparisons.

6.5 Discussion

The most prominent cardiac remodelling event associated with cardiac functional alterations is myocardial fibrosis with the accumulation of interstitial matrix components.^{86, 344, 345} The present study demonstrates that type-I and type III collagen deposition was increased in the non-infarcted myocardium of the STNx+MI compared to Sham+MI animals. In parallel, collagen I mRNA expression was also up-regulated in STNx+MI vs Sham+MI animals. In addition, increased collagen I mRNA expression without change in collagen I deposition was observed in STNx+MI vs STNx+Sham animals. Taken together, the significant increases in collagen deposition and collagen gene expression may contribute to pathological reactive fibrosis in the LV, resulting in the observed diastolic impairment seen in this setting.

Pathological cardiac remodelling in response to renal dysfunction was demonstrated in Chapter 5. Cardiomyocyte cross-sectional area was significantly greater in the non-infarcted myocardium of the STNx groups compared to sham-operated animals. These were accompanied by the increases in gene expression of LV hypertrophic marker ANP, this was similar to previous studies described by our group.¹²⁷ The subsequent MI increased STNx-induced cardiac myocyte hypertrophy as indicated by significant elevation in cardiomyocyte size in STNx+MI vs STNx+Sham animals. This was associated with a non-significant increase in ANP gene expression between the two groups.

Elevation in Ang II leads to increased collagen I gene expression in part through activation of MAPK pathways.³⁴⁶ Phospho-p38 MAPK and phospho-p44/42 MAPK signalling pathways were activated in the LV tissues accompanied by the increases in

collagen I mRNA expression in STNx+MI vs STNx+Sham animals. However, we did not observe major differences in cardiac protein levels between the STNx+MI and Sham+MI groups at week 12. These pathways do not readily provide an explanation for the further reduction in delta LVEF and delta FS between the MI groups.

KIM-1 is induced at the target site of injury, and its expression in renal tissue has been correlated with renal damage and worsening renal function in various human renal diseases.^{205, 206, 347, 348} KIM-1 positive staining in the tubules has been observed in animals with mild renal insufficiency caused by a large MI with mean infarct size of 41-46%, and it appears to be a potential tubular injury biomarker for the detection of progressive kidney failure in this setting.²¹⁰ In the present study, subsequent MI accelerated STNx-induced KIM-1 tissue levels in the kidney of STNx+MI compared to the STNx+Sham animals; and these increases between the STNx groups occurred with no changes in bp and renal function.

Recruitment of inflammatory cells (CD68) to the injured kidney was observed in STNx groups. These observations may provide a mechanistic link between poor renal outcomes and chronic inflammation in the setting of CKD.⁵⁸ These inflammatory cells may mediate tubulointerstitial injury by a number of mechanisms that include the production of ROS as well as secretion of proteolytic enzymes, vasoactive hormones, and growth factors.³¹⁴ The macrophages induced pro-fibrotic growth factor TGF β ₁,²⁴² is a key factor in the pathogenesis of progressive renal disease.³⁴⁹

Up-regulated mRNA expression of the fibrotic markers TGF β ₁ and collagen IV as well as pro-inflammatory cytokine IL-6 was observed in the kidney of STNx+MI and

STNx+Sham animals. Increases in TGF- β protein levels were also found in the kidney of the STNx groups. Thus, the TGF- β known as a common pathway to involve in fibroblast proliferation, extracellular matrix deposition and kidney hypertrophy,³⁵⁰⁻³⁵³ may at least in part contribute to the functional deterioration observed in the STNx groups. Increases in phospho-NF κ B protein levels were observed compared STNx groups to the Sham+Sham animals, however, no difference was found in phospho-p38 MAPK and phospho-p44/42 MAPK protein levels. Lack of significant differences among the groups may be related to the time point of the analysis.

By combining immunohistochemical and molecular biological techniques, the present study has investigated the pathology and mechanisms associated with cardiac remodelling and renal tubulointerstitial injury. Further intervention studies using this model may provide further mechanistic insights into the progression of CRS. KIM-1 may represent a useful renal injury biomarker for early detection and monitoring of disease progression, as well as potentially monitoring its response to therapy.

Chapter 7 Treatments for Indoxyl Sulfate- induced Cardiac Effects

7.1 Introduction

Indoxyl sulfate (IS), one of the non-dialysable uremic toxins, appears to be involved in the pathophysiology of CRS.¹²⁴ Significantly increased circulating IS levels have been observed in animals with CKD as described in Chapter 3 and 5. Furthermore, IS has been demonstrated to have direct pro-hypertrophic and pro-fibrotic effects on cardiac cells.¹²⁶ It significantly increased neonatal cardiac myocyte hypertrophy and fibroblast collagen synthesis in a clinically relevant concentration range.¹²⁶ In this chapter, we attempt to determine potential approaches to block IS-induced cardiac remodelling. Targeting the pathways associated with the IS-stimulated detrimental effects may represent a novel therapeutic approach to the management of CHF with concomitant CKD.

Neonatal cardiac myocytes (NCMs) and neonatal cardiac fibroblasts (NCFs) have been used in this study as they have been proven to be valid models of cardiac myocyte hypertrophy and fibroblast collagen synthesis as well as for evaluating the efficacy of therapeutic agents.^{126, 252} This *in vitro* study directly evaluates inhibition of IS-stimulated adverse cardiac effects, in comparison to the *in vivo* setting where many other systems may interfere with the findings.

OAT family has been found to play an important role in the absorption of a broad spectrum of substrates that include clinical drugs, their metabolites and uremic toxins.^{131, 133} Administration of IS to animals with CKD has resulted in IS being detected in the proximal and distal tubules where OAT1/3 have been localized.¹³³ Adverse cardiac and renal effects caused by IS may share a common pathogenesis

pathway. We therefore hypothesized that antagonists of OAT1/3 would suppress IS-induced cardiac myocyte hypertrophy and fibroblast collagen synthesis, which contribute to pathological cardiac remodelling (Figure 7.1).

ASK1 has been demonstrated to be a key element in the mechanisms of myocardial cell apoptosis and non-apoptotic cardiomyocyte death.^{68, 71, 72} It is a critical signalling molecule in LV remodelling including cardiac hypertrophy and cardiac interstitial fibrosis *via* activation of JNK, p38 MAPK and NFκB pathways.^{70, 73, 75, 77} Thus, it is proposed to be a potential therapeutic target for cardiac disease. Furthermore, the activation of ASK1 downstream p38, p44/42 MAPK and NFκB pathways has been shown to be involved in IS-induced cardiac remodelling.¹²⁶ Hence, we hypothesized that inhibition of ASK1 would also suppress IS-activated cardiac remodelling (Figure 7.1).

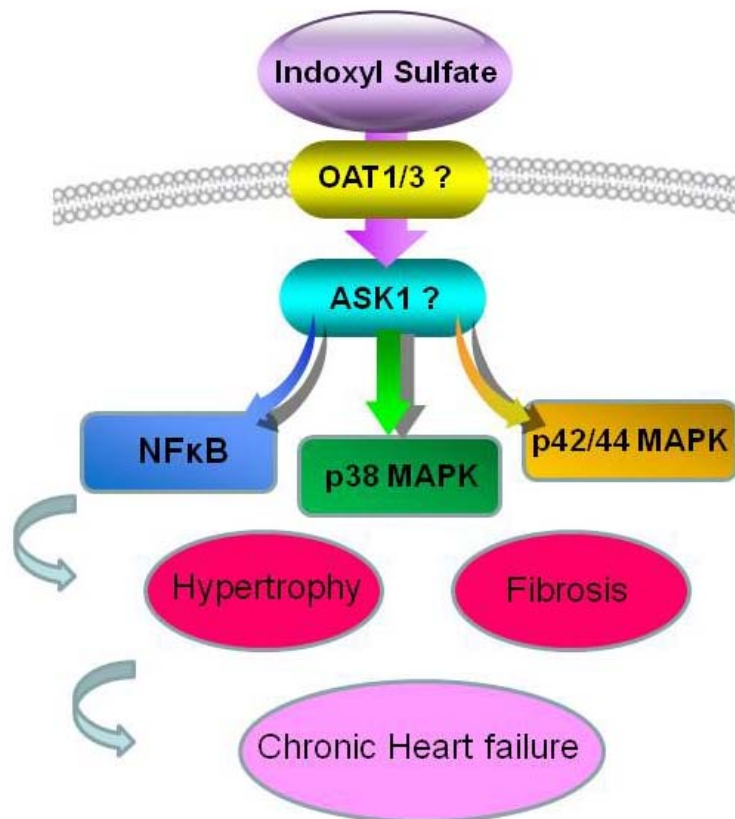


Figure 7.1 Potential pathways involved in the indoxyl sulfate-induced cardiac effects. OAT1/3, organic anion transporters 1 and 3; ASK1, apoptosis signal-regulating kinase-1; p38 and p44/42 MAPK, p38 and p44/42 mitogen-activated protein kinase; NFκB, nuclear factor-kappa B.

Based on above considerations, the hypothesis for this chapter is that the inhibition of OAT1/3 and/or ASK1 would suppress IS-induced cardiac myocyte hypertrophy and fibroblast collagen synthesis, which adversely affect cardiac function.

7.2 Aims

To investigate potential treatments for suppression of IS-induced cardiac myocyte hypertrophy and fibroblast collagen synthesis.

7.3 Materials and Methods

Sprague Dawley neonatal cardiac myocytes and fibroblasts were isolated and cultured as per Chapter 2.2.4. OAT1/3 antagonists [probenecid (Pro) and cilastatin (Cil)] and ASK1 inhibitors [GSK2261818A (G226) and GSK2358939 (G235)] were co-cultured at increasing doses for 48-hour with IS (10 μ M) in cardiac myocytes and fibroblasts. 3 H-leucine and 3 H-proline incorporation were used to assess myocyte hypertrophy and collagen turnover respectively. MTT assay was used to determine cardiac cell viability.

7.4 Results

7.4.1 OAT1/3 inhibition in cardiac myocytes

Stimulation of IS with a concentration of 10 μ M caused 21.0% increases in cardiomyocyte hypertrophy compared with unstimulated cells ($p < 0.001$), as determined by 3 H-leucine incorporation (Figure 7.2). Addition of OAT1/3 inhibitors, Pro and Cil, at concentration ranging from 0.1 to 100 μ M inhibited IS-stimulated hypertrophy down to unstimulated levels, indicating that OAT1/3 may be involved in IS-induced cardiomyocyte hypertrophy.

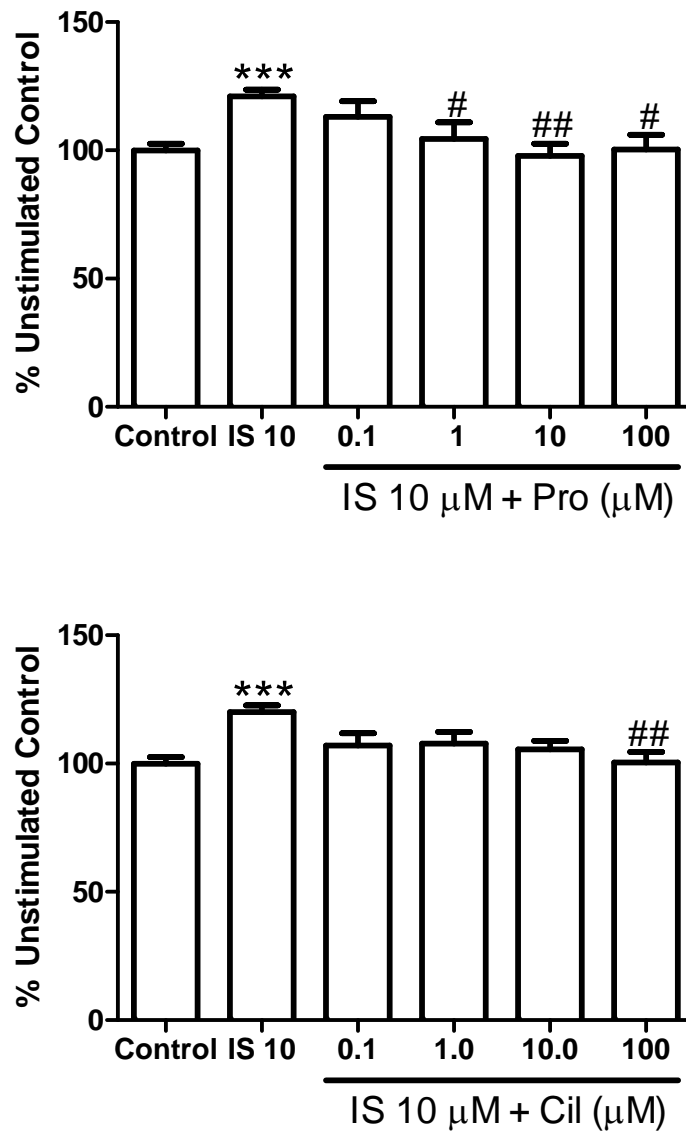


Figure 7.2 Inhibition effects of probenecid (Pro) and cilastatin (Cil) on indoxyl sulfate (IS)-induced neonatal cardiac myocyte hypertrophy. The stimulation effects of IS were inhibited by Pro and Cil in a dose-dependent manner, indicating that the effects may be in part *via* OAT1/3. Data are presented as means \pm SEM from three experiments each with triplicates. *** $p < 0.001$ 10 μ M IS vs unstimulated control, # $p < 0.05$, ## $p < 0.01$ vs 10 μ M IS.

7.4.2 OAT1/3 inhibition in cardiac fibroblasts

Stimulation of IS with a concentration of 10 μM caused 15.5% increases in cardiac fibroblast collagen synthesis ($p < 0.001$), as determined by ^3H -proline incorporation (Figure 7.3). Co-administration of OAT1/3 antagonists, Pro and Cil, at concentration ranging from 0.1 to 100 μM attenuated the increases in collagen synthesis in a dose-dependent manner, indicating that OAT1/3 may be involved in IS-induced cardiac fibroblast collagen synthesis. Pro appeared to be more potent in inhibiting collagen synthesis comparing to Cil.

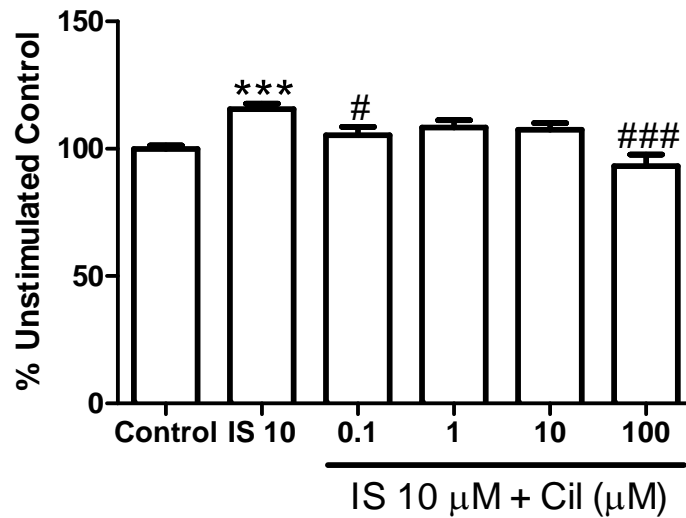
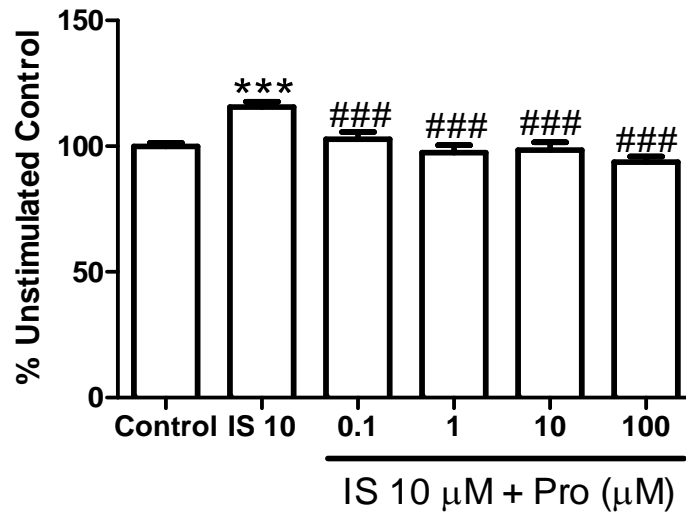


Figure 7.3 Inhibition effects of probenecid (Pro) and cilastatin (Cil) on indoxyl sulfate (IS)-induced neonatal cardiac fibroblast collagen synthesis. The stimulation effects of IS were inhibited by Pro and Cil in a dose-dependent manner, indicating that the effects may be in part *via* OAT1/3. Data are presented as means \pm SEM from three experiments each with triplicates. *** $p < 0.001$ 10 μ M IS vs unstimulated control, # $p < 0.05$, ### $p < 0.001$ vs 10 μ M IS.

7.4.3 ASK1 inhibition in cardiac myocytes

Stimulation of IS with a concentration of 10 μM caused significant increases in cardiomyocyte hypertrophy compared with unstimulated cells ($p < 0.001$), as determined by ^3H -leucine incorporation. Addition of ASK1 inhibitors, G226 and G235, at concentration ranging from 0.03 to 1.0 μM inhibited IS-stimulated myocyte hypertrophy in a dose-dependent manner, indicating that ASK1 may be involved in IS-induced cardiomyocyte hypertrophy (Figure 7.4). G226 appeared to be more potent in inhibiting hypertrophy comparing to G235.

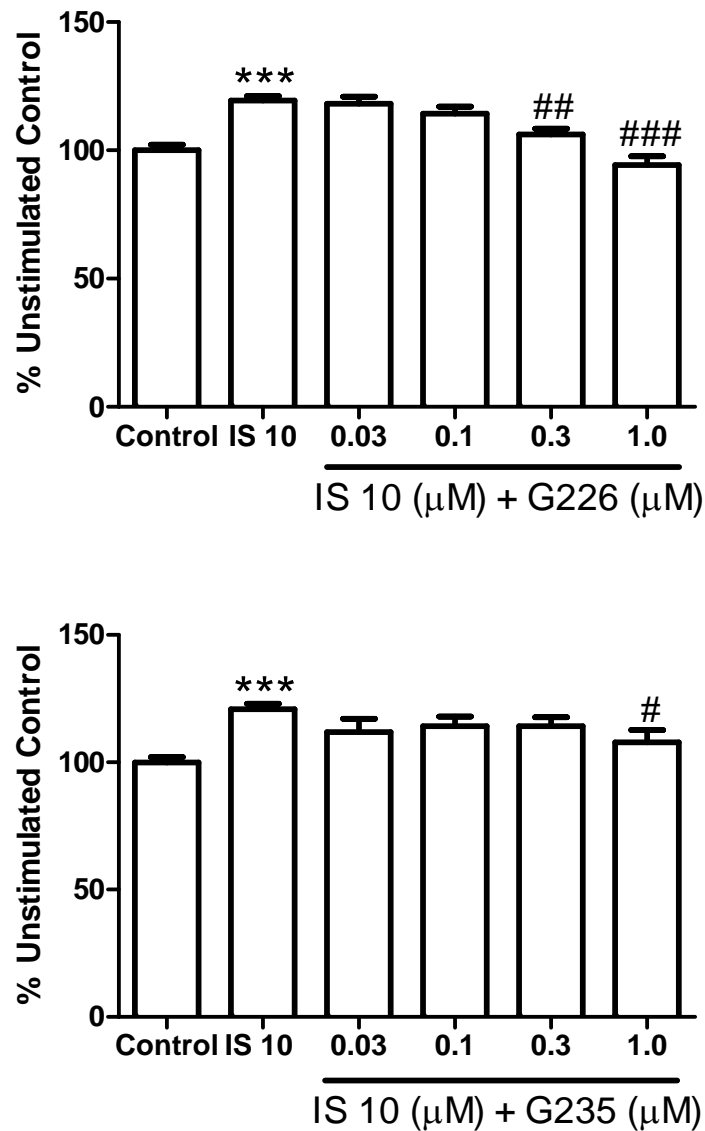


Figure 7.4 Inhibition effects of GSK2261818A (G226) and GSK2358939 (G235) on indoxyl sulfate (IS)-induced neonatal cardiac myocyte hypertrophy. The stimulation effects of IS were inhibited by G226 and G235 in a dose-dependent manner, indicating that the effects may be in part *via* ASK1. Data are presented as means \pm SEM from three experiments each with triplicates. *** $p < 0.001$ 10 μ M IS vs unstimulated control, # $p < 0.05$, ## $p < 0.01$, ### $p < 0.001$ vs 10 μ M IS.

7.4.4 ASK1 inhibition in cardiac fibroblasts

Cardiac fibroblast collagen synthesis was significantly increased by stimulation of IS with a concentration of 10 μM ($p < 0.001$), as determined by ^3H -proline incorporation. Addition of ASK1 inhibitors, G226 and G235, at concentration ranging from 0.03 to 1.0 μM inhibited IS-stimulated collagen synthesis down to unstimulated levels, indicating that ASK1 may be involved in IS-induced cardiac fibroblast collagen synthesis (Figure 7.5).

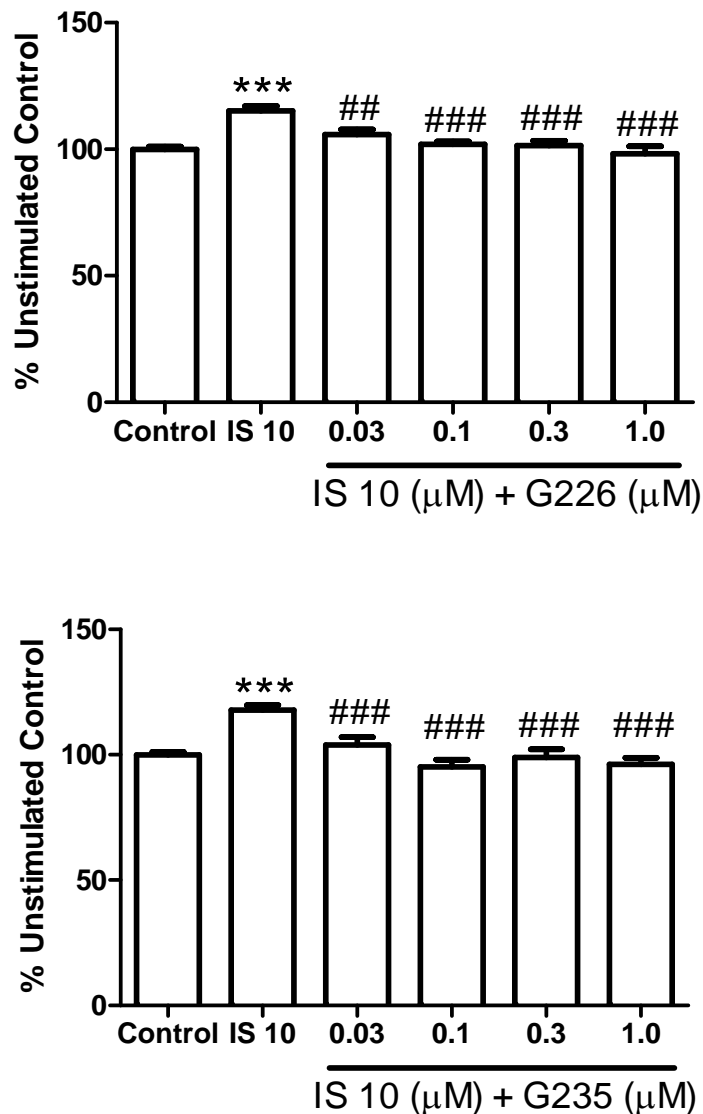


Figure 7.5 Inhibition effects of GSK2261818A (G226) and GSK2358939 (G235) on indoxyl sulfate (IS)-induced neonatal cardiac fibroblast collagen synthesis. The

stimulation effects of IS were inhibited by G226 and G235 in a dose-dependent manner, indicating that the effects may be in part *via* ASK1. Data are presented as means \pm SEM from three experiments each with triplicates. *** $p < 0.001$ 10 μ M IS vs unstimulated control, ## $p < 0.01$, ### $p < 0.001$ vs 10 μ M IS.

7.4.5 Effect of OAT1/3 and ASK1 inhibitors on cardiac cell viability

The effects of OAT1/3 and ASK1 inhibitors on cardiac cell viability were examined by MTT assay. OAT1/3 and ASK1 inhibitors did not affect cardiac cell viability at concentration ranging from 0.1 to 100, and 0.03 to 1.0 μ M respectively (Figure 7.6).

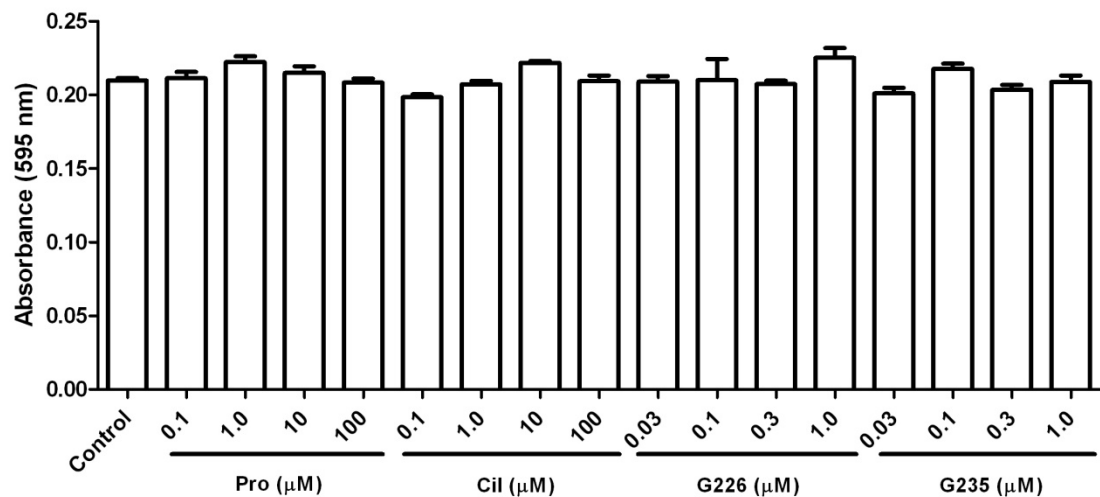


Figure 7.6 Effect of OAT1/3 inhibitors (Pro and Cil) and ASK1 inhibitors (G226 and G235) on neonatal cardiac fibroblast viability at concentration ranging from 0.1 to 100, and 0.03 to 1.0 μ M respectively. Data are presented as means \pm SEM. Pro, probenecid; Cil, cilastatin; G226, GSK2261818A; G235, GSK2358939.

7.5 Discussion

Cardiac hypertrophy and interstitial fibrosis, predominant features of uremic cardiomyopathy, are sustained in both CKD patients and animal models, even with well-controlled blood pressure.^{119, 124, 354, 355} In this chapter, we investigated NCMs and NCFs *via* approaches to block pro-hypertrophic and pro-fibrotic actions of IS. Circulating levels of IS in CKD patients vary from a few micromolars to hundreds of micromolars.^{134, 356} Thus, the concentration of 10 μ M for IS-induced cardiac effects falls into a clinically relevant pathophysiological concentration range. Inhibition of OAT1/3 and ASK1 suppressed IS-activated cardiac myocyte hypertrophy and fibroblast collagen synthesis. OAT1/3 and ASK1 antagonists appear to attenuate these effects by blocking the uptake of IS into cardiac cells and downstream intracellular pathway respectively.

These findings occurred in the absence of any significant reduction in cardiac cell survival and proliferation. Specifically, IS did not affect cardiac cell viability over the concentration range from 0.01 to 100 μ M.¹²⁶ Furthermore, OAT1/3 and ASK1 antagonists did not affect cardiac cell viability at the concentrations used in this study.

Intervention with other OAT inhibitors and/or suppression of other downstream intracellular actions post-uptake may be of therapeutic benefit. However, OAT1/3 and ASK1 antagonists may have additional, non-specific actions other than as OAT1/3 and ASK1 inhibitors.

Based on these findings, an *in vivo* STNx model can be proposed to confirm the effects of OAT inhibitors and ASK1 antagonists on amelioration of cardiac toxicity induced by

IS. Although there have been reports that show existence of OAT1/3 in the kidneys, further experiments need to be performed to support the localization of accumulated IS and sites of OAT1/3 in the heart using immunohistochemistry or mRNA expression.

In summary, OAT1/3 and ASK1 appear to play a role in IS-induced pathological cardiac remodelling, which are suppressed by OAT1/3 and ASK1 antagonists, in a dose-dependent manner. Blocking the cardiac uptake and/or the pathways it activates may represent a potential novel therapeutic strategy to ameliorate uremic toxin-stimulated cardiac effects in the setting of co-morbid CHF and CKD.

Chapter 8 Thesis Summary, Conclusions and Future Directions

Cardiorenal syndrome (CRS) is a complex clinical condition, and the management of this condition is still sub-optimal because the pathophysiology and mechanisms underlying this syndrome are yet to be fully explored. Therefore, this thesis was aimed to establish important new preclinical CRS models to provide original and further insights into the pathophysiology and the underlying mechanisms of CRS. Several important findings will be summarised and the conclusions drawn from these results will be described in this chapter. Furthermore, severe renal dysfunction and significantly increased circulating IS levels have been observed in uremic animals and human kidney disease. Our group has recently demonstrated a possible role of IS in the cell culture setting examining its effects on myocyte hypertrophy and fibroblast collagen synthesis. Findings from the potential treatments of IS-induced cardiac effects will also be described.

8.1 *In vivo* MI+STNx and STNx+MI studies

In Chapter 3 and 4, we have demonstrated in type II CRS model of MI complicated by the addition of STNx, subsequent kidney insult accelerated the reduction in LVEF and cardiac remodelling post-MI, whilst MI attenuated the STNx-induced changes in BP and accelerated STNx-induced renal tubulointerstitial fibrosis. However MI showed little effects on the STNx-associated KIM-1 tissue levels.

In Chapter 5 and 6, we have investigated the impact on the heart and kidney in type IV CRS model of STNx complicated by the addition of MI. The findings suggest that MI accelerated STNx-induced cardiac remodelling, and increased renal tubulointerstitial fibrosis and KIM-1 tissue levels; and all of these effects were BP independent.

Although CHF and CKD are heterogeneous disorders that result from multiple underlying diseases and involve various regulatory mechanisms, accelerated cardiac remodelling and increased renal tubulointerstitial fibrosis appear to be the common pathophysiological changes occurring in both models. The tubular injury biomarker KIM-1 can be considered as a sensitive renal biomarker for the early detection of progressive kidney failure.

To further evaluate the disease mechanisms and outcomes of these animal models, data from MI+STNx and STNx+MI studies were pooled and multiple analyses performed. Animals were categorized into Sham, MI, STNx, MI+STNx and STNx+MI animals (Table 8.1). MI groups (MI, MI+STNx and STNx+MI animals) had similar infarct size. The addition of STNx to MI further reduced LVEF and FS compared to MI only ($p<0.05$). STNx groups (STNx, MI+STNx and STNx+MI animals) had significantly increased circulating IS levels. The addition of MI to STNx did not further reduce GFR compared to STNx only.

Table 8.1 Pooled analysis of data from MI+STNx and STNx+MI studies, categorizing animals to Sham, MI, STNx, MI+STNx and STNx+MI groups.

	Sham	MI	STNx	MI+STNx	STNx+MI
Survival rate (%)	100.0	64.0	68.5	44.1	39.8
Infarct size (%)	-	35.2±1.9	-	33.7±1.5	34.4±2.4
BP (mmHg)	132.1±3.9	123.2±4.5	221.8±6.9 ***, §§§	176.6±9.3 ***, §§§, ###	204.9±11.6 ***, §§§
LVEF (%)	67.4±1.7	40.4±1.4 ***	73.2±2.0 §§§	31.2±1.3 ***, §, ###	42.7±3.5 ***, ###, aa
FS (%)	40.2±1.5	18.1±0.7 ***	45.5±2.1 §§§	15.1±0.9 ***, §, ###	18.1±1.2 ***, ###
ESPVR (mmHg/μl)	0.53±0.05	0.27±0.03 *	0.73±0.09 §§§	0.32±0.04 *, ##	0.38±0.03
EDPVR (mmHg/μl)	0.02±0.01	0.04±0.01 *	0.04±0.01 **	0.04±0.01 *	0.05±0.01 *
Tau logistic (ms)	10.7±0.4	12.6±0.5 **	17.1±0.9 ***, §§§	17.0±1.4 ***, §§	17.0±1.6 ***, §§
LVEDP (mmHg)	3.2±0.4	8.0±0.8 ***	7.4±1.0 ***	10.7±1.5 ***	8.8±1.8 ***
GFR (ml/min/Kg)	8.5±0.3	7.4±0.5	1.0±0.3 ***, §§§	1.5±0.4 ***, §§§	0.4±0.3 ***, §§§
CrCl (ml/min)	233.2±18.8	221.6±27.4	32.7±6.9 ***, §§§	33.8±7.9 ***, §§§	33.9±12.4 ***, §§§
Proteinuria (mg/24 hr)	23.9±1.5	18.8±1.3	366.9±37.9 ***, §§§	433.7±87.1 ***, §§§	380.0±89.1 ***, §§§
IS (μmol/L)	12.48±1.51	12.31±1.13	62.90±10.43 ***, §§§	64.05±13.58 ***, §§§	66.19±13.17 ***, §§§
KIM-1 (%)	0.014±0.003	0.014±0.002	0.322±0.064 ***, §§§	0.340±0.084 ***, §§§	0.807±0.160 ***, §§§, ###, aaa

Values are expressed as mean ± SEM. BP, blood pressure; LVEF, left ventricular ejection fraction; FS, fractional shortening; ESPVR and EDPVR, slope of end systolic and diastolic pressure-volume relationship; LVEDP: LV end diastolic pressure; GFR, glomerular filtration rate; CrCl, creatinine clearance; IS, indoxyl sulfate; KIM-1, kidney injury molecule-1. * p<0.05, ** p<0.01, *** p<0.001 vs Sham; § p<0.05, §§ p<0.01, §§§ p<0.001 vs MI; ## p<0.01, ### p<0.001 vs STNx; aa p<0.01, aaa p<0.001 vs MI+STNx.

MI+STNx animals had decreased LVEF ($p<0.01$) and almost significantly reduced FS ($p=0.055$) compared to STNx+MI animals, whilst a non-significant reduction in GFR ($p=0.064$) and increased KIM-1 tissue levels ($p<0.001$) were observed in STNx+MI vs MI+STNx animals. These changes occurred independent of BP. The findings indicate that animals with pre-morbid CHF had worsening cardiac outcomes; and that animals with pre-morbid CKD were likely to have more severe renal outcomes, suggesting that the severity of heart and kidney damage appears to be best related with the primary failing organ. The reduced LVEF may be caused by an extended MI follow-up period (14 vs 8 weeks) in MI+STNx animals, and conversely the non-significantly reduced GFR may be due to the longer STNx follow-up period in STNx+MI animals (12 vs 10 weeks).

8.2 Study limitations

STNx+MI animals were unable to be maintained for longer than 12 weeks due to the very high mortality observed over this duration, presumably due to the aggressive nature of STNx surgery. Thus, a longer follow-up to match our previous MI+STNx study of 14 weeks experimental time was difficult to conduct.

We did not observe any major evidence of deterioration in renal function in the MI+STNx and/or STNx+MI setting compared to the STNx only. Changes in renal fibrosis may not necessarily be accompanied by functional alterations at 14/12 weeks. This may be representative of the time it takes for pathological fibrosis to contribute to the subsequent dysfunction. Alternatively, the insult induced by STNx may be so aggressive that a further reduction in renal function following MI would be impossible to observe.

8.3 *In vitro* IS study

In isolated rat neonatal cardiac myocytes and fibroblasts, inhibition of OAT1/3 and ASK1 suppressed the myocyte hypertrophy and fibroblast collagen synthesis stimulated by IS, in a dose-dependent manner. These observations are of considerable clinical interest as hypertrophy and fibrosis are involved in the ongoing cardiac remodelling process and commonly found in association with HF. Therefore, the findings may suggest novel approaches in the prevention and management of IS-induced cardiac remodelling and failure.

8.4 Future directions

This thesis has focused on better understanding of the pathophysiology and potential mechanisms of CRS, and opportunities for early diagnosis through KIM-1. The animal models established within this thesis provide base models for future research including development of preventive strategies and application of mechanism-targeted management.

Neurohormonal over-activation and hemodynamic disturbances are major contributors to CRS. Despite available therapies to control neurohormonal overdrive and high BP, this condition remains associated with markedly reduced survival.³ Therefore, additional strategies are urgently needed to impact on this disease condition. Potential novel therapeutic strategies designed to reduce circulating IS levels in addition to current management can be examined employing the models established (e.g. MI+STNx and/or STNx+MI models). Key therapeutic approaches, such as RAAS blockade can be included as background therapy. Treatment effects of a gut adsorbent, AST-120 remain to be investigated in combination with a RAAS blocker in CRS

animal models. Addition of AST-120 to conventional management would be of major clinical relevance if its cardiorenal-protective effects can be confirmed.

To further investigate the MI+STNx and STNx+MI models, the blood pressure in the STNx animals should be controlled as that would differentiate the effect of hypertension for that of CKD.

To facilitate the identification of the progression of CRS, the present work measured tissue KIM-1 levels using immunohistochemistry. Further quantitative tests (e.g. sandwich ELISA) on urinary KIM-1 levels are needed to detect this protein as a potential biomarker in current pathophysiological models and/or other preclinical drug development studies. If this is the case, the evaluation of urinary KIM-1 levels may serve as a non-invasive, rapid, sensitive method to facilitate early assessment of pathophysiological influences and drug toxicity.

The accumulation of circulating IS was demonstrated in animals with STNx, MI+STNx, and STNx+MI. Further investigations on tissue IS levels in heart may provide strong evidence of IS-associated uremic cardiomyopathy. The question of whether IS-induced cardiac remodelling is linked to other common contributors described in the pathophysiology of CRS, particularly neurohormonal processes, remains currently unanswered.

The efficacy of OAT1/3 and ASK1 inhibitors *in vitro* makes these compounds potentially useful in the management of uremic cardiomyopathy. The fact that these compounds act on different IS signalling pathways, may at least in part provide useful

insights into the mechanisms of IS-induced cardiac fibrosis. Further studies are needed to determine whether blockade of OAT1/3 and ASK1 will be of benefit in relevant disease models (e.g. MI+STNx and/or STNx+MI models) or in man.

This thesis can therefore serve as a starting point for the future of basic research into the condition of CRS which adversely affects so many people worldwide.

References

1. Berl T, Henrich W. Kidney-heart interactions: epidemiology, pathogenesis, and treatment. *Clin J Am Soc Nephrol*. 2006;1(1):8-18.
2. Bock JS, Gottlieb SS. Cardiorenal Syndrome: New Perspectives. *Circulation*. 2010;121(23):2592-2600.
3. Ronco C, Haapio M, House AA, Anavekar N, Bellomo R. Cardiorenal syndrome. *J Am Coll Cardiol*. 2008;52(19):1527-1539.
4. Ronco C, McCullough P, Anker SD, Anand I, Aspromonte N, Bagshaw SM, Bellomo R, Berl T, Bobek I, Cruz DN, Daliento L, Davenport A, Haapio M, Hillege H, House AA, Katz N, Maisel A, Mankad S, Zanco P, Mebazaa A, Palazzuoli A, Ronco F, Shaw A, Sheinfeld G, Soni S, Vescovo G, Zamperetti N, Ponikowski P. Cardio-renal syndromes: report from the consensus conference of the Acute Dialysis Quality Initiative. *Eur Heart J*. 2010;31(6):703-711.
5. Han WK, Bonventre JV. Biologic markers for the early detection of acute kidney injury. *Curr Opin Crit Care*. 2004;10(6):476-482.
6. Heywood JT, Fonarow GC, Costanzo MR, Mathur VS, Wigneswaran JR, Wynne J. High Prevalence of Renal Dysfunction and Its Impact on Outcome in 118,465 Patients Hospitalized With Acute Decompensated Heart Failure: A Report From the ADHERE Database. *J Card Fail*. 2007;13(6):422-430.
7. Bagshaw SM, Cruz DN, Aspromonte N, Daliento L, Ronco F, Sheinfeld G, Anker SD, Anand I, Bellomo R, Berl T, Bobek I, Davenport A, Haapio M, Hillege H, House A, Katz N, Maisel A, Mankad S, McCullough P, Mebazaa A, Palazzuoli A, Ponikowski P, Shaw A, Soni S, Vescovo G, Zamperetti N, Zanco P, Ronco C, for the Acute Dialysis Quality Initiative Consensus G. Epidemiology of cardio-renal syndromes: workgroup statements from the 7th ADQI Consensus Conference. *Nephrol Dial Transplant*. 2010;25(5):1406-1416.
8. Bagshaw SM, George C, Dinu I, Bellomo R. A multi-centre evaluation of the RIFLE criteria for early acute kidney injury in critically ill patients. *Nephrol Dial Transplant*. 2008;23(4):1203-1210.
9. Uchino S, Bellomo R, Goldsmith D, Bates S, Ronco C. An assessment of the RIFLE criteria for acute renal failure in hospitalized patients. *Crit Care Med*. 2006;34(7):1913-1917.
10. Kellum JA, Levin N, Bouman C, Lameire N. Developing a consensus classification system for acute renal failure. *Curr Opin Crit Care*. 2002;8(6):509-514.
11. Bellomo R, Ronco C, Kellum JA, Mehta RL, Palevsky P. Acute renal failure - definition, outcome measures, animal models, fluid therapy and information technology needs: the Second International Consensus Conference of the Acute Dialysis Quality Initiative (ADQI) Group. *Crit Care*. 2004;8(4):R204-212.
12. Mehta RL, Kellum JA, Shah SV, Molitoris BA, Ronco C, Warnock DG, Levin A. Acute Kidney Injury Network: report of an initiative to improve outcomes in acute kidney injury. *Crit Care*. 2007;11(2):R31.
13. McCullough PA. Cardiovascular disease in chronic kidney disease from a cardiologist's perspective. *Curr Opin Nephrol Hypertens*. 2004;13(6):591-600.
14. Ronco C, Maisel A. Volume Overload and Cardiorenal Syndromes. *Congest Heart Fail*. 2010;16(4):Si-Siv.

15. McMurray JJV, Pfeffer MA. Heart failure. *Lancet*. 2005;365(9474):1877-1889.
16. Mosterd A, Hoes AW. Clinical epidemiology of heart failure. *Heart*. 2007;93(9):1137-1146.
17. Redfield MM, Jacobsen SJ, Burnett JC, Mahoney DW, Bailey KR, Rodeheffer RJ. Burden of systolic and diastolic ventricular dysfunction in the community: Appreciating the scope of the heart failure epidemic. *JAMA*. 2003;289(2):194-202.
18. Haldeman GA, Croft JB, Giles WH, Rashidee A. Hospitalization of patients with heart failure: National Hospital Discharge Survey, 1985 to 1995. *Am Heart J*. 1999;137(2):352-360.
19. Berry C, Murdoch DR, McMurray JJV. Economics of chronic heart failure. *Eur J Heart Fail*. 2001;3(3):283-291.
20. Hillege HL, van Gilst WH, van Veldhuisen DJ, Navis G, Grobbee DE, de Graeff PA, de Zeeuw D. Accelerated decline and prognostic impact of renal function after myocardial infarction and the benefits of ACE inhibition: the CATS randomized trial. *Eur Heart J*. 2003;24(5):412-420.
21. Forman DE, Butler J, Wang Y, Abraham WT, O'Connor CM, Gottlieb SS, Loh E, Massie BM, Rich MW, Stevenson LW, Young JB, Krumholz HM. Incidence, predictors at admission, and impact of worsening renal function among patients hospitalized with heart failure. *J Am Coll Cardiol*. 2004;43(1):61-67.
22. Hillege HL, Girbes ARJ, de Kam PJ, Boomsma F, de Zeeuw D, Charlesworth A, Hampton JR, van Veldhuisen DJ. Renal function, neurohormonal activation, and survival in patients with chronic heart failure. *Circulation*. 2000;102(2):203-210.
23. Dries DL, Exner DV, Domanski MJ, Greenberg B, Stevenson LW. The prognostic implications of renal insufficiency in asymptomatic and symptomatic patients with left ventricular systolic dysfunction. *J Am Coll Cardiol*. 2000;35(3):681-689.
24. Hillege HL, Nitsch D, Pfeffer MA, Swedberg K, McMurray JJV, Yusuf S, Granger CB, Michelson EL, Ostergren J, Cornel JH, de Zeeuw D, Pocock S, van Veldhuisen DJ. Renal function as a predictor of outcome in a broad spectrum of patients with heart failure. *Circulation*. 2006;113(5):671-678.
25. Shlipak MG. Pharmacotherapy for heart failure in patients with renal insufficiency. *Ann Intern Med*. 2003;138(11):917-924.
26. Smith GL, Vaccarino V, Kosiborod M, Lichtman JH, Cheng S, Watnick SG, Krumholz HM. Worsening renal function: What is a clinically meaningful change in creatinine during hospitalization with heart failure? *J Card Fail*. 2003;9(1):13-25.
27. Elsayed EF, Tighiouart H, Griffith J, Kurth T, Levey AS, Salem D, Sarnak MJ, Weiner DE. Cardiovascular disease and subsequent kidney disease. *Arch Intern Med*. 2007;167(11):1130-1136.
28. Smith GL, Lichtman JH, Bracken MB, Shlipak MG, Phillips CO, DiCapua P, Krumholz HM. Renal Impairment and Outcomes in Heart Failure Systematic Review and Meta-Analysis. *J Am Coll Cardiol*. 2006;47:1987-1996.
29. de Silva R, Nikitin NP, Witte KKA, Rigby AS, Goode K, Bhandari S, Clark AL, Cleland JGF. Incidence of renal dysfunction over 6 months in patients with chronic heart failure due to left ventricular systolic dysfunction: contributing factors and relationship to prognosis. *Eur Heart J*. 2006;27:569-581.
30. Al-Ahmad A, Rand WM, Manjunath G, Konstam MA, Salem DN, Levey AS, Sarnak MJ. Reduced kidney function and anemia as risk factors for mortality in

- patients with left ventricular dysfunction. *J Am Coll Cardiol*. 2001;38(4):955-962.
31. Bibbins-Domingo K, Lin F, Vittinghoff E, Barrett-Connor E, Grady D, Shlipak MG. Renal insufficiency as an independent predictor of mortality among women with heart failure. *J Am Coll Cardiol*. 2004;44(8):1593-1600.
 32. Ahmed A, Rich MW, Sanders PW, Perry GJ, Bakris GL, Zile MR, Love TE, Aban IB, Shlipak MG. Chronic Kidney Disease Associated Mortality in Diastolic Versus Systolic Heart Failure: A Propensity Matched Study. *Am J Cardiol*. 2007;99(3):393-398.
 33. Campbell RC, Sui X, Filippatos G, Love TE, Wahle C, Sanders PW, Ahmed A. Association of chronic kidney disease with outcomes in chronic heart failure: a propensity-matched study. *Nephrol Dial Transplant*. 2009;24(1):186-193.
 34. Gottlieb SS, Abraham W, Butler J, Forman DE, Loh E, Massie BM, O'Connor CM, Rich MW, Stevenson LW, Young J, Krumholz HM. The prognostic importance of different definitions of worsening renal function in congestive heart failure. *J Card Fail*. 2002;8(3):136-141.
 35. Smith GL, Shlipak MG, Havranek EP, Masoudi FA, McClellan WM, Foody JM, Rathore SS, Krumholz HM. Race and Renal Impairment in Heart Failure: Mortality in Blacks Versus Whites. *Circulation*. 2005;111(10):1270-1277.
 36. United States Renal Data System. USRDS 2012 Annual Data Report: Atlas of Chronic Kidney Disease and End-Stage Renal Disease in the United States. 2012.
 37. Sarnak MJ, Levey AS, Schoolwerth AC, Coresh J, Culleton B, Hamm LL, McCullough PA, Kasiske BL, Kelepouris E, Klag MJ, Parfrey P, Pfeffer M, Raij L, Spinosa DJ, Wilson PW. Kidney disease as a risk factor for development of cardiovascular disease: A statement from the American Heart Association Councils on kidney in cardiovascular disease, high blood pressure research, clinical cardiology, and epidemiology and prevention. *Hypertension*. 2003;42(5):1050-1065.
 38. Levey AS, Coresh J, Balk E, Kausz AT, Levin A, Steffes MW, Hogg RJ, Perrone RD, Lau J, Eknoyan G. National Kidney Foundation Practice Guidelines for Chronic Kidney Disease: Evaluation, Classification, and Stratification. *Ann Intern Med*. 2003;139(2):137-147.
 39. Sarnak MJ, Levey AS, Schoolwerth AC, Coresh J, Culleton B, Hamm LL, McCullough PA, Kasiske BL, Kelepouris E, Klag MJ, Parfrey P, Pfeffer M, Raij L, Spinosa DJ, Wilson PW. Kidney Disease as a Risk Factor for Development of Cardiovascular Disease: A Statement From the American Heart Association Councils on Kidney in Cardiovascular Disease, High Blood Pressure Research, Clinical Cardiology, and Epidemiology and Prevention. *Circulation*. 2003;108(17):2154-2169.
 40. Shulman N, Ford C, Hall W, Blaufox M, Simon D, Langford H, Schneider K. Prognostic value of serum creatinine and effect of treatment of hypertension on renal function. Results from the hypertension detection and follow-up program. The hypertension detection and follow-up program cooperative group. *Hypertension*. 1989;13(5 Suppl):I80-93.
 41. Tyralla K, Amann K. Cardiovascular changes in renal failure. *Blood Purificat*. 2002;20(5):462-465.
 42. Foley RN, Parfrey PS, Sarnak MJ. Clinical epidemiology of cardiovascular disease in chronic renal disease. *Am J Kidney Dis*. 1998;32(5 Suppl 3):S112-119.

43. Foley RN, Parfrey PS, Harnett JD, Kent GM, Martin CJ, Murray DC, Barre PE. Clinical and echocardiographic disease in patients starting end-stage renal disease therapy. *Kidney Int.* 1995;47(1):186-192.
44. Ritz E, Bommer J. Cardiovascular Problems on Hemodialysis: Current Deficits and Potential Improvement. *Clin J Am Soc Nephrol.* 2009;4(Suppl 1):S71-S78.
45. Herzog CA, Ma JZ, Collins AJ. Poor Long-Term Survival after Acute Myocardial Infarction among Patients on Long-Term Dialysis. *New Engl J Med.* 1998;339(12):799-805.
46. Herzog CA. Dismal long-term survival of dialysis patients after acute myocardial infarction: can we alter the outcome? *Nephrol Dial Transplant.* 2002;17(1):7-10.
47. Go AS, Chertow GM, Fan D, McCulloch CE, Hsu C-y. Chronic kidney disease and the risks of death, cardiovascular events, and hospitalization. *N Engl J Med* 2004;351(13):1296-1305.
48. Brewster UC, Setaro JF, Perazella MA. The renin-angiotensin-aldosterone system: cardiorenal effects and implications for renal and cardiovascular disease states. *Am J Med Sci.* 2003;326(1):15-24.
49. Sica DA. Sodium and water retention in heart failure and diuretic therapy: basic mechanisms. *Clev Clin J Med.* 2006;73(Suppl 2):S2.
50. Atlas SA. The Renin-Angiotensin Aldosterone System: Pathophysiological Role and Pharmacologic Inhibition. *J Manag Care Pharm.* 2007;13(8 Suppl B):9-20.
51. Long DA, Price KL, Herrera-Acosta J, Johnson RJ. How Does Angiotensin II Cause Renal Injury? *Hypertension.* 2004;43(4):722-723.
52. Hunt SA, Abraham WT, Chin MH, Feldman AM, Francis GS, Ganiats TG, Jessup M, Konstam MA, Mancini DM, Michl K, Oates JA, Rahko PS, Silver MA, Stevenson LW, Yancy CW. ACC/AHA 2005 Guideline update for the diagnosis and management of chronic heart failure in the adult. *Circulation.* 2005;112:e154-e235.
53. Brewster UC, Perazella MA. Cardiorenal effects of the renin-angiotensin-aldosterone system. *Hosp Physician.* 2004;40:11-26.
54. Sobotka P, Mahfoud F, Schlaich M, Hoppe U, Bohm M, Krum H. Sympatho-renal axis in chronic disease. *Clin Res Cardiol.* 2011;100(12):1049–1057.
55. DiBona GF. Physiology in perspective: The wisdom of the body. Neural control of the kidney. *Am J Physiol Regul Integr Comp Physiol* 2005;289(3):R633-641.
56. Esler M. The 2009 Carl Ludwig Lecture: pathophysiology of the human sympathetic nervous system in cardiovascular diseases: the transition from mechanisms to medical management. *J Appl Physiol* 2010;108(2):227-237.
57. Galle J. Oxidative stress in chronic renal failure. *Nephrol Dial Transplant.* 2001;16(11):2135-2137.
58. Himmelfarb J, Stenvinkel P, Ikizler TA, Hakim RM. The elephant in uremia: Oxidant stress as a unifying concept of cardiovascular disease in uremia. *Kidney Int.* 2002;62:1524-1538.
59. Darley-USmar V, Wiseman H, Halliwell B. Nitric oxide and oxygen radicals: a question of balance. *FEBS Lett.* 1995;369(2-3):131-135.
60. Wever R, Boer P, Hijmering M, Stroes E, Verhaar M, Kastelein J, Versluis K, Lagerwerf F, van Rijn H, Koomans H, Rabelink T. Nitric Oxide Production Is Reduced in Patients With Chronic Renal Failure. *Arterioscler Thromb Vasc Biol.* 1999;19(5):1168-1172.

61. Braunwald E. Biomarkers in Heart Failure. *N Engl J Med.* 2008;358(20):2148-2159.
62. Nakamura K, Fushimi K, Kouchi H, Mihara K, Miyazaki M, Ohe T, Namba M. Inhibitory effects of antioxidants on neonatal rat cardiac myocyte hypertrophy induced by tumor necrosis factor- α and angiotensin II. *Circulation.* 1998;98:794-799.
63. Hori M, Nishida K. Oxidative stress and left ventricular remodelling after myocardial infarction. *Cardiovasc Res* 2009;81:457-464.
64. Giordano FJ. Oxygen, oxidative stress, hypoxia, and heart failure. *J Clin Invest.* 2005;115:500-508.
65. Siwik DA, Tzortzis JD, Pimental DR, Chang DL, Pagano PJ, Singh K, Sawyer DB, Colucci WS. Inhibition of copper-zinc superoxide dismutase induces cell growth, hypertrophic phenotype, and apoptosis in neonatal rat cardiac myocytes in vitro. *Circ Res.* 1999;85:147-153.
66. Cesselli D, Jakoniuk I, Barlucchi L, Beltrami AP, Hintze TH, Nadal-Ginard B, Kajstura J, Leri A, Anversa P. Oxidative Stress-Mediated Cardiac Cell Death Is a Major Determinant of Ventricular Dysfunction and Failure in Dog Dilated Cardiomyopathy. *Circ Res.* 2001;89(3):279-286.
67. Liu Q, Sargent MA, York AJ, Molkentin JD. ASK1 regulates cardiomyocyte death but not hypertrophy in transgenic mice. *Circ Res.* 2009;105:1110-1117.
68. Ichijo H, Nishida E, Irie K, ten Dijke P, Saitoh M, Moriguchi T, Takagi M, Matsumoto K, Miyazono K, Gotoh Y. Induction of apoptosis by ASK1, a mammalian MAPKKK that activates SAPK/JNK and p38 signaling pathways. *Science.* 1997;275(5296):90-94.
69. Baines CP, Molkentin JD. STRESS signaling pathways that modulate cardiac myocyte apoptosis. *J Mol Cell Cardiol.* 2005;38(1):47-62.
70. Hikoso S, Ikeda Y, Yamaguchi O, Takeda T, Higuchi Y, Hirotani S, Kashiwase K, Yamada M, Asahi M, Matsumura Y, Nishida K, Matsuzaki M, Hori M, Otsu K. Progression of Heart Failure Was Suppressed by Inhibition of Apoptosis Signal-Regulating Kinase 1 Via Transcoronary Gene Transfer. *J Am Coll Cardiol.* 2007;50(5):453-462.
71. Watanabe T, Otsu K, Takeda T, Yamaguchi O, Hikoso S, Kashiwase K, Higuchi Y, Taniike M, Nakai A, Matsumura Y, Nishida K, Ichijo H, Hori M. Apoptosis signal-regulating kinase 1 is involved not only in apoptosis but also in non-apoptotic cardiomyocyte death. *Biochem Biophys Res Commun.* 2005;333(2):562-567.
72. Yamaguchi O, Higuchi Y, Hirotani S, Kashiwase K, Nakayama H, Hikoso S, Takeda T, Watanabe T, Asahi M, Taniike M, Matsumura Y, Tsujimoto I, Hongo K, Kusakari Y, Kurihara S, Nishida K, Ichijo H, Hori M, Otsu K. Targeted deletion of apoptosis signal-regulating kinase 1 attenuates left ventricular remodeling. *Proc Natl Acad Sci.* 2003;100(26):15883-15888.
73. Izumiya Y, Kim S, Izumi Y, Yoshida K, Yoshiyama M, Matsuzawa A, Ichijo H, Iwao H. Apoptosis Signal-Regulating Kinase 1 Plays a Pivotal Role in Angiotensin II-Induced Cardiac Hypertrophy and Remodeling. *Circ Res.* 2003;93(9):874-883.
74. Kompa AR, See F, Lewis DA, Adrahtas A, Cantwell DM, Wang BH, Krum H. Long-Term but Not Short-Term p38 Mitogen-Activated Protein Kinase Inhibition Improves Cardiac Function and Reduces Cardiac Remodeling Post-Myocardial Infarction. *J Pharmacol and Exp Ther.* 2008;325(3):741-750.

75. Tsujimoto I, Hikoso S, Yamaguchi O, Kashiwase K, Nakai A, Takeda T, Watanabe T, Taniike M, Matsumura Y, Nishida K, Hori M, Kogo M, Otsu K. The Antioxidant Edaravone Attenuates Pressure Overload-Induced Left Ventricular Hypertrophy. *Hypertension*. 2005;45(5):921-926.
76. Nagai H, Noguchi T, Takeda K, Ichijo H. Pathophysiological roles of ASK1-MAP kinase signaling pathways. *J Biochem Mol Biol*. 2007;40(1):1-6.
77. Hirotani S, Otsu K, Nishida K, Higuchi Y, Morita T, Nakayama H, Yamaguchi O, Mano T, Matsumura Y, Ueno H, Tada M, Hori M. Involvement of nuclear factor-kappaB and apoptosis signal-regulating kinase 1 in G-protein-coupled receptor agonist-induced cardiomyocyte hypertrophy. *Circulation*. 2002;105:509-515.
78. Wang AY-M, Wang M, Woo J, Lam CW-K, Lui S-F, Li PK-T, Sanderson JE. Inflammation, Residual Kidney Function, and Cardiac Hypertrophy Are Interrelated and Combine Adversely to Enhance Mortality and Cardiovascular Death Risk of Peritoneal Dialysis Patients. *J Am Soc Nephrol*. 2004;15(8):2186-2194.
79. Arici M, Walls J. End-stage renal disease, atherosclerosis, and cardiovascular mortality: Is C-reactive protein the missing link? *Kidney Int*. 2001;59:407-414.
80. Stenvinkel P. New insights on inflammation in chronic kidney disease-genetic and non-genetic factors. *Nephrol Ther*. 2006;2(3):111-119.
81. Yeun J, Levine R, Mantadilok V, Kaysen G. C-Reactive protein predicts all-cause and cardiovascular mortality in hemodialysis patients. *Am J Kidney Dis*. 2000;35(3):469-476.
82. Ridker PM, Cushman M, Stampfer MJ, Tracy RP, Hennekens CH. Inflammation, Aspirin, and the Risk of Cardiovascular Disease in Apparently Healthy Men. *N Engl J Med*. 1997;336(14):973-979.
83. Sutton MG, Sharpe N. Left ventricular remodeling after myocardial infarction: pathophysiology and therapy. *Circulation*. 2000;101(25):2981-2988.
84. Fahim M, Halim S, Kamel I. Tumor necrosis factor alpha in patients with acute myocardial infarction. *Egypt J Immunol*. 2004;11(1):31-37.
85. Guillen I, Blanes M, Gomez-Lechon MJ, Castell JV. Cytokine signaling during myocardial infarction: sequential appearance of IL-1 beta and IL-6. *Am J Physiol-Reg I*. 1995;269(2):R229-235.
86. Nian M, Lee P, Khaper N, Liu P. Inflammatory Cytokines and Postmyocardial Infarction Remodeling. *Circ Res*. 2004;94(12):1543-1553.
87. Vanden Berghe W, Plaisance S, Boone E, De Bosscher K, Schmitz ML, Fiers W, Haegeman G. p38 and Extracellular Signal-regulated Kinase Mitogen-activated Protein Kinase Pathways Are Required for Nuclear Factor- κ B p65 Transactivation Mediated by Tumor Necrosis Factor. *J Biol Chem*. 1998;273(6):3285-3290.
88. Wang Y. Signal transduction in cardiac hypertrophy - dissecting compensatory versus pathological pathways utilizing a transgenic approach. *Curr Opin Pharmacol*. 2001;1(2):134-140.
89. Bozkurt B, Kribbs SB, Clubb FJ, Jr, Michael LH, Didenko VV, Hornsby PJ, Seta Y, Oral H, Spinale FG, Mann DL. Pathophysiologically relevant concentrations of tumor necrosis factor-alpha promote progressive left ventricular dysfunction and remodeling in rats. *Circulation*. 1998;97(14):1382-1391.
90. Landray MJ, Wheeler DC, Lip GYH, Newman DJ, Blann AD, McGlynn FJ, Ball S, Townend JN, Baigent C. Inflammation, endothelial dysfunction, and

- platelet activation in patients with chronic kidney disease: the chronic renal impairment in Birmingham (CRIB) study. *Am J Kidney Dis*. 2004;43(2):244-253.
91. Shlipak MG, Fried LF, Crump C, Bleyer AJ, Manolio TA, Tracy RP, Furberg CD, Psaty BM. Elevations of Inflammatory and Procoagulant Biomarkers in Elderly Persons With Renal Insufficiency. *Circulation*. 2003;107(1):87-92.
 92. Kelly KJ. Distant effects of experimental renal ischemia/reperfusion injury. *J Am Soc Nephrol*. 2003;14(6):1549-1558.
 93. Bryant D, Becker L, Richardson J, Shelton J, Franco F, Peshock R, Thompson M, Giroir B. Cardiac Failure in Transgenic Mice With Myocardial Expression of Tumor Necrosis Factor- α . *Circulation*. 1998;97(14):1375-1381.
 94. Long CS. The Role of Interleukin-1 in the Failing Heart. *Heart Fail Rev*. 2001;6(2):81-94.
 95. Raine AE. Hypertension and the kidney. *Brit Med Bull*. 1994;50(2):322-341.
 96. Levy D, Larson M, Vasan R, Kannel W, Ho K. The progression from hypertension to congestive heart failure. *JAMA*. 1996;275(20):1557-1562.
 97. Levy D, Garrison R, Savage D, Kannel W, Castelli W. Left ventricular mass and incidence of coronary heart disease in an elderly cohort: The Framingham Heart Study. *Ann Intern Med*. 1989;110(2):101-107.
 98. Lorell BH, Carabello BA. Left Ventricular Hypertrophy: Pathogenesis, Detection, and Prognosis. *Circulation*. 2000;102(4):470-479.
 99. Meredith PA, Ostergren J. From hypertension to heart failure-are there better primary prevention strategies? *J Renin Angiotensin Aldosterone Syst*. 2006;7(2):64-73.
 100. Drazner MH. The Progression of Hypertensive Heart Disease. *Circulation*. 2011;123(3):327-334.
 101. Klapholz M. β -Blocker Use for the Stages of Heart Failure. *Mayo Clin Proc*. 2009;84(8):718-729.
 102. Levin A. The relationship of haemoglobin level and survival: direct or indirect effects? *Nephrol Dial Transplant*. 2002;17(Suppl 5):8-13.
 103. Keane WF, Brenner BM, De Zeeuw D, Grunfeld J-P, McGill J, Mitch WE, Ribeiro AB, Shahinfar S, Simpson RL, Snapinn SM, Toto R. The risk of developing end-stage renal disease in patients with type 2 diabetes and nephropathy: The RENAAL Study. *Kidney Int*. 2003;63(4):1499-1507.
 104. Silverberg D, Wexler D, Iaina A, Steinbruch S, Wollman Y, Schwartz D. Anemia, chronic renal disease and congestive heart failure - the cardio renal anemia syndrome: the need for cooperation between cardiologists and nephrologists. *Int Urol Nephrol*. 2006;38(2):295-310.
 105. Bansal N, Tighiouart H, Weiner D, Griffith J, Vlagopoulos P, Salem D, Levin A, Sarnak MJ. Anemia as a risk factor for kidney function decline in individuals with heart failure. *Am J Cardiol*. 2007;99(8):1137-1142.
 106. Silverberg D, Wexler D, Blum M, Wollman Y, Iaina A. The cardio-renal anaemia syndrome: does it exist? *Nephrol Dial Transplant*. 2003;18(Suppl 8):viii7-12.
 107. Fine LG, Bandyopadhyay D, Norman JT. Is there a common mechanism for the progression of different types of renal diseases other than proteinuria? Towards the unifying theme of chronic hypoxia. *Kidney Int*. 2000;57(Suppl. 75):22-26.
 108. Silberberg JS, Rahal DP, Patton DR, Sniderman AD. Role of anemia in the pathogenesis of left ventricular hypertrophy in end-stage renal disease. *Am J Cardiol*. 1989;64(3):222-224.

109. Grune T, Sommerburg O, Siems W. Oxidative stress in anemia. *Clin Nephrol*. 2000;53(Suppl 1):18-22.
110. Palazzuoli A, Gallotta M, Loving F, Nuti R, Siverberg D. Anaemia in heart failure: a common interaction with renal insufficiency called the cardio-renal anaemia syndrome. *Int J Clin pract*. 2008;62(2):281-286.
111. Jie KE, Verhaar MC, Cramer M-JM, van der Putten K, Gaillard CAJM, Doevendans PA, Koomans HA, Joles JA, Braam B. Erythropoietin and the cardiorenal syndrome: cellular mechanisms on the cardiorenal connectors. *Am J Physiol-Renal*. 2006;291(5):F932-944.
112. Phrommintikul A, Haas SJ, Elisk M, Krum H. Mortality and target haemoglobin concentrations in anaemic patients with chronic kidney disease treated with erythropoietin: a meta-analysis. *Lancet*. 369(9559):381-388.
113. Schwarz S, Trivedi BK, Kalantar-Zadeh K, Kovesdy CP. Association of Disorders in Mineral Metabolism with Progression of Chronic Kidney Disease. *Clin J Am Soc Nephrol*. 2006;1(4):825-831.
114. Block GA, Hulbert-Shearon TE, Levin NW, Port FK. Association of serum phosphorus and calcium x phosphate product with mortality risk in chronic hemodialysis patients: A national study. *Am J kidney Dis*. 1998;31(4):607-617.
115. Block G, Raggi P, Bellasi A, Kooienga L, Spiegel D. Mortality effect of coronary calcification and phosphate binder choice in incident hemodialysis patients. *Kidney Int*. 2007;71:438-441.
116. Sangiorgi G, Rumberger JA, Severson A, Edwards WD, Gregoire J, Fitzpatrick LA, Schwartz RS. Arterial Calcification and Not Lumen Stenosis Is Highly Correlated With Atherosclerotic Plaque Burden in Humans: A Histologic Study of 723 Coronary Artery Segments Using Nondecalcifying Methodology. *J Am Coll Card*. 1998;31(1):126-133.
117. Keelan PC, Bielak LF, Ashai K, Jamjoum LS, Denktas AE, Rumberger JA, Sheedy IIPF, Peyser PA, Schwartz RS. Long-Term Prognostic Value of Coronary Calcification Detected by Electron-Beam Computed Tomography in Patients Undergoing Coronary Angiography. *Circulation*. 2001;104(4):412-417.
118. Custodio MR, Koike MK, Neves KR, dos Reis LM, Gracioli FG, Neves CL, Batista DG, Magalhaes AO, Hawlitschek P, Oliveira IB, Dominguez WV, Moyses RMA, Jorgetti V. Parathyroid hormone and phosphorus overload in uremia: impact on cardiovascular system. *Nephrol Dial Transplant*. 2012;27(4):1437-1445.
119. Gross ML, Ritz E. Hypertrophy and fibrosis in the cardiomyopathy of uremia-beyond coronary heart disease. *Semin Dial*. 2008;21(4):308-318.
120. Slinin Y, Foley RN, Collins AJ. Calcium, Phosphorus, Parathyroid Hormone, and Cardiovascular Disease in Hemodialysis Patients: The USRDS Waves 1, 3, and 4 Study. *J Am Soc Nephrol*. 2005;16(6):1788-1793.
121. Ganesh SK, Stack AG, Levin NW, Hulbert-Shearon T, Port FK. Association of Elevated Serum PO(4), Ca x PO(4) Product, and Parathyroid Hormone with Cardiac Mortality Risk in Chronic Hemodialysis Patients. *J Am Soc Nephrol*. 2001;12(10):2131-2138.
122. Palmer SC, Hayen A, Macaskill P, Pellegrini F, Craig JC, Elder GJ, Strippoli GFM. Serum levels of phosphorus, parathyroid hormone, and calcium and risks of death and cardiovascular disease in individuals with chronic kidney disease: A systematic review and meta-analysis. *JAMA*. 2011;305(11):1119-1127.
123. Meyer TW, Hostetter TH. Uremia. *N Engl J Med*. 2007;357:1316-1325.

124. Lekawanvijit S, Kompa AR, Wang BH, Kelly DJ, Krum H. Cardiorenal Syndrome: The Emerging Role of Protein-Bound Uremic Toxins. *Circ Res*. 2012;111(11):1470-1483.
125. Dhondt A, Vanholder R, Van Biesen W, Lameire N. The removal of uremic toxins. *Kidney Int*. 2000;58(Suppl 76):47-59.
126. Lekawanvijit S, Adrahtas A, Kelly DJ, Kompa AR, Wang BH, Krum H. Does indoxyl sulfate, a uraemic toxin, have direct effects on cardiac fibroblasts and myocytes? *Eur Heart J*. 2010;31(14):1771-1779.
127. Lekawanvijit S, Kompa AR, Manabe M, Wang BH, Langham RG, Nishijima F, Kelly DJ, Krum H. Chronic kidney disease-induced cardiac fibrosis is ameliorated by reducing circulating levels of a non-dialysable uremic toxin, indoxyl sulfate. *PLoS ONE*. 2012;7(7):e41281.
128. Fujii H, Nishijima F, Goto S, Sugano M, Yamato H, Kitazawa R, Kitazawa S, Fukagawa M. Oral charcoal adsorbent (AST-120) prevents progression of cardiac damage in chronic kidney disease through suppression of oxidative stress. *Nephrol Dial Transplant*. 2009;24(7):2089-2095.
129. Peng YS, Ding HC, Lin YT, Syu JP, Chen Y, Wang SM. Uremic toxin p-cresol induces disassembly of gap junctions of cardiomyocytes. *Toxicology*. 2012;302(1):11-17.
130. Lee JC, Downing SE. Negative inotropic effects of phenol on isolated cardiac muscle. *Am J Pathol*. 1981;102:367-372.
131. Enomoto A, Endou H. Roles of organic anion transporters (OATs) and a urate transporter (URAT1) in the pathophysiology of human disease. *Clin Exp Nephrol*. 2005;9:195-205.
132. Shimizu H, Bolati D, Adijiang A, Muteliefu G, Enomoto A, Nishijima F, Dateki M, Niwa T. NF- κ B plays an important role in indoxyl sulfate-induced cellular senescence, fibrotic gene expression, and inhibition of proliferation in proximal tubular cells. *Am J Physiol Cell Physiol*. 2011;301(5):C1201-C1212.
133. Enomoto A, Takeda M, Tojo A, Sekine T, Cha S, Khamdang S, Takayama F, Aoyama I, Nakamura S, Endou H, Niwa T. Role of organic anion transporters in the tubular transport of indoxyl sulfate and the induction of its nephrotoxicity. *J Am Soc Nephrol*. 2002;13(7):1711-1720.
134. Niwa T, Ise M. Indoxyl sulfate, a circulating uremic toxin, stimulates the progression of glomerular sclerosis. *J Lab Clin Med*. 1994;124(1):96-104.
135. Niwa T, Nomura T, Sugiyama S, Miyazaki T, Tsukushi S, Tsutsui S. The protein metabolite hypothesis, a model for the progression of renal failure: an oral adsorbent lowers indoxyl sulfate levels in undialyzed uremic patients. *Kidney Int*. 1997;52(Suppl 62):S23-28.
136. Aoyama I, Niwa T. Molecular insights into preventive effects of AST-120 on the progression of renal failure. *Clin Exp Nephrol*. 2001;5:209-216.
137. Vanholder R, De Smet R, Glorieux G, Argiles A, Baurmeister U, Brunet P, Clark W, Cohen G, De Deyn PP, Deppisch R, Descamps-Latscha B, Henle T, Jorres A, Lemke HD, Massy ZA, Passlick-Deetjen J, Rodriguez M, Stegmayr B, Stenvinkel P, Tetta C, Wanner C, Zidek W. Review on uremic toxins: Classification, concentration, and interindividual variability. *Kidney Int*. 2003;63(5):1934-1943.
138. Meert N, Schepers E, De Smet R, Argiles A, Cohen G, Deppisch R, Drüeke T, Massy Z, Spasovski G, Stegmayr B, Zidek W, Jankowski J, Vanholder R. Inconsistency of Reported Uremic Toxin Concentrations. *Artif Organs*. 2007;31(8):600-611.

139. Swan JS, Kragten EY, Veening H. Liquid-chromatographic study of fluorescent materials in uremic fluids. *Clin Chem.* 1983;29(6):1082-1084.
140. Niwa T, Takeda N, Tatematsu A, Maeda K. Accumulation of indoxyl sulfate, an inhibitor of drug-binding, in uremic serum as demonstrated by internal-surface reversed-phase liquid chromatography. *Clin Chem.* 1988;34(11):2264-2267.
141. Miyazaki T, Ise M, Seo H, Niwa T. Indoxyl sulfate increases the gene expressions of TGF-beta 1, TIMP-1 and pro-alpha 1(I) collagen in uremic rat kidneys. *Kidney Int Suppl.* 1997;62:S15-22.
142. Owada S, Goto S, Bannai K, Hayashi H, Nishijima F, Niwa T. Indoxyl Sulfate Reduces Superoxide Scavenging Activity in the Kidneys of Normal and Uremic Rats. *Am J Nephrol.* 2008;28(3):446-454.
143. Miyazaki T, Aoyama I, Ise M, Seo H, Niwa T. An oral sorbent reduces overload of indoxyl sulphate and gene expression of TGF- β 1 in uraemic rat kidneys. *Nephrol Dial Transplant.* 2000;15(11):1773-1781.
144. Schocken DD, Benjamin EJ, Fonarow GC, Krumholz HM, Levy D, Mensah GA, Narula J, Shor ES, Young JB, Hong Y. Prevention of Heart Failure: A Scientific Statement From the American Heart Association Councils on Epidemiology and Prevention, Clinical Cardiology, Cardiovascular Nursing, and High Blood Pressure Research; Quality of Care and Outcomes Research Interdisciplinary Working Group; and Functional Genomics and Translational Biology Interdisciplinary Working Group. *Circulation.* 2008;117(19):2544-2565.
145. Brown RD, Ambler SK, Mitchell MD, Long CS. The cardiac fibroblast: Therapeutic target in myocardial remodeling and failure. *Annu Rev Pharmacol Toxicol.* 2005;45(1):657-687.
146. Frey N, Olson EN. Cardiac hypertrophy: the good, the bad, and the ugly. *Annu Rev Physiol.* 2003;65(1):45-79.
147. Warren SE, Royal HD, Markis JE, Grossman W, McKay RG. Time course of left ventricular dilation after myocardial infarction: Influence of infarct-related artery and success of coronary thrombolysis. *J Am Coll Cardiol.* 1988;11(1):12-19.
148. Cleutjens JPM, Kandala JC, Guarda E, Guntaka RV, Weber KT. Regulation of collagen degradation in the rat myocardium after infarction. *J Mol Cell Cardiol.* 1995;27(6):1281-1292.
149. Peterson JT, Li H, Dillon L, Bryant JW. Evolution of matrix metalloprotease and tissue inhibitor expression during heart failure progression in the infarcted rat. *Cardiovasc Res.* 2000;46:307-315.
150. Cleutjens JP, Verluyten MJ, Smiths JF, Daemen MJ. Collagen remodeling after myocardial infarction in the rat heart. *Am J Pathol.* 1995;147(2):325-338.
151. Sun Y, Zhang JQ, Zhang J, Ramires FJA. Angiotensin II, transforming growth factor-beta1 and repair in the infarcted heart. *J Mol Cell Cardiol.* 1998;30(8):1559-1569.
152. See F, Kompa A, Jennifer M, Lewis DA, Krum H. Fibrosis as a therapeutic target post-myocardial infarction. *Curr Pharm Design.* 2005;11:477-487.
153. Díez J. Mechanisms of cardiac fibrosis in hypertension. *J Clin Hypertens* 2007;9(7):546-550.
154. Bakth S, Arena J, Lee W, Torres R, Haider B, Patel BC, Lyons MM, Regan TJ. Arrhythmia susceptibility and myocardial composition in diabetes. Influence of physical conditioning. *J Clin Invest.* 1986;77(2):382-395.

155. Rigatto C, Parfrey P. Uraemic Cardiomyopathy: an Overload Cardiomyopathy. *J Clin Basic Cardiol*. 2001;4(2):93-95.
156. London G, Parfrey P. Cardiac disease in chronic uremia: pathogenesis. *Adv Ren Replace Ther*. 1997;4(3):194-211.
157. Amann K, Breitbart M, Ritz E, Mall G. Myocyte/capillary mismatch in the heart of uremic patients. *J Am Soc Nephrol*. 1998;9:1018-1022.
158. Schrier RW, Abraham WT. Hormones and Hemodynamics in Heart Failure. *N Engl J Med*. 1999;341(8):577-585.
159. Metcalfe W. How does early chronic kidney disease progress?: A Background Paper prepared for the UK Consensus Conference on Early Chronic Kidney Disease. *Nephrol Dial Transplant*. 2007;22(Suppl 9):ix26-ix30.
160. Remuzzi G, Bertani T. Pathophysiology of Progressive Nephropathies. *N Engl J Med*. 1998;339(20):1448-1456.
161. Sporn MB, Roberts AB, Wakefield LM, Assoian RK. Transforming growth factor-beta: biological function and chemical structure. *Science* 1986;233:532-534.
162. Roberts AB, Sporn MB, Assoian RK, Smith JM, Roche NS, Wakefield LM, Heine UI, Liotta LA, Falanga V, Kehrl JH. Transforming growth factor type beta: rapid induction of fibrosis and angiogenesis in vivo and stimulation of collagen formation in vitro. *Proc Natl Acad Sci*. 1986;83:4167-4171.
163. Okada H, Danoff TM, Kalluri R, Neilson EG. Early role of Fsp1 in epithelial-mesenchymal transformation. *Am J Physiol Renal Physiol*. 1997;273(4):F563-F574.
164. Zeisberg EM, Tarnavski O, Zeisberg M, Dorfman AL, McMullen JR. Endothelial-to-mesenchymal transition contributes to cardiac fibrosis. *Nat Med*. 2007;13:952-961.
165. Liu Y. Renal fibrosis: New insights into the pathogenesis and therapeutics. *Kidney Int*. 2006;69(2):213-217.
166. Hewitson TD. Renal tubulointerstitial fibrosis: common but never simple. *Am J Physiol Renal Physiol*. 2009;296(6):F1239-F1244.
167. Gilbert RE, Wu LL, Kelly DJ, Cox A, Wilkinson-Berka JL, Johnston CI, Cooper ME. Pathological Expression of Renin and Angiotensin II in the Renal Tubule after Subtotal Nephrectomy: Implications for the Pathogenesis of Tubulointerstitial Fibrosis. *Am J Pathol*. 1999;155(2):429-440.
168. George SM, Kalantarina K. The role of imaging in the management of cardiorenal syndrome. *Int J Nephrol*. 2011;doi:10.4061/2011/245241.
169. Galderisi M, Henein MY, D'Hooge J, Sicari R, Badano LP, Zamorano JL, Roelandt JRTC. Recommendations of the European Association of Echocardiography How to use echo-Doppler in clinical trials: different modalities for different purposes. *Eur J Echocardiogr*. 2011;12(5):339-353.
170. Lang RM, Bierig M, Devereux RB, Flachskampf FA, Foster E, Pellikka PA, Picard MH, Roman MJ, Seward J, Shanewise J, Solomon S, Spencer KT, St. John Sutton M, Stewart W. Recommendations for chamber quantification. *Eur J Echocardiogr*. 2006;7(2):79-108.
171. Palmieri V, Dahlof B, DeQuattro V, Sharpe N, Bella JN, de Simone G, Paranicas M, Fishman D, Devereux RB. Reliability of echocardiographic assessment of left ventricular structure and function: The PRESERVE study. *J Am Coll Cardiol*. 1999;34(5):1625-1632.
172. Krum H, Jelinek M, Stewart S, Sindone A, Atherton J, Wilson J, Ishami V, Waddell J. National Heart Foundation of Australia and the Cardiac Society of

- Australia and New Zealand. Guidelines for the prevention, detection and management of chronic heart failure in Australia. 2011.
173. Damman K, van Deursen VM, Navis G, Voors AA, van Veldhuisen DJ, Hillege HL. Increased Central Venous Pressure Is Associated With Impaired Renal Function and Mortality in a Broad Spectrum of Patients With Cardiovascular Disease. *J Am Coll Cardiol*. 2009;53(7):582-588.
 174. Zethelius B, Berglund L, Sundstrom J, Ingelsson E, Basu S, Larsson A, Venge P, Arnlov J. Use of Multiple Biomarkers to Improve the Prediction of Death from Cardiovascular Causes. *N Engl J Med*. 2008;358(20):2107-2116.
 175. Nguyen MT, Ross GF, Dent CL, Devarajan P. Early prediction of acute renal injury using urinary proteomics. *Am J Nephrol*. 2005;25(4):318-326.
 176. Devarajan P, Mishra J, Supavekin S, Patterson LT, Steven Potter S. Gene expression in early ischemic renal injury: clues towards pathogenesis, biomarker discovery, and novel therapeutics. *Mol Genet Metab*. 2003;80(4):365-376.
 177. Tang WHW, Francis GS, Morrow DA, Newby LK, Cannon CP, Jesse RL, Storrow AB, Christenson RH, Committee M, Apple FS, Ravkilde J, Tang WHW, Wu AHB. National academy of clinical biochemistry laboratory medicine practice guidelines: clinical utilization of cardiac biomarker testing in heart failure. *Circulation*. 2007;116(5):e99-109.
 178. Cruz D, Soni S, Slavin L, Ronco C, Maisel A. Biomarkers of cardiac and kidney dysfunction in cardiorenal syndromes. *Contrib Nephrol*. 2010;165:83-92.
 179. de Boer RA, Voors AA, Muntendam P, van Gilst WH, van Veldhuisen DJ. Galectin-3: a novel mediator of heart failure development and progression. *Eur J Heart Fail*. 2009;11(9):811-817.
 180. Monserrat L, Lopez B, Gonzalez A, Hermida M, Fernandez X, Ortiz M, Barriales-Villa R, Castro-Beiras A, Diez J. Cardiotrophin-1 plasma levels are associated with the severity of hypertrophy in hypertrophic cardiomyopathy. *Eur Heart J*. 2011;32(2):177-183.
 181. Gonzalez A, Lopez B, Ravassa S, Beaumont J, Zudaire A, Gallego I, Brugnolaro C, Diez J. Cardiotrophin-1 in hypertensive heart disease. *Endocrine*. 2012;42(1):9-17.
 182. Talwar S, Squire IB, Downie PF, O'Brien RJ, Davies JE, Ng LL. Elevated circulating cardiotrophin-1 in heart failure: relationship with parameters of left ventricular systolic dysfunction. *Clin Sci*. 2000;99(1):83-88.
 183. Ng LL, O'Brien RJ, Demme B, Jennings S. Non-competitive immunochemiluminometric assay for cardiotrophin-1 detects elevated plasma levels in human heart failure. *Clin Sci*. 2002;102(4):411-416.
 184. Lopez B, Gonzalez A, Querejeta R, Barba J, Diez J. Association of plasma cardiotrophin-1 with stage C heart failure in hypertensive patients: Potential diagnostic implications. *J Hypertens*. 2009;27(2):418-424.
 185. Tsutamoto T, Asai S, Tanaka T, Sakai H, Nishiyama K, Fujii M, Yamamoto T, Ohnishi M, Wada A, Saito Y, Horie M. Plasma level of cardiotrophin-1 as a prognostic predictor in patients with chronic heart failure. *Eur J Heart Fail*. 2007;9(10):1032-1037.
 186. Shimp M, Morrow DA, Weinberg EO, Sabatine MS, Murphy SA, Antman EM, Lee RT. Serum Levels of the Interleukin-1 Receptor Family Member ST2 Predict Mortality and Clinical Outcome in Acute Myocardial Infarction. *Circulation*. 2004;109(18):2186-2190.

187. Weinberg EO, Shimpo M, De Keulenaer GW, MacGillivray C, Tominaga S-i, Solomon SD, Rouleau J-L, Lee RT. Expression and regulation of ST2, an interleukin-1 receptor family member, in cardiomyocytes and myocardial infarction. *Circulation*. 2002;106(23):2961-2966.
188. Schmitter D, Cotter G, Voors A. Clinical use of novel biomarkers in heart failure: towards personalized medicine. *Heart Fail Rev*. 2013;doi:10.1007/s10741-10013-19396-10745.
189. Lok DJ, Van Der Meer P, de la Porte PW, Lipsic E, Van Wijngaarden J, Hillege HL, van Veldhuisen DJ. Prognostic value of galectin-3, a novel marker of fibrosis, in patients with chronic heart failure: data from the DEAL-HF study. *Clin Res Cardiol*. 2010;99:323-328.
190. Lopez-Andres N, Rossignol P, Iraqi W, Fay R, Nuee J, Ghio S, Cleland JGF, Zannad F, Lacolley P. Association of galectin-3 and fibrosis markers with long-term cardiovascular outcomes in patients with heart failure, left ventricular dysfunction, and dyssynchrony: insights from the CARE-HF (Cardiac Resynchronization in Heart Failure) trial. *Eur J Heart Fail*. 14(1):74-81.
191. van Kimmenade RR, Januzzi Jr JL, Ellinor PT, Sharma UC, Bakker JA, Low AF, Martinez A, Crijns HJ, MacRae CA, Menheere PP, Pinto YM. Utility of Amino-Terminal Pro-Brain Natriuretic Peptide, Galectin-3, and Apelin for the Evaluation of Patients With Acute Heart Failure. *J Am Coll Cardiol*. 2006;48(6):1217-1224.
192. Shah RV, Chen-Tournoux AA, Picard MH, van Kimmenade RRJ, Januzzi JL. Galectin-3, cardiac structure and function, and long-term mortality in patients with acutely decompensated heart failure. *Eur J Heart Fail*. 2010;12(8):826-832.
193. Fermann GJ, Lindsell CJ, Storrow AB, Hart K, Sperling M, Roll S, Weintraub NL, Miller KF, Maron DJ, Naftilan AJ, McPherson JA, Sawyer DB, Christenson R, Collins SP. Galectin 3 complements BNP in risk stratification in acute heart failure. *Biomarkers*. 2012;17(8):706-713.
194. De Boer RA, Wanner C, Blouin K, Drechsler C. Galectin-3 and Outcomes in Patients with End-Stage Renal Disease: Data from the German Diabetes and Dialysis Study. *Circulation*. 2011;124:A11743.
195. Jafar TH, Schmid CH, Levey AS. Serum Creatinine as Marker of Kidney Function in South Asians: A Study of Reduced GFR in Adults in Pakistan. *J Am Soc Nephrol*. 2005;16:1413-1419.
196. Dharnidharka VR, Kwon C, Stevens G. Serum cystatin C is superior to serum creatinine as a marker of kidney function: a meta-analysis. *Am J Kidney Dis*. 2002;40(2):221-226.
197. Herget-Rosenthal S, Bökenkamp A, Hofmann W. How to estimate GFR-serum creatinine, serum cystatin C or equations? *Clin Biochem*. 2007;40(3-4):153-161.
198. Bagshaw S, Gibney R. Conventional markers of kidney function. *Crit Care Med*. 2008;36(Suppl 4):152-158.
199. Perrone RD, Madias NE, Levey AS. Serum creatinine as an index of renal function: new insights into old concepts. *Clin Chem*. 1992;38(10):1933-1953.
200. Zolezzi C, Ferrari S, Fasano MC, Telentinis L, Bacci G, Pizzoferrato A. Correlation between cystatin C and serum creatinine as markers of renal function in patients with neoplasms of the locomotor system. *J Chemother*. 2001;13(3):316-323.
201. Mishra J, Ma Q, Prada A, Mitsnefes M, Zahedi K, Yang J, Barasch J, Devarajan P. Identification of neutrophil gelatinase-associated lipocalin as a novel early

- urinary biomarker for ischemic renal injury. *J Am Soc Nephrol*. 2003;14(10):2534-2543.
202. de Geus HRH, Bakker J, Lesaffre EMEH, le Noble JLML. Neutrophil Gelatinase-associated Lipocalin at ICU Admission Predicts for Acute Kidney Injury in Adult Patients. *Am J Respir Crit Care Med*. 2013;183(7):907-914.
 203. Nickolas TL, O'Rourke MJ, Yang J, Sise ME, Canetta PA, Barasch N, Buchen C, Khan F, Mori K, Giglio J, Devarajan P, Barasch J. Sensitivity and Specificity of a Single Emergency Department Measurement of Urinary Neutrophil Gelatinase-Associated Lipocalin for Diagnosing Acute Kidney Injury. *Ann Intern Med*. 2008;148(11):810-819.
 204. Alvelos M, Pimentel R, Pinho E, Gomes A, Lourenco P, Teles MJ, Almeida P, Guimaraes JT, Bettencourt P. Neutrophil Gelatinase-Associated Lipocalin in the Diagnosis of Type 1 Cardio-Renal Syndrome in the General Ward. *Clin J Am Soc Nephrol*. 2011;6(3):476-481.
 205. Han WK, Bailly V, Abichandani R, Thadhani R, Bonventre JV. Kidney injury molecule-1 (KIM-1): a novel biomarker for human renal proximal tubule injury. *Kidney Int*. 2002;62(1):237-244.
 206. Ichimura T, Hung CC, Yang SA, Stevens JL, Bonventre JV. Kidney injury molecule-1: a tissue and urinary biomarker for nephrotoxicant-induced renal injury. *Am J Physiol Renal Physiol*. 2004;286(3):F552-563.
 207. Jungbauer CG, Birner C, Jung B, Buchner S, Lubnow M, von Bary C, Endemann D, Banas B, Mack M, Boger CA, Riegger G, Luchner A. Kidney injury molecule-1 and N-acetyl- β -D-glucosaminidase in chronic heart failure: possible biomarkers of cardiorenal syndrome. *Eur J Heart Fail*. 2011;13(10):1104-1110.
 208. Muntner P, He J, Hamm L, Loria C, Whelton PK. Renal Insufficiency and Subsequent Death Resulting from Cardiovascular Disease in the United States. *J Am Soc Nephrol*. 2002;13(3):745-753.
 209. Damman K, Van Veldhuisen DJ, Navis G, Vaidya VS, Smilde TDJ, Westenbrink BD, Bonventre JV, Voors AA, Hillege HL. Tubular damage in chronic systolic heart failure is associated with reduced survival independent of glomerular filtration rate. *Heart*. 2010;96(16):1297-1302.
 210. Lekawanvijit S, Kompa AR, Zhang Y, Wang BH, Kelly DJ, Krum H. Myocardial Infarction Impairs Renal Function, Induces Renal Interstitial Fibrosis and Increases renal KIM-1 Expression: Implications for Cardiorenal Syndrome. *Am J Physiol Heart Circ Physiol*. 2012;302(9):H1884-H1893.
 211. Nickolas TL, Barasch J, Devarajan P. Biomarkers in acute and chronic kidney disease. *Curr Opin Nephrol Hypertens*. 2008;17(2):127-132.
 212. Haase M, Bellomo R, Story D, Davenport P, Haase-Fielitz A. Urinary interleukin-18 does not predict acute kidney injury after adult cardiac surgery: a prospective observational cohort study. *Crit Care*. 2008;12(4):1-8.
 213. Bosomworth MP, Aparicio SR, Hay AW. Urine N-acetyl-beta-D-glucosaminidase - a marker of tubular damage? *Nephrol Dial Transplant*. 1999;14(3):620-626.
 214. Liangos O, Perianayagam MC, Vaidya VS, Han WK, Wald R, Tighiouart H, MacKinnon RW, Li L, Balakrishnan VS, Pereira BJG, Bonventre JV, Jaber BL. Urinary N-Acetyl- β -(D)-Glucosaminidase Activity and Kidney Injury Molecule-1 Level Are Associated with Adverse Outcomes in Acute Renal Failure. *J Am Soc Nephrol*. 2007;18(3):904-912.

215. Matsushima H, Yoshida H, Machiguchi T, Muso E, Matsuyama E, Tamura T, Sasayama S. Urinary albumin and TGF β 1 levels as renal damage indices in patients with congestive heart failure. *Clin Exp Nephrol*. 2002;6(1):21-29.
216. Patten RD, Hall-Porter MR. Small Animal Models of Heart Failure: Development of Novel Therapies, Past and Present. *Circ Heart Fail*. 2009;2(2):138-144.
217. Kenchaiah S, Narula J, Vasan RS. Risk factors for heart failure. *Med Clin North Am*. 2004;88(5):1145-1172.
218. Ozcan A, Ware K, Calomeni E, Nadasdy T, Forbes R, Satoskar AA, Nadasdy G, Rovin BH, Hebert LA, Brodsky SV. 5/6 Nephrectomy as a Validated Rat Model Mimicking Human Warfarin-Related Nephropathy. *Am J Nephrol*. 2012;35(4):356-364.
219. Fletcher P, Pfeffer J, Pfeffer M, Braunwald E. Left ventricular diastolic pressure-volume relations in rats with healed myocardial infarction: effects on systolic function. *Circ Res*. 1981;49:618-626.
220. Tan SM, Zhang Y, Connelly KA, Gilbert RE, Kelly DJ. Targeted inhibition of activin receptor-like kinase 5 signaling attenuates cardiac dysfunction following myocardial infarction. *Am J Physiol Heart Circ Physiol*. 2010;298(5):H1415-1425.
221. Pfeffer MA, Pfeffer JM, Fishbein MC, Fletcher PJ, Spadaro J, Kloner RA, Braunwald E. Myocardial infarct size and ventricular function in rats. *Circ Res*. 1979;44(4):503-512.
222. Gaballa MA, Goldman S. Ventricular remodeling in heart failure. *J Card Fail*. 2004;8(Suppl 6):476-485.
223. Burrell LM, Risvanis J, Kubota E, Dean RG, MacDonald PS, Lu S, Tikellis C, Grant SL, Lew RA, Smith AI, Cooper ME, Johnston CI. Myocardial infarction increases ACE2 expression in rat and humans. *Eur Heart J*. 2005;26(4):369-375.
224. Crackower MA, Sarao R, Oudit GY, Yagil C, Kozieradzki I, Scanga SE, Oliveira-dos-Santos AJ, da Costa J, Zhang L, Pei Y, Scholey J, Ferrario CM, Manoukian AS, Chappell MC, Backx PH, Yagil Y, Penninger JM. Angiotensin-converting enzyme 2 is an essential regulator of heart function. *Nature*. 2002;417:822-828.
225. Pfeffer JM, Pfeffer MA, Braunwald E. Influence of chronic captopril therapy on the infarcted left ventricle of the rat. *Circ Res*. 1985;57(1):84-95.
226. Pfeffer MA, Pfeffer JM, Steinberg C, Finn P. Survival after an experimental myocardial infarction: beneficial effects of long-term therapy with captopril. *Circulation*. 1985;72(2):406-412.
227. Smits JF, van Krimpen C, Schoemaker RG, Cleutjens JP, Daemen MJ. Angiotensin II receptor blockade after myocardial infarction in rats: effects on hemodynamics, myocardial DNA synthesis, and interstitial collagen content. *J Cardiovasc Pharmacol*. 1992;20(5):772-778.
228. Pfeffer MA, Braunwald E, Moya LA, Basta L, Brown EJ, Cuddy TE, Davis BR, Geltman EM, Goldman S, Flaker GC, Klein M, Lamas GA, Packer M, Rouleau J, Rouleau JL, Rutherford J, Wertheimer JH, Hawkins CM. Effect of Captopril on Mortality and Morbidity in Patients with Left Ventricular Dysfunction after Myocardial Infarction. *N Engl J Med*. 1992;327(10):669-677.
229. St John Sutton M, Pfeffer MA, Plappert T, Rouleau JL, Moya LA, Dagenais GR, Lamas GA, Klein M, Sussex B, Goldman S. Quantitative two-dimensional echocardiographic measurements are major predictors of adverse cardiovascular

- events after acute myocardial infarction. The protective effects of captopril. *Circulation*. 1994;89(1):68-75.
230. Pfeffer MA, Lamas GA, Vaughan DE, Parisi AF, Braunwald E. Effect of Captopril on Progressive Ventricular Dilatation after Anterior Myocardial Infarction. *N Engl J Med*. 1988;319(2):80-86.
 231. Velkoska E, Dean RG, Griggs K, Burchill L, Burrell LM. Angiotensin-(1-7) infusion is associated with increased blood pressure and adverse cardiac remodelling in rats with subtotal nephrectomy. *Clin Sci*. 2010;120:335-345.
 232. Suzuki H, Schaefer L, Ling H, Schaefer RM, Dammrich J, Teschner M, Heidland A. Prevention of cardiac hypertrophy in experimental chronic renal failure by long-term ACE inhibitor administration: potential role of lysosomal proteinases. *Am J Nephrol*. 1995;15(2):129-136.
 233. Burchill L, Velkoska E, Dean RG, Lew RA, Smith AI, Levidiotis V, Burrell LM. Acute kidney injury in the rat causes cardiac remodelling and increases angiotensin-converting enzyme 2 expression. *Exp Physiol*. 2008;93(5):622-630.
 234. Grobe JL, Mecca AP, Lingis M, Shenoy V, Bolton TA, Machado JM, Speth RC, Raizada MK, Katovich MJ. Prevention of angiotensin II-induced cardiac remodeling by angiotensin-(1-7). *Am J Physiol Heart Circ Physiol*. 2007;292(2):H736-H742.
 235. Grobe JL, Mecca AP, Mao H, Katovich MJ. Chronic angiotensin-(1-7) prevents cardiac fibrosis in DOCA-salt model of hypertension. *Am J Physiol Heart Circ Physiol*. 2006;290(6):H2417-H2423.
 236. Hostetter TH, Olson JL, Rennke HG, Venkatachalam MA, Brenner BM. Hyperfiltration in remnant nephrons: a potentially adverse response to renal ablation. *Am J Physiol Renal Physiol*. 1981;241(1):F85-F93.
 237. Kelly DJ, Zhang Y, Gow R, Gilbert RE. Tranilast attenuates structural and functional aspects of renal injury in the remnant kidney model. *J Am Soc Nephrol*. 2004;15:2619-2629.
 238. Kelly DJ, Zhang Y, Cox AJ, Gilbert RE. Combination therapy with tranilast and angiotensin-converting enzyme inhibition provides additional renoprotection in the remnant kidney model. *Kidney Int*. 2006;69(11):1954-1960.
 239. Gilbert RE, Zhang Y, Williams SJ, Zammit SC, Stapleton DI. A Purpose-Synthesised Anti-Fibrotic Agent Attenuates Experimental Kidney Diseases in the Rat. *PLoS ONE*. 2012;7(10):e47160.
 240. Border WA, Noble NA, Yamamoto T, Harper JR, Yamaguchi Y. Natural inhibitor of transforming growth factor-beta protects against scarring in experimental kidney disease. *Nature*. 1992;360:361-364.
 241. Fine LG, Norman JT. Chronic hypoxia as a mechanism of progression of chronic kidney diseases: from hypothesis to novel therapeutics. *Kidney Int*. 2008;74(7):867-872.
 242. Wu LL, Cox A, Roe CJ, Dziadek M, Cooper ME, Gilbert RE. Transforming growth factor beta1 and renal injury following subtotal nephrectomy in the rat: role of the renin-angiotensin system. *Kidney Int*. 1997;51(5):1553-1567.
 243. Socha MJ, Manhiani M, Said N, Imig JD, Motamed K. Secreted Protein Acidic and Rich in Cysteine Deficiency Ameliorates Renal Inflammation and Fibrosis in Angiotensin Hypertension. *Am J Pathol*. 2007;171(4):1104-1112.
 244. Sakai N, Baba M, Nagasima Y, Kato Y, Hirai K, Kondo K-I, Kobayashi K, Yoshida M, Kaneko S, Kishida T, Kawakami S, Hosaka M, Inayama Y, Yao M. SPARC expression in primary human renal cell carcinoma: Upregulation of SPARC in sarcomatoid renal carcinoma. *Hum Pathol*. 2001;32(10):1064-1070.

245. Wu LL, Cox A, Roe CJ, Dziadek M, Cooper ME, Gilbert RE. Secreted protein acidic and rich in cysteine expression after subtotal nephrectomy and blockade of the renin-angiotensin system. *J Am Soc Nephrol*. 1997;8(9):1373-1382.
246. Homma T, Sonoda H, Manabe K, Arai K, Mizuno M, Sada T, Ikeda M. Activation of renal angiotensin type 1 receptor contributes to the pathogenesis of progressive renal injury in a rat model of chronic cardiorenal syndrome. *Am J Physiol Renal Physiol*. 2012;302(6):F750-F761.
247. Ochodnický P, de Zeeuw D, Henning RH, Kluppel CA, van Dokkum RPE. Endothelial function predicts the development of renal damage after combined nephrectomy and myocardial infarction. *J Am Soc Nephrol*. 2006;17(4 Suppl 2):S49-52.
248. Van Dokkum RPE, Eijkelkamp WBA, Kluppel ACA, Henning RH, van Goor H, Citgez M, Windt WAKM, van Veldhuisen DJ, de Graeff PA, de Zeeuw D. Myocardial infarction enhances progressive renal damage in an experimental model for cardio-renal interaction. *J Am Soc Nephrol*. 2004;15(12):3103-3110.
249. Windt WAKM, Eijkelkamp WBA, Henning RH, Kluppel ACA, de Graeff PA, Hillege HL, Schafer S, de Zeeuw D, van Dokkum RPE. Renal damage after myocardial infarction is prevented by renin-angiotensin-aldosterone-system intervention. *J Am Soc Nephrol*. 2006;17(11):3059-3066.
250. Bongartz LG, Joles JA, Verhaar MC, Cramer MJ, Goldschmeding R, Tilburgs C, Gaillard CA, Doevendans PA, Braam B. Subtotal nephrectomy plus coronary ligation leads to more pronounced damage in both organs than either nephrectomy or coronary ligation. *Am J Physiol Heart Circ Physiol*. 2012;302(3):H845-H854.
251. Liu S, Kompa AR, Kumfu S, Nishijima F, Kelly DJ, Krum H, Wang BH. Subtotal nephrectomy accelerates pathological cardiac remodeling post-myocardial infarction: Implications for cardiorenal syndrome. *Int J Cardiol*. 2013;doi:10.1016/j.ijcard.2012.12.065.
252. Kompa AR, Wang BH, Xu G, Zhang Y, Ho P-Y, Eisennagel S, Thalji RK, Marino JP, Kelly DJ, Behm DJ, Krum H. Soluble epoxide hydrolase inhibition exerts beneficial anti-remodeling actions post-myocardial infarction. *Int J Cardiol*. 2013;167(1):210-219.
253. Windt WAKM, Henning RH, Kluppel ACA, Xu Y, de Zeeuw D, van Dokkum RPE. Myocardial infarction does not further impair renal damage in 5/6 nephrectomized rats. *Nephrol Dial Transplant*. 2008;23(10):3103-3110.
254. Sata Y, Krum H. The future of pharmacological therapy for heart failure. *Circ J*. 2010;74:809-817.
255. Risler T, Schwab A, Kramer B, Braun N, Erley C. Comparative pharmacokinetics and pharmacodynamics of loop diuretics in renal failure. *Cardiology*. 1994;84 (Suppl 2):155-161.
256. Steiner JF, Robbins LJ, Hammermeister KE, Roth SC, Hammond WS. Incidence of digoxin toxicity in outpatients. *West J Med*. 1994;161:474-478.
257. Philbin EF, Santella RN, Rocco TA. Angiotensin-converting enzyme inhibitor use in older patients with heart failure and renal dysfunction. *J Am Geriatr Soc*. 1999;47:302-308.
258. Biasioli S, Barbaresi F, Barbiero M, Petrosino L, Cavallini L, Zambello A, Cavalcanti G, Foroni R, Bonofiglio C. Intermittent venovenous hemofiltration as a chronic treatment for refractory and intractable heart failure. *ASAIO J*. 1992;38(3):M658-M663.

259. Iorio L, Simonelli R, Nacca RG, DeSanto LS. Daily hemofiltration in severe heart failure. *Kidney Int Suppl* 1997;59(S62-S65).
260. Dickstein K, Cohen-Solal A, Filippatos G, McMurray J, Ponikowski P, Poole-Wilson P, Strömberg A, van Veldhuisen D, Atar D, Hoes A, Keren A, Mebazaa A, Nieminen M, Priori S, Swedberg K. ESC guidelines for the diagnosis and treatment of acute and chronic heart failure 2008: the Task Force for the diagnosis and treatment of acute and chronic heart failure 2008 of the European Society of Cardiology. Developed in collaboration with the Heart Failure Association of the ESC (HFA) and endorsed by the European Society of Intensive Care Medicine (ESICM). *Eur J Heart Fail*. 2008;10(10):933-989.
261. Krum H, Cameron P. Diuretics in the treatment of heart failure: mainstay of therapy or potential hazard? *J Card Fail*. 2006;12(5):333-335.
262. Attanasio P, Ronco C, Anker M, Ponikowski P, Anker S. Management of chronic cardiorenal syndrome. *Contrib Nephrol*. 2010;165:129-139.
263. Fliser D, Schroter M, Neubeck M, Ritz E. Coadministration of thiazides increases the efficacy of loop diuretics even in patients with advanced renal failure. *Kidney Int*. 1994;46(2):482-488.
264. Sackner-Bernstein JD, Skopicki HA, Aaronson KD. Risk of Worsening Renal Function With Nesiritide in Patients With Acutely Decompensated Heart Failure. *Circulation*. 2005;111(12):1487-1491.
265. Krum H, Iyngkaran P, Lekawanvijit S. Pharmacologic management of the cardiorenal syndrome in heart failure. *Curr Heart Fail Rep*. 2009;6(2):105-111.
266. Ellison DH. Diuretic therapy and resistance in congestive heart failure. *Cardiology*. 2001;96:132-143.
267. Krum H. Heart-Kidney Connection in Hypertension and Heart Failure, Cardiac Society of Australia and New Zealand 59th Annual Scientific Meeting. 2011.
268. Boerrigter G, Burnett J. Cardiorenal syndrome in decompensated heart failure: Prognostic and therapeutic implications. *Curr Heart Fail Rep*. 2004;1(3):113-120.
269. Felker GM, Lee KL, Bull DA, Redfield MM, Stevenson LW, Goldsmith SR, LeWinter MM, Deswal A, Rouleau JL, Ofili EO, Anstrom KJ, Hernandez AF, McNulty SE, Velazquez EJ, Kfoury AG, Chen HH, Givertz MM, Semigran MJ, Bart BA, Mascette AM, Braunwald E, O'Connor CM. Diuretic Strategies in Patients with Acute Decompensated Heart Failure. *N Engl J Med*. 2011;364(9):797-805.
270. Eshaghian S, Horwich TB, Fonarow GC. Relation of loop diuretic dose to mortality in advanced heart failure. *Am J Cardiol*. 2006;97(12):1759-1764.
271. Costanzo MR, Guglin ME, Saltzberg MT, Jessup ML, Bart BA, Teerlink JR, Jaski BE, Fang JC, Feller ED, Haas GJ, Anderson AS, Schollmeyer MP, Sobotka PA. Ultrafiltration Versus Intravenous Diuretics for Patients Hospitalized for Acute Decompensated Heart Failure. *J Am Coll Cardiol*. 2007;49(6):675-683.
272. Bart BA, Goldsmith SR, Lee KL, Givertz MM, O'Connor CM, Bull DA, Redfield MM, Deswal A, Rouleau JL, LeWinter MM, Ofili EO, Stevenson LW, Semigran MJ, Felker GM, Chen HH, Hernandez AF, Anstrom KJ, McNulty SE, Velazquez EJ, Ibarra JC, Mascette AM, Braunwald E. Ultrafiltration in Decompensated Heart Failure with Cardiorenal Syndrome. *N Engl J Med*. 2012;367(24):2296-2304.
273. Nicklas J, Pitt B, Timmis G, Breneman G, Jafri S, Duvernoy W, Davis S, Goldberg M, Blair J, Mancini G, Johnson T, Luckoff C, Henry G. Effect of

- Enalapril on Mortality and the Development of Heart Failure in Asymptomatic Patients with Reduced Left Ventricular Ejection Fractions. *N Engl J Med*. 1992;327(10):685-691.
274. Fleming I. Signaling by the angiotensin-converting enzyme. *Circ Res*. 2006;98(7):887-896.
 275. Shlipak MG, Massie BM. The clinical challenge of cardiorenal syndrome. *Circulation*. 2004;110(12):1514-1517.
 276. Cano N, Fiaccadori E, Tesinsky P, Toigo G, Druml W, Kuhlmann M, Mann H, Hörl WH. ESPEN guidelines on enteral nutrition: adult renal failure. *Clin Nutr*. 2006;25(2):295-310.
 277. Lefebvre J, Murphey LJ, Hartert TV, Jiao Shan R, Simmons WH, Brown NJ. Dipeptidyl Peptidase IV Activity in Patients With ACE-Inhibitor-Associated Angioedema. *Hypertension*. 2002;39(2):460-464.
 278. Israili ZH, Hall WD. Cough and Angioneurotic Edema Associated with Angiotensin-Converting Enzyme Inhibitor Therapy. A Review of the Literature and Pathophysiology. *Ann Intern Med*. 1992;117(3):234-242.
 279. Krum H, Jelinek MV, Stewart S, Sindone A, Atherton JJ. 2011 update to National Heart Foundation of Australia and Cardiac Society of Australia and New Zealand Guidelines for the prevention, detection and management of chronic heart failure in Australia, 2006. *Med J Aust*. 2011;194(8):405-409.
 280. Terra SG. Angiotensin Receptor Blockers. *Circulation*. 2003;107(24):e215-e216.
 281. Siragy H. AT1 and AT2 receptors in the kidney: role in disease and treatment. *Am J Kidney Dis*. 2000;36(3 Suppl 1):4-9.
 282. Yusuf S, Pfeffer MA, Swedberg K, Granger CB, Held P, McMurray JJV, Michelson EL, Olofsson B, Östergren J. Effects of candesartan in patients with chronic heart failure and preserved left-ventricular ejection fraction: the CHARM-Preserved Trial. *Lancet*. 2003;362(9386):777-781.
 283. CIBIS-II Investigators and Committees. The Cardiac Insufficiency Bisoprolol Study II (CIBIS-II): a randomised trial. *Lancet*. 1999;353(9146):9-13.
 284. Silke B. Beta-blockade in CHF: pathophysiological considerations. *Eur Heart J Suppl*. 2006;8(Suppl C):C13-C18.
 285. Bristow MR. β -Adrenergic Receptor Blockade in Chronic Heart Failure. *Circulation*. 2000;101(5):558-569.
 286. Lefkowitz RJ, Rockman HA, Koch WJ. Catecholamines, Cardiac β -Adrenergic Receptors, and Heart Failure. *Circulation*. 2000;101(14):1634-1637.
 287. Frishman WH. Beta-Adrenergic Blockers. *Circulation*. 2003;107(18):e117-e119.
 288. Krum H, Haas SJ, Eichhorn E, Ghali J, Gilbert E, Lechat P, Packer M, Roecker E, Verkenne P, Wedel H, Wikstrand J. Prognostic benefit of beta-blockers in patients not receiving ACE-Inhibitors. *Eur Heart J*. 2005;26:2154-2158.
 289. Castagno D, Jhund PS, McMurray JJV, Lewsey JD, Erdmann E, Zannad F, Remme WJ, Lopez-Sendon JL, Lechat P, Follath F, Hoglund C, Mareev V, Sadowski Z, Seabra-Gomes RJ, Dargie HJ. Improved survival with bisoprolol in patients with heart failure and renal impairment: an analysis of the cardiac insufficiency bisoprolol study II (CIBIS-II) trial. *Eur J Heart Fail*. 2010;12(6):607-616.
 290. Pitt B, Zannad F, Remme WJ, Cody R, Castaigne A, Perez A, Palensky J, Wittes J. The effect of spironolactone on morbidity and mortality in patients with severe heart failure. *N Engl J Med*. 1999;341(10):709-717.

291. Pitt B, Remme W, Zannad F, Neaton J, Martinez F, Roniker B, Bittman R, Hurley S, Kleiman J, Gatlin M. Eplerenone, a selective aldosterone blocker, in patients with left ventricular dysfunction after myocardial infarction. *N Engl J Med*. 2003;348(14):1309-1321.
292. Zannad F, McMurray JJV, Krum H, van Veldhuisen DJ, Swedberg K, Shi H, Vincent J, Pocock SJ, Pitt B. Eplerenone in patients with systolic heart failure and mild symptoms. *N Engl J Med*. 2011;364(1):11-21.
293. Vanholder R, Baurmeister U, Brunet P, Cohen G, Glorieux G, Jankowski J, for the European Uremic Toxin Work G. A Bench to Bedside View of Uremic Toxins. *J Am Soc Nephrol*. 2008;19(5):863-870.
294. Eloot S, Van Biesen W, Dhondt A, Van de Wynkele H, Glorieux G, Verdonck P, Vanholder R. Impact of hemodialysis duration on the removal of uremic retention solutes. *Kidney Int*. 2007;73(6):765-770.
295. Fagugli RM, De Smet R, Buoncristiani U, Lameire N, Vanholder R. Behavior of non-protein-bound and protein-bound uremic solutes during daily hemodialysis. *Am J Kidney Dis*. 2002;40(2):339-347.
296. Mucsi I, Hercz G, Uldall R, Ouwendyk M, Francoeur R, Pierratos A. Control of serum phosphate without any phosphate binders in patients treated with nocturnal hemodialysis. *Kidney Int*. 1998;53(5):1399-1404.
297. Schulman G, Agarwal R, Acharya M, Berl T, Blumenthal S, Kopyt N. A multicenter, randomized, double-blind, placebo-controlled, dose-ranging study of AST-120 (kremezin) in patients with moderate to severe CKD. *Am J kidney Dis* 2006;47(4):565-577.
298. Ueda H, Shibahara N, Takagi S, Inoue T, Katsuoka Y. AST-120 treatment in pre-dialysis period affects the prognosis in patients on hemodialysis. *Ren Fail*. 2008;30(9):856-860.
299. Tamada S, Asai T, Kuwabara N, Iwai T, Uchida J, Teramoto K, Kaneda N, Yukimura T, Komiya T, Nakatani T, Miura K. Molecular Mechanisms and Therapeutic Strategies of Chronic Renal Injury: The Role of Nuclear Factor kappa B Activation in the Development of Renal Fibrosis. *J Pharmacol Sci*. 2006;100(1):17-21.
300. Kompa AR, Samuel CS, Summers RJ. Inotropic responses to human gene 2 (B29) relaxin in a rat model of myocardial infarction (MI): effect of pertussis toxin. *Brit J Pharmacol*. 2002;137:710-718.
301. Kompa AR, Summers RJ. Lidocaine and surgical modification reduces mortality in a rat model of cardiac failure induced by coronary artery ligation *J Pharmacol Toxicol Meths*. 2000;43:199-203.
302. Bunag RD. Validation in awake rats of a tail-cuff method for measuring systolic pressure. *J Appl Physiol*. 1973;34(2):279-282.
303. Pfeffer JM, Pfeffer MA, Frohlich ED. Validity of an indirect tail-cuff method for determining systolic arterial pressure in unanesthetized normotensive and spontaneously hypertensive rats. *J Lab Clin Med*. 1971;78(6):957-962.
304. Connelly KA, Kelly DJ, Zhang Y, Prior DL, Martin J, Cox AJ, Thai K, Feneley MP, Tsoporis J, White KE, Krum H, Gilbert RE. Functional, structural and molecular aspects of diastolic heart failure in the diabetic (mRen-2)27 rat. *Cardiovasc Res*. 2007;76(2):280-291.
305. Schiller N, Shah P, Crawford M, DeMaria A, Devereux R, Feigenbaum H, Gutgesell H, Reichek N, Sahn D, Schnittger I. Recommendations for quantitation of the left ventricle by two-dimensional echocardiography. American Society of Echocardiography Committee on Standards,

- Subcommittee on Quantitation of Two-Dimensional Echocardiograms. *J Am Soc Echocardiogr*. 1989;2(5):358-367.
306. Connelly KA, Prior DL, Kelly DJ, Feneley MP, Krum H, Gilbert RE. Load-sensitive measures may overestimate global systolic function in the presence of left ventricular hypertrophy: a comparison with load-insensitive measures. *Am J Physiol Heart Circ Physiol*. 2006;290(4):H1699-H1705.
 307. Georgakopoulos D, Mitzner WA, Chen C-H, Byrne BJ, Millar HD, Hare JM, Kass DA. In vivo murine left ventricular pressure-volume relations by miniaturized conductance micromanometry. *Am J Physiol Heart Circ Physiol*. 1998;274(4):H1416-H1422.
 308. Ito H, Takaki M, Yamaguchi H, Tachibana H, Suga H. Left ventricular volumetric conductance catheter for rats. *Am J Physiol Heart Circ Physiol*. 1996;270(4):H1509-H1514.
 309. Georgakopoulos D, Kass DA. Estimation of parallel conductance by dual-frequency conductance catheter in mice. *Am J Physiol Heart Circ Physiol*. 2000;279(1):H443-H450.
 310. Yang B, Larson DF, Beischel J, Kelly R, Shi J, Watson RR. Validation of conductance catheter system for quantification of murine pressure-volume loops. *J Invest Surg*. 2001;14(6):341-355.
 311. Kelly DJ, Skinner SL, Gilbert RE, Cox AJ, Cooper ME, Wilkinson-Berka JL. Effects of endothelin or angiotensin II receptor blockade on diabetes in the transgenic (mRen-2)27 rat. *Kidney Int*. 2000;57:1882-1894.
 312. Wilkinson-Berka JL, Kelly DJ, Koerner SM, Jaworski K, Davis B, Thallas V, Cooper ME. ALT-946 and Aminoguanidine, Inhibitors of Advanced Glycation, Improve Severe Nephropathy in the Diabetic Transgenic (mREN-2)27 Rat. *Diabetes*. 2002;51(11):3283-3289.
 313. Kelly JD, Wilkinson-Berka JL, Allen TJ, Cooper ME, Skinner SL. A new model of diabetic nephropathy with progressive renal impairment in the transgenic (mRen-2)27 rat (TGR). *Kidney Int*. 1998;54(2):343-352.
 314. Kelly DJ, Chanty A, Gow RM, Zhang Y, Gilbert RE. Protein Kinase C β Inhibition Attenuates Osteopontin Expression, Macrophage Recruitment, and Tubulointerstitial Injury in Advanced Experimental Diabetic Nephropathy. *J Am Soc Nephrol*. 2005;16(6):1654-1660.
 315. Tran L, Kompa AR, Kemp W, Phrommintikul A, Wang BH, Krum H. Chronic urotensin-II infusion induces diastolic dysfunction and enhances collagen production in rats. *Am J Physiol Heart Circ Physiol*. 2010;298(2):H608-H613.
 316. Burnette WN. "Western Blotting": Electrophoretic transfer of proteins from sodium dodecyl sulfate-polyacrylamide gels to unmodified nitrocellulose and radiographic detection with antibody and radioiodinated protein A. *Anal Biochem*. 1981;112(2):195-203.
 317. Imamura T, Takase M, Nishihara A, Oeda E, Hanai J, Kawabata M, Miyazono K. Smad6 inhibits signalling by the TGF- β superfamily. *Nature*. 1997;389:622-626.
 318. Simpson P. Stimulation of Hypertrophy of Cultured Neonatal Rat Heart Cells through an alpha-Adrenergic Receptor and Induction of Beating through an alpha1- and beta1-Adrenergic Receptor Interaction. Evidence for Independent Regulation of Growth and Beating. *Circ Res*. 1985;56:884-894.
 319. Woodcock EA, Wang BH, Arthur JF, Lennard A, Matkovich SJ, Du X-J, Brown JH, Hannan RD. Inositol Polyphosphate 1-Phosphatase Is a Novel Antihypertrophic Factor. *J Biol Chem*. 2002;277(25):22734-22742.

320. Tzanidis A, Hannan RD, Thomas WG, Onan D, Autelitano DJ, See F, Kelly DJ, Gilbert RE, Krum H. Direct Actions of Urotensin II on the Heart: Implications for Cardiac Fibrosis and Hypertrophy. *Circ Res*. 2003;93(3):246-253.
321. Hannan RD, Rothblum LI. Regulation of ribosomal DNA transcription during neonatal cardiomyocyte hypertrophy. *Cardiovasc Res*. 1995;30(4):501-510.
322. Thomas WG, Brandenburger Y, Autelitano DJ, Pham T, Qian H, Hannan RD. Adenoviral-Directed Expression of the Type 1A Angiotensin Receptor Promotes Cardiomyocyte Hypertrophy via Transactivation of the Epidermal Growth Factor Receptor. *Circ Res*. 2002;90(2):135-142.
323. See F, Thomas W, Way K, Tzanidis A, Kompa A, Lewis D, Itescu S, Krum H. P38 mitogen-activated protein kinase inhibition improves cardiac function and attenuates left ventricular remodeling following myocardial infarction in the rat. *J Am Coll Cardiol*. 2004;44(8):1679-1689.
324. Mosmann T. Rapid colorimetric assay for cellular growth and survival: Application to proliferation and cytotoxicity assays. *J Immunol Methods*. 1983;65:55-63.
325. Liu S, Lekawanvijit S, Kompa AR, Wang BH, Kelly DJ, Krum H. Cardiorenal Syndrome: Pathophysiology, Preclinical Models, Management and Potential Role of Uraemic Toxins. *Clin Exp Pharmacol Physiol*. 2012;39(8):692-700.
326. Liu S, Wang BH, Kompa AR, Lekawanvijit S, Krum H. Antagonists of organic anion transporters 1 and 3 ameliorate adverse cardiac remodelling induced by uremic toxin indoxyl sulfate. *Int J Cardiol*. 2012;158(3):457-458.
327. Szymanski MK, de Boer RA, Navis GJ, van Gilst WH, Hillege HL. Animal models of cardiorenal syndrome: a review *Heart Fail Rev*. 2012;17:411-420.
328. Aoyagi T, Fujii AM, Flanagan MF, Arnold LW, Brathwaite KW, Colan SD, Mirsky I. Transition from compensated hypertrophy to intrinsic myocardial dysfunction during development of left ventricular pressure-overload hypertrophy in conscious sheep. Systolic dysfunction precedes diastolic dysfunction. *Circulation*. 1993;88(5):2415-2425.
329. Onodera T, Tamura T, Said S, McCune SA, Gerdes AM. Maladaptive Remodeling of Cardiac Myocyte Shape Begins Long Before Failure in Hypertension. *Hypertension*. 1998;32(4):753-757.
330. Jois P, Mebazaa A. Cardio-Renal Syndrome Type 2: Epidemiology, Pathophysiology, and Treatment. *Semin Nephrol*. 2012;32(1):26-30.
331. Gao Z, Barth AS, DiSilvestre D, Akar FG, Tian Y, Tanskanen A, Kass DA, Winslow RL, Tomaselli GF. Key pathways associated with heart failure development revealed by gene networks correlated with cardiac remodeling. *Physiol Genomics*. 2008;35:222-230.
332. Deten A, Holzl A, Leicht M, Barth W, Zimmer H-G. Changes in Extracellular Matrix and in Transforming Growth Factor Beta Isoforms After Coronary Artery Ligation in Rats. *J Mol Cell Cardiol*. 2001;33(6):1191-1207.
333. Bonventre JV. Kidney injury molecule-1 (KIM-1): a urinary biomarker and much more. *Nephrol Dial Transplant*. 2009;24(11):3265-3268.
334. Ko GJ, Boo C-S, Jo S-K, Cho WY, Kim HK. Macrophages contribute to the development of renal fibrosis following ischaemia/reperfusion-induced acute kidney injury. *Nephrol Dial Transplant*. 2008;23(3):842-852.
335. Bar-Joseph Z, Gitter A, Simon I. Studying and modelling dynamic biological processes using time-series gene expression data. *Nat Rev Genet*. 2012;13(8):552-564.

336. Border WA, Noble NA. Transforming Growth Factor β in Tissue Fibrosis. *N Engl J Med*. 1994;331(19):1286-1292.
337. Gui T, Sun Y, Shimokado A, Muragaki Y. The Roles of Mitogen-Activated Protein Kinase Pathways in TGF- β -Induced Epithelial-Mesenchymal Transition. *J Sig Transd*. 2012;doi:10.1155/2012/289243.
338. Cheung A, Sarnak M, Yan G, Berkoben M, Heyka R, Kaufman A, Lewis J, Rocco M, Toto R, Windus D, Ornt D, Levey A. Cardiac diseases in maintenance hemodialysis patients: results of the HEMO Study. *Kidney Int*. 2004;65:2380-2389.
339. Johnson DW, Craven AM, Isbel NM. Modification of cardiovascular risk in hemodialysis patients: an evidence-based review. *Hemodial Int*. 2007;11(1-14).
340. Tonelli M, Wiebe N, Culleton B, House A, Rabbat C, Fok M, McAlister F, Garg AX. Chronic Kidney Disease and Mortality Risk: A Systematic Review. *J Am Soc Nephrol*. 2006;17(7):2034-2047.
341. McCullough P, Jurkovitz C, Pergola P, McGill J, Brown W, Collins A, Chen S, Li S, Singh A, Norris K, Klag M, Bakris G. Independent components of chronic kidney disease as a cardiovascular risk state: Results from the kidney early evaluation program (keep). *Arch Intern Med*. 2007;167(11):1122-1129.
342. Bujak M, Frangogiannis N. The role of TGF- β signaling in myocardial infarction and cardiac remodeling. *Cardiovasc Res*. 2007;74:184-195.
343. Mall G, Rambausek M, Neumeister A, Kollmar S, Vetterlein F, Ritz E. Myocardial interstitial fibrosis in experimental uremia-implications for cardiac compliance. *Kidney Int*. 1988;33(4):804-811.
344. Lopez B, Gonzalez A, Diez J. Circulating Biomarkers of Collagen Metabolism in Cardiac Diseases. *Circulation*. 2010;121(14):1645-1654.
345. Kitamura M, Shimizu M, Ino H, Okeie K, Yamaguchi M, Funjino N, Mabuchi H, Nakanishi I. Collagen remodeling and cardiac dysfunction in patients with hypertrophic cardiomyopathy: the significance of type III and VI collagens. *Clin Cardiol*. 2001;24(4):325-329.
346. Tharaux P-L, Chatziantoniou C, Fakhouri F, Dussaule J-C. Angiotensin II Activates Collagen I Gene Through a Mechanism Involving the MAP/ER Kinase Pathway. *Hypertension*. 2000;36(3):330-336.
347. Vaidya V, Ramirez V, Ichimura T, Bobadilla N, Bonventre J. Urinary kidney injury molecule-1: a sensitive quantitative biomarker for early detection of kidney tubular injury. *Am J Physiol Renal Physiol* 2006;290:F517-529.
348. van Timmeren MM, van den Heuvel MC, Bailly V, Bakker SJL, van Goor H, Stegeman CA. Tubular kidney injury molecule-1 (KIM-1) in human renal disease. *J Pathol*. 2007;212(2):209-217.
349. Border W, Brees D, Noble N. Transforming growth factor-beta and extracellular matrix deposition in the kidney. *Contrib Nephrol*. 1994;107:140-145.
350. Frantz S, Bauersachs J, Ertl G. Post-infarct remodelling: contribution of wound healing and inflammation. *Cardiovasc Res*. 2009;81:474-481.
351. Border W, Noble N. TGF- β in kidney fibrosis: A target for gene therapy. *Kidney Int*. 1997;51:1388-1396.
352. Sharma K, Jin Y, Guo J, Ziyadeh F. Neutralization of TGF- β by anti-TGF- β antibody attenuates kidney hypertrophy and the enhanced extracellular matrix gene expression in STZ-induced diabetic mice. *Diabetes*. 1996;45:522-530.

- 353. Sharma K, Ziyadeh F. Renal hypertrophy is associated with upregulation of TGF- β 1 gene expression in diabetic BB rat and NOD mouse. *Am J Physiol Renal Physiol*. 1994;267(6):F1094-F1001.
- 354. Siedlecki A, Jin X, Muslin A. Uremic cardiac hypertrophy is reversed by rapamycin but not by lowering of blood pressure. *Kidney Int*. 2009;75(8):800-808.
- 355. Kennedy DJ, Elkareh J, Shidyak A, Shapiro AP, Smaili S, Mutgi K, Gupta S, Tian J, Morgan E, Khouri S, Cooper CJ, Periyasamy SM, Xie Z, Malhotra D, Fedorova OV, Bagrov AY, Shapiro JI. Partial nephrectomy as a model for uremic cardiomyopathy in the mouse. *Am J Physiol Renal Physiol*. 2008;294:F450-F454.
- 356. Stanfel LA, Gulyassy PF, Jarrard EA. Determination of indoxyl sulfate in plasma of patients with renal failure by use of ion-pairing liquid chromatography. *Clin Chem*. 1986;32(6):938-942.

Appendices

Appendix 1: Cardiorenal syndrome: Pathophysiology, preclinical models, management and potential role of uraemic toxins

This review article was written in the first PhD year and has been published in the *Clinical and Experimental Pharmacology and Physiology* 2012; 39: 692-700. The paper in a PDF format was enclosed.

3rd Australia-China Biomedical Research Conference (ACBRC2011)

Cardiorenal syndrome: Pathophysiology, preclinical models, management and potential role of uraemic toxinsShan Liu,* Suree Lekawanvijit,* Andrew R Kompa,*[†] Bing H Wang,* Darren J Kelly[†] and Henry Krum***Centre for Cardiovascular Research and Education in Therapeutics, Department of Epidemiology and Preventive Medicine, Monash University and [†]Department of Medicine, University of Melbourne, St Vincent's Hospital, Melbourne, Victoria, Australia***SUMMARY**

1. Cardiorenal syndrome (CRS) describes the primary dysfunction in either the kidney or heart that initiates the combined impairment of both organs. The heart and kidney exert reciprocal control of the respective function to maintain constant blood volume and organ perfusion under continuously changing conditions.

2. The pathophysiology of CRS is not fully understood, but appears to be caused by a complex combination of haemodynamic, neurohormonal, immunological and biochemical feedback pathways. Of these pathways, the contributory role of uraemic toxins that accumulate in CRS has been underexplored. One such toxin, namely indoxyl sulphate, has been found to have direct adverse effects on relevant cardiac cells.

3. Early diagnosis by assessing cardiac and renal injury biomarkers may be critical for timely therapeutic intervention. Such therapies are directed at attenuation of neurohormonal activation, control of elevated blood pressure, correction of anaemia and relief of hypervolaemia. Reduction of non-dialysable uraemic toxins is a further potentially beneficial therapeutic strategy.

Key words: cardiorenal syndrome, indoxyl sulphate, management, pathophysiology, preclinical models, uraemic toxin.

INTRODUCTION

A close relationship between renal dysfunction and heart failure (HF) has been demonstrated, both clinically and using basic research methodologies. A diseased heart has numerous negative effects on kidney function, whereas renal insufficiency can significantly impair cardiac function.^{1,2} To describe this interrelationship, the term

'cardiorenal syndrome' (CRS) has been increasingly used in recent years. Cardiorenal syndrome has been generally defined as a pathophysiological disorder of the heart and kidney whereby acute or chronic dysfunction of one organ may induce acute or chronic dysfunction of the other.³ The primary failing organ can be either the heart or kidney. Systemic disorders, such as sepsis, are also proposed to be a subtype of CRS.³

EPIDEMIOLOGY

Acceleration of coronary artery disease and left ventricular hypertrophy (LVH) are major cardiac problems observed in patients with renal failure and may be contributory to chronic heart failure (CHF) that is also frequently seen in patients with chronic kidney disease (CKD).^{1,4} Patients with CKD are more likely to die of CHF than kidney failure.⁵ Mortality rates for renal disease remain above 20% annually with the use of dialysis, with more than half the deaths related to cardiovascular disease.⁶

Renal dysfunction is common in patients with HF, with a prevalence of approximately 25%.^{7–9} The degree of renal dysfunction is a powerful independent risk factor for all-cause mortality in CHF patients.⁹

PATHOPHYSIOLOGY OF CRS**Pathophysiological contributors to CRS***Neurohormonal activation*

The primary organ insult causes activation of a series of response mechanisms by neural and hormonal systems (Fig. 1). Although in some cases these mechanisms are initially compensatory, many contribute to the further functional worsening and progression of CRS over the long term.

Changes in cardiac function associated with CHF lead to a decline in cardiac output, which may cause diminished blood flow and renal hypoperfusion (Fig. 1). This leads to baroreceptor-mediated renal vasoconstriction, activation of the renal sympathetic nervous system (SNS) and release of catecholaminergic hormones.² Activation of the SNS further stimulates renal vasoconstriction and causes fluid retention (Fig. 1).²

Elevated central sympathetic tone caused by renal somatic afferent nerve activation and the consequences of excessive efferent

Correspondence: Dr Henry Krum, Department of Epidemiology and Preventive Medicine, Level 6 The Alfred Centre, 99 Commercial Road, Melbourne, Victoria 3004, Australia. Email: [REDACTED]

Presented at the 3rd Australia-China Biomedical Research Conference (ACBRC 2011) Melbourne, Australia, 28–30 April 2011. The papers in these proceedings have been peer reviewed.

Received 13 July 2011; revision 30 September 2011; accepted 13 October 2011.

© 2011 The Authors

Clinical and Experimental Pharmacology and Physiology

© 2011 Blackwell Publishing Asia Pty Ltd

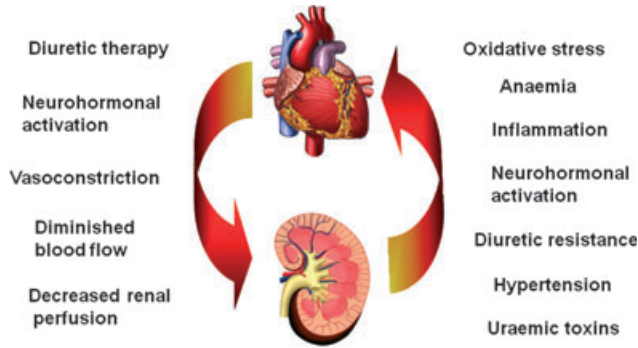


Fig. 1 Pathophysiological interactions between heart and kidney in cardio-renal syndrome (CRS).

sympathetic signals to the kidney are closely associated with the development of CRS.¹⁰ Various stimuli, such as renal ischaemia, hypoxia, oxidative stress and intrinsic renal diseases are likely to activate renal sensory afferent signalling.¹¹ These signalling pathways affect the hypothalamus, which provides the basis for targeting the renal somatic afferent nerves as modulators of central integration in the brain stem.^{10,11} This integration subsequently causes increased sympathetic efferent signalling to kidneys and directly influences the entire sympathetic system.^{10,12} Interventional renal nerve ablation has been demonstrated to reduce blood pressure and improve insulin resistance in patients with resistant hypertension.^{13–17}

Overactivity of the renin–angiotensin–aldosterone system (RAAS) as an essential pathophysiological consequence in either CHF or CKD may activate the SNS and play a role in endothelial dysfunction and the progression of atherosclerosis, as well as inhibition of the fibrinolytic system.¹⁸ Also, angiotensin (Ang) II increases blood pressure and stimulates the secretion of aldosterone, which increases reabsorption of sodium and water, as well as acting as a circulating hormone, exerting damaging effects on the heart and kidney.¹⁸ The haemodynamic consequences of systemic hypertension, as well as the direct pro-inflammatory and pro-fibrotic effects of AngII and aldosterone, play important roles in subsequent CRS.¹⁹

Intracellular signalling pathways

Oxidative stress defines an imbalance in the formation of anti-oxidants and reactive oxygen species (ROS). Reactive oxygen species are known to stimulate inflammatory cytokines (e.g. tumour necrosis factor (TNF)- α , interleukin (IL)-1 β and IL-6), which regulate cell survival and death.²⁰ Increased oxidative stress has been demonstrated in patients with CKD, which may contribute to the pathophysiology of CRS (Fig. 1).²¹ Angiotensin II has been demonstrated to activate ROS in rat neonatal cardiomyocytes and pretreatment with anti-oxidants suppresses AngII-induced cardiac hypertrophy.²² These results suggest a critical role for ROS-dependent signal transduction in cardiac hypertrophy.

Apoptosis signal-regulating kinase-1 (ASK1) is a ROS-sensitive, mitogen-activated protein kinase kinase kinase (MAPKKK).²³ It has been shown that ASK1 activates two different subgroups of mitogen-activated protein kinase kinases (MAPKK), namely MKK3/6 and MKK4/7; these, in turn, activate p38 and c-Jun N-terminal kinase (JNK) subgroups of mitogen-activated protein kinases (MAPK), respectively (Fig. 2).²⁴ The p38 MAPK signalling cascade has been found to be an important pathway in the progression of left ventricu-

lar (LV) dysfunction and pathological remodelling after myocardial infarction (MI).²⁵ It has been demonstrated that ASK1 is involved in G-protein-coupled receptor agonist-induced nuclear factor (NF)- κ B activation and resulting cardiomyocyte hypertrophy.²⁶ The ROS/ASK1 pathway is involved in cellular necrosis and apoptosis, indicating that ASK1 may be a therapeutic target to reduce LV remodelling after MI.²⁷

Inflammatory response

Cardiac injury results in the migration of macrophages, monocytes and neutrophils into the myocardium. This initiates intracellular signalling and neurohormonal activation, which localizes the inflammatory response.²⁸ Increases in plasma IL-1 β and IL-6 have been observed in patients early after MI.²⁹ Patients with HF express elevated circulating levels of TNF- α , which promotes progressive LV dysfunction and remodelling.³⁰ In renal injury, increased levels of TNF- α , IL-1 β and intercellular adhesion molecule-1 (ICAM-1) mRNA have been found in the heart after renal ischaemia–reperfusion (Fig. 1).³¹

Other factors

Several chronic conditions, such as hypertension, anaemia and uraemic toxins, may contribute to CRS (Fig. 1). Hypertension itself frequently causes severe renal disease and hypertension also commonly develops in patients with underlying renal disease.³² The coexistence of hypertension with renal diseases greatly accelerates the progression of renal failure.³² In the heart, hypertension results in pressure overload and is the major precursor for the development of LVH, associated with progressive changes in cardiac myocyte enlargement and accumulation of collagen, which may cause diastolic dysfunction.^{33,34} Hypertension also increases the risk of MI via acceleration of atherosclerosis, which may lead to systolic dysfunction.³⁵ Thus, both diastolic and systolic dysfunction may develop, especially when other precipitant factors are present.³⁵

Anaemia, CHF and CKD interact in a vicious circle to cause or worsen each other.^{36,37} Anaemia, as a result of erythropoietin (EPO) insufficiency, is frequently associated with CKD.³⁷ Erythrocytes contain many anti-oxidants; thus, anaemia may cause increases in oxidative stress.^{36,38} The lack of oxygen supply to the heart associated

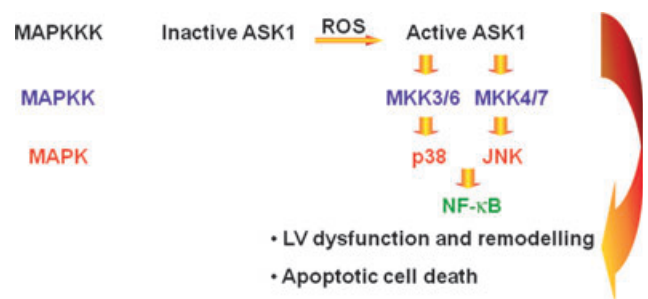


Fig. 2 Apoptosis signal-regulating kinase-1 (ASK1) is a mitogen-activated protein kinase kinase kinase (MAPKKK) that activates mitogen-activated protein kinase kinases (MAPKK), namely MKK3/6 and MKK4/7, which, in turn, activate p38 and c-Jun N-terminal kinase (JNK) mitogen-activated protein kinases (MAPK), respectively. In addition, ASK1 is involved in the activation of the transcription factor nuclear factor (NF)- κ B.²⁰

with anaemia may be compensated for by increasing heart rate and stroke volume and this may activate the SNS and RAAS, causing renal vasoconstriction and fluid retention.^{36,39} Exogenous EPO treatment has been shown to have anti-apoptotic, anti-oxidative and anti-inflammatory effects with improved renal and cardiovascular function.⁴⁰

Apart from hypertension and anaemia, there may also be additional factors contributing to CHF in CKD patients. The normal kidney is able to filter harmful chemicals (i.e. toxins). In the setting of CKD there is systemic accumulation of such toxins, many of which can be eliminated by dialysis. However, removal of some toxins, including indoxyl sulphate, phenyl acetic acid, *m/p*-cresol and *m/p*-cresylsulphate, is limited owing to their high protein-binding capacity.^{41,42} Of these non-dialysable toxins, indoxyl sulphate has been demonstrated to have profibrotic effects to the kidney and, most recently, its profibrotic and prohypertrophic effects on relevant cardiac cells have been demonstrated.^{42–46} In addition, the increased cardiac fibrosis in animals with CKD has been shown to be correlated with indoxyl sulphate serum levels.⁴⁷

Several uraemic toxins, namely asymmetrical dimethyl L-arginine (ADMA), homocysteine, advanced glycation end-products, *p*-cresyl sulphate, indoxyl sulphate etc., are mostly protein bound and are linked to endothelial dysfunction, atherosclerosis and insulin resistance in end-stage renal disease and advanced CKD.^{48,49} Asymmetrical dimethyl L-arginine, an endogenous compound that accumulates in patients with CKD, inhibits nitric oxide synthesis and may thus contribute to hypertension and immune dysfunction.⁵⁰ In addition, ADMA accelerates the senescence of endothelial cells via oxidative stress *in vitro* and its accumulation could contribute to the increased risk in cardiovascular events in patients with CKD.^{51,52} Homocysteine also has adverse effects on vascular endothelial cells, as observed in the condition of hyperhomocysteinaemia, and these effects are mediated through oxidative stress mechanisms.⁵³ Advanced glycation end-products that accumulate in patients with CKD as a result of inflammation, oxidative stress and carbamoylation in turn promote a pro-inflammatory and oxidant pattern in endothelial cells.⁴⁸ *p*-Cresyl sulphate has been suggested to alter endothelial function in dialysis patients by inducing shedding of endothelial microparticles.⁵⁴ Indoxyl sulphate induces oxidative stress in endothelial cells by enhancing ROS production, increasing NAD(P)H oxidase activity and decreasing glutathione levels.⁵⁵

Consequences of CRS

Cardiac changes

Left ventricular remodelling refers to changes in myocardial structure and function in response to cardiac injury, which is associated with reduced heart pump function and low cardiac output.⁵⁶ These changes result in end-organ ischaemia, increased right atrial pressure and volume retention. Postinfarction, infarct expansion occurs within hours of myocyte injury, resulting in myocyte hypertrophy, wall thinning and ventricular dilatation, with accompanying myocyte apoptosis or necrosis.^{28,56,57} Myocyte hypertrophy leads to LVH, which is an adaptive response during LV remodelling.²⁸ Although it offsets increased load, attenuates progressive dilation and stabilizes the contractile function, remodelling leads to a worse prognostic outcome via either sudden death or progressive pump dysfunction.⁵⁸

Postinjury, cardiac fibroblasts also undergo phenotypic transformation to myofibroblasts, which have an increased capacity for colla-

gen synthesis.^{59,60} Therefore collagen deposition in the heart is increased both at the site of the infarct to prevent further ventricular deformation and in remote regions, including the peri-infarct region and the interventricular septum.^{61,62} Fibroblast activation and collagen synthesis are regulated by signals of local and systemic origin, including AngII, endothelin-1 and transforming growth factor (TGF)- β 1.⁶³ Increased cardiac fibrosis results in exaggerated mechanical stiffness and contributes to diastolic dysfunction.⁵⁶ Progressive increases in fibrosis may also cause systolic dysfunction and LVH, as well as electrical instability leading to fatal arrhythmias.⁵⁶

Cardiac changes in the setting of CKD, or the so-called 'uraemic cardiomyopathy', comprise LVH, cardiac fibrosis and a decrease in myocardial capillary density.^{34,64} Left ventricular hypertrophy is found in 75% of CKD patients commencing dialysis treatment.⁶⁵ Cardiac fibrosis contributes to diastolic HF and sudden cardiac death, the most common cause of cardiovascular death in CKD patients.^{64,66,67} A decrease in myocardial capillary density, sometimes considered as a microvascular change, can increase the risk of ischaemic heart disease.

Renal changes

Renal fibrosis is contributory to glomerulosclerosis, tubulointerstitial fibrosis and tubular atrophy. After the initial insult, the affected kidney undergoes a series of events in an attempt to repair and recover from the injury, such as fibroblast activation. Accumulated renal collagen is cross-linked and resistant to degradation, which invariably results in loss of function when normal tissue is replaced with scar tissue.^{68,69} Glomerulosclerosis, which is the scarring of the glomerulus, may result in the occlusion of the capillary loops and ultimately lead to loss of glomerular function.⁷⁰

The prolonged renal hypoxia caused by both anaemia and CHF can cause chronic renal ischaemia and eventual nephron loss and renal fibrosis.⁷¹ Several previous studies have shown that anaemia is an independent risk factor for the progression of end-stage renal disease.^{72,73} However, a recent study has demonstrated that anaemia is associated with a more rapid progression of kidney disease in patients with CHF.⁷⁴

In the setting of CHF, renal dysfunction is a common complication associated with poor clinical outcomes.^{75,76} However, little is known with regard to renal structural changes in patients with CHF. To date, only increased renal fibrosis has been demonstrated in post-MI animals.^{77,78}

BIOMARKERS

Biomarkers can contribute to the early diagnosis of injury and thus to timely therapeutic intervention. Natriuretic peptides, particularly B-type natriuretic peptide (BNP) and its amino-terminal metabolite N-terminal pro-BNP are powerful predictors of cardiac events.⁷⁹ Postinfarction, it is common for BNP to be secreted from the ventricles causing natriuresis and vasodilation. A BNP level < 100 pg/mL yielded a 90% sensitivity and 76% specificity for separating cardiac from non-cardiac aetiologies of dyspnoea.⁸⁰ Patients with a BNP level < 130 pg/mL had a 1% risk of sudden cardiac death compared with a 19% risk at higher concentrations.⁸⁰ Cardiotrophin-1 is a member of the family of IL-6-related cytokines and its plasma levels are elevated in HF in relation to the severity of LV systolic

dysfunction.^{81,82} Serum soluble suppression of tumourigenicity 2 (ST2), an IL-1 receptor family member, is increased in the serum of patients early after acute MI.⁸³ Galectin-3 has stimulatory effects on macrophage migration, fibroblast proliferation and fibrosis synthesis.⁸⁴ Its expression is maximal at peak fibrosis and absent after recovery; thus, it may develop as a novel mediator of HF development and progression.⁸⁴

Increased levels of serum creatinine remain the most commonly used standard for assessment of renal function in clinical practice.^{85,86} Recently, cystatin C has been suggested as a better predictor of glomerular function than serum creatinine in patients with CKD because its serum levels are not affected by age, gender, race or muscle mass.⁸⁷ For early diagnosis, neutrophil gelatinase-associated lipocalin appears to be one of the earliest markers detected in the blood and urine of patients with acute kidney injury.⁸⁸ Kidney injury molecule 1 (KIM-1) is a protein detectable in the urine after ischaemic or nephrotoxic insults to proximal tubular cells and seems to be highly specific for ischaemic acute kidney injury.^{89,90}

Preclinical models

A variety of experimental models with cardiac and renal impairment have been developed, with rat models predominating. Left anterior descending coronary artery ligation is often used to induce experimental MI, whereas experimental subtotal nephrectomy (STNx) by infarction of extrarenal branches of the left renal artery is used as a model of CKD.

Myocardial infarction model

Cardiac effects

Cardiac systolic function is reduced in MI animals. Fractional shortening and ejection fraction are substantially decreased in this model.⁷⁷ Left ventricular weight/bodyweight (BW) and lung weight/BW ratios are significantly greater in MI animals 5 weeks after MI.⁹¹ Infarcted wall thinning with scarring tissue and non-infarcted myocardium hypertrophies are observed in MI animals 3 weeks after MI.^{92,93} Histological analysis shows that the cardiomyocyte cross-sectional area, the expression of interstitial fibrosis, collagen I/III, TGF- β protein, α -smooth muscle actin and macrophages are significantly increased in the non-infarct zone of the heart in MI animals.⁹¹ Western blot analysis demonstrates a significant increase in phosphorylated (p-) Smad2 protein expression in MI animals 5 weeks after MI.⁹¹

Renal effects

Myocardial infarction has detrimental effects on the renal function over time, as assessed at 4, 8, 12 and 16 weeks after MI.⁷⁷ Glomerular filtration rate (GFR) significantly decreases in MI animals at 4 weeks, but not at 8 and 12 weeks, and deteriorates further at 16 weeks. Histological analysis reveals that renal cortical interstitial fibrosis and TGF- β bioactivity (p-smad2) are significantly greater in MI animals at all time points. The degree of fibrosis increases progressively and is maximal at 16 weeks. Furthermore positive staining in the tubules of the biomarker KIM-1 is more prominent in MI animals over time and increased cardiac mRNA expression of TGF- β 1 and TNF- α are observed in MI animals at 16 weeks.⁷⁷

Subtotal nephrectomy model

Cardiac effects

Early LV diastolic dysfunction has been demonstrated by an increase of the peak velocity of atrial filling (A and A' waves) and a decrease in the E/A and E'/A' ratios in STNx animals, as determined by echocardiography.⁴⁷ Heart weight/BW ratio, myocyte cross-sectional area and LV interstitial fibrosis are significantly increased in STNx animals.^{47,94} Increases in gene expression of profibrotic (TGF- β , connective tissue growth factor) and hypertrophic (atrial natriuretic peptide, β -myosin heavy chain and α -skeletal muscle actin) markers, as well as TGF- β and p-NF- κ B protein expression are also observed in STNx animals.⁴⁷ In addition the observed cardiac remodelling in this model is associated with a significant increase in cardiac angiotensin-converting enzyme 2 (ACE2) gene expression and ACE2 activity.⁹⁵

Renal effects

Subtotal nephrectomy animals develop hypertension, substantial albuminuria, reduced creatinine clearance and reduced GFR.^{47,96,97} Subtotal nephrectomy leads to significant increases in glomerulosclerosis and tubulointerstitial fibrosis, tubular atrophy and expression of p-Smad2.^{96,97} Significant increases in TGF- β 1 gene expression are observed in STNx animals, which is localized to the sclerotic glomeruli, areas of tubulointerstitial injury and sites of mononuclear cell infiltration observed by *in situ* hybridization.⁹⁸

The above studies clearly indicate that impairment of one organ has detrimental effects on the other, with changes at the functional, biochemical and molecular levels. In an attempt to rapidly progress the dysfunction in both organs, several attempts have been made to combine the two models, as described below.

Combination of MI and STNx models

Subtotal nephrectomy + MI model

Very few attempts of combining these models have been evaluated. One study reports a combined STNx + MI model where STNx animals were maintained for 1 week before MI was induced and animals followed for a further 15 weeks.⁹⁹ In that study, maximal LV pressure was correlated with proteinuria in the STNx + MI compared with STNx + sham-operated animals.⁹⁹ In addition, proteinuria and the incidence of focal glomerulosclerosis were significantly increased in STNx + MI compared with STNx + sham animals.⁹⁹ Another study reported on a combined STNx model (STNx for 2 weeks, followed by MI for a further 10 weeks).¹⁰⁰ In that study, renal blood flow and creatinine clearance were reduced in STNx + MI compared with STNx + sham animals.¹⁰⁰

Myocardial infarction + STNx model

We have recently examined a combined post-MI model, where 4 weeks after MI animals underwent STNx and were followed for a further 10 weeks. The heart weight/BW and lung weight/BW ratios were significantly greater in the MI + STNx compared with MI + sham animals, despite no difference in infarct size between the two groups.¹⁰¹ Fractional shortening and ejection fraction were further reduced in the MI + STNx compared with MI + Sham animals.

Significant increases in cardiomyocyte cross-sectional area and cardiac interstitial fibrosis in the non-infarct zone were observed in the MI + STNx compared with MI + Sham animals. Despite a lower blood pressure in the MI + STNx animals, greater renal interstitial fibrosis in the non-infarct zone was observed compared with MI + Sham animals.¹⁰¹

MANAGEMENT OF CRS

Managing CRS is a major therapeutic challenge in clinical practice because many of the drugs used to control HF can worsen renal function and *vice versa*. Successful drug therapies in the setting of HF have focused on diuretics and key neurohormonal systems activated as part of the pathophysiology of this disease process.¹⁰² In particular, the SNS and RAAS represent key neurohormonal targets.¹⁰²

Diuretics

Diuretic therapy has been a mainstay in the management of acute decompensated HF. It has been used to remove fluid in volume overloaded patients and to maintain normal body fluid volume after this has been achieved.¹⁰³ However, conventional diuretic therapy in CHF can cause electrolyte abnormalities, development of prerenal azotaemia and worsening renal function (Fig. 1). Thiazide diuretics inhibit sodium reabsorption in the distal renal tubule, which causes increased salt and water excretion, decreasing blood volume and decreasing blood pressure. Thiazide diuretics tend to be ineffective in patients with advanced renal failure; thus, loop diuretics are preferred over thiazide diuretics in patients with creatinine clearance < 30 mL/min per 1.73 m².^{104,105} An optimal dose is needed to be titrated in individual patients for the highest efficacy with the least neurohormonal activation, which may occur secondary to diuretic-induced hypovolaemia and renal hypoperfusion.¹⁰⁶ Many patients with CRS become resistant to conventional diuretic treatment, indicated by persistent pulmonary congestion and the need for still higher doses. In this 'diuretic resistant' setting, higher doses of diuretics are needed to achieve effective concentrations in renal tubules when renal function worsens (Fig. 1).¹⁰⁷ However, renal blood flow may be more potently reduced than congestive HF symptoms improved. Higher doses of loop diuretics for patients with HF are suggested to be associated with a high risk of mortality.¹⁰⁸ Thus, worsening diuretic resistance is a powerful predictor in the progression of CRS.

Angiotensin converting enzyme inhibitors

Angiotensin-converting enzyme inhibitors (ACEI) are the first-line treatment for patients with LV systolic dysfunction and they also prevent progressive renal dysfunction in diabetic nephropathy and other forms of CKD.¹⁰⁹ In addition, ACEI inhibit the degradation by angiotensin-converting enzyme (ACE) of bradykinin, an endogenous vasodilator,¹¹⁰ and act on tissue ACE, including in the heart, to exert direct beneficial effects on remodelling. The ACEI are also able to lower blood pressure and reduce cardiac after load and may be used in combination with AngII receptor blockers (ARBs). Unfortunately, in the presence of underlying renal disease, the use of ACEI and other RAAS inhibitors may be associated with increases in creatinine, thereby creating a therapeutic dilemma.¹⁰⁹ Patients with renal artery stenosis and CKD are at a higher risk of developing renal dys-

function in response to the introduction of ACEI and/or ARBs. In addition, ACEI and ARBs cause potassium retention; thus, CKD patients are advised to restrict dietary sodium and potassium.¹¹¹

Angiotensin receptor blockers

The effects of AngII include vasoconstriction, sodium reabsorption, SNS stimulation, aldosterone secretion and inhibition of renin synthesis and these effects are mediated through the angiotensin AT₁ receptor.¹¹² The ARBs act differently to ACEI and inhibit these effects of AngII by preventing it from binding to its receptor. The ARBs are mainly used in the treatment of hypertension, diabetic nephropathy and congestive HF.¹¹³

Mineralocorticoid receptor antagonists

Mineralocorticoid receptor antagonists play an important role in the management of CHF.¹¹⁴ The selective mineralocorticoid receptor antagonist eplerenone improved mortality in patients with mild LV systolic dysfunction and postacute myocardial infarction HF.^{115,116} However, hyperkalaemia is a major concern in patients with reduced estimated GFR receiving mineralocorticoid antagonists for HF.¹⁰⁶

Beta-blockers

Beta-blockers are recommended in the treatment of hypertension and systolic CHF.^{117,118} They act by suppressing the action of endogenous catecholamines, released by the SNS, on β -adrenoceptors. The magnitude of the prognostic benefit conferred by beta-blockers appear to be similar to those of ACEI in patients with systolic CHF.¹¹⁸ The Cardiac Insufficiency Bisoprolol Study II investigated bisoprolol, a highly selective β_1 -adrenoceptor antagonist, which is found to be effective in patients with HF and concomitant renal dysfunction.^{119,120}

Treatment for the accumulation of uraemic toxins

Two major therapeutic options exist to minimize the detrimental effects of uraemic toxins: (i) to reduce the concentrations of protein-bound uraemic toxins; and (ii) to neutralize their toxic effects by pharmacological strategies.¹²¹ Prolonged dialysis time and/or increasing the treatment frequency or using higher permeability membranes may offer benefits to enhance uraemic toxin removal.^{121–124} AST-120, an oral charcoal adsorbant, shows a strong adsorptive ability for uraemic toxins that are known to accumulate in patients with CKD and are believed to accelerate renal dysfunction.¹²⁵ Treatment with AST-120 reduces circulating levels of uraemic toxins such as indoxyl sulphate, as well as serum creatinine and proteinuria, in animals with CKD.⁴⁷ Serum indoxyl sulphate is reduced by 79% with AST-120 treatment; this is accompanied by a significant reduction in LV fibrosis as well as cardiac TGF- β and p-NF- κ B protein expression.⁴⁷ AST-120 is approved for use in Japan to prolong the time to dialysis therapy and improve uraemic symptoms in patients with CKD.¹²⁵ In patients with moderate to severe CKD, AST-120 reduces serum indoxyl sulphate levels, but it does not directly affect serum creatinine or urine creatinine levels.¹²⁵

In addition to enhancing uraemic toxin removal, another option is to alleviate the toxic effects using currently applied pharmacological

strategies, such as ACEI, ARBs, beta-blockers and many others.¹²¹ In cell culture, we have observed that indoxyl sulphate significantly increases neonatal rat cardiac myocyte hypertrophy and fibroblast collagen synthesis in a clinically relevant concentration range.⁴⁵ These effects are due, in part, to activation of p38 MAPK, p42/44 MAPK and NF- κ B pathways.⁴⁵ Organic anion transporters 1 and 3 play an important role in the transcellular transport of indoxyl sulphate in both cardiac and renal cells.^{126,127} Administration of indoxyl sulphate to animals with CKD has resulted in indoxyl sulphate being detected in the proximal and distal tubules where organic anion transporters 1 and 3 have been localized.¹²⁷ The effects of indoxyl sulphate uptake in cardiac myocytes and fibroblasts, as well as in proximal tubular cells, are inhibited by probenecid and cilastatin, organic anion transport 1 and 3 inhibitors.^{126,127} Other potential pathways activated by uraemic toxins should be explored and novel therapeutic targets could be identified for the amelioration of the CRS in comorbid CHF and CKD.

CONCLUSIONS

Despite the growing recognition of CRS, its underlying pathophysiology is not well understood. Therefore, recognition of pathophysiological interactions between the heart and kidney during dysfunction of either one organ or both organs has important clinical implications. Early diagnosis is critical for the effective management of CRS. There have been several novel therapeutic strategies that target CRS directly, such as selective adenosine A₁ receptor blockers, natriuretic peptides, vasopressin antagonists, soluble guanylate cyclase activators, ultrafiltration and many others. Ongoing clinical trials of these potential pharmacological agents will clarify their safety and efficacy in the management of CRS. Finally, targeting uraemic toxins that may have cardiac and renal effects may provide therapeutic benefit complementary to the above approaches.

REFERENCES

- Berl T, Henrich W. Kidney–heart interactions. Epidemiology, pathogenesis, and treatment. *Clin. J. Am. Soc. Nephrol.* 2006; **1**: 8–18.
- Bock JS, Gottlieb SS. Cardiorenal syndrome: New perspectives. *Circulation* 2010; **121**: 2592–600.
- Ronco C, Haapio M, House AA, Anavekar N, Bellomo R. Cardiorenal syndrome. *J. Am. Coll. Cardiol.* 2008; **52**: 1527–39.
- Tyralla K, Amann K. Cardiovascular changes in renal failure. *Blood Purif.* 2002; **20**: 462–5.
- Shulman N, Ford C, Hall W *et al.* Prognostic value of serum creatinine and effect of treatment of hypertension on renal function. Results from the Hypertension Detection and Follow-up Program. The Hypertension Detection and Follow-up Program Cooperative Group. *Hypertension* 1989; **13** (Suppl.): I80–93.
- Go AS, Chertow GM, Fan D, McCulloch CE, Hsu C-Y. Chronic kidney disease and the risks of death, cardiovascular events, and hospitalization. *N. Engl. J. Med.* 2004; **351**: 1296–305.
- Hillege HL, Girbes ARJ, de Kam PJ *et al.* Renal function, neurohormonal activation, and survival in patients with chronic heart failure. *Circulation* 2000; **102**: 203–10.
- Dries DL, Exner DV, Domanski MJ, Greenberg B, Stevenson LW. The prognostic implications of renal insufficiency in asymptomatic and symptomatic patients with left ventricular systolic dysfunction. *J. Am. Coll. Cardiol.* 2000; **35**: 681–9.
- Hillege HL, Nitsch D, Pfeiffer MA *et al.* Renal function as a predictor of outcome in a broad spectrum of patients with heart failure. *Circulation* 2006; **113**: 671–8.
- Sobotka P, Mahfoud F, Schlaich M, Hoppe U, Bohm M, Krum H. Sympatho-renal axis in chronic disease. *Clin. Res. Cardiol.* 2011; Epub June 19, 2011; doi:10.1007/s00392-011-0335-y.
- DiBona GF. Physiology in perspective: The wisdom of the body. Neural control of the kidney. *Am. J. Physiol. Regul. Integr. Comp. Physiol.* 2005; **289**: R633–41.
- Esler M. The Carl Ludwig Lecture. Pathophysiology of the human sympathetic nervous system in cardiovascular diseases: The transition from mechanisms to medical management. *J. Appl. Physiol.* 2010; **108**: 227–37.
- Krum H, Schlaich M, Whitbourn R *et al.* Catheter-based renal sympathetic denervation for resistant hypertension: A multicentre safety and proof-of-principle cohort study. *Lancet* 2009; **373**: 1275–81.
- Schlaich MP, Sobotka PA, Krum H, Lambert E, Esler MD. Renal sympathetic-nerve ablation for uncontrolled hypertension. *N. Engl. J. Med.* 2009; **361**: 932–4.
- Schlaich MP, Straznicki N, Grima M *et al.* Renal denervation: A potential new treatment modality for polycystic ovary syndrome? *J. Hypertens.* 2011; **29**: 991–6.
- Mahfoud F, Schlaich M, Kindermann I *et al.* Effect of renal sympathetic denervation on glucose metabolism in patients with resistant hypertension. *Circulation* 2011; **123**: 1940–6.
- Esler M, Krum H, Sobotka P, Schlaich M, Schneider R, Bohm M. Renal sympathetic denervation in patients with treatment-resistant hypertension (The Symplicity HTN-2 Trial): A randomised controlled trial. *Lancet* 2010; **376**: 1904–9.
- Brewster UC, Setaro JF, Perazella MA. The renin–angiotensin–aldosterone system. Cardiorenal effects and implications for renal and cardiovascular disease states. *Am. J. Med. Sci.* 2004; **326**: 15–24.
- Brewster UC, Perazella MA. Cardiorenal effects of the renin–angiotensin–aldosterone system. *Hosp. Physician* 2004; **40**: 11–26.
- Hori M, Nishida K. Oxidative stress and left ventricular remodelling after myocardial infarction. *Cardiovasc. Res.* 2009; **81**: 457–64.
- Galle J. Oxidative stress in chronic renal failure. *Nephrol. Dial. Transplant.* 2001; **16**: 2135–7.
- Nakamura K, Fushimi K, Kouchi H *et al.* Inhibitory effects of antioxidants on neonatal rat cardiac myocyte hypertrophy induced by tumor necrosis factor- α and angiotensin II. *Circulation* 1998; **98**: 794–9.
- Liu Q, Sargent MA, York AJ, Molkentin JD. ASK1 regulates cardiomyocyte death but not hypertrophy in transgenic mice. *Circ. Res.* 2009; **105**: 1110–7.
- Ichijo H, Nishida E, Irie K *et al.* Induction of apoptosis by ASK1, a mammalian MAPKKK that activates SAPK/JNK and p38 signaling pathways. *Science* 1997; **275**: 90–4.
- See F, Thomas W, Way K *et al.* P38 mitogen-activated protein kinase inhibition improves cardiac function and attenuates left ventricular remodeling following myocardial infarction in the rat. *J. Am. Coll. Cardiol.* 2004; **44**: 1679–89.
- Hirotsu S, Otsu K, Nishida K *et al.* Involvement of nuclear factor- κ B and apoptosis signal-regulating kinase 1 in G-protein-coupled receptor agonist-induced cardiomyocyte hypertrophy. *Circulation* 2002; **105**: 509–15.
- Yamaguchi O, Higuchi Y, Hirotsu S *et al.* Targeted deletion of apoptosis signal-regulating kinase 1 attenuates left ventricular remodeling. *Proc. Natl. Acad. Sci.* 2004; **100**: 15883–8.
- Sutton MG, Sharpe N. Left ventricular remodeling after myocardial infarction: Pathophysiology and therapy. *Circulation* 2000; **101**: 2981–8.
- Guillen I, Blanes M, Gomez-Lechon MJ, Castell JV. Cytokine signaling during myocardial infarction. Sequential appearance of IL-1 beta and IL-6. *Am. J. Physiol.* 1995; **269**: R229–35.
- Bozkurt B, Kribbs SB, Clubb FJ Jr *et al.* Pathophysiologically relevant concentrations of tumor necrosis factor- α promote progressive left ventricular dysfunction and remodeling in rats. *Circulation* 1998; **97**: 1382–91.

31. Kelly KJ. Distant effects of experimental renal ischemia/reperfusion injury. *J. Am. Soc. Nephrol.* 2004; **14**: 1549–58.
32. Raine AE. Hypertension and the kidney. *Br. Med. Bull.* 1994; **50**: 322–41.
33. Levy D, Garrison R, Savage D, Kannel W, Castelli W. Left ventricular mass and incidence of coronary heart disease in an elderly cohort: The Framingham Heart Study. *Ann. Intern. Med.* 1989; **110**: 101–7.
34. Sarnak MJ, Levey AS, Schoolwerth AC *et al.* Kidney disease as a risk factor for development of cardiovascular disease: A statement from the American Heart Association Councils on kidney in cardiovascular disease, high blood pressure research, clinical cardiology, and epidemiology and prevention. *Hypertension* 2004; **42**: 1050–65.
35. Meredith PA, Ostergren J. From hypertension to heart failure: Are there better primary prevention strategies? *J. Renin Angiotensin Aldosterone Syst.* 2006; **7**: 64–73.
36. Silverberg D, Wexler D, Blum M, Wollman Y, Iaina A. The cardio-renal anaemia syndrome: Does it exist? *Nephrol. Dial. Transplant.* 2004; **18** (Suppl. 8): viii7–12.
37. Silverberg D, Wexler D, Iaina A, Steinbruch S, Wollman Y, Schwartz D. Anemia, chronic renal disease and congestive heart failure: The cardio renal anemia syndrome. The need for cooperation between cardiologists and nephrologists. *Int. Urol. Nephrol.* 2006; **38**: 295–310.
38. Grune T, Sommerburg O, Siems W. Oxidative stress in anemia. *Clin. Nephrol.* 2000; **53** (Suppl. 1): 18–22.
39. Palazzuoli A, Gallotta M, Loving F, Nuti R, Siverberg D. Anaemia in heart failure: A common interaction with renal insufficiency called the cardio-renal anaemia syndrome. *Int. J. Clin. Pract.* 2008; **62**: 281–6.
40. Jie KE, Verhaar MC, Cramer M-JM *et al.* Erythropoietin and the cardiorenal syndrome: Cellular mechanisms on the cardiorenal connectors. *Am. J. Physiol.* 2006; **291**: F932–44.
41. Dhondt A, Vanholder R, Van Biesen W, Lameire N. The removal of uremic toxins. *Kidney Int.* 2000; **58** (Suppl. 76): 47–59.
42. Iyngkaran P, Tuck KL, Ma J *et al.* Do all protein bound renal toxins exert physiological effects on cardiac cells? *Heart Lung Circ.* 2009; **18** (Suppl. 3): S250–1 (Abstract).
43. Niwa T, Ise M. Indoxyl sulfate, a circulating uremic toxin, stimulates the progression of glomerular sclerosis. *J. Lab. Clin. Med.* 1994; **124**: 96–104.
44. Vanholder R, De Smet R, Glorieux G *et al.* Review on uremic toxins: Classification, concentration, and interindividual variability. *Kidney Int.* 2004; **63**: 1934–44.
45. Lekawanvijit S, Adrahtas A, Kelly DJ, Kompa AR, Wang BH, Krum H. Does indoxyl sulfate, a uraemic toxin, have direct effects on cardiac fibroblasts and myocytes? *Eur. Heart J.* 2010; **31**: 1771–9.
46. Miyazaki T, Ise M, Seo H, Niwa T. Indoxyl sulfate increases the gene expressions of TGF-beta 1, TIMP-1 and pro-alpha 1(I) collagen in uremic rat kidneys. *Kidney Int. Suppl.* 1997; **62**: S15–22.
47. Lekawanvijit S, Kompa A, Manabe M, Kelly DJ, Krum H. Chronic kidney disease-induced cardiac fibrosis is ameliorated by reducing circulating levels of a non-dialysable uremic toxin, indoxyl sulfate. *J. Am. Coll. Cardiol.* 2011; **57** (Suppl.): E192 (Abstract).
48. Jourde-Chiche N, Dou L, Cerini C, Dignat-George F, Brunet P. Vascular incompetence in dialysis patients: Protein-bound uremic toxins and endothelial dysfunction. *Semin. Dial.* 2011; **24**: 327–37.
49. Mak R. Insulin and its role in chronic kidney disease. *Pediatr. Nephrol.* 2008; **23**: 355–62.
50. Leone A, Moncada S, Vallance P, Calver A, Collier J. Accumulation of an endogenous inhibitor of nitric oxide synthesis in chronic renal failure. *Lancet* 1992; **339**: 572–5.
51. Zoccali C, Bode-Boger SM, Mallamaci F *et al.* Plasma concentration of asymmetrical dimethylarginine and mortality in patients with end-stage renal disease: A prospective study. *Lancet* 2001; **358**: 2113–7.
52. Scalera F, Borlak J, Beckmann B *et al.* Endogenous nitric oxide synthesis inhibitor asymmetric dimethyl L-arginine accelerates endothelial cell senescence. *Arterioscler. Thromb. Vasc. Biol.* 2004; **24**: 1816–22.
53. Chambers JC, McGregor A, Jean-Marie J, Obeid OA, Kooner JS. Demonstration of rapid onset vascular endothelial dysfunction after hyperhomocysteinemia: An effect reversible with vitamin C therapy. *Circulation* 1999; **99**: 1156–60.
54. Meijers BKJ, Van kerckhoven S, Verbeke K *et al.* The uremic retention solute *p*-cresyl sulfate and markers of endothelial damage. *Am. J. Kidney Dis.* 2009; **54**: 891–901.
55. Dou L, Jourde-Chiche N, Faure V *et al.* The uremic solute indoxyl sulfate induces oxidative stress in endothelial cells. *J. Thromb. Haemost.* 2007; **5**: 1302–8.
56. Brown RD, Ambler SK, Mitchell MD, Long CS. The cardiac fibroblast: Therapeutic target in myocardial remodeling and failure. *Annu. Rev. Pharmacol. Toxicol.* 2005; **45**: 657–87.
57. Warren SE, Royal HD, Markis JE, Grossman W, McKay RG. Time course of left ventricular dilation after myocardial infarction: Influence of infarct-related artery and success of coronary thrombolysis. *J. Am. Coll. Cardiol.* 1988; **11**: 12–9.
58. Frey N, Olson EN. Cardiac hypertrophy: The good, the bad, and the ugly. *Annu. Rev. Physiol.* 2004; **65**: 45–79.
59. Cleutjens JPM, Kandala JC, Guarda E, Guntaka RV, Weber KT. Regulation of collagen degradation in the rat myocardium after infarction. *J. Mol. Cell. Cardiol.* 1995; **27**: 1281–92.
60. Peterson JT, Li H, Dillon L, Bryant JW. Evolution of matrix metalloprotease and tissue inhibitor expression during heart failure progression in the infarcted rat. *Cardiovasc. Res.* 2000; **46**: 307–15.
61. Cleutjens JP, Verluyten MJ, Smiths JF, Daemen MJ. Collagen remodeling after myocardial infarction in the rat heart. *Am. J. Pathol.* 1995; **147**: 325–38.
62. Sun Y, Zhang JQ, Zhang J, Ramires FJA. Angiotensin II, transforming growth factor-beta1 and repair in the infarcted heart. *J. Mol. Cell. Cardiol.* 1998; **30**: 1559–69.
63. See F, Kompa A, Jennifer M, Lewis DA, Krum H. Fibrosis as a therapeutic target post-myocardial infarction. *Curr. Pharm. Des.* 2005; **11**: 477–87.
64. Gross M-L, Ritz E. Non-coronary heart disease in dialysis patients. Hypertrophy and fibrosis in the cardiomyopathy of uremia: Beyond coronary heart disease. *Semin. Dial.* 2008; **21**: 308–18.
65. Foley RN, Parfrey PS, Hamett JD *et al.* Clinical and echocardiographic disease in patients starting end-stage renal disease therapy. *Kidney Int.* 1995; **47**: 186–92.
66. Díez J. Mechanisms of cardiac fibrosis in hypertension. *J. Clin. Hypertens.* 2007; **9**: 546–50.
67. Bakth S, Arena J, Lee W *et al.* Arrhythmia susceptibility and myocardial composition in diabetes. Influence of physical conditioning. *J. Clin. Invest.* 1986; **77**: 382–95.
68. Liu Y. Renal fibrosis: New insights into the pathogenesis and therapeutics. *Kidney Int.* 2006; **69**: 213–7.
69. Hewitson TD. Renal tubulointerstitial fibrosis: Common but never simple. *Am. J. Physiol. Renal Physiol.* 2009; **296**: F1239–44.
70. Pozzi A, Voziyan PA, Hudson BG, Zent R. Regulation of matrix synthesis, remodeling and accumulation in glomerulosclerosis. *Curr. Pharm. Des.* 2009; **15**: 1318–34.
71. Fine LG, Bandyopadhyay D, Norman JT. Is there a common mechanism for the progression of different types of renal diseases other than proteinuria? Towards the unifying theme of chronic hypoxia. *Kidney Int.* 2000; **57** (Suppl. 75): S22–6.
72. Levin A. The relationship of haemoglobin level and survival: Direct or indirect effects? *Nephrol. Dial. Transplant.* 2002; **17** (Suppl. 5): 8–13.
73. Keane WF, Brenner BM, De Zeeuw D *et al.* The risk of developing end-stage renal disease in patients with type 2 diabetes and nephropathy: The RENAAL Study. *Kidney Int.* 2004; **63**: 1499–507.
74. Bansal N, Tighiouart H, Weiner D *et al.* Anemia as a risk factor for kidney function decline in individuals with heart failure. *Am. J. Cardiol.* 2007; **99**: 1137–42.
75. Shlipak MG. Pharmacotherapy for heart failure in patients with renal insufficiency. *Ann. Intern. Med.* 2004; **138**: 917–24.

76. Smith GL, Vaccarino V, Kosiborod M *et al.* Worsening renal function: What is a clinically meaningful change in creatinine during hospitalization with heart failure? *J. Card. Fail.* 2004; **9**: 13–25.
77. Lekawanvijit S, Kompa A, Zhang Y, Wang BH, Kelly DJ, Krum H. Myocardial infarction impairs renal function, induces renal interstitial fibrosis and increases Kim-1 expression: Implications for the cardiorenal syndrome. *Circulation* 2009; **120** (Suppl.): S1076 (Abstract).
78. Martin FL, Huntley BK, Harders GE, Sandberg SM, Chen HH, Burnett JC. Myocardial infarction mediates renal fibrosis and activates renal molecular remodeling in the absence of heart failure. *Circulation* 2007; **116** (Suppl.): II60.
79. Tang WHW, Francis GS, Morrow DA *et al.* National academy of clinical biochemistry laboratory medicine practice guidelines: Clinical utilization of cardiac biomarker testing in heart failure. *Circulation* 2007; **116**: E99–109.
80. Cruz D, Soni S, Slavin L, Ronco C, Maisel A. Biomarkers of cardiac and kidney dysfunction in cardiorenal syndromes. *Contrib. Nephrol.* 2010; **165**: 83–92.
81. Talwar S, Squire IB, Downie PF, O'Brien RJ, Davies JE, Ng LL. Elevated circulating cardiotrophin-1 in heart failure: Relationship with parameters of left ventricular systolic dysfunction. *Clin. Sci.* 2000; **99**: 83–8.
82. Ng LL, O'Brien RJ, Demme B, Jennings S. Non-competitive immunochemiluminometric assay for cardiotrophin-1 detects elevated plasma levels in human heart failure. *Clin. Sci.* 2002; **102**: 411–6.
83. Weinberg EO, Shimp M, De Keulenaer GW *et al.* Expression and regulation of ST2, an interleukin-1 receptor family member, in cardiomyocytes and myocardial infarction. *Circulation* 2002; **106**: 2961–6.
84. de Boer RA, Voors AA, Muntendam P, van Gilst WH, van Veldhuisen DJ. Galectin-3: A novel mediator of heart failure development and progression. *Eur. J. Heart Fail.* 2009; **11**: 811–7.
85. Herget-Rosenthal S, Bökenkamp A, Hofmann W. How to estimate GFR-serum creatinine, serum cystatin C or equations? *Clin. Biochem.* 2007; **40**: 153–61.
86. Bagshaw S, Gibney R. Conventional markers of kidney function. *Crit. Care Med.* 2008; **36** (Suppl. 4): S152–8.
87. Dhamidharka VR, Kwon C, Stevens G. Serum cystatin C is superior to serum creatinine as a marker of kidney function: A meta-analysis. *Am. J. Kidney Dis.* 2002; **40**: 221–6.
88. Mishra J, Ma Q, Prada A *et al.* Identification of neutrophil gelatinase-associated lipocalin as a novel early urinary biomarker for ischemic renal injury. *J. Am. Soc. Nephrol.* 2004; **14**: 2534–43.
89. Han WK, Bailly V, Abichandani R, Thadhani R, Bonventre JV. Kidney injury molecule-1 (KIM-1): A novel biomarker for human renal proximal tubule injury. *Kidney Int.* 2002; **62**: 237–44.
90. Ichimura T, Hung CC, Yang SA, Stevens JL, Bonventre JV. Kidney injury molecule-1: A tissue and urinary biomarker for nephrotoxicant-induced renal injury. *Am. J. Physiol. Renal Physiol.* 2004; **286**: F552–63.
91. Tan SM, Zhang Y, Connelly KA, Gilbert RE, Kelly DJ. Targeted inhibition of activin receptor-like kinase 5 signaling attenuates cardiac dysfunction following myocardial infarction. *Am. J. Physiol. Heart Circ. Physiol.* 2010; **298**: H1415–25.
92. Pfeffer MA, Pfeffer JM, Fishbein MC *et al.* Myocardial infarct size and ventricular function in rats. *Circ. Res.* 1979; **44**: 503–12.
93. Gaballa MA, Goldman S. Ventricular remodeling in heart failure. *J. Card. Fail.* 2004; **8** (Suppl. 6): S476–85.
94. Suzuki H, Schaefer L, Ling H *et al.* Prevention of cardiac hypertrophy in experimental chronic renal failure by long-term ACE inhibitor administration: Potential role of lysosomal proteinases. *Am. J. Nephrol.* 1995; **15**: 129–36.
95. Burchill L, Velkoska E, Dean RG *et al.* Acute kidney injury in the rat causes cardiac remodelling and increases angiotensin-converting enzyme 2 expression. *Exp. Physiol.* 2008; **93**: 622–30.
96. Kelly DJ, Zhang Y, Gow R, Gilbert RE. Tranilast attenuates structural and functional aspects of renal injury in the remnant kidney model. *J. Am. Soc. Nephrol.* 2004; **15**: 2619–29.
97. Kelly DJ, Zhang Y, Cox AJ, Gilbert RE. Combination therapy with tranilast and angiotensin-converting enzyme inhibition provides additional renoprotection in the remnant kidney model. *Kidney Int.* 2006; **69**: 1954–60.
98. Wu LL, Cox A, Roe CJ, Dziadek M, Cooper ME, Gilbert RE. Transforming growth factor beta1 and renal injury following subtotal nephrectomy in the rat: Role of the renin–angiotensin system. *Kidney Int.* 1997; **51**: 1553–67.
99. Van Dokkum RPE, Eijkelkamp WBA, Kluppel ACA *et al.* Myocardial infarction enhances progressive renal damage in an experimental model for cardio-renal interaction. *J. Am. Soc. Nephrol.* 2004; **15**: 3103–10.
100. Windt WAKM, Henning RH, Kluppel ACA, Xu Y, de Zeeuw D, van Dokkum RPE. Myocardial infarction does not further impair renal damage in 5/6 nephrectomized rats. *Nephrol. Dial. Transplant.* 2008; **23**: 3103–10.
101. Liu S, Kompa A, Kelly D, Krum H, Wang B. Combined subtotal nephrectomy and myocardial infarction accelerates heart and kidney disease: A new model of the cardiorenal syndrome. *Heart Lung Circ.* 2011; **20** (Suppl. 2): S61–2 (Abstract).
102. Sata Y, Krum H. The future of pharmacological therapy for heart failure. *Circ. J.* 2010; **74**: 809–17.
103. Krum H, Cameron P. Diuretics in the treatment of heart failure: Mainstay of therapy or potential hazard? *J. Card. Fail.* 2006; **12**: 333–5.
104. Attanasio P, Ronco C, Anker M, Ponikowski P, Anker S. Management of chronic cardiorenal syndrome. *Contrib. Nephrol.* 2010; **165**: 129–39.
105. Fliser D, Schroter M, Neubeck M, Ritz E. Coadministration of thiazides increases the efficacy of loop diuretics even in patients with advanced renal failure. *Kidney Int.* 1994; **46**: 482–8.
106. Krum H, Iyngkaran P, Lekawanvijit S. Pharmacologic management of the cardiorenal syndrome in heart failure. *Curr. Heart Fail. Rep.* 2009; **6**: 105–11.
107. Boerrigter G, Burnett J. Cardiorenal syndrome in decompensated heart failure: Prognostic and therapeutic implications. *Curr. Heart Fail. Rep.* 2004; **1**: 113–20.
108. Eshaghian S, Horwich TB, Fonarow GC. Relation of loop diuretic dose to mortality in advanced heart failure. *Am. J. Cardiol.* 2006; **97**: 1759–64.
109. Shlipak MG, Massie BM. The clinical challenge of cardiorenal syndrome. *Circulation* 2004; **110**: 1514–7.
110. Fleming I. Signaling by the angiotensin-converting enzyme. *Circ. Res.* 2006; **98**: 887–96.
111. Cano N, Fiaccadori E, Tesinsky P *et al.* ESPEN guidelines on enteral nutrition: Adult renal failure. *Clin. Nutr.* 2006; **25**: 295–310.
112. Siragy H. AT₁ and AT₂ receptors in the kidney: Role in disease and treatment. *Am. J. Kidney Dis.* 2000; **36** (Suppl. 1): S4–9.
113. Willenheimer R, Dahlöf B, Rydberg E, Erhardt L. AT₁-receptor blockers in hypertension and heart failure. Clinical experience and future directions. *Eur. Heart J.* 1999; **20**: 997–1008.
114. Pitt B, Zannad F, Remme WJ *et al.* The effect of spironolactone on morbidity and mortality in patients with severe heart failure. *N. Engl. J. Med.* 1999; **341**: 709–17.
115. Pitt B, Remme W, Zannad F *et al.* Eplerenone, a selective aldosterone blocker, in patients with left ventricular dysfunction after myocardial infarction. *N. Engl. J. Med.* 2004; **348**: 1309–21.
116. Zannad F, McMurray JJV, Krum H *et al.* Eplerenone in patients with systolic heart failure and mild symptoms. *N. Engl. J. Med.* 2011; **364**: 11–21.
117. Bangalore S, Messerli FH, Kostis JB, Pepine CJ. Cardiovascular protection using beta-blockers: A critical review of the evidence. *J. Am. Coll. Cardiol.* 2007; **50**: 563–72.
118. Krum H, Haas SJ, Eichhorn E *et al.* Prognostic benefit of beta-blockers in patients not receiving ACE-inhibitors. *Eur. Heart J.* 2005; **26**: 2154–8.
119. CIBIS-II Investigators and Committees. The Cardiac Insufficiency Bisoprolol Study II (CIBIS-II): A randomised trial. *Lancet* 1999; **353**: 9–13.

120. Castagno D, Jhund PS, McMurray JJV *et al.* Improved survival with bisoprolol in patients with heart failure and renal impairment: An analysis of the Cardiac Insufficiency Bisoprolol Study II (CIBIS-II) trial. *Eur. J. Heart Fail.* 2010; **12**: 607–16.
121. Vanholder R, Baurmeister U, Brunet P *et al.* A bench to bedside view of uremic toxins. *J. Am. Soc. Nephrol.* 2008; **19**: 863–70.
122. Eloot S, Van Biesen W, Dhondt A *et al.* Impact of hemodialysis duration on the removal of uremic retention solutes. *Kidney Int.* 2007; **73**: 765–70.
123. Fagugli RM, De Smet R, Buoncristiani U, Lameire N, Vanholder R. Behavior of non-protein-bound and protein-bound uremic solutes during daily hemodialysis. *Am. J. Kidney Dis.* 2002; **40**: 339–47.
124. Mucci I, Hercz G, Uldall R, Ouwendyk M, Francoeur R, Pierratos A. Control of serum phosphate without any phosphate binders in patients treated with nocturnal hemodialysis. *Kidney Int.* 1998; **53**: 1399–404.
125. Schulman G, Agarwal R, Acharya M, Berl T, Blumenthal S, Kopyt N. A multicenter, randomized, double-blind, placebo-controlled, dose-ranging study of AST-120 (kremezin) in patients with moderate to severe CKD. *Am. J. Kidney Dis.* 2006; **47**: 565–77.
126. Liu S, Lekawanvijit S, Xu G, Kompa A, Krum H, Wang B. Organic ion transporters ameliorate the adverse cardiac effects of the non-dialysable uremic toxin indoxyl sulphate in cardiac cell culture. Implications for the treatment of the cardiorenal syndrome. *Heart Lung Circ.* 2010; **19** (Suppl. 2): S77 (Abstract).
127. Enomoto A, Takeda M, Tojo A *et al.* Role of organic anion transporters in the tubular transport of indoxyl sulfate and the induction of its nephrotoxicity. *J. Am. Soc. Nephrol.* 2002; **13**: 1711–20.

Appendix 2: Antagonists of organic anion transporters 1 and 3 ameliorate adverse cardiac remodelling induced by uremic toxin indoxyl sulfate

This peer reviewed article was written in the second PhD year and has been published in the *International Journal of Cardiology* 2012; 158(3): 457-458. The paper in a PDF format was enclosed.

scaffold: 6 months and 1 year follow-up assessment. A virtual histology intravascular ultrasound study from the first In man, ABSORB Cohort B Trial. JACC Cardiovasc Interv in press.

- [4] Costa MA, Angiolillo DJ, Tannenbaum M, et al. Impact of stent deployment procedural factors on long-term effectiveness and safety of sirolimus-eluting stents (final results of the multicenter prospective STLLR trial). Am J Cardiol 2008;101:1704–11.
- [5] Hoffmann R, Guagliumi G, Musumeci G, et al. Vascular response to sirolimus-eluting stents delivered with a nonaggressive implantation technique: comparison of

intravascular ultrasound results from the multicenter, randomized e-sirius, and sirius trials. Catheter Cardiovasc Interv 2005;66:499–506.

- [6] Gogas BD, Radu M, Onuma Y, et al. Evaluation with in vivo optical coherence tomography and histology of the vascular effects of the everolimus-eluting bioresorbable vascular scaffold at two years following implantation in a healthy porcine coronary artery model: implications of pilot results for future pre-clinical studies. Int J Cardiovasc Imaging 2012;28(3):499–511.
- [7] Coats AJ, Shewan LG. Statement on authorship and publishing ethics in the International Journal of Cardiology. Int J Cardiol Dec 2 2011;153(3):239–40.

0167-5273/\$ – see front matter © 2012 Elsevier Ireland Ltd. All rights reserved.
doi:10.1016/j.ijcard.2012.05.023

Antagonists of organic anion transporters 1 and 3 ameliorate adverse cardiac remodelling induced by uremic toxin indoxyl sulfate

Shan Liu ^a, Bing H. Wang ^a, Andrew R. Kompa ^{a,b}, Suree Lekawanvijit ^a, Henry Krum ^{a,*}

^a Centre for Cardiovascular Research and Education in Therapeutics, Department of Epidemiology and Preventive Medicine, Monash University, Melbourne, Victoria, Australia

^b Department of Medicine, University of Melbourne, St. Vincent's Hospital, Melbourne, Victoria, Australia

ARTICLE INFO

Article history:

Received 11 April 2012

Accepted 4 May 2012

Available online 26 May 2012

Keywords:

Organic anion transporters 1 and 3

Indoxyl sulfate

Cardiac cells

Hypertrophy

Collagen synthesis

Circulating toxins in patients with chronic kidney disease may attenuate cardiac function [1,2]. Specifically, indoxyl sulfate, one such non-dialysable uremic toxin, has direct pro-hypertrophic and pro-fibrotic effects on cardiac myocytes and fibroblasts [3]. This toxin significantly increases neonatal cardiac myocyte hypertrophy and fibroblast collagen synthesis within a clinically relevant concentration range [3]. We sought to determine potential approaches to blockade of indoxyl sulfate-induced cardiac remodelling.

Organic anion transporters 1 and 3 play an important role in the trans-cellular uptake of indoxyl sulfate in renal cells [4]. Administration of indoxyl sulfate to animals with chronic kidney disease results in indoxyl sulfate being detected in the proximal and distal tubules of the kidney where organic anion transporters 1 and 3 have been localized [4]. We therefore hypothesized that antagonists of organic anion transporters 1 and 3 would suppress indoxyl sulfate-induced cardiac myocyte hypertrophy and fibroblast collagen synthesis, which contribute to pathological cardiac remodelling.

Sprague–Dawley neonatal cardiac myocytes and fibroblasts were isolated and cultured, as described previously [3]. Organic anion transporters 1 and 3 antagonists (probenecid and cilastatin, respectively) were co-cultured at increasing doses for 48 h with indoxyl sulfate (10 μ M) in cardiac myocytes and fibroblasts. ³H-leucine and ³H-proline incorporation were used to assess myocyte hypertrophy and collagen turnover, respectively. 3-(4,5-Dimethylthiazol-2-yl)-2,5-diphenyltetrazolium bromide assay was used to determine cell viability, as described previously [3].

Stimulation of cells with indoxyl sulfate caused a 21.0% increase in cardiac myocyte hypertrophy and 15.5% increase in collagen synthesis, compared with unstimulated cells ($p < 0.001$ and $p < 0.001$ respectively) (Fig. 1). Co-administration of organic anion transporter 1 and 3 antagonists, probenecid and cilastatin, at concentrations ranging from 0.1 to 100 μ M inhibited indoxyl sulfate-stimulated myocyte hypertrophy in a dose-dependent manner (Fig. 1A). Probenecid and cilastatin also attenuated the increases in indoxyl sulfate-stimulated collagen synthesis, again, in a dose-dependent manner (Fig. 1B). Probenecid appeared to be more potent in inhibiting collagen synthesis compared to cilastatin. These findings indicate that organic anion transporters 1 and 3 may be involved in indoxyl sulfate-induced cardiac effects.

Hypertrophy and fibrosis are major contributors to cardiac remodelling, leading to heart failure. In this study, we investigated cardiac cells via an approach to blockade of pro-hypertrophic and pro-fibrotic actions of indoxyl sulfate in cardiac myocytes and fibroblasts. Inhibition of organic anion transporters 1 and 3 with probenecid and cilastatin suppressed indoxyl sulfate-activated cardiac myocyte hypertrophy and fibroblast collagen synthesis. These findings occurred in the absence of any significant reduction in cardiac cell viability, as assessed by 3-(4,5-Dimethylthiazol-2-yl)-2,5-diphenyltetrazolium bromide assay. Specifically, indoxyl sulfate did not affect cardiac cell viability at the concentration range from 0.01 to 100 μ M [3]. Furthermore, organic anion transporter 1 and 3 antagonists did not affect cardiac cell viability at the concentrations used in this study.

This *in vitro* study directly evaluates inhibition of indoxyl sulfate-stimulated adverse cardiac effects, in comparison to the *in vivo* setting where many other systems may interfere with the findings. Circulating levels of indoxyl sulfate in chronic kidney disease patients vary from a few micromolars to hundreds of micromolars [5,6]. Thus, the concentration of 10 μ M for indoxyl sulfate-induced cardiac effects falls into the clinical pathophysiological concentration range. Organic anion transporter 1 and 3 antagonists appear to attenuate these effects by blocking the uptake of indoxyl sulfate into cardiac cells. Intervention with other organic anion transporters 1 and 3 inhibitors and/or suppression of downstream intracellular actions post-uptake may be of therapeutic benefit. However, probenecid and cilastatin may have additional, non-specific actions other than as organic anion transporter inhibitors.

In summary, organic anion transporters 1 and 3 appear to play a role in indoxyl sulfate-induced pathological cardiac remodelling, which are suppressed by organic anion transporter 1 and 3 antagonists, in a dose-dependent manner. Reducing circulating indoxyl sulfate levels may represent a potential novel therapeutic strategy to ameliorate

* Corresponding author at: Department of Epidemiology and Preventive Medicine, Level 6, The Alfred Centre, 99 Commercial Road, Melbourne, Victoria 3004, Australia.
E-mail address: [redacted] (H. Krum).

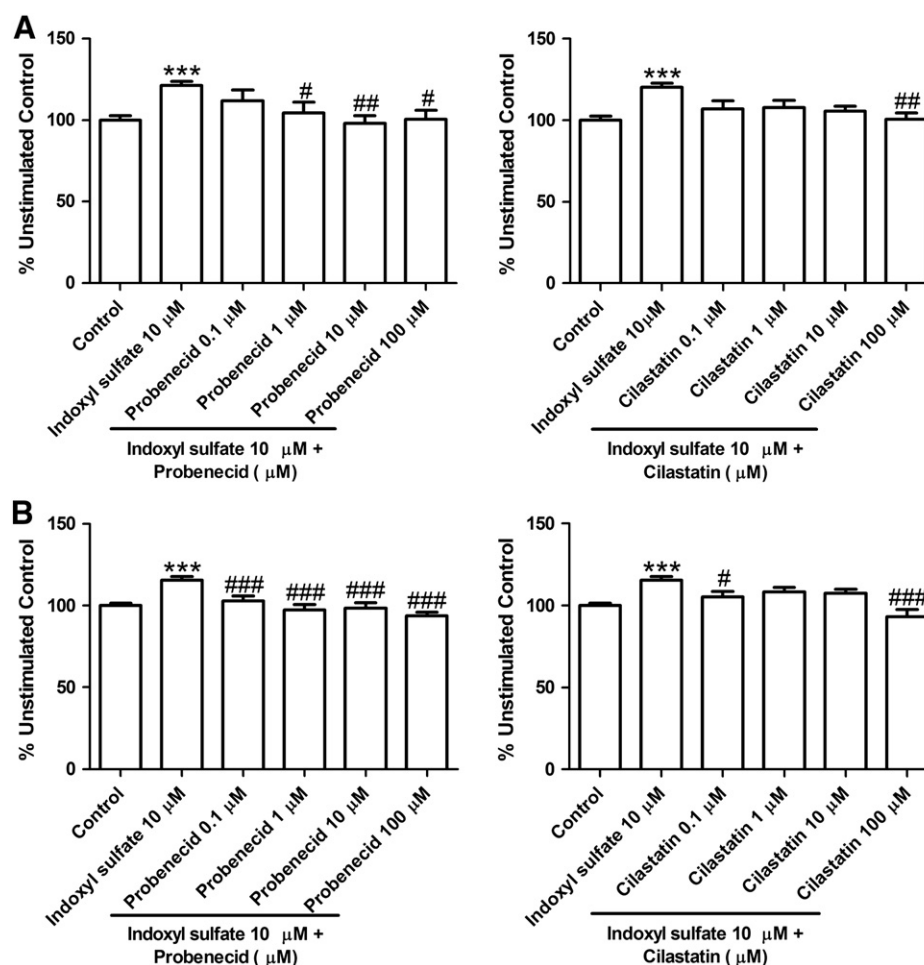


Fig. 1. Inhibition effects of probenecid and cilastatin on indoxyl sulfate-induced myocyte hypertrophy (A) and fibroblast collagen synthesis (B). The stimulation effects of indoxyl sulfate were inhibited by probenecid and cilastatin in a dose-dependent manner, indicating that the effects may be in part via organic anion transporters 1 and 3. Data analyzed by 1-way ANOVA and presented as means \pm SEM from three experiments with triplicates. *** p < 0.001 10 μ M indoxyl sulfate vs. unstimulated control, # p < 0.05 vs. 10 μ M indoxyl sulfate, ## p < 0.01 vs. 10 μ M indoxyl sulfate, ### p < 0.001 vs. 10 μ M indoxyl sulfate.

uremic toxin-stimulated cardiac effects in the setting of co-morbid chronic heart failure and chronic kidney disease.

References

- [1] Fujii H, Nakai K, Fukagawa M. Role of oxidative stress and indoxyl sulfate in progression of cardiovascular disease in chronic kidney disease. *Ther Apher Dial* 2011;15:125–8.
- [2] Niwa T. Role of indoxyl sulfate in the progression of chronic kidney disease and cardiovascular disease: experimental and clinical effects of oral sorbent AST-120. *Ther Apher Dial* 2011;15:120–4.
- [3] Lekawanvijit S, Adrahtas A, Kelly DJ, Kompa AR, Wang BH, Krum H. Does indoxyl sulfate, a uraemic toxin, have direct effects on cardiac fibroblasts and myocytes? *Eur Heart J* 2010;31:1771–9.
- [4] Enomoto A, Takeda M, Tojo A, et al. Role of organic anion transporters in the tubular transport of indoxyl sulfate and the induction of its nephrotoxicity. *J Am Soc Nephrol* 2002;13:1711–20.
- [5] Niwa T, Takeda N, Tatematsu A, Maeda K. Accumulation of indoxyl sulfate, an inhibitor of drug-binding, in uremic serum as demonstrated by internal-surface reversed-phase liquid chromatography. *Clin Chem* 1988;34:2264–7.
- [6] Stanfel LA, Gulyassy PF, Jarrard EA. Determination of indoxyl sulfate in plasma of patients with renal failure by use of ion-pairing liquid chromatography. *Clin Chem* 1986;32:938–42.

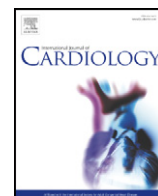
Appendix 3: Subtotal nephrectomy accelerates pathological cardiac remodeling post-myocardial infarction: Implications for cardiorenal syndrome

This peer reviewed article was written in the third PhD year and has been published in the *International Journal of Cardiology* DOI: 10.1016/j.ijcard.2012.12.065. The paper in a PDF format was enclosed.



Contents lists available at SciVerse ScienceDirect

International Journal of Cardiology

journal homepage: www.elsevier.com/locate/ijcard

Subtotal nephrectomy accelerates pathological cardiac remodeling post-myocardial infarction: Implications for cardiorenal syndrome☆☆☆★

Shan Liu^{a,1}, Andrew R. Kompa^{a,b,1}, Sirinart Kumfu^{a,c}, Fuyuhiko Nishijima^d, Darren J. Kelly^b, Henry Krum^{a,*}, Bing H. Wang^a

^a Centre of Cardiovascular Research and Education in Therapeutics, Department of Epidemiology and Preventive Medicine, Monash University, Melbourne, Australia

^b Department of Medicine, University of Melbourne, St. Vincent's Hospital, Melbourne, Australia

^c Department of Physiology, Faculty of Medicine, Chiang Mai University, Chiang Mai, Thailand

^d Pharmaceutical Department, Kureha Corporation, Tokyo, Japan

ARTICLE INFO

Article history:

Received 23 August 2012

Received in revised form 27 November 2012

Accepted 25 December 2012

Available online xxxx

Keywords:

Cardiorenal syndrome

Myocardial infarction

Subtotal nephrectomy

Cardiac remodeling

Renal fibrosis

ABSTRACT

Background: To further understand the pathophysiology of concomitant cardiac and renal dysfunction, we investigated molecular, structural and functional changes in heart and kidney that occur when a kidney insult (5/6 nephrectomy–STNx) follows myocardial infarction (MI).

Methods: Male Sprague Dawley rats (n=43) were randomized into four groups: Sham-operated MI + Sham-operated STNx (Sham + Sham), MI + Sham-operated STNx (MI + Sham), Sham-operated MI + STNx (Sham + STNx) and MI + STNx. MI/Sham surgery was followed by STNx/Sham surgery 4 weeks later. Cardiac and renal function was assessed prior to STNx/Sham surgery and again 10 weeks later. Hemodynamic parameters were measured prior to sacrifice.

Results: Compared to the MI + Sham group, STNx further accelerated the reduction in left ventricular (LV) ejection fraction by 21% (p<0.01), and increased tau logistic by 38% (p<0.01) in MI + STNx animals. Heart weight/body weight (BW) and lung weight/BW ratios were 39% (p<0.001) and 16% (p<0.01) greater in MI + STNx compared to MI + Sham animals. Similarly, myocyte cross-sectional area (p<0.001), cardiac interstitial fibrosis (p<0.01) and collagen I (p<0.01) were increased in the LV non-infarct zone of the myocardium in the MI + STNx group. These changes were associated with significant increases in atrial natriuretic peptide (p<0.001), transforming growth factor β_1 (p<0.05) and collagen I (p<0.05) gene expression in MI + STNx animals. In comparison with the Sham + STNx group, renal tubulointerstitial fibrosis was increased by 64% in MI + STNx animals (p<0.001), with no further deterioration in renal function.

Conclusions: STNx accelerated cardiac changes post-MI whilst MI accelerated STNx-induced renal fibrosis, supporting bidirectional interactions in cardiorenal syndrome (CRS). This animal model may be of use in assessing the impact of therapies to treat CRS.

© 2012 Published by Elsevier Ireland Ltd.

1. Introduction

Renal dysfunction frequently coexists with myocardial infarction (MI) and heart failure (HF), manifesting in the so-called cardiorenal syndrome (CRS) [1]. The prevalence of renal disease in patients with chronic HF (CHF) is approximately 25% [2–4]. The degree of renal dysfunction is a powerful independent risk factor for all-cause mortality in HF patients [3–8]. Studies have indicated that even a slight worsening

of renal function is associated with increased mortality and prolonged hospital stay [9].

The pathophysiology and potential mechanisms underlying CRS are poorly understood. The heart and the kidney exert reciprocal control in maintaining constant blood volume and organ perfusion under continuously changing conditions. A complex combination of hemodynamic, neurohormonal, immunological, biochemical feedback pathways and other unknown factors such as uremic toxins contribute to CRS [10].

In the event of a cardiac insult, such as MI, the ensuing hemodynamic disturbances trigger neurohormonal and pro-inflammatory cytokine activation. Short-term adaptive responses, such as activation of the renin–angiotensin and sympathetic nervous systems, may become maladaptive in the heart and kidney with prolonged activation [11]. Recently, we have demonstrated that progressive renal tubulointerstitial fibrosis occurs post-MI [12]. Kidney injury molecule-1 (KIM-1), a trans-membrane tubular protein, whose expression is observed following

☆ Statement of authorship: This author takes responsibility for all aspects of the reliability and freedom from bias of the data presented and their discussed interpretation.

☆☆ This work was supported by the NHMRC of Australia (program grant no. 546272).

★ No conflicts of interest.

* Corresponding author at: Department of Epidemiology and Preventive Medicine, Level 6 The Alfred Centre, 99 Commercial Road, Melbourne, Vic, 3004, Australia. Tel: +61 3 9903 0042.

E-mail address: h.krum@monash.edu (H. Krum).

¹ Authors contributed equally to the manuscript.

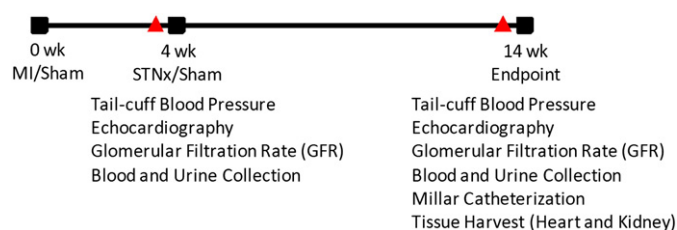


Fig. 1. Experimental design. MI, myocardial infarction; STNx, 5/6 nephrectomy.

kidney injury, also appears to be a sensitive and early marker of post-MI kidney injury [12,13].

Furthermore, in response to MI, inflammatory cells and various cytokines, such as interleukin-6 (IL-6) and tumor necrosis factor- α appear at the site of injury that occur in response to local tissue injury [14]. Although they play a role in stabilization of the infarct, long term, their activation not only contributes to pathological fibrosis [14]. In addition to inflammatory responses, indoxyl sulfate, a non-dialysable uremic toxin, has been demonstrated as a contributory factor in cardiac hypertrophy and fibrosis [15,16]. In a rat model of chronic kidney disease (CKD) induced by 5/6 nephrectomy (STNx), we have demonstrated that cardiac fibrosis correlated closely with indoxyl sulfate plasma levels [17].

A number of experimental rat models with cardiac or renal impairment have been developed [10]. However, very few have attempted to combine elements of cardiac and renal dysfunction as a potential model of CRS [18–22]. Specifically, no study has been performed where MI-induced left ventricular (LV) systolic dysfunction is complicated by the addition of CKD. Given the multiplicity of heart-kidney interactions and lack of systematic investigation of CRS, the present study aimed to establish a new model of MI (induced by left anterior descending coronary ligation) followed by a kidney insult (induced by STNx) in rats. We sought to identify subsequent cardiac and renal changes (molecular, structural and functional) and examine in detail the potential mechanisms that may underlie the changes observed.

2. Methods

2.1. Study design and rat model

Male Sprague Dawley rats ($n=43$) weighing 200–250 g were randomized into four groups: Sham-operated MI + Sham-operated STNx (Sham + Sham), MI + Sham-operated STNx (MI + Sham), Sham-operated MI + STNx (Sham + STNx) and MI + STNx. MI/Sham surgery was induced initially and STNx/Sham surgery performed 4 weeks later (Fig. 1). Systolic blood pressure (BP) was measured using tail cuff plethysmography and cardiac and renal function was assessed as described below prior to STNx/Sham surgery and again 10 weeks later. Hemodynamic parameters were measured prior to sacrifice, tissues

Table 1
Primer sequences used in real-time PCR.

Gene	Primer sequence
TGF β ₁	Forward: 5' CCA GCC GCG GGA CTC T 3' Reverse: 5' TTC CGT TTC ACC AGC TCC AT 3'
cTGF	Forward: 5' GCG GCG AGT CCT TCC AA 3' Reverse: 5' CCA CGG CCC CAT CCA 3'
Collagen I	Forward: 5' TGC CGA TGT CGC TAT CCA 3' Reverse: 5' TCT TGC AGT GAT AGG TGA TGT TCTG 3'
Collagen IV	Forward: 5'-ATCCGGCCCTTCATTAGCA-3' Reverse: 5'-GACTGTGACCCGCCATCA-3'
ANP	Forward: 5'-ATCTGATGGATTCAAGAAC-3' Reverse: 5'-CTCTGAGACGGGTTGACTTC-3'
β -MHC	Forward: 5'-TTGGCAGCGACTGCGTCATC-3' Reverse: 5'-GAGCTCCAGAGTTTCTCCGAAGGA-3'
IL-6	Forward: 5' GCT ATG AAG TTT CTC TCC GCA AGA 3' Reverse: 5' GGC AGT GGC TGT CAA CAA CAT 3'
GAPDH	Forward: 5'-GACATGCCCGCTGGAGAAAC-3' Reverse: 5'-AGCCCAGGATGCCCTTGTAGT-3'
18S	Forward: 5' TCG AGG CCC TGT AAT TGG AA 3' Reverse: 5' CCC TCC AAT GGA TCC TCG TT 3'

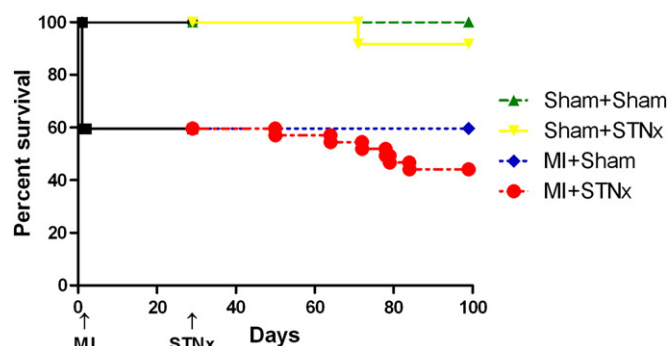


Fig. 2. Kaplan–Meier curves for groups of Sham + Sham, MI + Sham, Sham + STNx and MI + STNx respectively.

then collected for histology, gene and protein analysis. The survival analysis was performed by GraphPad Prism 5 and displayed by Kaplan–Meier survival curves. All experiments adhered to the Guidelines for Animal Welfare of National Health and Medical Research Council of Australia and approved by the Ethics Committee of St Vincent's Hospital (Animal Ethics Committee Number 027/10).

2.2. Animal surgery

MI surgery was performed as previously described with modifications [23]. Briefly, at week 0, isoflurane anesthetized animals were intubated and a thoracotomy performed. The left anterior descending coronary artery was identified and permanently ligated 3 mm below its origin. Buprenorphine (0.03 mg/kg, sc) was administered for analgesia. Sham animals underwent the same procedure except that the coronary artery was not ligated.

Four-weeks post-MI, MI/Sham-operated animals underwent either STNx or Sham-operated STNx as previously described [17]. Briefly, isoflurane-anesthetized rats underwent right subcapsular nephrectomy and infarction of approximately 2/3 of the left kidney by selective ligation of two of 3–4 extra-renal branches of the left renal artery. Sham animals underwent laparotomy and manipulation of both kidneys before wound closure.

2.3. Cardiac functional assessment

2.3.1. Echocardiography

Transthoracic echocardiography was performed prior to STNx/Sham surgery and again at the endpoint using a Vivid 7 (GE Vingmed, Horten, Norway) echocardiography machine with a 10 MHz phased array probe as routinely performed in our laboratory [24]. Parasternal short-axis views of the heart were used to obtain measures of LV internal dimension in diastole and systole, and LV posterior and anterior wall thicknesses in diastole. Parasternal long-axis views were used to obtain LV end diastolic (LVEDV) and end systolic (LVESV) volumes. Ejection fraction (EF) and fractional

Table 2

Animal number, survival rate, infarct size, tissue weight and quantitation of the immuno-histochemical staining for cardiac collagen III in the LV non-infarct zone. Values are mean \pm SEM. BW: body weight. * $p<0.05$ versus Sham + Sham, ** $p<0.01$ versus Sham + Sham, *** $p<0.001$ versus Sham + Sham; $^{\S}p<0.05$ versus MI + Sham, $^{\S\S}p<0.01$ versus MI + Sham, $^{\S\S\S}p<0.001$ versus MI + Sham.

	Sham + Sham	MI + Sham	Sham + STNx	MI + STNx
Animal Number	10	11	11	11
Survival rate (%)	100.0	59.7	91.7	44.1
Infarct size (%)	–	34.6 \pm 2.2	–	33.7 \pm 1.5
Tissue weight				
Heart weight/BW ratio (mg/g)	2.4 \pm 0.1	2.8 \pm 0.1	3.9 \pm 0.2	3.9 \pm 0.2
		***	***, §§§	***, §§§
Lung weight/BW ratio (mg/g)	3.0 \pm 0.1	3.1 \pm 0.1	3.6 \pm 0.1	3.6 \pm 0.2
			**, §§	**, §§
LV weight/BW ratio (mg/g)	1.73 \pm 0.07	1.94 \pm 0.03	2.93 \pm 0.14	2.88 \pm 0.10
		**	***, §§§	***, §§§
Atria weight/BW ratio (mg/g)	0.24 \pm 0.01	0.32 \pm 0.02	0.35 \pm 0.03	0.42 \pm 0.04
		**	**	***, §
Left kidney weight/BW ratio (mg/g)	3.1 \pm 0.1	3.1 \pm 0.1	4.6 \pm 0.1	5.0 \pm 0.2
			***, §§§	***, §§§
Immunohistochemical staining				
Cardiac collagen III (%)	0.08 \pm 0.02	0.11 \pm 0.03	0.17 \pm 0.04	0.19 \pm 0.04
			*	*

Table 3

Blood pressure and echocardiography data at week 4 (prior to STNx/Sham surgery) and week 14. Values are mean \pm SEM. FS: fractional shortening; EF: ejection fraction; LVEDV and LVESV: LV end diastolic and end systolic volume; DT: deceleration time; IVRT: isovolumetric relaxation time. Ejection fraction was significantly decreased in MI+STNx animals compared to the MI+Sham group at week 14. * $p<0.05$ versus Sham+Sham, ** $p<0.01$ versus Sham+Sham, *** $p<0.001$ versus Sham+Sham; § $p<0.05$ versus MI+Sham, §§ $p<0.01$ versus MI+Sham, §§§ $p<0.001$ versus MI+Sham; # $p<0.05$ versus Sham+STNx, ## $p<0.01$ versus Sham+STNx, ### $p<0.001$ versus Sham+STNx.

	Week 4				Week 14			
	Sham + Sham	MI + Sham	Sham + STNx	MI + STNx	Sham + Sham	MI + Sham	Sham + STNx	MI + STNx
Blood pressure								
Blood pressure (mmHg)	128.2 \pm 6.8	115.5 \pm 6.3	122.3 \pm 3.5	111.4 \pm 4.2	125.8 \pm 6.0	118.8 \pm 4.7	221.8 \pm 10.9 ***, §§§	176.6 \pm 9.3 ***, §§§, ##
Echocardiography								
FS (%)	40.5 \pm 1.5	21.4 \pm 1.5 ***	45.3 \pm 1.5 §§§	18.1 \pm 0.5 ***, ###	40.4 \pm 2.9	19.1 \pm 0.9 ***	47.6 \pm 3.3 §§§	15.1 \pm 0.9 ***, §§, ###
Anterior wall thickness (mm)	1.45 \pm 0.03	0.91 \pm 0.04 ***	1.49 \pm 0.05 §§§	0.83 \pm 0.03 ***, ###	1.64 \pm 0.04	0.78 \pm 0.02 ***	2.04 \pm 0.06 ***, §§§	0.73 \pm 0.03 ***, ###
Posterior wall thickness (mm)	1.57 \pm 0.05	1.81 \pm 0.06 *	1.67 \pm 0.06	1.65 \pm 0.04	1.69 \pm 0.06	1.93 \pm 0.05 **	2.24 \pm 0.08 ***, §	1.69 \pm 0.08 §, ###
EF (%)	67.1 \pm 2.2	42.7 \pm 2.3 ***	72.2 \pm 2.0 §§§	37.7 \pm 1.4 ***, ###	67.8 \pm 2.9	39.4 \pm 1.8 ***	71.8 \pm 3.1 §§§	31.2 \pm 1.3 ***, §§, ###
LVEDV (mL)	0.66 \pm 0.02	0.83 \pm 0.05 **	0.60 \pm 0.04 §§	0.90 \pm 0.05 ***, ###	0.76 \pm 0.04	1.11 \pm 0.05 ***	0.81 \pm 0.04 §§	1.23 \pm 0.07 ***, ###
LVESV (mL)	0.22 \pm 0.05	0.48 \pm 0.04 ***	0.17 \pm 0.02 §§§	0.56 \pm 0.04 ***, ###	0.25 \pm 0.03	0.68 \pm 0.04 ***	0.22 \pm 0.03 §§§	0.85 \pm 0.06 ***, §, ###
LV mass (gram/m ²)	1.41 \pm 0.04	1.47 \pm 0.05	1.40 \pm 0.04	1.51 \pm 0.03	1.70 \pm 0.04	1.80 \pm 0.11	2.13 \pm 0.07 **, §	1.78 \pm 0.08 #
DT (ms)	31.3 \pm 1.5	36.0 \pm 1.8	38.3 \pm 1.1 *	39.0 \pm 1.5 **	32.1 \pm 1.8	37.2 \pm 1.8	31.8 \pm 2.1	36.7 \pm 2.3
IVRT (ms)	23.0 \pm 1.4	31.3 \pm 1.2 ***	21.9 \pm 1.3 §§§	30.3 \pm 1.6 **, ###	24.2 \pm 1.6	34.7 \pm 1.7 **	26.2 \pm 1.6 §	35.4 \pm 2.5 **, ##
E wave velocity (m/s)	1.04 \pm 0.04	1.07 \pm 0.04	1.06 \pm 0.03	1.05 \pm 0.04	0.99 \pm 0.04	0.97 \pm 0.04	1.10 \pm 0.04	1.03 \pm 0.05
A wave velocity (m/s)	0.64 \pm 0.06	0.49 \pm 0.03	0.53 \pm 0.04	0.48 \pm 0.03	0.45 \pm 0.05	0.37 \pm 0.04	0.66 \pm 0.05 *, §§	0.53 \pm 0.06 §
E' wave velocity (cm/s)	4.8 \pm 0.3	4.0 \pm 0.3	4.4 \pm 0.2	3.7 \pm 0.2 *	4.0 \pm 0.2	3.6 \pm 0.3	4.4 \pm 0.4	4.1 \pm 0.3
A' wave velocity (cm/s)	3.3 \pm 0.3	2.7 \pm 0.3	3.5 \pm 0.4	2.5 \pm 0.1	2.7 \pm 0.4	2.5 \pm 0.3	4.4 \pm 0.3 **, §§	3.1 \pm 0.3 #
E/E' wave ratio	22.4 \pm 1.1	26.7 \pm 1.1	25.1 \pm 1.5	28.3 \pm 1.7 *	25.0 \pm 1.4	28.2 \pm 2.2	26.2 \pm 2.3	26.0 \pm 1.8
E/A wave ratio	1.8 \pm 0.1	2.3 \pm 0.2	2.1 \pm 0.2	2.3 \pm 0.2	2.6 \pm 0.5	3.0 \pm 0.4	1.7 \pm 0.1	2.2 \pm 0.4
E'/A' wave ratio	1.5 \pm 0.1	1.6 \pm 0.3	1.4 \pm 0.1	1.5 \pm 0.1	1.7 \pm 0.2	1.6 \pm 0.3	1.1 \pm 0.1 *	1.5 \pm 0.2

shortening (FS) were calculated according to standard formulae. Doppler and tissue Doppler images were obtained from the apical 4-chamber view of the heart for measures of diastolic function, namely early and late transmitral peak diastolic flow velocity (E and A waves),

mitral valve inflow E wave deceleration time (DT), isovolumic relaxation time (IVRT) and peak early and late (E' and A') diastolic tissue velocity at the septal side of the mitral annulus. All parameters were assessed using an average of three beats and calculations

Table 4

Hemodynamic parameters assessed at week 14. Values are mean \pm SEM. dP/dt max, dP/dt min: the maximal rate of pressure rise and fall; LVEDP: LV end diastolic pressure; ESPVR, slope of end systolic pressure–volume relationship; EDPVR, slope of end diastolic pressure–volume relationship; PRSW, slope of preload recruitable stroke work relationship. Tau logistic was significantly increased in MI+STNx animals compared to the MI+Sham group. * $p<0.05$ versus Sham+Sham, ** $p<0.01$ versus Sham+Sham, *** $p<0.001$ versus Sham+Sham; § $p<0.05$ versus MI+Sham, §§ $p<0.01$ versus MI+Sham, §§§ $p<0.001$ versus MI+Sham; # $p<0.05$ versus Sham+STNx, ### $p<0.001$ versus Sham+STNx.

	Sham + Sham	MI + Sham	Sham + STNx	MI + STNx
Systolic blood pressure (mmHg)	104.4 \pm 6.3	91.8 \pm 2.0	116.7 \pm 6.4 §§	111.8 \pm 6.0 §§
Diastolic blood pressure (mmHg)	77.3 \pm 5.7	66.3 \pm 2.4	87.6 \pm 5.4 §§	88.6 \pm 5.7 §§
Heart rate (beats/min)	306 \pm 19	302 \pm 23	309 \pm 17	314 \pm 17
dP/dt max (mmHg/ms)	6123 \pm 215	4763 \pm 163	6193 \pm 301 §§§	4633 \pm 253 ***, ###
– dP/dt min (mmHg/ms)	5229 \pm 295	3212 \pm 180 ***	4124 \pm 356 *, §	3065 \pm 207 ***, #
LVEDP (mmHg)	3.9 \pm 0.6	7.3 \pm 0.9 *	10.1 \pm 1.4 **	10.7 \pm 1.5 **
ESPVR (mmHg/ μ l)	0.58 \pm 0.07	0.29 \pm 0.04 **	0.47 \pm 0.07 §	0.32 \pm 0.04 **
EDPVR (mmHg/ μ l)	0.03 \pm 0.01	0.03 \pm 0.01	0.05 \pm 0.01	0.04 \pm 0.01
PRSW (mmHg)	78.9 \pm 5.5	58.2 \pm 6.1 *	62.7 \pm 8.9	49.2 \pm 4.5 ***
Cardiac output (mmHg)	45070 \pm 3670	44678 \pm 4975	53724 \pm 8169	30761 \pm 4775 *, #
Tau logistic (ms)	10.0 \pm 0.5	12.3 \pm 0.7 *	16.5 \pm 1.6 ***, §	17.0 \pm 1.4 ***, §§

Table 5

Renal function and indoxyl sulfate levels at week 4 (prior to STNx/Sham surgery) and week 14. Values are mean \pm SEM. STNx animals developed severe renal dysfunction and had increased indoxyl sulfate levels compared the non-STNx groups at week 14. * $p < 0.05$ versus Sham + Sham, ** $p < 0.01$ versus Sham + Sham, *** $p < 0.001$ versus Sham + Sham; $^{\S}p < 0.05$ versus MI + Sham, $^{\S\S}p < 0.01$ versus MI + Sham, $^{\S\S\S}p < 0.001$ versus MI + Sham.

	Week 4				Week 14			
	Sham + Sham	MI + Sham	Sham + STNx	MI + STNx	Sham + Sham	MI + Sham	Sham + STNx	MI + STNx
Glomerular filtration rate (ml/min/kg)	10.0 \pm 1.1	11.2 \pm 0.9	12.1 \pm 0.4	11.3 \pm 0.9	8.4 \pm 0.3	6.9 \pm 0.8	1.1 \pm 0.5 ***, §§§	1.5 \pm 0.4 ***, §§§
Creatinine clearance (ml/min)	206.4 \pm 14.5	162.3 \pm 22.4	202.1 \pm 24.1	185.1 \pm 13.1	222.8 \pm 27.5	192.6 \pm 36.9	33.7 \pm 12.4 ***, §§	33.8 \pm 7.9 ***, §§§
Serum creatinine (μ mol/l)	28.2 \pm 1.0	29.3 \pm 1.1	30.6 \pm 0.7	29.4 \pm 0.5	37.9 \pm 4.7	45.3 \pm 6.7	101.8 \pm 12.3 ***, §§	110.4 \pm 25.3 *
Proteinuria (mg/24 hr)	20.1 \pm 1.5	16.9 \pm 1.1	19.6 \pm 1.4	14.8 \pm 1.9	24.8 \pm 2.2	20.4 \pm 1.7	391.4 \pm 60.1 ***, §§§	433.7 \pm 87.1 ***, §§§
Indoxyl sulfate (mg/dl)	0.15 \pm 0.01	0.16 \pm 0.05	0.18 \pm 0.02	0.22 \pm 0.03	0.13 \pm 0.03	0.16 \pm 0.02	0.76 \pm 0.19 **, §	0.72 \pm 0.15 *, §

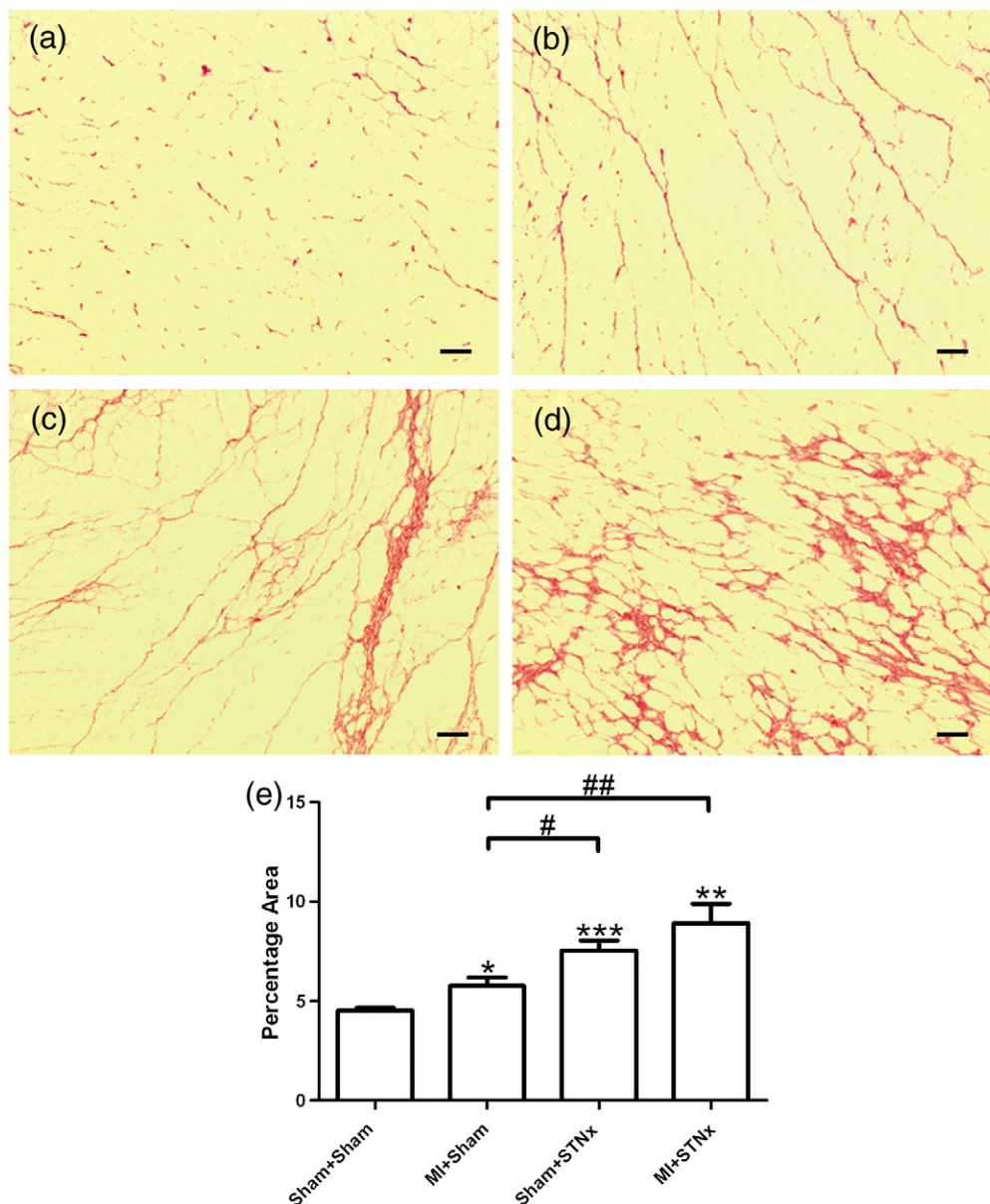


Fig. 3. Representative images of the LV non-infarct zone showing picrosirius red staining from the following groups (a) Sham + Sham, (b) MI + Sham, (c) Sham + STNx and (d) MI + STNx. Scale bar, 100 μ m. Quantitation of picrosirius red staining (e) showing MI + STNx animals had significantly greater cardiac interstitial fibrosis compared to the MI + Sham group. Data are expressed as mean \pm SEM. * $p < 0.05$ versus Sham + Sham, ** $p < 0.01$ versus Sham + Sham, *** $p < 0.001$ versus Sham + Sham; # $p < 0.05$, ## $p < 0.01$ for between group comparisons.

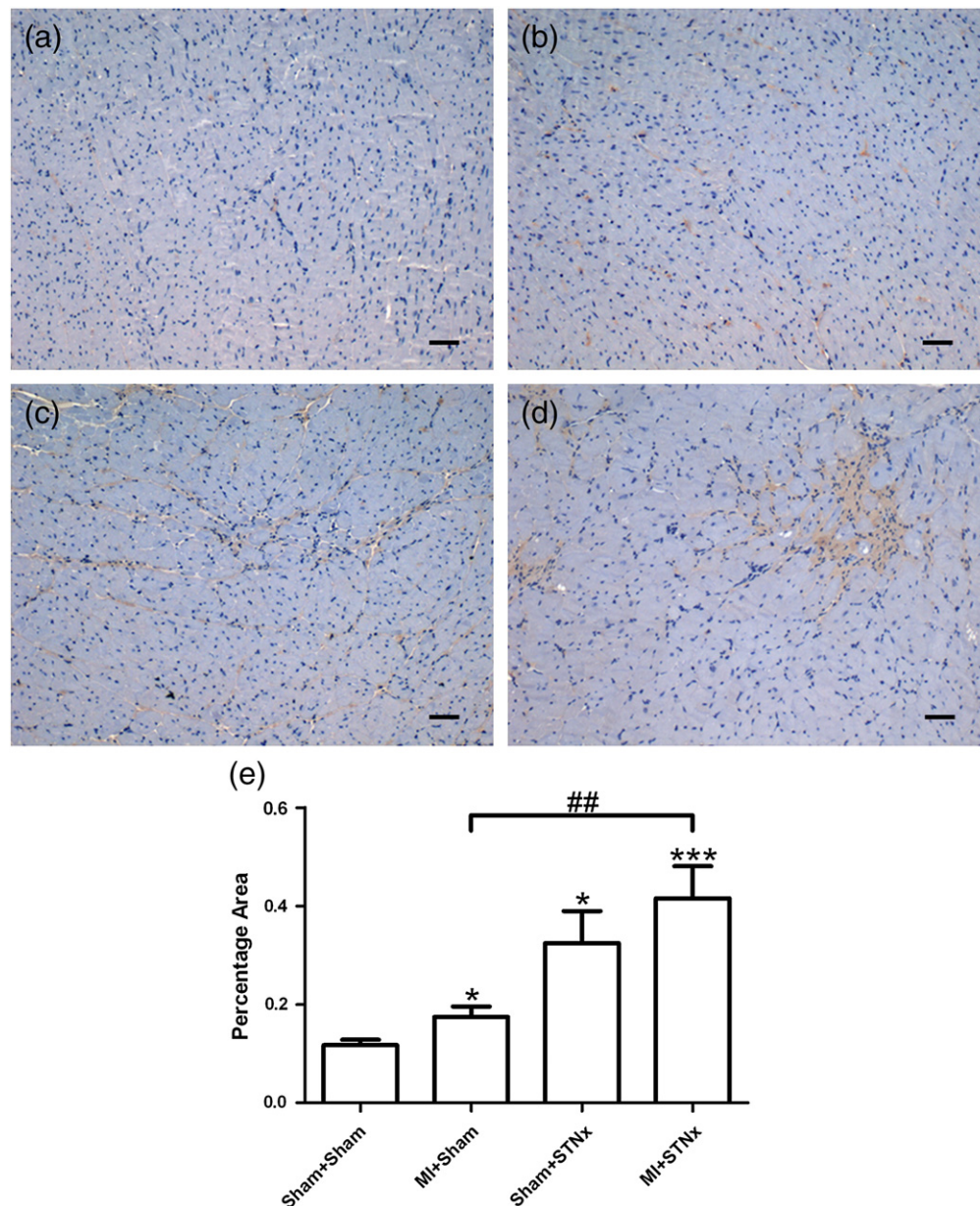


Fig. 4. Representative images of the LV non-infarct zone showing collagen I immunostaining from the following groups (a) Sham + Sham, (b) MI + Sham, (c) Sham + STNx and (d) MI + STNx. Scale bar, 30 μm. Quantitation of collagen I (e) showing MI + STNx animals had significantly greater immunostaining than the MI + Sham group. Data are expressed as mean ± SEM. * $p < 0.05$ versus Sham + Sham, *** $p < 0.001$ versus Sham + Sham; ## $p < 0.01$ for between group comparisons.

were made in accordance with the American Society of Echocardiography guidelines. All data were acquired and analysed by a single blinded observer using Echo PAC (GE Vingmed) offline processing.

2.3.2. Cardiac catheterization

Hemodynamic measurements were performed prior to tissue collection as previously described [17]. Briefly, a 2 F miniaturized combined catheter/micromanometer (Model SPR838 Millar instruments, Houston, TX) was inserted into the right common carotid artery to obtain aortic BP, and then advanced into the LV to obtain LV pressure–volume (PV) loops. PV loops were recorded at steady state and during transient preload reduction, achieved by occlusion of the inferior vena cava and portal vein with the ventilator turned off and rat apnoeic. The following validated parameters were assessed using Millar conductance data acquisition and analysis software PVAN 3.2: LV end diastolic pressure (LVEDP), the maximal rate of pressure rise (dp/dtmax) and fall (dp/dtmin), the slope of the end systolic PV relationship (ESPVR), the slope of the end diastolic PV relationship (EDPVR), Tau (t Logistic), and the slope of the preload recruitable stroke work (PRSW) relationship.

2.4. Renal functional assessment

2.4.1. Glomerular filtration rate

Glomerular filtration rate (GFR) was assessed prior to STNx/Sham surgery and again at the endpoint as previously described [17]. Animals were intravenously injected with a radioactive isotope, ^{99}Tc -diethylene triamine penta-acetic acid (^{99}Tc -DTPA) which is excreted solely by the glomerulus. Blood was sampled 43 min after injection and plasma radioactivity measured to evaluate the rate of DTPA excretion, this was compared to the counts of the standard reference prepared at the time of injection. The calculated GFR was corrected for body weight (BW) and reported as GFR ml/min/kg.

2.4.2. Creatinine clearance, proteinuria and plasma indoxyl sulphate levels

Prior to STNx/Sham surgery and at the endpoint, rats were bled and then housed in metabolic cages for 24 h for urine collection. Serum creatinine, urinary creatinine and proteinuria were measured using a Cobas Integra® 400 Plus Bioanalyzer (Roche, Indianapolis, IN) as per manufacturers' instructions. Creatinine clearance was calculated according to standard formula [17]. Plasma indoxyl sulfate levels were measured using a high performance liquid chromatography method as previously described [17,25].

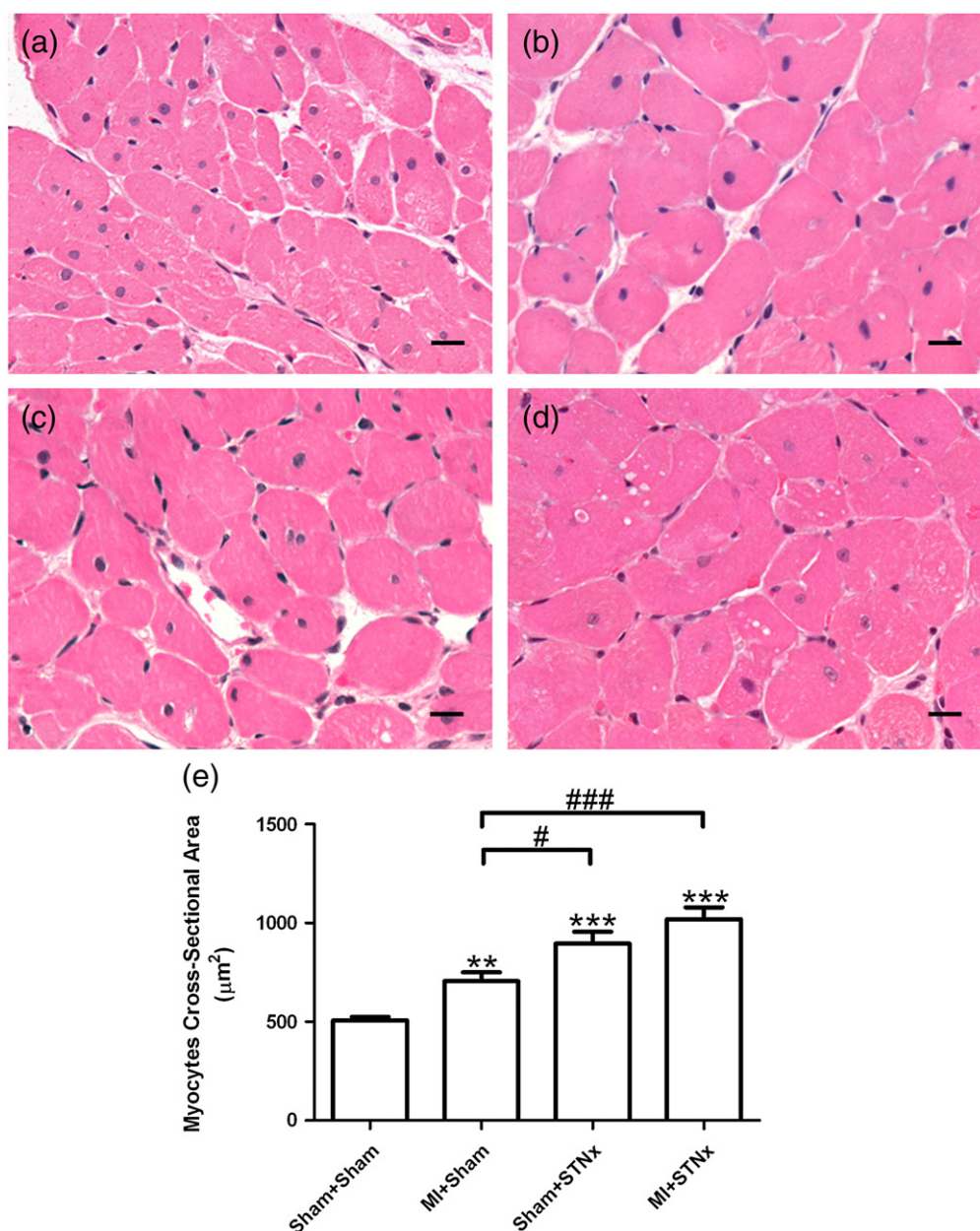


Fig. 5. Representative images of the LV non-infarct zone showing hematoxylin and eosin staining in myocytes from the following groups (a) Sham+Sham, (b) MI+Sham, (c) Sham+STNx and (d) MI+STNx. Scale bar, 30 μm. Quantitation of the data (e) showing that MI+STNx animals had significantly larger cardiomyocytes compared to the MI+Sham group. Data are expressed as mean ± SEM. ***p*<0.01 versus Sham+Sham, ****p*<0.001 versus Sham+Sham; #*p*<0.05, ###*p*<0.001 for between group comparisons.

2.5. Histology and immunohistochemistry

Cross sections of LV (4 μm) from all MI animals were stained with picosirius red and scanned using Aperio ScanScope Console v.8.0.0.1058 (Aperio Technologies, Inc) for infarct size analysis. Infarct size was expressed as an averaged percentage of the endocardial and epicardial scarred circumferences of the LV. Animals with small infarcts (<20%) were omitted from the analysis.

LV and kidney tissue sections from all animals, stained with picosirius red, were analysed for interstitial fibrosis using Aperio ScanScope Console v.8.0.0.1058 (Aperio Technologies, Inc). Picosirius red stained interstitial fibrosis in the non-infarct zone of the LV and kidney, excluding perivascular fibrosis, was selected for its intensity of red staining, and the percentage area was calculated using a pre-set algorithm [17]. The intensity and algorithm was preset and maintained constant for the analysis of all sections.

LV tissue sections from all animals were stained with hematoxylin–eosin to determine myocyte cross-sectional area in the non-infarct zone of the LV sub-endocardium. Sections were scanned and images analysed using Aperio ScanScope Console v.8.0.0.1058 (Aperio Technologies, Inc). Myocytes in the same plane, as assessed by selecting cells with similar sized nuclei and intact cellular membranes in the non-infarct zone of the myocardium, were outlined and the average calculated from 50 myocytes per LV [12]. Similar sized nuclei were consistently selected for all groups.

Antibody staining of the non-infarct zone of the LV from all animals for collagen I and collagen III was assessed immunohistochemically, using goat anti-type I collagen (Southern Biotech, Birmingham, AL, USA) and goat anti-type III collagen (BioGenex, San Ramon, CA, USA) antibodies respectively with horseradish peroxidase (HRP)-linked secondary antibodies. Images were digitally captured using an AxioImager.A1 microscope (Carl Zeiss AxioVision) attached to an AxioCamMRC5 digital camera (Carl Zeiss AxioVision). The positive brown staining was quantified using image analysis software AIS (Analytic Imaging Station version 6.0, Imaging Research Inc., Ontario, Canada) [26]. Results were expressed as average percentage area of 10 fields at ×100 magnification in the subendocardial region of the non-infarct zone of the LV for all animals. Antibody staining was selected for its intensity which was preset and maintained constant for the analysis of all sections.

Tissue expression of KIM-1 in the non-infarct zone of the kidney cortex from all animals was assessed immunohistochemically, using goat anti-KIM-1 antibodies (R&D Systems, Minneapolis, MN, USA). Sections were scanned and images were analysed using Aperio ScanScope Console v.8.0.0.1058 (Aperio Technologies, Inc). The positive brown staining in the non-infarct zone of the kidney cortex was selected for its intensity, and results were expressed as percentage area calculated using a pre-set algorithm [12]. The intensity of antibody staining and the algorithm was preset and maintained constant for the analysis of all sections.

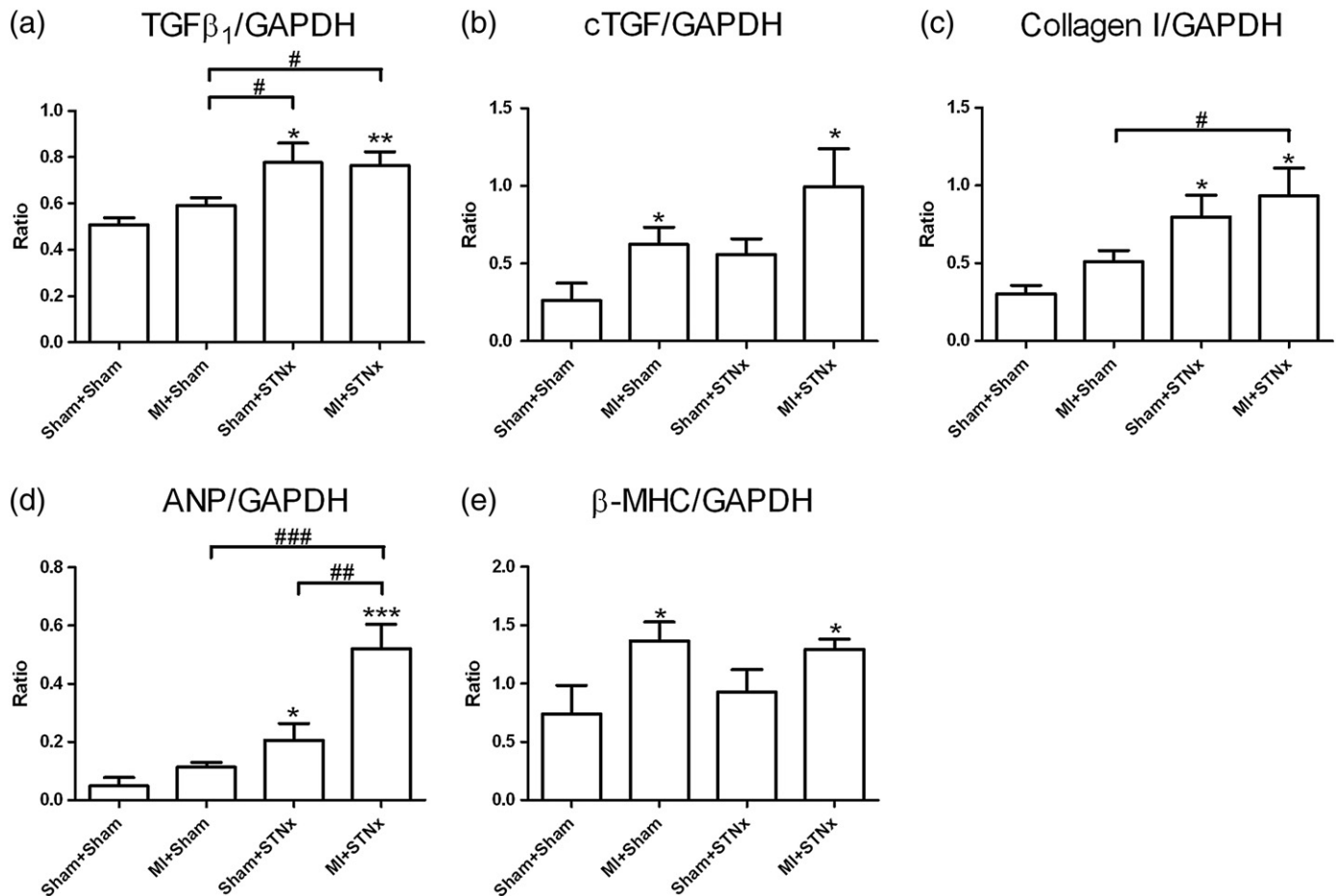


Fig. 6. mRNA expression of pro-fibrotic related markers TGFβ₁ (a), cTGF (b) and collagen I (c) and hypertrophic related markers ANP (d) and β-MHC (e) gene expression, expressed as a ratio of GAPDH in the LV non-infarct zone. Data are expressed as mean ± SEM. **p*<0.05 versus Sham + Sham, ***p*<0.01 versus Sham + Sham, ****p*<0.001 versus Sham + Sham; #*p*<0.05, ##*p*<0.01, ###*p*<0.001 for between group comparisons.

Tissue expression of macrophage infiltration in the non-infarct zone of the kidney cortex from all animals was assessed immunohistochemically, using mouse anti-CD 68 antibodies (AbD Serotec, Raleigh, NC, USA). Sections were scanned using Aperio ScanScope Console v.8.0.0.1058 (Aperio Technologies, Inc). The total number of macrophages (CD 68 immunoreactive cells) in the non-infarct zone of the kidney cortex was individually counted [26]. All histological and immunohistochemical data were acquired and analysed by a single blinded observer.

2.6. Quantitative mRNA expression

Total RNA was extracted from frozen non-infarct zone cardiac and renal tissue using Ambion RNAqueous® Kit (Ambion, Austin, TX, USA). mRNA was reverse transcribed into cDNA, and triplicate cDNA aliquots were amplified using sequence-specific primers (Geneworks, Adelaide, SA, Australia) with SYBR Green detection (Applied Biosystems) using an ABI prism 7900HT sequence detection system (Applied Biosystems). Real-time PCR was used to quantify mRNA expression of transforming growth factor (TGF) β₁, connective tissue growth factor (cTGF), collagen I, collagen IV, atrial natriuretic peptide (ANP), β-myosin heavy chain (β-MHC) and IL-6. Quantitation was standardized to the housekeeping genes GAPDH (cardiac tissue) and 18S (renal tissue). The primer pair sequences are shown in Table 1.

2.7. Western blot analysis

Total protein was extracted from frozen non-infarct zone cardiac tissues and renal tissues with modified RIPA buffer containing protease and phosphatase inhibitors using a polytron homogenizer as previously described [17]. Protein concentrations were determined by Bradford assay (Bio-Rad, Hercules, CA, USA). Equal amounts of protein (30 μg) were separated by 10% sodium dodecyl sulfate-polyacrylamide gel electrophoresis, and electrophoretically transferred to nitrocellulose membranes (Amersham Biosciences) [27]. Western blot analysis was performed as per manufacturer's protocol with specific antibodies (phospho-smad2, TGF-β precursor, phospho-p44/42 mitogen-activated protein kinase (MAPK), phospho-p38 MAPK and phospho-nuclear factor kappa B (NFκB) antibodies-Cell Signaling Technology, Beverly, MA, USA; pan-actin antibody-NeoMarkers, Fremont, CA, USA) and then visualized by enhanced chemiluminescence reagents

(Thermo Scientific). Band intensity was analysed using ImageJ software (National Center for Biotechnology Information) [15]. Pan-actin was used as the endogenous control.

2.8. Statistical analyses

Results are expressed as the mean ± SEM. Significance was determined by a one-way ANOVA with Bonferroni's multiple comparison test. For comparisons between 2 groups, unpaired Student *t*-test was used. All statistical analyses were performed using GraphPad Prism 5. Significant differences compared to Sham + Sham animals are expressed as **p*<0.05, ***p*<0.01, and ****p*<0.001; significant differences compared to MI + Sham animals are expressed as §*p*<0.05, §§*p*<0.01, and §§§*p*<0.001; significant differences compared to Sham + STNx animals are expressed as #*p*<0.05, ##*p*<0.01, and ###*p*<0.001.

3. Results

3.1. Survival rate

Survival rates for the different groups were 100%, 59.7%, 91.7% and 44.1% for Sham + Sham, MI + Sham, Sham + STNx and MI + STNx animals respectively (Fig. 2). The number of animals in each group at the endpoint is shown in Table 2.

3.2. Blood pressure, tissue weight and infarct size

There was no difference in BP between all groups prior to STNx/Sham (Table 3). As a consequence of STNx, all STNx animals were hypertensive. MI + STNx animals had reduced systolic BP compared to the Sham + STNx group (*p*<0.01) (Table 3).

There was no difference in infarct size between MI + STNx and MI + Sham groups (Table 2). All tissue weights were corrected for

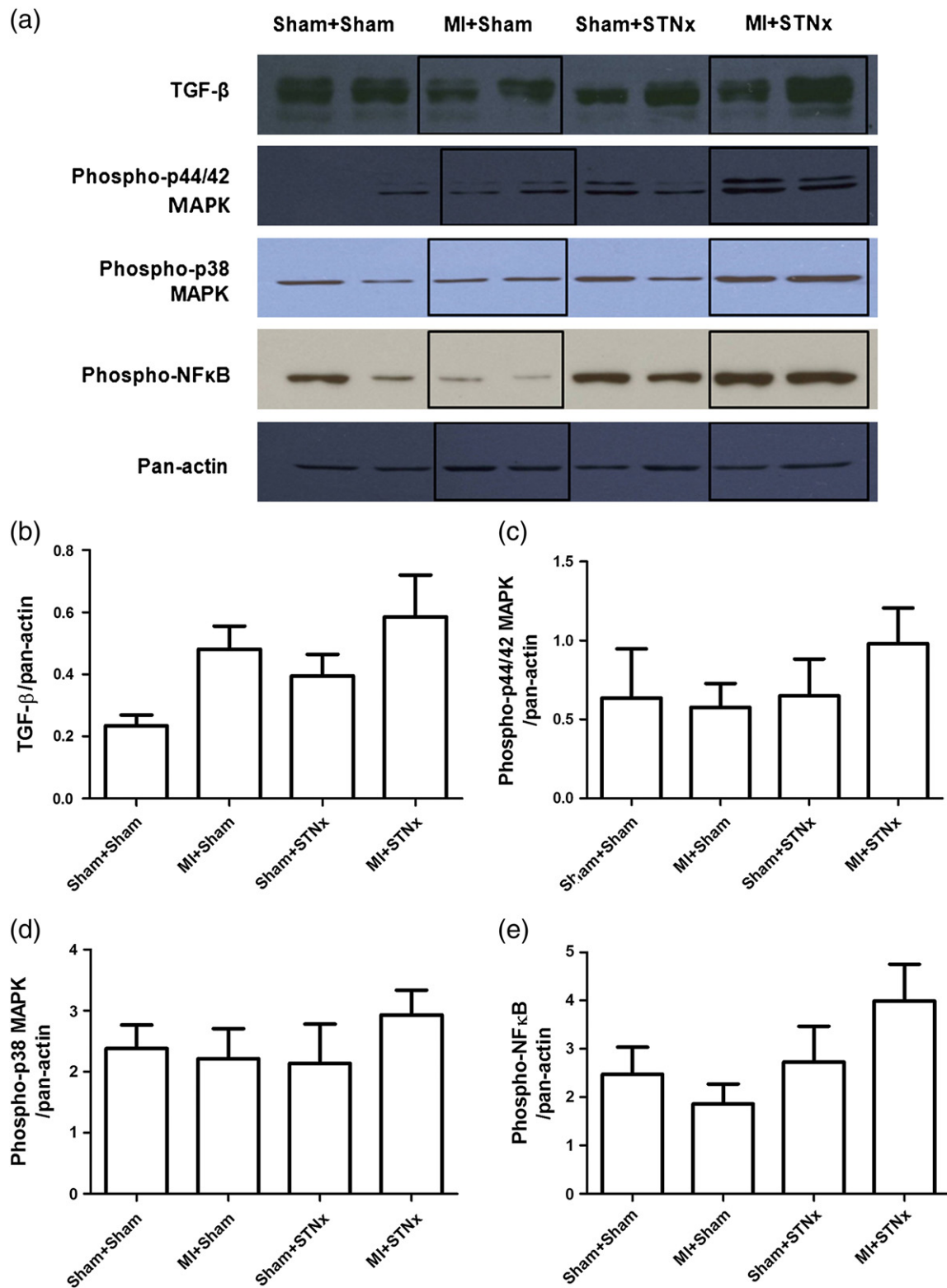


Fig. 7. Representative images of the Western blot showing cardiac protein levels in the LV non-infarct zone from Sham + Sham, MI + Sham, Sham + STNx and MI + STNx groups (a). Quantitation of the protein levels of TGF-β (b), phospho-p44/42 MAPK (c), phospho-p38 MAPK (d), and phospho-NFκB (e) in the non-infarct zone of the myocardium as normalized with pan-actin. Data are expressed as mean ± SEM.

BW. Heart weight/BW, LV weight/BW, atria weight/BW, lung weight/BW and left kidney weight/BW ratios were significantly greater in MI + STNx animals compared to the MI + Sham group (Table 2). Heart weight/BW and LV weight/BW ratios were higher in Sham + STNx

animals compared with MI + Sham animals ($p < 0.001$), because the MI injury removed 34% of the LV free wall mass and replaced it with a scar, this was also evident in the echocardiography measure of anterior wall thickness which was significantly reduced compared to the

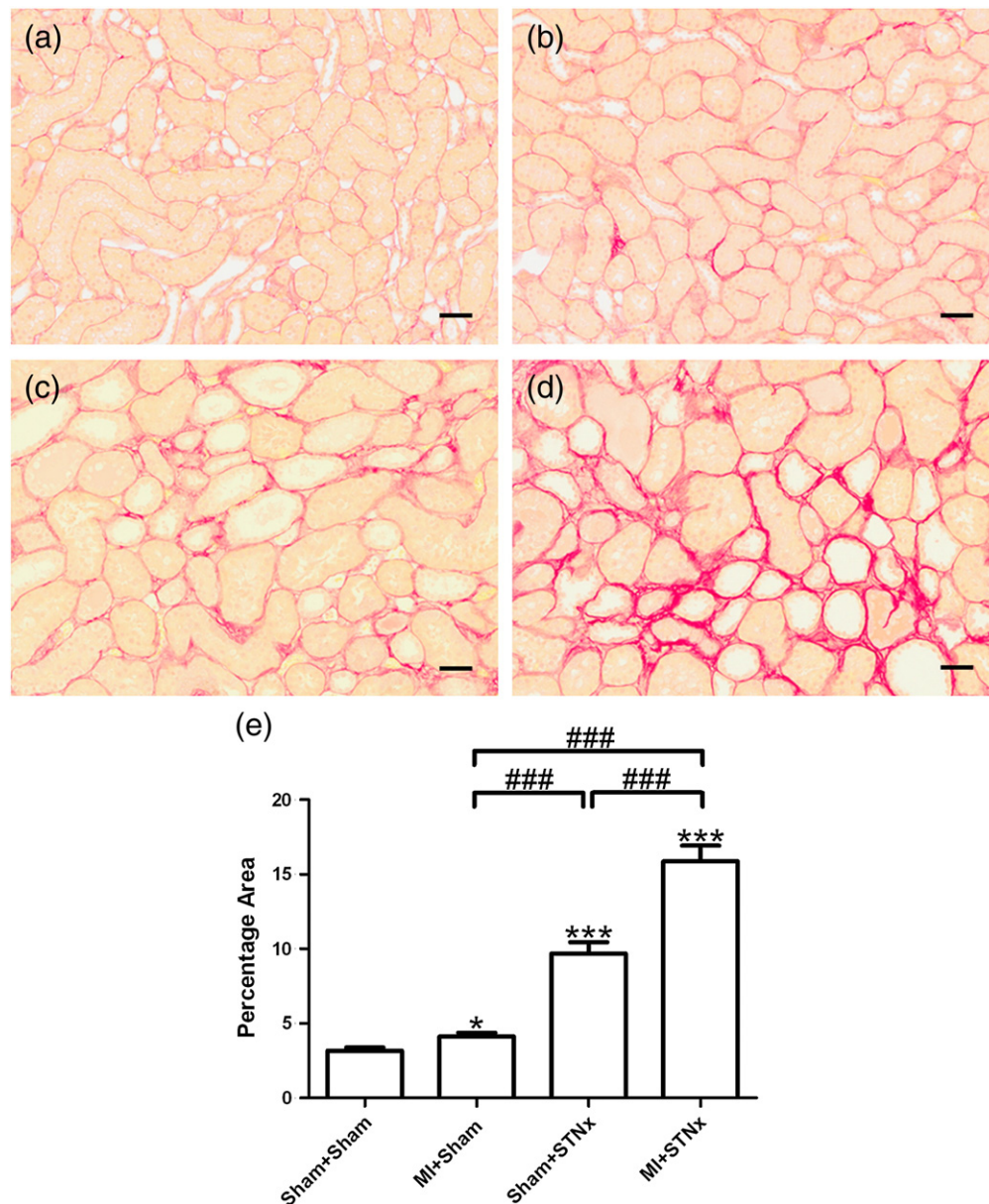


Fig. 8. Representative images of the non-infarct zone of the remaining left kidney showing picrosirius red staining from the following groups (a) Sham+Sham, (b) MI+Sham, (c) Sham+STNx and (d) MI+STNx. Scale bar, 50 μm. Quantitation of renal tubulointerstitial fibrosis (e) showing MI+STNx animals had significantly greater tubulointerstitial fibrosis than the MI+Sham and Sham+STNx groups. Data are expressed as mean ± SEM. * $p < 0.05$ versus Sham+Sham, *** $p < 0.001$ versus Sham+Sham; ### $p < 0.001$ for between group comparisons.

Sham+Sham group at week 14 ($p < 0.001$) (Table 3). Also both anterior and posterior wall thickness in the Sham+STNx animals was significantly increased compared to MI+Sham animals ($p < 0.001$ and $p < 0.05$ respectively) suggesting that there was more muscle mass in the STNx group, and hence the LV and total heart weight as a ratio of BW was greater. A major driver of this hypertrophy was the increase in BP that was observed in the Sham+STNx group compared to the MI+Sham group (Table 3).

3.3. Cardiac function

Significant reductions in LV EF and FS were observed in animals that underwent MI compared to sham-operated animals at 4 weeks post-MI (Table 3). Animals that underwent MI+STNx had a further 21% reduction in both LV EF and FS compared to the MI+Sham group at 10 weeks post-STNx ($p < 0.01$). Although no difference in A

wave velocity was observed between all groups at 4 weeks post-MI; a significant increase was seen in MI+STNx animals compared to the MI+Sham group at 10 weeks post-STNx ($p < 0.05$).

The time constant of active relaxation, Tau logistic, was significantly prolonged by 38% in MI+STNx animals compared to the MI+Sham group ($p < 0.01$) (Table 4). Significant increases in systolic and diastolic BP were observed in MI+STNx animals compared to the MI+Sham group ($p < 0.01$). LVEDP in MI+STNx animals compared to the MI+Sham group did not reach significance ($p = 0.08$). MI+STNx animals had a 31% reduction in cardiac output compared to the MI+Sham group ($p = 0.06$).

The rate of rise and fall of pressure in the LV, dP/dt (max) and dP/dt (min), were significantly reduced in MI animals compared to the non-MI groups; however, no difference was observed comparing MI+STNx animals with the MI+Sham group. PRSW and ESPVR were significantly reduced in animals that underwent MI compared to

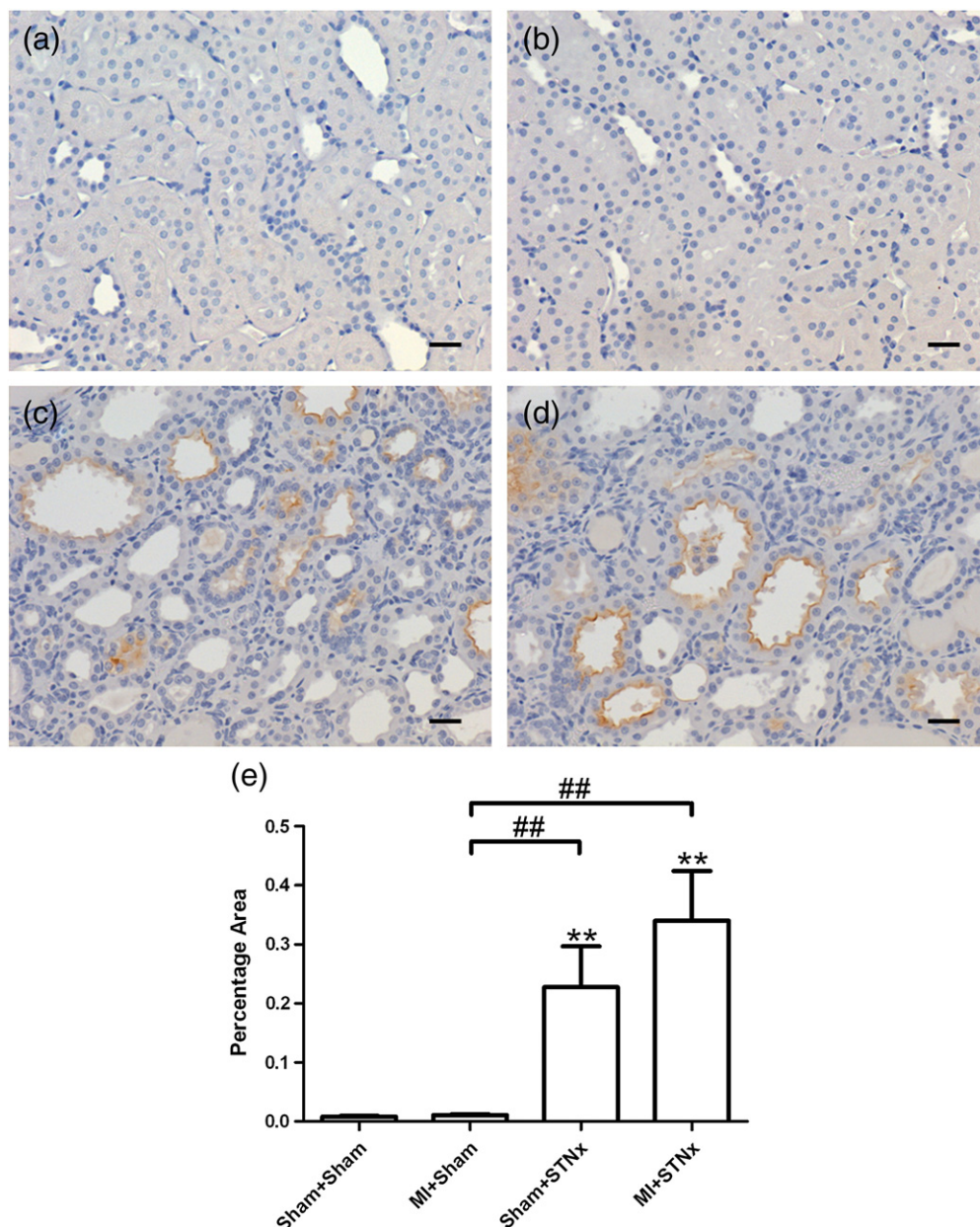


Fig. 9. Representative images of the non-infarct cortex region of the remaining left kidney showing immunostaining of the renal injury biomarker KIM-1 from the following groups (a) Sham + Sham, (b) MI + Sham, (c) Sham + STNx and (d) MI + STNx. Scale bar, 30 μm. Quantitation of KIM-1 (e) showing STNx animals had significantly greater levels of the KIM-1 compared to the non-STNx groups. Data are expressed as mean ± SEM. ***p* < 0.01 versus Sham + Sham; ##*p* < 0.01 for between group comparisons.

Sham + Sham control animals; while EDPVR was not statistically different among the groups.

3.4. Renal function

There was no difference in renal function among the groups prior to STNx/Sham surgery (Table 5). At 14 weeks, STNx animals developed severe renal dysfunction as indicated by reduced GFR, reduced creatinine clearance and increased proteinuria compared the non-STNx groups. However, no further deterioration was observed between MI + STNx and Sham + STNx groups at 14 weeks.

3.5. Indoxyl sulfate levels

There was no difference in plasma indoxyl sulfate levels among the groups prior to STNx/Sham (Table 5). STNx animals had significantly

higher indoxyl sulfate levels at 14 weeks, and there was no significant difference between MI + STNx and Sham + STNx groups.

3.6. Cardiac interstitial fibrosis

Cardiac interstitial fibrosis in the LV non-infarct zone, determined from picrosirius red staining, was significantly increased in MI + STNx animals compared to the MI + Sham group (*p* < 0.01) (Fig. 3a–e). LV fibrosis was also greater in MI + Sham and Sham + STNx animals compared to Sham + Sham control animals (*p* < 0.05 and *p* < 0.001 respectively). Antibody staining for collagen I in the LV non-infarct zone was significantly increased in MI + STNx animals compared to the MI + Sham group (*p* < 0.01) (Fig. 4a–e); while antibody staining for collagen III in the LV non-infarct zone was non-significantly elevated between MI + STNx and MI + Sham groups (*p* = 0.08) (Table 2).

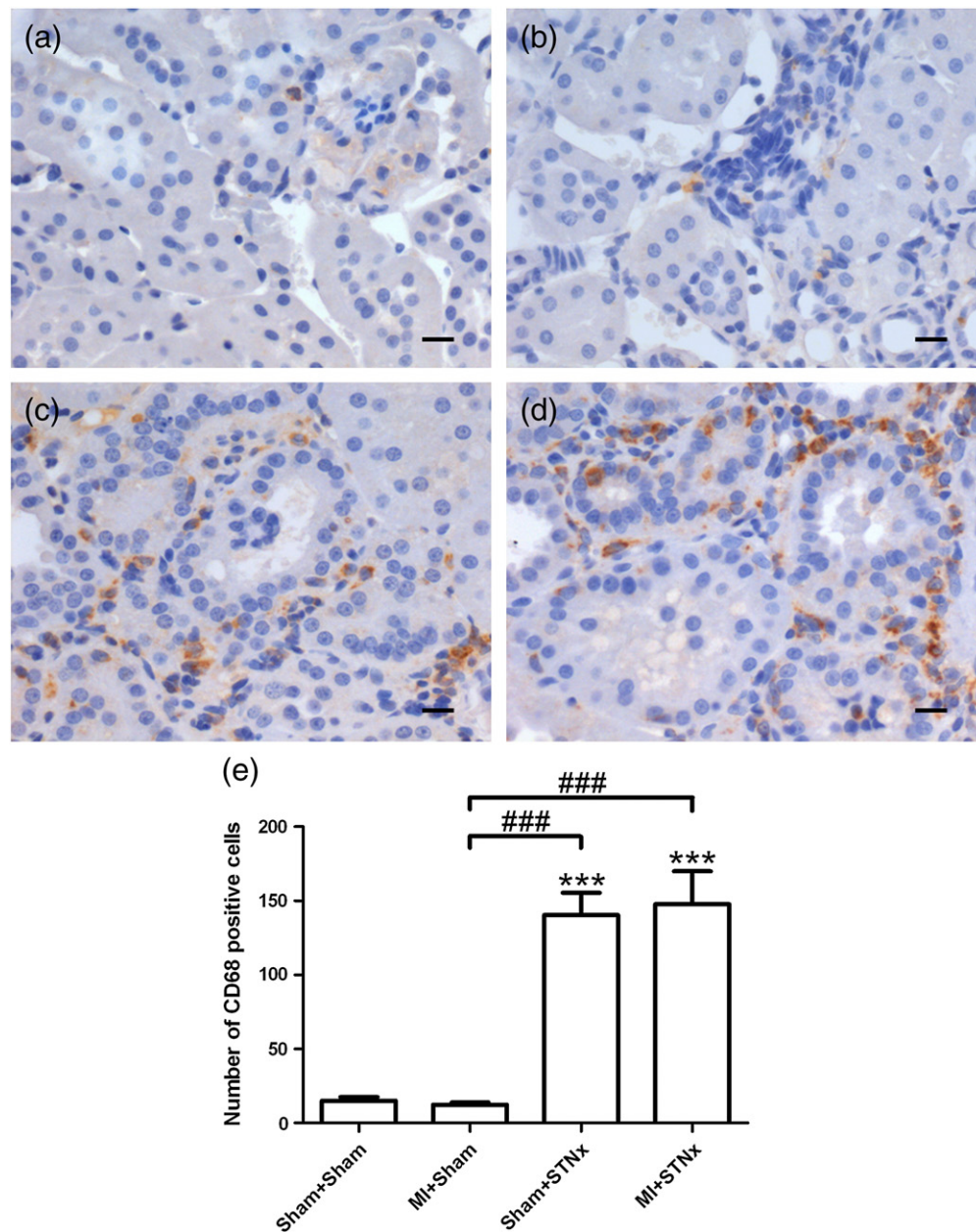


Fig. 10. Representative images of the non-infarct cortex region of the remaining left kidney showing immunostaining of macrophage infiltration from the following groups (a) Sham + Sham, (b) MI + Sham, (c) Sham + STNx and (d) MI + STNx. Scale bar, 30 μ m. Quantitation of number of CD68 positive cells (e) showing STNx animals had significantly increased macrophage infiltration compared to the non-STNx groups. Data are expressed as mean \pm SEM. *** p < 0.001 versus Sham + Sham; ### p < 0.001 for between group comparisons.

3.7. Myocyte cross-sectional area

Myocyte cross-sectional area in the LV non-infarct zone, determined from hematoxylin and eosin stained sections, was elevated by 44% in MI + STNx animals compared to the MI + Sham group (p < 0.001) (Fig. 5a–e). The myocyte cross-sectional area was also greater in MI + Sham and Sham + STNx animals compared to Sham + Sham control animals (p < 0.01 and p < 0.001 respectively).

3.8. Cardiac mRNA expression

Real time PCR was used to determine gene expression of the pro-fibrotic related markers TGF β ₁, cTGF and collagen I in the LV non-infarct zone at the endpoint (Fig. 6a–c). Compared to Sham + Sham control animals, TGF β ₁ and collagen I were significantly increased in the Sham + STNx and MI + STNx groups (p < 0.05), whereas cTGF expression was significantly elevated in the MI + Sham and MI + STNx

groups (p < 0.05). TGF β ₁ and collagen I, but not cTGF showed significant increases in MI + STNx animals compared to the MI + Sham group (p < 0.05).

The hypertrophic related marker ANP was increased in Sham + STNx and MI + STNx animals compared to the Sham + Sham control group (p < 0.05 and p < 0.001 respectively) (Fig. 6d). In MI + STNx animals ANP was significantly elevated compared to either MI + Sham or Sham + STNx group (p < 0.001 and p < 0.01 respectively). The hypertrophic related marker β -MHC was significantly increased in MI + Sham and MI + STNx animals compared to the Sham + Sham control group (p < 0.05), but there was no significant difference between MI + STNx and MI + Sham groups (Fig. 6e).

3.9. Cardiac signaling pathway activation

Activation of phospho-smad2 was not detectable in the LV non-infarct zone using Western blot analysis. Although no significant

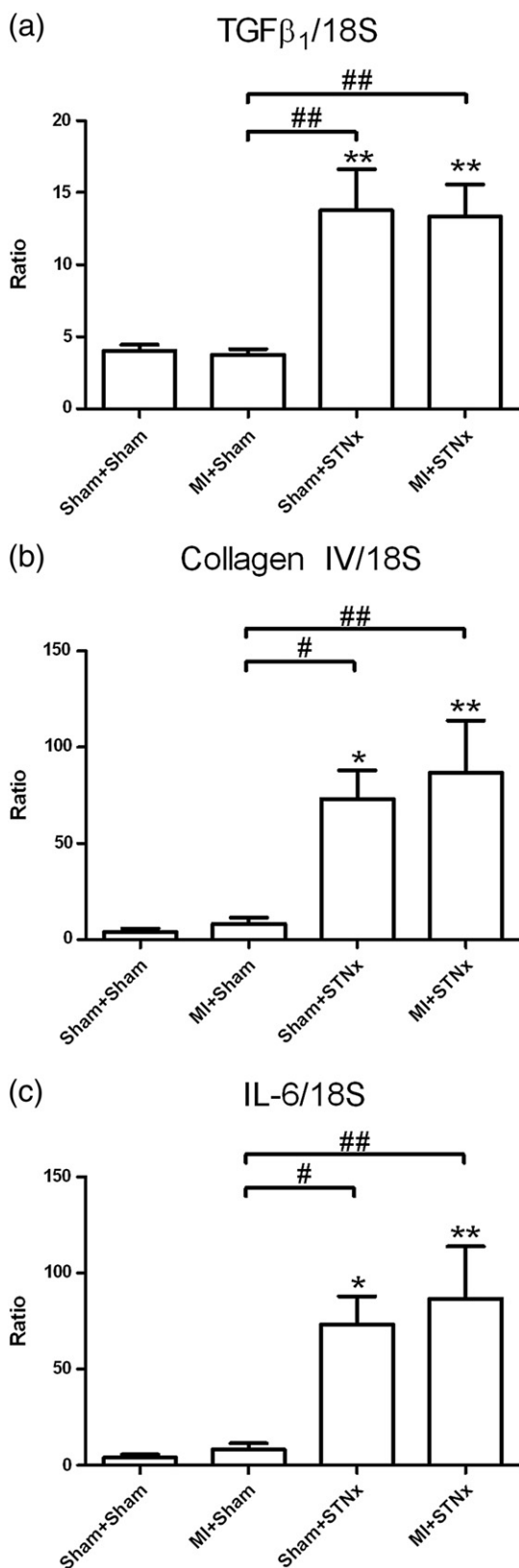


Fig. 11. mRNA expression of pro-fibrotic related markers TGFβ₁ (a) and collagen IV (b); and the pro-inflammatory cytokine IL-6 (c) in the remaining left kidney, expressed as a ratio of 18S. Data are expressed as mean ± SEM. *p<0.05 versus Sham+Sham, **p<0.01 versus Sham+Sham; #p<0.05, ##p<0.01 for between group comparisons.

differences in the levels of TGF-β/pan-actin, phospho-p44/42 MAPK/pan-actin, phospho-p38 MAPK/pan-actin and phospho-NFκB/pan-actin were found among the groups, there was an indicating trend towards an increase in TGF-β/pan-actin between Sham+Sham and MI+STNx groups (Fig. 7a-e). There was also a definite trend toward an increase in phospho-NFκB/pan-actin between MI+Sham and MI+STNx groups.

3.10. Renal tubulointerstitial fibrosis

MI+Sham (p<0.05), Sham+STNx (p<0.001) and MI+STNx (p<0.001) animals demonstrated significantly greater tubulointerstitial fibrosis in the non-infarct zone of the kidney compared to Sham+Sham control group. Both STNx groups had significantly greater renal tubulointerstitial fibrosis compared to the MI+Sham group (p<0.001). MI+STNx animals had incrementally greater tubulointerstitial fibrosis compared to the Sham+STNx group (p<0.001) (Fig. 8a-e).

3.11. Renal injury biomarker and macrophage infiltration

STNx animals demonstrated significantly greater expression of the renal injury biomarker KIM-1 (Fig. 9a-e) and had increased macrophage infiltration (Fig. 10a-e) in the non-infarct cortex region of the remaining left kidney compared to the non-STNx groups; and no significant difference was observed between MI+STNx and Sham+STNx groups.

3.12. Renal mRNA expression

Renal pro-fibrotic related markers TGFβ₁ and collagen IV as well as pro-inflammatory cytokine IL-6 were significantly increased in STNx animals compared the non-STNx groups (Fig. 11a-c); and no further increase was observed between MI+STNx and Sham+STNx groups.

3.13. Renal signaling pathway activation

Activation of phospho-smad2 was not detectable in the kidney using Western blot analysis. There were significant increases in the levels of TGF-β, phospho-NFκB and phospho-p38 MAPK but not phospho-p44/42 MAPK as normalized with pan-actin comparing both Sham+STNx and MI+STNx groups to the Sham+Sham control animals (Fig. 12a-e). The levels of TGF-β, phospho-NFκB and phospho-p38 MAPK as normalized with pan-actin were significantly up-regulated in MI+STNx animals compared to the MI+Sham group.

4. Discussion

The present study demonstrates that MI followed by STNx may be a potentially useful model to assess the pathophysiology and mechanisms underlying CRS as well as the impact of potential therapies in this setting. Impairment of cardiac function and accelerated cardiac remodeling as well as increased renal tubulointerstitial fibrosis was observed in animals that underwent MI followed by STNx. These findings are of considerable interest as this model appears to successfully recapitulate features of the phenotype of both ventricular remodeling and kidney impairment which occurs clinically. Few studies have investigated the effects of MI on animals with primary CKD, however no report has described the effects of 5/6 STNx on animals with a primary cardiac disease [28]. A previous study examining a model of unilateral nephrectomy followed by MI did not reproduce the condition of primary CKD contributing to decreased cardiac function as renal function was preserved in those animals [19,20], suggesting unilateral nephrectomy takes longer for renal impairment to evolve. In this study, we allowed 4 weeks post-MI for animals to develop cardiac dysfunction before inducing 5/6 STNx, a further 10 weeks allows for the development of CKD whilst at the same time preserving survival as much as possible to permit adequate

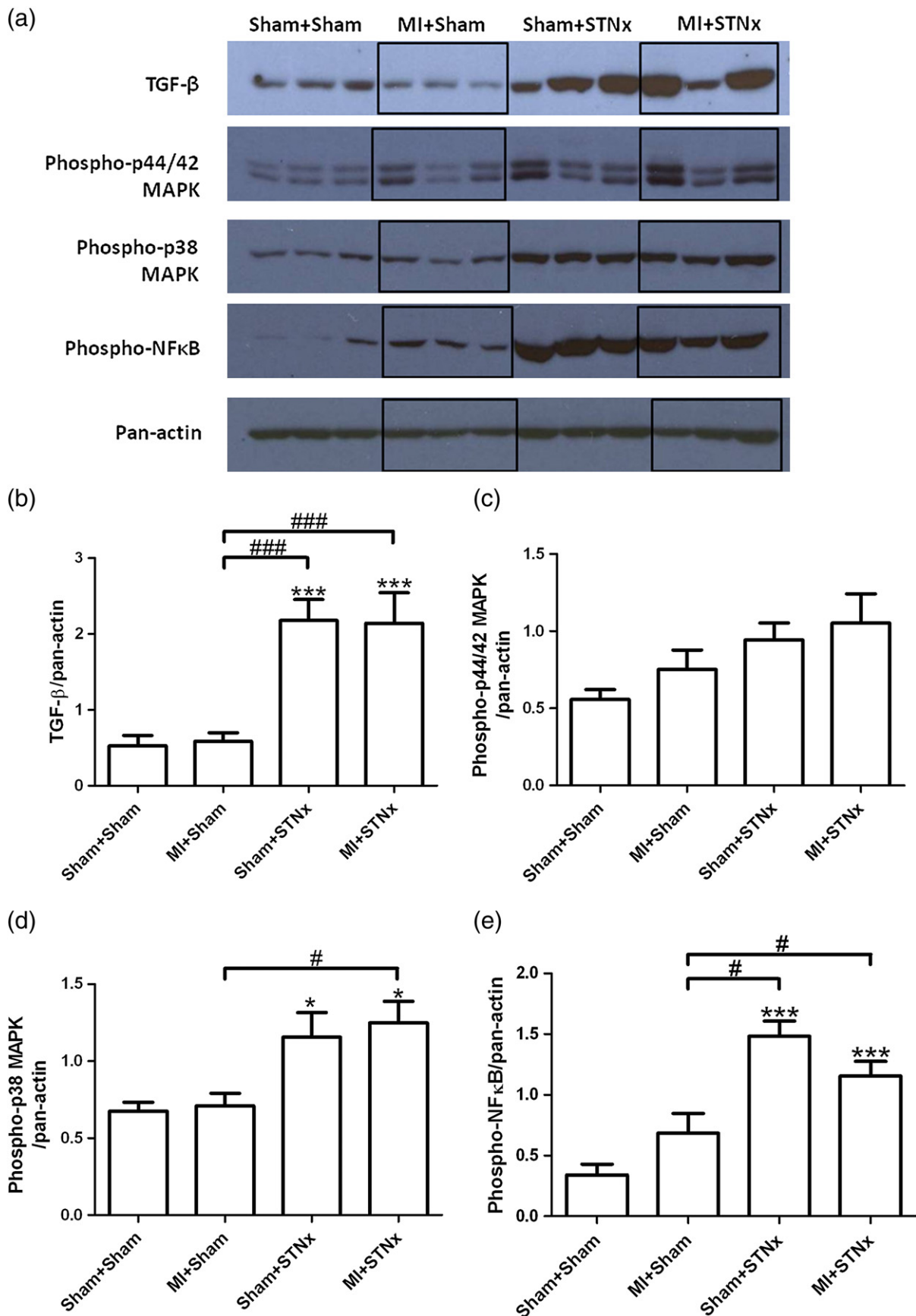


Fig. 12. Representative images of the Western blot showing renal protein levels from Sham + Sham, MI + Sham, Sham + STNx and MI + STNx groups (a). Quantitation of the protein levels of TGF-β (b), phospho-p44/42 MAPK (c), phospho-p38 MAPK (d), and phospho-NFκB (e) as normalized with pan-actin. Data are expressed as mean ± SEM. **p* < 0.05 versus Sham + Sham, ****p* < 0.001 versus Sham + Sham; #*p* < 0.05, ###*p* < 0.001 for between group comparisons.

tissue analysis. To our knowledge, this paper is the first description of progressive functional, structural and molecular changes on heart and kidney in a pre-clinical model of MI followed by STNx that replicates the clinical scenario leading to CRS [1].

Worsening renal function in the context of HF is associated with adverse outcomes [29]. Reflecting this, mortality was increased by 26% in MI + STNx animals than the MI + Sham group, despite no difference in infarct size as well as attenuation rather than an increase in BP in MI + STNx animals.

MI animals developed systolic dysfunction, as indicated by significant decreases in LV EF and FS at 4 weeks post-MI. The subsequent STNx accelerated the progression of cardiac remodeling leading to a further reduction in LV EF and FS in MI + STNx animals compared to the MI + Sham group. Cardiac remodeling was also accompanied by pulmonary congestion as lung weight was significantly increased in MI + STNx animals compared to the MI + Sham group. It is therefore likely that MI + STNx animals had some degree of decompensated HF.

In this study, we specifically explored progressive structural, molecular and biochemical changes to the myocardium that progress to LV dysfunction. A prominent cardiac remodeling event associated with functional alterations is myocardial fibrosis, assessed by the extent of collagen deposition. MI + STNx animals had significantly greater collagen I protein expression compared to the MI + Sham group, consistent with a significant elevation in cardiac extra-cellular fibrosis accumulation. These changes were associated with significant increases in LV gene expression of fibrotic related markers TGF β ₁ and collagen I in MI + STNx animals compared to the MI + Sham group.

Increased fibrosis in the LV impedes cardiac relaxation and led to a deterioration in diastolic function as observed by a significant increase in A wave velocity in MI + STNx animals compared to the MI + Sham group. Furthermore, a significant increase in the hemodynamic parameter of Tau logistic, a load independent measure of isovolumetric relaxation and LV chamber stiffness, suggested impaired ventricular relaxation.

In addition, compensatory eccentric hypertrophy of the viable myocardium contributes to ventricular dysfunction [30]. Increases in myocyte cross-sectional area as well as elevated heart weight were observed in MI + STNx animals compared to the MI + Sham group, which may be contributory to and reflective of the detrimental effects of pathological cardiac remodeling [31,32]. These were associated with significant increases in gene expression of the hypertrophic related marker ANP in MI + STNx animals compared to the MI + Sham group.

A definite trend toward an increase in the levels of phospho-NF κ B between MI + Sham and MI + STNx animals, and an indicating trend toward an elevation in the levels of TGF- β between Sham + Sham and MI + STNx animals were observed, indicating these pathways may be operating under the setting of MI + STNx. Lack of significant differences among the groups may be related to the time point of the analysis. Cardiac signaling pathway activation occurs immediately or very early in the cardiac remodeling response to MI [33]. The TGF- β precursor increases within the first day post-MI [34]. After inflammation has subsided, peak levels of differently activated signaling pathways are likely to decrease in the post-MI heart. Therefore, the alterations may be difficult to observe at the 14-week time-point at which tissues were harvested.

Renal fibrosis, another pathological process that occurs post-MI [12] was accelerated by STNx. Renal tubulointerstitial fibrosis was increased in MI + STNx animals despite significantly lower BP compared to the Sham + STNx group, indicating that this detrimental effect had a BP-independent component. Up-regulated gene expression of the fibrotic related markers TGF β ₁ and collagen IV as well as pro-inflammatory cytokine IL-6 was observed in the kidney in STNx animals. Although gene changes in the kidney between MI + STNx and Sham + STNx animals were not observed, these are likely to have occurred considerably earlier than the 14-week time-point. Activation of gene expression is a dynamic process [35], hence the increases in transcription in MI + STNx animals at

14-weeks post-MI may have returned back to the levels in the Sham + STNx group. Increases in TGF- β , phospho-p38 MAPK and phospho-NF κ B protein levels were found in the kidney in Sham + STNx and MI + STNx animals compared to the Sham + Sham control group. Thus activation of fibrotic related pathways, namely TGF- β , p38 MAPK and NF κ B, may at least in part contribute to the functional worsening observed in STNx animals. These changes were accompanied by increases in renal injury biomarker (KIM-1) and macrophage infiltration in STNx animals, all of which may be contributory to the subsequent renal fibrosis [36,37].

Two insults within a 4-week period may not ideally replicate the clinical scenario of heart failure followed by renal insufficiency and is a limitation of the current study. However, the features of accelerated organ worsening have clinical implications. Functional changes in the kidney between MI + STNx and Sham + STNx animals were not observed, at least at the 14-week time-point. We did, however, observe structural changes in the kidney which were greater in MI + STNx compared to Sham + STNx animals. This may translate to functional changes over a time period beyond our study duration (10 weeks post STNx). Alternatively, the insult induced by STNx may be so aggressive that a further reduction in renal function following MI would be difficult to observe.

In conclusion, the present study has systematically examined the pathophysiology and the mechanisms underlying cardiac and renal changes in the setting of MI followed by STNx. STNx accelerates cardiac hypertrophy, fibrosis and cardiac dysfunction post-MI, whilst MI accelerates STNx-induced renal fibrosis. These findings have clinical implications with regard to the pathophysiology of the so-called cardiorenal syndrome in man specifically renal impairment post MI, and it may represent a useful pre-clinical model that recapitulates some of the clinical features of this condition. We have thus established a new proof-of-concept CRS model to improve understanding of organ crosstalk and potentially assess the efficacy of mechanism-targeted therapies in attenuating both cardiac and renal injury in the CRS setting.

Acknowledgement/support

We would like to acknowledge Ms Mariana Pacheco, Ms Jemma Court and Ms Alysha Holland for their technical assistance with the animal studies, Mrs Sylwia Glowacka for assistance with Cobas assays and Dr Yuan Zhang for assistance with immunohistochemistry. Shan Liu is a recipient of International Postgraduate Research Scholarship funded by Australian Government and Monash Graduate Scholarship funded by Monash University, Australia. This work was supported by the NHMRC of Australia (program grant no. 546272).

The authors of this manuscript have certified that they comply with the Principles of Ethical Publishing in the International Journal of Cardiology [38].

References

- [1] Ronco C, Haapio M, House AA, Anavekar N, Bellomo R. Cardiorenal syndrome. *J Am Coll Cardiol* 2008;52:1527–39.
- [2] Dries DL, Exner DV, Domanski MJ, Greenberg B, Stevenson LW. The prognostic implications of renal insufficiency in asymptomatic and symptomatic patients with left ventricular systolic dysfunction. *J Am Coll Cardiol* 2000;35:681–9.
- [3] Hillege HL, Girbes ARJ, de Kam PJ, et al. Renal function, neurohormonal activation, and survival in patients with chronic heart failure. *Circulation* 2000;102:203–10.
- [4] Hillege HL, Nitsch D, Pfeffer MA, et al. Renal function as a predictor of outcome in a broad spectrum of patients with heart failure. *Circulation* 2006;113:671–8.
- [5] Al-Ahmad A, Rand WM, Manjunath G, et al. Reduced kidney function and anemia as risk factors for mortality in patients with left ventricular dysfunction. *J Am Coll Cardiol* 2001;38:955–62.
- [6] Bibbins-Domingo K, Lin F, Vittinghoff E, Barrett-Connor E, Grady D, Shlipak MG. Renal insufficiency as an independent predictor of mortality among women with heart failure. *J Am Coll Cardiol* 2004;44:1593–600.
- [7] de Silva R, Nikitin NP, Witte KKA, et al. Incidence of renal dysfunction over 6 months in patients with chronic heart failure due to left ventricular systolic dysfunction: contributing factors and relationship to prognosis. *Eur Heart J* 2006;27:569–81.
- [8] Smith GL, Lichtman JH, Bracken MB, et al. Renal impairment and outcomes in heart failure systematic review and meta-analysis. *J Am Coll Cardiol* 2006;47:1987–96.

- [9] Gottlieb SS, Abraham W, Butler J, et al. The prognostic importance of different definitions of worsening renal function in congestive heart failure. *J Card Fail* 2002;8:136–41.
- [10] Liu S, Lekawanvijit S, Kompa AR, Wang BH, Kelly DJ, Krum H. Cardiorenal syndrome: pathophysiology, preclinical models, management and potential role of uraemic toxins. *Clin Exp Pharmacol Physiol* 2012;39:692–700.
- [11] Xu X, Wan W, Ji L, et al. Exercise training combined with angiotensin II receptor blockade limits post-infarct ventricular remodelling in rats. *Cardiovasc Res* 2008;78:523–32.
- [12] Lekawanvijit S, Kompa AR, Zhang Y, Wang BH, Kelly DJ, Krum H. Myocardial infarction impairs renal function, induces renal interstitial fibrosis and increases renal KIM-1 Expression: implications for cardiorenal syndrome. *Am J Physiol Heart Circ Physiol* 2012;302:H1884–93.
- [13] van Timmeren MM, van den Heuvel MC, Bailly V, Bakker SJL, van Goor H, Stegeman CA. Tubular kidney injury molecule-1 (KIM-1) in human renal disease. *J Pathol* 2007;212:209–17.
- [14] Nian M, Lee P, Khaper N, Liu P. Inflammatory cytokines and postmyocardial infarction remodeling. *Circ Res* 2004;94:1543–53.
- [15] Lekawanvijit S, Adrahtas A, Kelly DJ, Kompa AR, Wang BH, Krum H. Does indoxyl sulfate, a uraemic toxin, have direct effects on cardiac fibroblasts and myocytes? *Eur Heart J* 2010;31:1771–9.
- [16] Liu S, Wang BH, Kompa AR, Lekawanvijit S, Krum H. Antagonists of organic anion transporters 1 and 3 ameliorate adverse cardiac remodeling induced by uremic toxin indoxyl sulfate. *Int J Cardiol* 2012;158:457–8.
- [17] Lekawanvijit S, Kompa AR, Manabe M, et al. Chronic kidney disease-induced cardiac fibrosis is ameliorated by reducing circulating levels of a non-dialysable uremic toxin indoxyl sulfate. *PLoS One* 2012;7:e41281.
- [18] Bongartz LG, Joles JA, Verhaar MC, et al. Subtotal nephrectomy plus coronary ligation leads to more pronounced damage in both organs than either nephrectomy or coronary ligation. *Am J Physiol Heart Circ Physiol* 2012;302:H845–54.
- [19] Homma T, Sonoda H, Manabe K, et al. Activation of renal angiotensin type 1 receptor contributes to the pathogenesis of progressive renal injury in a rat model of chronic cardiorenal syndrome. *Am J Physiol Renal Physiol* 2012;302:F750–61.
- [20] Van Dokkum RPE, Eijkelkamp WBA, Kluppel ACA, et al. Myocardial infarction enhances progressive renal damage in an experimental model for cardio-renal interaction. *J Am Soc Nephrol* 2004;15:3103–10.
- [21] Windt WAKM, Eijkelkamp WBA, Henning RH, et al. Renal damage after myocardial infarction is prevented by renin–angiotensin–aldosterone-system intervention. *J Am Soc Nephrol* 2006;17:3059–66.
- [22] Windt WAKM, Henning RH, Kluppel ACA, Xu Y, de Zeeuw D, van Dokkum RPE. Myocardial infarction does not further impair renal damage in 5/6 nephrectomized rats. *Nephrol Dial Transplant* 2008;23:3103–10.
- [23] Kompa AR, Summers RJ. Lidocaine and surgical modification reduces mortality in a rat model of cardiac failure induced by coronary artery ligation. *J Pharmacol Toxicol Methods* 2000;43:199–203.
- [24] Phrommintikul A, Tran L, Kompa A, et al. Effects of a Rho kinase inhibitor on pressure overload induced cardiac hypertrophy and associated diastolic dysfunction. *Am J Physiol Heart Circ Physiol* 2008;294:1804–14.
- [25] Owada S, Goto S, Bannai K, Hayashi H, Nishijima F, Niwa T. Indoxyl sulfate reduces superoxide scavenging activity in the kidneys of normal and uremic rats. *Am J Nephrol* 2008;28:446–54.
- [26] Kompa AR, Wang BH, Xu G, et al. Soluble epoxide hydrolase inhibition exerts beneficial anti-remodeling actions post-myocardial infarction. *Int J Cardiol* (in press); <http://dx.doi.org/10.1016/j.ijcard.2011.12.062>.
- [27] Kompa AR, See F, Lewis DA, et al. Long-term but not short-term p38 mitogen-activated protein kinase inhibition improves cardiac function and reduces cardiac remodeling post-myocardial infarction. *J Pharmacol Exp Ther* 2008;325:741–50.
- [28] Szymanski MK, de Boer RA, Navis GJ, van Gilst WH, Hillege HL. Animal models of cardiorenal syndrome: a review. *Heart Fail Rev* 2012;17:411–20.
- [29] McCullough PA. Contrast-induced acute kidney injury. *J Am Coll Cardiol* 2008;51:1419–28.
- [30] Aoyagi T, Fujii AM, Flanagan MF, et al. Transition from compensated hypertrophy to intrinsic myocardial dysfunction during development of left ventricular pressure-overload hypertrophy in conscious sheep. Systolic dysfunction precedes diastolic dysfunction. *Circulation* 1993;88:2415–25.
- [31] Onodera T, Tamura T, Said S, McCune SA, Gerdes AM. Maladaptive remodeling of cardiac myocyte shape begins long before failure in hypertension. *Hypertension* 1998;32:753–7.
- [32] Sutton MGSJ, Sharpe N. Left ventricular remodeling after myocardial infarction. *Circulation* 2000;101:2981–8.
- [33] Gao Z, Barth AS, DiSilvestre D, et al. Key pathways associated with heart failure development revealed by gene networks correlated with cardiac remodeling. *Physiol Genomics* 2008;35:222–30.
- [34] Deten A, Holzl A, Leicht M, Barth W, Zimmer H-G. Changes in extracellular matrix and in transforming growth factor beta isoforms after coronary artery ligation in rats. *J Mol Cell Cardiol* 2001;33:1191–207.
- [35] Bar-Joseph Z, Gitter A, Simon I. Studying and modelling dynamic biological processes using time-series gene expression data. *Nat Rev Genet* 2012;13:552–64.
- [36] Bonventre JV. Kidney injury molecule-1 (KIM-1): a urinary biomarker and much more. *Nephrol Dial Transplant* 2009;24:3265–8.
- [37] Ko GJ, Boo C-S, Jo S-K, Cho WY, Kim HK. Macrophages contribute to the development of renal fibrosis following ischaemia/reperfusion-induced acute kidney injury. *Nephrol Dial Transplant* 2008;23:842–52.
- [38] Shewan LG, Coats AJ. Ethics in the authorship and publishing of scientific articles. *Int J Cardiol* 2010;144:1–2.